The immunopathogenesis of Primary Biliary Cholangitis from T cell prospective

by

Vincenzo Ronca

A Thesis submitted to the University of Birmingham for the Degree of DOCTOR OF PHILOSOPHY

UNIVERSITY OF BIRMINGHAM

Institute of Immunology and Immunotherapy

College of Medical and Dental Sciences

University of Birmingham

October 2024

Table of Contents

Abstract……6

Acknowledgements ……8

1. Introduction ……18

1.1. The liver and immune system an history of tolerance ……18

1.1.1. Liver microanatomy ……20

1.1.2. Liver as lymphoid organ ……23

1.2. Biliary epithelial cells: physiology and their immune role ……30

1.2.1. Anatomy and physiology of the BECs……30

1.2.2. BECs role in liver immunology……32

1.3. The breach of tolerance and the autoimmunity in the liver: the case of primary biliary cholangitis ……34

1.3.1. Definition and Epidemiology……35

1.4. PBC: Clinical Manifestation and disease burden ……37

1.4.1. Treatment and Unmet Need……37

1.4.2. PBC pathogenesis……38

1.5. Cell-in-cell structure ……51

1.5.1. Definition and Historical Background ……51

1.5.2. Classification ……52

1.5.3. Emperipolesis……55

1.5.4. Entosis……57

1.5.5. Cell-cannibalism ……58

1.5.6. Phagocytosis and Phagoptosis ……60

1.5.7. Enclysis……62

1.5.8. Cell-in-cell structures in the liver ……62

2. Material and Methods.....66

2.1. Ethical approval 66

2.2. Human samples 66

2.3. Antibodies 67

2.4. Biliary epithelial cell isolation and culture 70

2.5. T cell isolation and culture 71

2.6. Flow Cytometry..... 71

2.7. Quantitative Co-culture Assays 72

2.8. CellProfiler high content analysis 73

2.9. T cell siRNA knockdown 74

2.10. Fluorescence Activated Cell Sorting of E-cadherin+ cells..... 75

2.11. Paraffin-embedding of tissue 76

2.12. Immunohistochemistry 77

2.13. Semi-quantitative analysis of tissues..... 78

2.14. Immunocytochemistry 78

2.15. Inhibitors 79

2.16. Live imaging..... 80

2.17. Electron microscopy..... 80

2.18. Characterization of the epigenetic profile of PBC T cells. 81

2.19. Chromatin Immunoprecipitation Followed by Sequencing (ChIP-seq)..... 82

2.20. Assay for Transposase-Accessible Chromatin Using Sequencing (ATAC-seq) 84

2.20.1. Cell Lysis and Nuclei Preparation: 84

2.20.2. Transposition Reaction: 85

2.20.3. Library Amplification: 86

2.20.4. Library Purification and Quality Control: 86

2.20.5. Sequencing and Data Analysis: 86

2.21. Bisulfite sequencing 87

2.22. Generation and testing of Stable and functioning induced regulatory T cells... 88

2.23. Generation of antigen specific stable and functioning induced regulatory T cells 89

2.24. Statistics 90

3. Results 91

3.1. Biliary epithelial cells invaded by T CD8 cells: a cell-in-cell structure..... 91

3.1.1. Introduction 91

3.1.2. Live $CD8^+$ T cells are internalised into biliary epithelial cells in vivo and in vitro whereas $CD4^+$ T cells are not..... 92

3.1.3. CD8+ T cells are larger, more eccentric, and more frequently internalised within BEC after activation in vitro. 101

3.1.4. CD8+ T cells internalisation required actin cytoskeleton rearrangements to form discreet junctions with biliary epithelial cells and invade them. 107

3.1.5. Discussion 112

3.2. The expression of E-cadherin is instrumental for biliary epithelial cells invasion and is expressed by T CD8 cells..... 114

3.2.1. Introduction 114

3.2.2. Internalised CD8+ T cells observed within biliary epithelial cells *in vivo* are CD69+CD103+, and are enriched in patients with Primary Biliary Cholangitis. 115

3.2.3. The expression patterns of E-cadherin by activated T cells is consistent with the characteristics of their internalisation into biliary epithelial cells. 125

3.2.4. CD8+ T cells from adherens junction through E-cadherin-β-catenin interaction. 127

3.2.5. E-cadherin expression increases the frequency of internalisation of CD8+ T cells into biliary epithelial cells. 131

3.2.6. CD8+ cell internalisation into BEC is a consistent event in PBC and driven by E-cadherin expression 135

3.2.7. Discussion 141

3.3. The generation of PDCE-2 specific, stable and functioning induced regulatory T cells from peripheral blood of patients with PBC. 143

3.3.1. Introduction 143

3.3.2. The generation of SFiTreg is effective and reliable. 144

3.3.3. SFiTregs remain stable and functional in inflammatory environment. 147

3.3.4. SFiTregs cell epigenetic profile is different from natural Tregs. 150

3.3.5. Discussion 160

4. Final Discussion and conclusions 162

5. Reference 169

6. Appendix 200

Abstract

This thesis aims to reinforce the role of the biliary epithelial cells (BEC)-T cells crosstalk as central mechanism in the pathogenesis of primary biliary cholangitis (PBC). I will also explore the role of regulatory T cells (Tregs) in the pathogenesis of PBC, proposing a new approach to use induced Tregs as cell therapy for the treatment of PBC.

In the first chapter, I will explore at first the complex processes involved in maintaining the immune tolerance within the liver in homeostatic condition. I will, then, discussed the anatomy and physiology of the BECs, introducing their role as immune active cells. A general overview of PBC will be then provided, fading into its pathogenesis with a particular focus on the BEC-T cell interaction and the role of Tregs. I will mention emperipolesis as an under identified entity in PBC pathology and potential factor in PBC pathogenesis. Finally, I will describe the general biology and classification of cell-in-cell (CIC) structure, focusing on its role within the liver.

To my entire family for being my rock,

to my grandfather to light the fire,

to my wife for believing so bluntly in me

to my children who are the fundamental reason of my being

and the answer to all my questions.

Acknowledgments

As I begin this chapter, which I intended to be the easiest and shortest, I realize it won't be brief at all.

Before getting started, I would like to dedicate this thesis to Lorenzo. He is a great example of the young minds that the science beyond this text and the passion that filled my PhD days aim to inspire. I looked to him and considered what someone with his brilliant mind would be interested in knowing as I moved my research forward. You have been in my thoughts every day throughout these three years. I hope and know I will be reading your PhD thesis very soon.

The journey to completing this PhD has been long, and there are countless people I want to thank. I apologize if I have left anyone out for the sake of brevity. However, if you feel like you should have been here, I probably thought so too. Please text me in that case, and I will tell you what you have represented in my life and how you contributed to this PhD. I strongly believe that words like these should be said more often, as people are not always aware of how important they are in other people's stories.

The first person I want to address in this chapter is you, reader. If you have this thesis in your hands, it’s either because I sent it to you (and if that’s the case, I apologize for the countless minutes of reading ahead) or you downloaded or opened it in its paper version. Thank you for taking the time to read this work. It

has cost me a lot of time and tears, and while the experiments were happening, life was happening too. Beyond these lines is the story of a boy who became a man. Behind the scenes is a challenging yet amazing life, filled with incredible people.

My life has changed at least twice since I started in 2021, and even more so since I moved to the UK in 2019. While the PhD progressed, so did life, and the challenges were deeply intertwined.

I want to start by acknowledging what amazed me the most—the welcoming and warm society I found in the UK. The media often portray moving and integrating into a new country as difficult, and I was told the same before leaving Italy. However, my own experience was rather different. I will always be grateful to those who were kind enough to wait a second or ask me to repeat what must have been, at best, odd English when I arrived. The only way to truly connect with people is through spoken language, and being oneself goes through words. It took a long time to fully be myself, but I found that everyone I met put in the effort to know me, reaching out for the meaning beyond the words. I will now address some of these amazing people, leaving aside formalities and focusing on emotions—which is what acknowledgments should convey.

How can you build the abstract concept of a safe place, a home? You should ask Marylin. She welcomed me into her house and made sure I could survive the induction into a new country and the crazy rhythms of my work life. She was the wisest advisor and the right person to ask about literally anything. She, along with David and Matthew, made me feel part of their family. In fact, I never felt alone

and always felt looked after. I'm not sure she knows how grateful I am and how personal and deep my feelings toward her truly are. She went from being a stranger to a friend and ultimately family. I sincerely thank you, Marylin, for who you are and for what you have represented in my (our, including Agostina and the kids) life.

Dan, the biggest man I have ever met—I'm not sure whether there are anatomical reasons to justify that he also has the biggest heart on earth. You are incredible, bro. You turn grey days into golden memories with your smile. You took me with you into your huge social bubble and taught me how to live in a different country and how to laugh at difficulties. Most importantly, you reminded me what faith is. I wish I could look to tomorrow with your eyes, man, but meeting you certainly changed my life.

Martina, I don't want to thank you as it sounds like this is the end of a chapter. Instead, I feel this is just the beginning. As I once told you, you have been my other family and have been there for me in my darkest hours. I can never fully express the deep gratitude and love I feel for you. Something I really want is for you to be the perfect aunt for Sveva and Tommy, as I know you will be in our life forever.

The reason I managed to get through everything in the lab, and for most of what I can do now, is my almighty friend Scott. We started a journey together, filled with distressing disappointments, false hopes, and fascinating discoveries. I could be shallow and thank him for helping me produce data or collaborate as a co-investigator in this exciting project. However, the main reason I want to thank

him is for teaching me how to overcome the frustration that comes from the gap between what creativity pushes me to do and what I can actually do. He made even the worst days bearable. To him goes my deepest gratitude.

The reasons all of this happened—a mixture of merit and blame—are my supervisors. Pietro Invernizzi is the man to whom I owe my passion for liver immunology. With his vision, he "created" my career, and with his enthusiasm for discovery and science, he fueled my will to progress and become a voice in this amazing field. I still sometimes read the first email I wrote in 2014 asking if I could work with him. Now, ten years later, I know that everything I have ever done is ultimately because of him. Professor, I can never find the right words to express my immense gratitude.

I would like to thank Marco Carbone. He tried to teach me things I could only understand years later, and they are still of great use to me. Having him as a mentor shaped how I think about scientific problems and perceive the scientific community. However, what I am most grateful to him for is his friendship. I treasure the memories we built over the years, and to him and his family, I am grateful for welcoming me as a member. Thank you for collecting the pieces of my broken expectations too many times and helping me put them back together with your wise guidance.

I also want to deeply thank Ye. He walked beside me all the way through this incredible and difficult journey. It hasn’t always been easy, but looking back, I can say that everything I achieved was thanks to his unwavering mentorship and support.

Working in the liver lab has been a privilege for me. What Prof. Adams created remains strong and still one of the best places to be a liver scientist in the world. I still can't believe I had this great opportunity. However, while infrastructure makes things strong, it is the people who animate it and push science forward. I will always be thankful to everyone I met in the lab over the past four years. I will never forget your kind words and wonderful presence.

Despite a PhD being focused on science and supposedly spent in the lab, one of the best decisions I ever made was to become a clinician in the UK. First, I would like to thank the NHS. I am Italian, coming from a public healthcare system, but what I witnessed during my years in the UK is a wonder. The service the NHS offers, through its infrastructure but even more so through the passion of the people working in it, is absolutely astonishing. Over the years, I took pride in being part of the NHS. Thank you, NHS, for being, in my opinion, a virtuous example of democratic access to the right to healthcare.

I had the privilege of working with some of the finest clinicians in a place that surpassed every expectation I ever had for my career. The Liver Unit at Queen Elizabeth Hospital isn't just a dream come true for any liver physician—it's a rare and inspiring environment where the highest standards of medicine coexist with warmth, camaraderie, and an unshakeable sense of purpose. It still amazes me how such a demanding job could be so fulfilling and yet so enjoyable.

Being part of this team has not only shaped me into the best clinician I could hope to be but has also made me a better person. There is no greater privilege than

doing what I love, surrounded by inspiring minds and an atmosphere that fosters growth. Truly, it's the best job in the world.

Now, moving to the people who have always been there. Dad, you gave me something that I never thought would be of use: a distaste for showing off. It may sound strange, but the need and will to meet your expectations made me embrace the most difficult challenges for the wrong reasons, only to realize that I loved what I was doing. You pushed me so hard that I was mad at you for the first half of my life. However, every time I failed, you were there to support me regardless of what happened. Thank you for being that dad, my dad.

Mum, you taught me kindness and what strength means. Looking back, I know that you have always been the best person in the room. You kept things together, in our family and with your friends. You always avoided conflicts, allowing others to lean on you, and you did so with a smile, letting them choose you as the one to blame. I am amazed, Mum, by how generous, strong, and gracious you are. Thank you both for being my parents and making my past and present special. Thank you for being the best grandparents Sveva and Tommy could ask for.

Nana, you don't know this, as I don't say it to you, but I am so proud of the human being and the woman you have become. We had the privilege of watching you grow up, and you don't yet know how scary that can be—you will find out in the future. When I look at you today, I see a strong, independent, and kind woman. You know where you are going, and you know how to get there. Well done. Even more, you are an amazing human being. Things have changed, and these days you are the pillar supporting me rather than the other way around.

Mary, look at you and how many things you have done and achieved. You shaped your existence in your own way and took everything you ever wanted. One could argue against the approach of "I want everything, and I want it now," but it certainly worked for you. You gave me two new tiny, amazing humans that I love with all my heart and who fill me with joy every time I have the chance to spend time with them. I will always be there for you, and if, in any circumstance, you felt my support lacking, I apologize. I am and want to be there for you for however long my life may be.

Nonna, ciao questa parte la scrivo completamente in italiano perché voglio che tu la legga così come l'ho pensata. Quello che hai fatto per me, emotivamente e praticamente non potrò mai dimenticarlo. Ho la fortuna di ricordare ogni piccolo dettaglio, finanche la sensazione delle calze calde che toccano il tuo pavimento liscio e pulito, dopo il bagno. Quel senso di protezione e di amore è il fondamento della mia forza e del mio coraggio. Da che io posso ricordare hai perso tanto, tantissimo, anche quella casa dove sei entrata sposa. Eppure, ancora riesci ad essere te stessa, e trovi modo e spazio per accoglierci tutti nel tuo cuore, nonostante tutte le nostre stranezze. Io non so cosa ho fatto per meritarti, ma sappi che ti voglio un bene indescrivibile. Grazie nonna.

I always argue that two parents cannot be the full package of someone’s care. In my case, the mixture of uncles and grandparents has contributed so much to who I am and what I have done that a big, heartfelt thank you is certainly required. I recently had the chance to spend time with Zia Ida and Zio Carmine, who were incredible in shaping my happy and perfect childhood. I missed you both so much,

and I will never be able to tell you how much I love you. I would love to have you around every day and for you to be the huge parental figures for my kids that you were for me.

If I had done all this ten years ago, when I was fresh, I would have said to you, Nonno, "Look, I have done it again, for you, as if you were here with me." Now, after twenty years since you left me—after high school graduation, medical school graduation, the internal medicine board, the master's degree in transplant medicine, and the PhD—the only thing I want to tell you is, "Meet my family: this is Agostina, my wonderful wife; this is Tommy—he bears your name; and this is Sveva—she is the sweetest thing I have ever seen." I cannot tell you this in person, but I hope you are somewhere watching, with Zia Rosaria telling you that Tommy was "as beautiful as a painting" (her words). What I realized, Grandpa, is that degrees and jobs don't bring one close to happiness, but family does—and you taught me that too with your example. The same goes for you, Zia—you are still present in every corner as that incredible character in our lives. I miss you both so much.

We researchers are fascinated by things we cannot explain, and we dedicate our lives to solving mysteries, often without fully succeeding. This is the perfect analogy for my marriage. In my mind, love is personal; everyone experiences it and gives it in their own way. You cannot ask for a specific type of love or define it, as it is a manifestation of something deep and personal. Agostina, my wife, has loved me in her own way since she met me. It has always been so intense that it confuses and amazes me at the same time. I struggled since day one to

understand her and the purpose of many things she does for me, especially since I clearly express my needs. However, she gives me all of herself in the way she knows and likes, as the strong and stubborn woman she is. She taught me what being loved means and how wrong I was in thinking I already knew. She is my life, my everything, because looking at what I have, and even more so at what we have done, I realize that nothing would have been possible without her, and without her being who she is. Still, I try to understand her, but somehow the need to understand is the need to possess, and I love how free and wildly independent she is. I am happy knowing I will never fully understand her. She is my other half, and this PhD is not dedicated to her, as I think she deserves to be awarded the PhD with me.

This thesis is not dedicated to my kids either. Tommy was born in Birmingham in the middle of my PhD, and being with him filled my heart more than I thought possible. Sveva arrived three years later in Milan. The thought of her began in what Agostina calls home in Greenfield Road. I realized that holding them made me feel defined for the first time. I am a dad—this is who I am. I have always struggled to define myself as a doctor, as I never thought it added anything to my definition as a person. I felt awkward introducing myself as "Dr. Ronca." Being a dad, on the other hand, changed me. Saying "I am a dad" makes me want to talk about this incredible experience, and it would make sense to tell people, while shaking their hands, "I am Vincenzo, Tommy and Sveva's father," as this defines who I have become and tells our story.

However, this thesis is not dedicated to them either, as they are unaware of science and medicine. I want them to look at this amazing world and society as individuals, flying free and independent, experiencing it thoroughly, and trying to find their place in it. I will love watching them grow and find their way—this is what I want to do with my life.

Thank you all for being part of my story that I am loving so much.

1. Introduction

Disclaimer: The themes discussed in this chapter have been discussed in reviews I have published(1-4) or are currently accepted but not published yet. The figures are all from the same papers and all of them have been produced as results of my work.

1.1. The liver and immune system an history of tolerance

The liver has been of great interest for humans since ancient times. Early detection of such interest is proven by paintings of liver vasculature found in cave paintings in southern France(5). Around 700 BCE, it was common practice, in Mesopotamia, to divine the will of the gods by inspecting the liver as reported by Ezekiel(6, 7). Later in time the Romans thought not only that the liver housed the soul but it was the centre of blood production and emotions(8).

Leonardo da Vinci in 16th-century was the first to document that precise liver anatomy(9). In "De Humani Corporis Fabrica Septum", Andreas Vesalius, shortly after, described the anatomical relationship between the liver parenchyma and the biliary tree(10). However, insight of the functioning of the liver should wait until the early microscope came along and Marcello Malpighi in 1666 described the liver's lobules and vasculature(11). The technical advancement in research tools and the introduction of electron microscopy boosted the liver research.

The biochemical role of the liver became evident, and its immunological features emerged during the transplant era of the 1960s. In fact the liver transplants appeared to be more tolerated, compared with other organs, even in presence of major histocompatibility complex (MHC) mismatches and minimal immunosuppression(12). Intriguingly, when other organs were transplanted at the same time of the liver, the other organs were better tolerated as well(13).

Cantor and colleagues tested the liver tolerance, trying to understand whether it was functional also to regulate systemic immune response. They infused load of antigens through the portal vein and subcutaneously. The systemic infusion triggered the production of circulating antibodies directed against the infused antigens. Surprisingly, when the infusion was done through the portal vein and sequentially subcutaneously, the antibodies in the circulation were undetectable, suggesting that the liver can indeed induce tolerance toward the antigens passing through the portal circulation(14). This unique feature is crucial since the liver processes over 2000 litres of blood daily from the portal vein (75%) and hepatic artery (25%). The blood in the portal vein collects all the venous bloods from the gut and is enriched with a plethora of antigens, from microbial products to food antigen. Therefore, the liver's immune system has evolved to tolerate benign antigens while effectively combating genuine threats.

The liver is now recognized as an immune organ(15, 16). The shift from maintaining immunological balance to the acute or chronic activation of the liver's innate or adaptive immune response underpins liver diseases.

1.1.1. Liver microanatomy

The liver sinusoids receive mixed bloods from the portal vein, draining from the intestine and the hepatic artery, coming from the systemic arterial circulation(17, 18). The sinusoidal endothelium lacks basal membrane and has got pores of 150-200 nm and it is a highly permeable structure.

The main epithelial cells in liver tissue are the hepatocytes. They are distributed in cords, typically one to two cells thick. Before reaching the lymphatic vessels, the lymph produced by the liver drains in a virtual space positioned between the hepatocytes cords and the sinusoidal channels called “space of Disse”, which houses the hepatic stellate cells(19). This internal recirculation facilitates the movement of immune cells from the blood into the liver tissue and then to the lymph nodes.

The liver's reticuloendothelial system acts as the primary barrier for the immunogenic factors (antigens or microbes) that eludes the gut barrier. It plays a pivotal role in maintaining liver immune balance orchestrating the immune response by regulating the lymphocyte activation and shaping the microenvironment(20).

The first line of defence is represented by the endothelium and particularly by the liver sinusoidal endothelial cells (LSECs). In a well-orchestrated function along with Kupffer cells (KCs), they form an efficient barrier capturing and processing any antigenic molecules in the sinusoidal blood, either initiating signalling pathways through Toll-like receptors (TLRs) or scavenger receptors or presenting the antigens to resident immune cells(21-23).

The figure 1.1 is a schematic representation of the tolerogenic process of the antigens in the sinusoids.

KCs is a unique population of hepatic macrophages positioned within the sinusoids.

They originate from erythromyeloid progenitors in the yolk sac that can self-renew (24, 25).

Their position allows frequent interaction with circulating immune cells. Under homeostatic condition they modulate the liver's immune activation by secreting IL-10 and prostaglandin-E2, preventing harmful inflammatory response, against harmless antigens(20, 26, 27). The chronic exposure to lipopolysaccharides (LPS), triggers the consistent secretion of IL-10 and the expression of Programm death-ligand 1 (PD-L1), both causing the inhibition of T cell responses(26, 28).

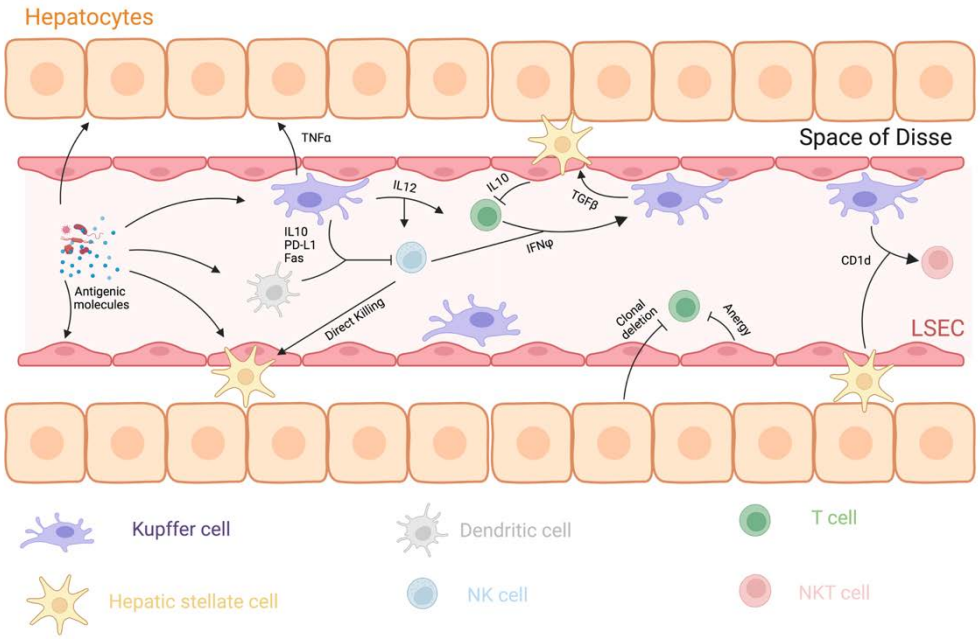

Figure 1.1 **Antigen presentation within the liver.** The molecules that trigger a response enter the body through the portal vein and activate various types of cells responsible for presenting antigens (such as KCs, DCs, HSCs, hepatocytes and LSECs). Normally under conditions, KCs and DCs suppress NK and T cells, by expressing PD L1 and releasing IL 10. LSECs also produce IL 10. When hepatocytes antigens it can either cause T cell inactivation or lead to their elimination. However, during times of inflammation activated KCs produce IL 12. Stimulate NK and T cells to produce IFN φ. A high level of this molecule helps sustain the activated state of KCs which can contribute to liver damage by releasing TNF α. Both HSCs and KCs are capable of presenting lipid antigens to NKT cells using CD1d.

LSECs express both MHC class I and II and they can, in fact, function as antigen-presenting cells to both T CD4+ and CD8+ cells. The outcome of the antigen presentation varies based on the amount of the available antigen and can trigger either a tolerogenic response or activate the immune cascade(29, 30) or even induce apoptosis in activated CD4 lymphocytes(30).

Hepatic stellate cells (HSCs) in the subendothelial space can interact with immune cells. While they play a role in chronic inflammation and fibrosis, they also contribute to immune balance in normal conditions(31-34).

Immune cells can traverse the LSEC barrier and interact with hepatocytes. These liver cells, like KCs and LSECs, can act as non-professional antigen-presenting cells. They typically express MHC class I but can also express MHC class II under certain conditions. This interaction can influence the course of infections, potentially favouring chronic infections over viral clearance(35-38).

1.1.2. Liver as lymphoid organ

The multifaceted functions the liver has, makes challenging to define this organ functionally. However, despite not being a traditional lymphoid organ like the spleen or thymus, it hosts a diverse range of resident cells within its parenchyma and portal tract (Figure 1.2).

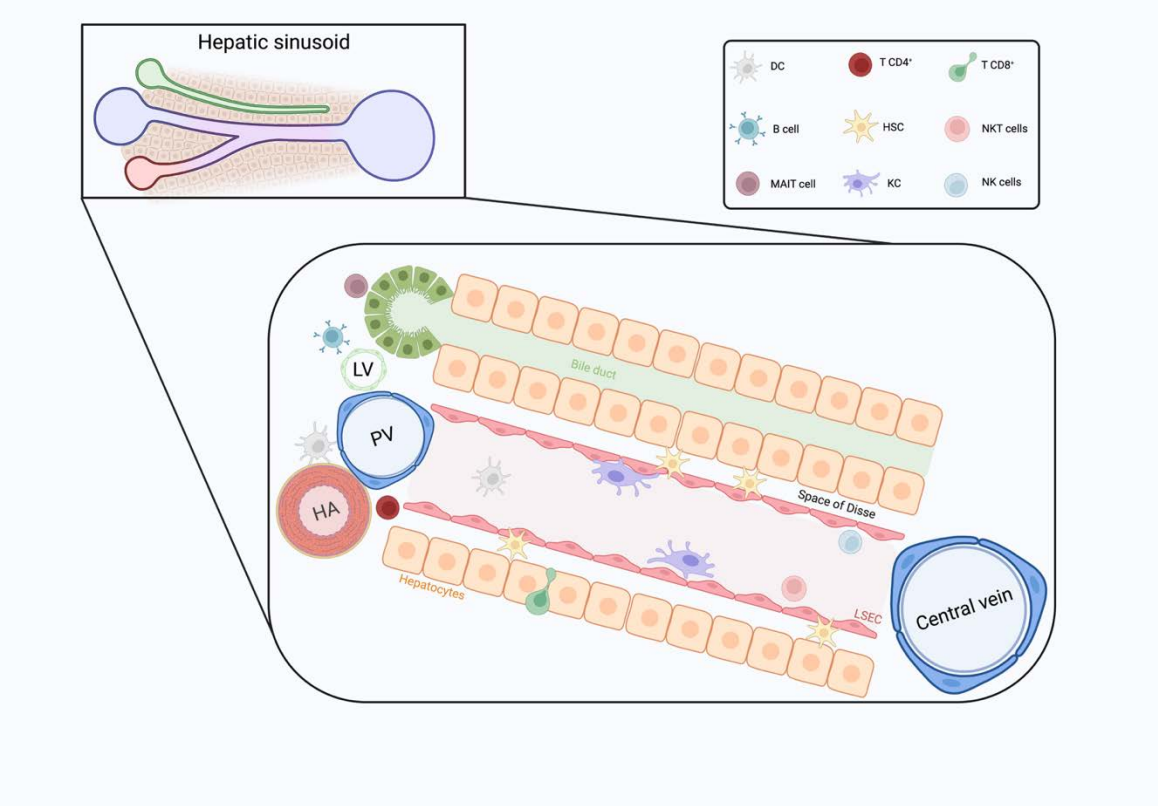

Figure 1.2 **Immune cells distribution in the hepatic sinusoids.** Representative scheme of the immune cells within the hepatic sinusoids and of their distribution in the sinusoidal structure. *PV= portal vein; HA = hepatic artery; LV = lymphatic vessel*

The state of activation and the function of the resident populations relies tightly on the liver's immune environment. In fact, the act as keepers of the immune tolerance, switching to central players of the immune response during inflammation.

The epithelial cells, namely hepatocytes and biliary epithelial cells (BECs) can instead become unintended targets of immune damage, resulting in acute or chronic liver conditions. When "activated", both BECs and hepatocytes transition from mere bystanders to active participants in the pathological process, either as antigen-presenting cells or as sources of inflammatory cytokines. The subsequent sections detail the feature of the liver's immune resident network.

1.1.2.1. Dendritic Cells (DCs)

DCs are professional antigen-presenting cells (APCs) and they are commonly abundant in skin, lungs, gut, and liver. Liver DCs can be sub-categorized into three groups: the conventional lymphoid (CD8α-, B220-, CD11b+) and myeloid (CD8α+, CD103+, B220-, CD11b-, CD1c+), preferentially found in the periportal region and around the central vein, and the plasmacytoid DCs (B220+, CD11b-) located within the liver parenchyma(39, 40). The latter, characterized by BDCA-2 and CD123 expression(41), play a pivotal role in viral defence upon the TLR 7/8 singling. The effect of the antigen presentation may have different outcomes based on the liver microenvironment. In fact, their response to low levels of LPS or IFN-γ results in the expression of indoleamine-2,3-dioxygenase (IDO), an enzyme that increase the levels of kynurenine, an immune-tolerogenic molecule(42, 43). Immature DCs remain triggers tolerogenic response, however,

chronic inflammation can stimulate their maturation upon CD80 signal and participate in the inflammatory process. (44).

1.1.2.2. Natural Killer Cells (NK)

NK cells are the most represented immune population within the liver(45, 46). Classically they are classified based on CD56 surface expression levels into $CD56^{bright}$ or $CD56^{dim}$, with the former showing low cytotoxic activity but with intense cytokine secreting activity and the latter with more cytolytic function(47). These cells are strategically located near KCs and LSECs(48). The liver resident killer (lrNK) cells exhibit functional and phenotypic differences compared to the circulating NK cells (cNK). Although both types originate from the bone marrow, the development and maintenance of lrNK cells depend on T bet and aryl hydrocarbon while cNK cells require Eomesodermin(49). Recent studies at the single cell level indicates that lrNKs have got an augmented expression of inhibitory receptors such as TIGIT and KLRB1 compared to cNK cells suggesting a potential role in maintaining tissue immune homeostasis(50, 51). These findings require validation through functional studies and, as such, the clear function of these cell population at the steady state remains to be better defined.

1.1.2.3. Natural Killer T Cells (NKT)

NKT are atypical lymphocytes that get peculiarly activated by lipid antigens or TLR pathways. They are enriched within the liver parenchyma and functionally and phenotypically divided into type I and type II, with the latter being more suppressive(52). They have a restricted T cell receptor (TCR) and often recognize self-antigens such as glycolipid sulfatide. When the type II cells get activated they release IL-4 which promotes the growth of hepatocytes and plays

a role, in liver regeneration(53). Additionally, they interact with DCs controlling the activation of type I NKT cells that are more proinflammatory and produce IFN-γ.

1.1.2.4. Mucosal Associated Invariant T Cells (MAIT)

MAIT cells are a group of unconventional T cells that are predominantly found in liver tissue. Their activation is specifically regulated by a polymorphic MHC class I related protein called MR1. This protein has the ability to present metabolites derived from vitamin B2 and B9 to the MAIT cells(54). The MAIT cells have been recognized as a barrier for the biliary epithelium shielding it from potential microbial triggers originating from the gut. BECs play a role in this process by producing CXCL16 and CCL20, which act as ligands for receptors (CXCR6 and CCR6) expressed on the surface of MAIT cells(55). The importance of MAIT cells as sentinels against infections in the liver is evident when considering their dysfunction in individuals, with alcoholic liver disease, which significantly increases their susceptibility to infections(56, 57).

1.1.2.5. Tissue Resident Memory T Cells (T_{RM})

Another central player in maintaining the intricate balance between tolerance and effective immune response, is a subset of memory T cells known as tissue-resident memory T cells (T_{RM}).

They provide sustained local intravascular immunosurveillance, allowing them to rapidly respond to threats such as hepatitis B, malaria, and even liver cancers like hepatocellular carcinoma(58). Their constant presence within the liver is not mere confinement; it's a strategic placement, ensuring they are the frontline defense against pathogens and tissue damage(59-61).

Liver T_{RM} maturation differs from the ones in other tissues. The usual maturation route is the antigen priming in lymphoid tissue and the following migration toward the organ of residency. Liver T_{RM}s instead are primed in situ, promoting the local maturation of this cell subset. This unique feature is instrumental to keep the cells close to the location of the cognate antigen encounter. The long local retention likely allows the clonal selection for the best adapted cells to the liver environment, promoting the tolerogenic role of this cells at the steady state(62, 63).

The liver's sinusoidal vessels play a pivotal role in the retention and behaviour of T_{RM}. Markers like CD69, CXCR6, CXCR3 and CD103 have been identified as defining features of these cells, suggesting their long-term residency within the liver(60, 64, 65).

Lessons about the protective role of T_{RM} comes from viral and parasite infections(66-71).

CD8+ T_{RM} was demonstrated to provide protection against malaria infections at the liver stage(64, 72-76). Early experiment showed the secretion of IFN-γ by intrahepatic populations and subsequent accumulation of memory T cells within the liver. These cells were instrumental for malaria protection(77, 78). This evidence was later confirmed by the formation of T_{RM} in the liver following malaria vaccination(64, 79).

Maini's group pioneered the understanding of virus specific CD8+ T_{RM} response and revealed their potential for long lasting effects(59-61). They described the presence of virus-specific T_{RM} directed against all the major virus antigens, correlating with well-controlled infection and low viral load. Such specific T_{RM} keep residing withing the liver even after resolving an infection(59).

In fact, they represent a first anti-viral defence, ready to release high load of IFN-γ and TNF upon TCR stimulation(80). These agents can inhibit HBV replication without causing cell damage(81-83).

However, their prolonged residence and interaction with the liver's rich cellular network make T_{RM} susceptible to influences from their environment. In conditions where the liver's homeostatic balance is disrupted, T_{RM} can contribute to tissue damage.

In studies on murine models on non-alcoholic steatohepatitis (NASH), associated with hepatocellular carcinoma (HCC)(84, 85), it was noticed an accumulation of activated hepatic CD8+ T cells with markers indicating tissue residency. This accumulation was linked to immune mediated liver damage and the progression of HCC. Dudek et al. Proposed a concept called "auto-aggression " where these CD8+ T_{RM} cells specifically attack hepatocytes. Interestingly blocking the FasL pathway showed effects against this auto aggression suggesting a potential therapeutic approach for chronic liver diseases, like NASH(84). On the hand Pfister et al., found that these T_{RM} cells produce significant amounts of TNF which is hypothesised to impair immunosurveillance and reduces the effectiveness of immunotherapies(85).

Based on the findings in mice it has been discovered that humans with levels of CD69 expression in their liver CD8+ T cells can cause liver damage through pathways induced by IL-15. The severity of liver failure in patients with end stage cirrhosis is directly related to the number of these cells(86). Recent studies using techniques like single cell RNA sequencing have also linked hepatic CD8+ T cells

to non-specific cytotoxic activity in patients experiencing hepatitis B virus (HBV) flares. Similar increases in CD8+ T_{RM} cells have been observed in cases of acute liver failure(87) and autoimmune hepatitis(88) with the latter showing a correlation with disease severity.

Further research may be able to distinguish between pathogenic subsets of liver CD8+ T_{RM} cells. Alternatively, these T_{RM} cells may play a role under certain conditions and a pathogenic role under others depending on specific inflammatory and metabolic signals.

1.2. Biliary epithelial cells: physiology and their immune role

1.2.1. Anatomy and physiology of the BECs

The biliary system is characterised by an intricate network of bile ducts lined by the BECs. It can be divided in intrahepatic and extrahepatic systems. The human intrahepatic biliary epithelium can be divided in *hepatic ducts* being the largest, measuring over 800 μm, followed by *segmental ducts* ranging between 400–800 μm, *area ducts* spanning 300–400 μm, *septal bile ducts* around 100 μm, *interlobular ducts* varying between 15–100 μm, and the smallest being the *bile ductules*, which are less than 15 μm(89-91).

According with the bile duct size, the morphology of BECs changes with them being classified as small or large BECs. Small BECs are found in the bile ductules (<15 mm in diameter), are cuboidal in shape and have a high nucleus-to-

cytoplasm ratio. On the other hand, the large BECs are positioned in larger bile ducts and are columnar, rich in organelles, and have a reduced nucleus/cytoplasm ratio(92). Small BECs are less specialised cells, compared with the large BEC that participate in the final bile formation. They have cilia on their surface which function as sensors within the bile duct lumen, detecting changes in bile flow and composition(93). After the bile has been secreted in the bile canaliculus by the hepatocytes, the BECs are involved in the final composition of the bile. They are responsible for up to 40% of the bile-salt independent bile flow(94). BECs main role in the bile formation is the secretion of bicarbonate into the bile upon the secretin stimulation in a process involving cystic fibrosis transmembrane conductance (CFTR) and $Cl^-/HCO3^-$ anion exchanger 2 (AE2)(95).

Supporting their functional difference, the molecular expression of surface transporters involved in the secretin-stimulated bicarbonate secretion varies along the biliary epithelium. Large BECs express molecules like secretin receptor (SR), CFTR, and AE2, which are pivotal for biliary fluid secretion through a cyclic adenin monophosphate (cAMP)-dependent pathway(96, 97). In contrast, small BECs relies on $Ca2^+$ -activated signalling pathways to increase the intracellular cAMP and participate in the bicarbonate secretion(98, 99).

Large BECs are more susceptible to damage compared with their smaller counterparts which, instead, exhibits greater resistance to liver injury(96) (98, 100, 101). Small BECs are also responsible to replenish large BECs in case of damage to the biliary epithelium.

BECs also play a crucial role in the liver's response to injury. They are quiescent at their baseline, however, when they are injured they become activated and highly proliferative(102-104). The pattern of response can however be several and span from ductopenia to biliary hyperplasia and ductular reaction (105-107). The biliary hyperplasia is common in cholestatic disease like primary sclerosing cholangitis (PSC). The loss of BECs triggers what seems a compensatory regenerative mechanism, which also triggers an increased secretion of $HCO3^-$ (105). The ductular reaction is typical of chronic disease like MASH and it is characterised by the proliferation of small and immature bile ductulus at the interface between portal tracts and liver parenchyma. The ductopenia is, instead, characterised by the reduction or loss of small bile ducts. This is a common histological feature observed in toxic injuries or autoimmune cholangiopathies such as primary biliary cholangitis (PBC)(106).

1.2.2. BECs role in liver immunology

BECs were thought to be just lining the biliary epithelium, shaping the final content of the bile. However, the evidence of their immune role piled up over the last 20 years. They are in fact instrumental in homeostatic protection of the biliary tree or active responder when an injury is perpetrated toward the biliary tract.

1.2.2.1. Homeostatic Immunobiology of BECs

In a state of equilibrium, BECs contribute significantly to the liver's immune defence. BECs luminal secretion include a plethora of proteins with potential antimicrobial and immunological functions(108). The most abundant of these molecules is certainly immunoglobulin (IgA). Notably, in humans, the responsibility of biliary IgA secretion falls on BECs, distinguishing them from the

rodent whereby the hepatocytes perform this function(109, 110). The IgA from the biliary epithelium fortifies the local antimicrobial defence systems in the bile ducts and upper intestine, potentially aiding to the systemic clearance of antigens(111, 112).

BECs also secrete defensins, mucins, lactoferrin, and cathelicidin, bolstering the antimicrobial effect of the bile(108, 113, 114). Furthermore, BECs can detect pathogen-associated molecular patterns (PAMPs) upon TLRs binding(113, 115). To support their role in the biliary epithelium protection, both the secretory machinery and TLR expression is increased by infections(115-117).

BECs express HLA class I at the steady state and can act as APCs. They also express adhesion molecules to recruit leukocyte at the biliary site. However, when they are quiescent, such antigen presentation results in apoptosis of the immune cells (118-120). Recent findings suggest cholangiocytes can present antigens to unconventional T cells, like mucosa-associated invariant T (MAIT) cells and natural killer T (NKT) cells, which are abundant near the gut microflora(121).

1.2.2.2. Immunobiology of Activated BECs

BECs can get activated when they are injured in cholestatic processes or infections(122, 123). Besides their proliferation pattern discussed earlier, they change their phenotype and become crucial players of the immune cascade(124, 125).

Activated BECs can engage in crosstalk with T cells and potentially act as APCs. Highly relevant for the recruitment in the peri-biliary region are CCL20 and CXCL16 which are active on CXCR6+ T cells. BECs express several adhesion molecules to interact with the immune cells with the most relevant being ICAM-1 and VCAM-1, CD40, CD44, CD95, LFA3(119, 126-129). Furthermore, when stimulated they start expressing MHC class II (119, 130). There are some controversies around the possibility they might be effective APCs. In fact, there is not data confirming any co-stimulatory molecule expression (i.e. CD80/CD86) to trigger second immune signal and activate T cells and their role as APC remain theoretical.

Activated BECs can also recruit monocytes in the biliary tract upon IL-8 secretion, which is upregulated in the bile of cholestatic liver disease patients(131-135).

In conclusion, BECs play a multifaceted role in liver immunology, both under homeostatic conditions and after being activated. Their secretions, receptor expressions, and interactions with other immune cells underscore their importance in maintaining liver health and responding to injuries.

1.3. The breach of tolerance and the autoimmunity in the liver: the case of primary biliary cholangitis

Autoimmunity occurs when the immune system mistakenly targets its self-structures. The activation of such aberrant immune response triggers a vicious circle, in which the inflammation is fed by the continue release of the self-antigen. The current understanding of autoimmunity suggests that a combination of

genetic background predisposition and environmental factors contributes to the process onset. One proposed theory suggests that the immune system responds to self-antigens that share similarities with microbial peptides, a phenomenon known as molecular mimicry(135, 136). In fact, genetic polymorphism may cause a disruption in the immune regulation and affect the clonal immune selection or reduce the immune activation threshold. Furthermore, various pieces of evidence have indicated the involvement of xenobiotic substances in mimicking antigens(137) or causing changes in endogenous proteins to form neoantigens (138) triggering the immune response.

Both, molecular mimicry, and the neo-antigen generation by xenobiotics have been proposed as triggers for the tolerance loss in PBC. The immune response in PBC targets a mitochondrial antigen, the lipoic acid binding residue of the inner lipoyl-domain of pyruvate dehydrogenase complex (PDC-E2). This protein structure is highly conserved among species and the human protein sequence is similar to *Escherichia Coli (E.Coli)* PDCE-E2(139). This data is interesting in consideration that recurrent urinary tract infections, often caused by *E.coli*, are correlated with the risk of developing PBC(140). The modification of the mitochondrial antigen by certain chemical compounds found especially in cosmetic products such as nail polish, namely 2 octynoic acids(141), may contribute to the higher prevalence of PBC among females(142).

1.3.1. Definition and Epidemiology

PBC is a chronic, cholestatic autoimmune liver disease that affects predominantly women. The histological picture is characterized by a chronic granulomatous

lymphocytic cholangitis targeting small and medium bile ducts with a specific seroreactivity for antimitochondrial antibodies (AMA)(143).

Despite being defined a rare disease, magnifying its epidemiological picture on the individuals at risk, namely middle-aged women, PBC is not rare at all. It has been estimated that every year at least 100,000 individuals got diagnosed with PBC and that at least one in 1000 women over the age of 40 years might be living with PBC(144). The prevalence of PBC has steadily increased across the whole world, with the latest report estimating a range from 3.7 to 29.9/ 100000 in North America (1981-2020), 3.2-20.7/100000 in Europe (1971-2020) and 2.0-15.3 in Asia-Pacific (1991-2020) (145, 146). The incidence trends have increased over the world up to 2000 and they stabilised afterwards with yearly incidence of 2.75, 1.86 and 0.84/100000 in North America, Europe, and Asia-Pacific, respectively (145, 146). These disparities in prevalence rates across regions suggest potential genetic, environmental, or even diagnostic variations that might influence the disease's manifestation.

Several genetic studies have shown several hereditary factors predisposing individuals to develop PBC (147-152). The geographical variation in the epidemiological picture, raise the question the different environmental exposure in different part of the world might be accountable for such variation. This includes risks such as smoking prevalence as well as exposure to environmental toxins like those, from toxic waste, historical coal mining activities or high levels of environmental cadmium(140, 153, 154).

1.4. PBC: Clinical Manifestation and disease burden

PBC is a slowly progressive disease. It is usually identified in early stages and the main referral pathways is through abnormal routine blood tests showing abnormal cholestatic enzymes (i.e. ALP) (143).

The main prognostic factor for patient with PBC is the response to the first line treatment, the ursodeoxychoclic acid (UDCA)(155-160) and the main prognostic score developed so far, both dichotomic and continuous, are computed after one year of treatment(157-160). Unfortunately, up to now 20-40% of patients do not have a complete response to treatment and face the risk of disease progression toward cirrhosis and potentially liver transplant(161, 162).

The burden of the disease goes however far beyond the life expectancy. In fact, despite the good overall prognosis of the patients who respond to the treatment, the plethora of symptoms experienced by PBC patients, significantly decrease their quality of life(163). The most common are pruritus and fatigue(143). However, other common symptoms include sicca complex (dryness of mouth and eyes) and abdominal pain.

1.4.1. Treatment and Unmet Need

The treatments for PBC to date are two biliary acids: the first line is the UDCA and for whom have an incomplete response after 12-month of adequate treatment the Obethicolic acid as add-on treatment(164, 165). UDCA exerts its function changing the bile acids pool and protecting the BECs from the action of the hydrophobic bile acids(166). Furthermore, increase the bile flow increasing the bicarbonate-rich choleresis(167). OCA on the other is a semi-synthetic bile

acid analog and it is a potent agonist of the farnesoid X receptor (FXR). The activation of FXR and in gut and the liver, effectively decrease the amount of bile acids produced, reducing the toxic effect on the BECs(168, 169). FXR signalling activation, has got an effect also on the inflammatory pathways in the liver(170). Additionally, off-label therapy with the pan-PPAR agonist bezafibrate has gained recognition as an effective alternative(171).

Despite these advancements, a significant gap remains in the treatment landscape of PBC. There is no current treatment available targeting the underlying immune dysregulation seen in PBC. The recurrence of PBC post-liver transplantation is a clear indication of the disease's immune-mediated nature(172). However, the lack of understanding of the immunopathogenesis of the disease, obstacle the process of an immune-targeted treatment, highlighting the need for further research on the basic mechanism of PBC.

1.4.2. PBC pathogenesis

PBC is a prototypical autoimmune disease with a well-recognized and characterised autoantigen and the presence of specific antibody the AMA in the blood (summary of the current pathogenetic hypothesis of PBC is given in figure 1.3). In fact, one of the diagnostic pillars, as discussed earlier is the detection of serum AMAs, which are found in almost 95% of patients. Besides specific disease being markers, AMAs also play a crucial role in the immunopathology of PBC(173, 174). In the early 90’s ground-breaking studies on PBCs identified all the autoantigens recognized by AMAs, pinpointing the unique dominant epitope (no determinant spreading) within the lipoyl-binding site(175-177). When tested with

the specific recombinant peptides, AMAs are almost exclusively present in PBC patients, if they can be detected even years before clinical symptoms appear(178-180). To reinforce the central role of this epitope, xenobiotic proteins can mimic the dominant epitope of the PDC-E2 and they are reactive with AMAs(181-184). Such proteins are typically used to immunize murine models, inducing AMAs and PBC-specific signs of cholangitis(185, 186).

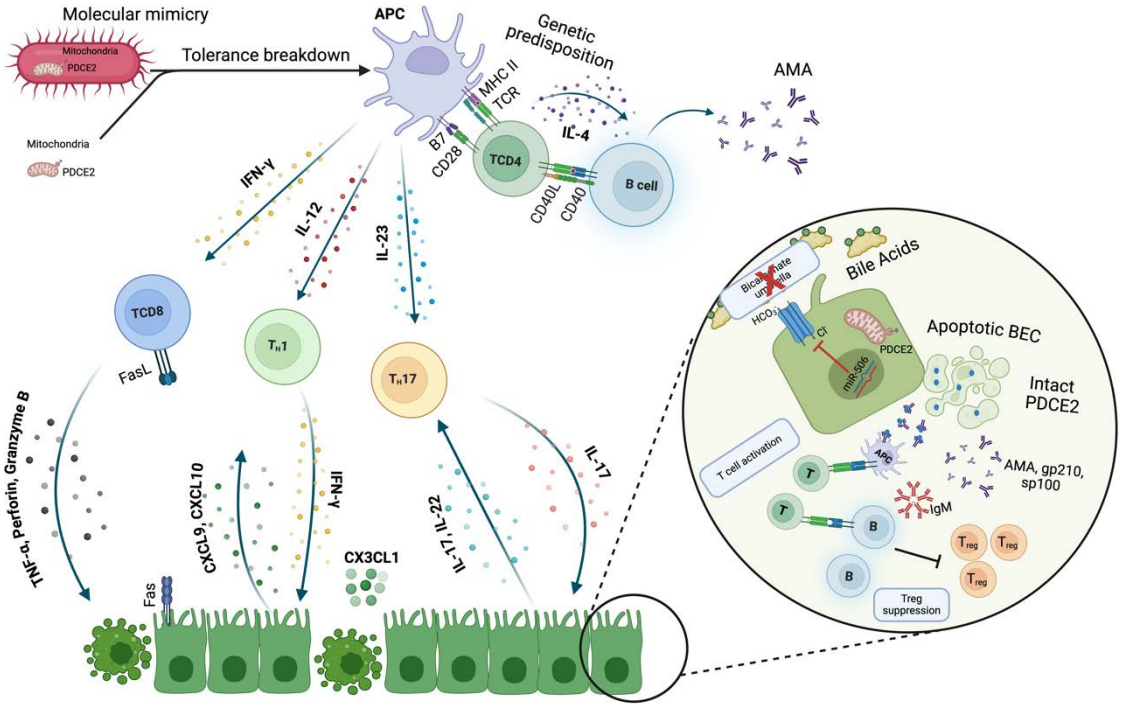

Figure 1.3 **Pathogenesis of primary biliary cholangitis**. PBC is thought to be the results of genetic and environmental interplay. Once the tolerance is broken the autoantigen PDC-E2 presented intact on the surface of the apoptotic blebs triggers the proliferation of the autoreactive B cells clone resulting in the production of AMAs. T cells response is a key player in the disease pathogenesis. The early-stage disease is characterized by a Th1-like response, whilst the late stage is characterized by a Th17-like response. The inflammation triggers a defective bicarbonate secretion, causing a reduced protection of the biliary epithelium surface. A similar effect is due to the post-transcriptional downregulation of the anion exchange protein 2 as effect of the overexpression of miR-506.

The role of the adaptive immune system in the pathogenesis of PBC is well recognized and summarised in figure 1.4.

Common histological finding in PBC is the infiltration of mononuclear cells around the small-medium sized bile ducts. These cells are infiltrating the injured bile ducts and are in proximity with BECs. Further characterisation of the immune populations through immunohistochemistry have revealed a dominance of CD4 and CD8 T cells along with B cells and killer (NK) cells.

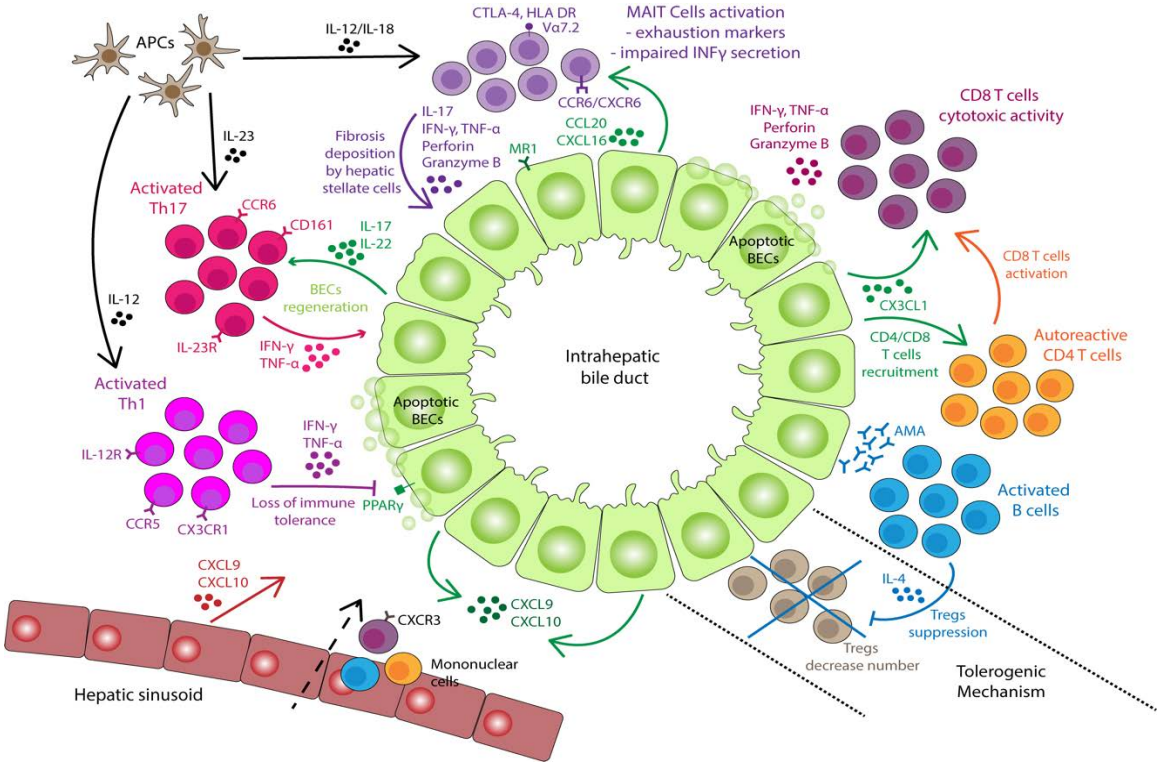

Figure 1.4 **Adaptive immunity in PBC** Th1 cells secrete IFN-γ and TNF-α, contributing to the loss of tolerance down-regulating peroxisome proliferator-activated receptor γ (PPARγ). Th17 secrete IL17 potentially inducing BECs regeneration. CCR6 and CXCR6 expressed on MAIT cells surface allow them to get in proximity of biliary epithelium (secreting CCL20 and CXCL16) and participate to the damage. The role of B cells includes AMA secretion but they have also a suppressive effect on regulatory T cells (Tregs) though IL-4 secretion. Adapted from(1)

The plethora of evidence pointing toward the antigen specific immune reaction is in fact the presence of PDC-E2-specific T CD4 and CD8 cells in PBC livers(187-190). A study conducted using blood mononuclear cells (PBMCs) from PBC patients by Kita and colleagues identified an HLA A2 restricted cytotoxic T lymphocyte epitope of PDC E2 that triggered a specific response after in vitro stimulation with dendritic cells loaded with antigens. They also emphasized that not only can autoantigen immune complexes be presented through cross presentation but that the efficiency of autoantigen presentation is relatively enhanced(187, 189).

Both IL 12 and IL 23 are cytokines, with functions and strong pro inflammatory properties playing crucial roles in various autoimmune disorders(191). Similarly, elements related to the IL-12/Th1 signalling pathway such as IL 12A, IL 12Rβ2 and STAT4 have been identified as genetic risk factors for PBC based on genome wide association studies (GWAS)(152, 192). Moreover, liver samples from PBC patients have shown a presence of Th17 lymphocytic infiltrates primarily around compromised interlobular bile ducts. This prevalence of Th17 becomes more pronounced in late stage of PBC with increased secretion of IL 23p19 from inflamed hepatocytes surrounding deteriorated BECs expressing IL 23R, IL 12Rβ2 and IFN γ(193, 194). It is believed that while Th1 plays a role in disease onset, Th17 is crucial, for sustaining the existing pathology during advanced stages of PBC(194).

The innate immune system on the other hand is multifaced and, plays certainly a role in initiating or sustaining the autoimmune response (Figure 1.5).

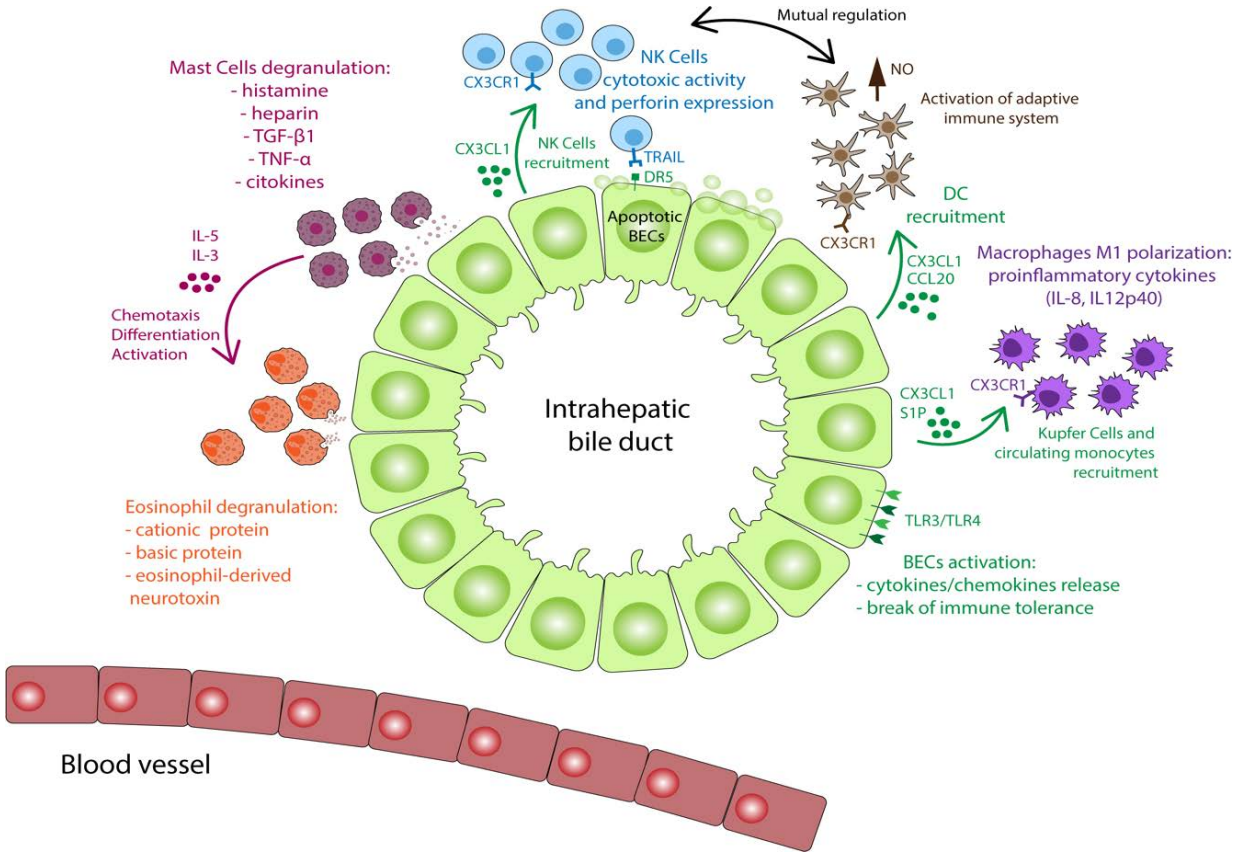

Figure 1.5 **Innate immunity in PBC.** BECs express more Tool-like-receptor (TLR) 4 in PBC patients, which binds bacterial LPS the receptor for bacterial LPS, and TLR 3 which binds instead, viral dsRNA. These two signals can activate BECs and induce the secretion of proinflammatory cytokines and contribute to breaking immune tolerance. CCL20 and CX3CL1 are chemoattractant causing the recruitment of several cell populations as natural killer cells, macrophages, dendritic cells and mast cells at the site of inflammation. The microenvironment is enriched with IL-5 and IL-3 produced by the mast cells, which acts as chemoattractant and activating factors for eosinophils. Adapted from(1)

There is evidence suggesting that monocytes derived by patients with PBC produce higher levels of proinflammatory cytokines in-vitro after being exposed to TLR ligands(195). Additionally, PBC patients show a rise in the frequency and quantity of NK cells in their blood and liver(196). These NK cells in the liver exhibit enhanced cytotoxic activity against their own BEC, resulting in further release of the autoantigens, maintaining the aberrant activation of the autoreactive T cells(197). IFN-γ bridges the gap between the role of the innate immunity and the acquired immunity(198, 199). All the APCs express a protein called CD40, which interacts with its ligand, CD40L, on the surface of activated CD4 T cells. CD40 is also expressed on the surface of B cells, and its activation, is central in the process of Ig class switching. The dysregulation of CD40-CD40L signal has been linked to an increase Fas/FasL- mediated BEC apoptosis(200, 201). Furthermore, the high IgM levels found as common features in PBC patients can be linked to epigenetic defect in CD40L resulting in disrupted Ig class switching(201).

MAIT cells, are a type of T cells are innate like T cells that have conserved and unchanging TCR α and β chains, specifically Vα 7.2. These cells are abundant in tissues throughout the body and particularly abundant in the liver accounting for up to 50% of T lymphocytes(202). A reduction in the circulating MAIT cells with parallel increase in their level within the liver has been reported in PBC patients. Furthermore, low numbers of MAIT cells in the peripheral blood has been correlated with biochemical signs of cholestasis (i.e. ALP) (203). In relatively recent study Botcher et al. demonstrated that the chronic stimulation of MAIT cells, by IL-12 leads to increased secretion of IL-17. This heightened secretion may potentially contribute to fibrosis deposition by stellate cells(57).

1.4.2.1. BECs and T cells crosstalk

BECs play a role in protecting the biliary tree from inflammatory challenges. Like the epithelium of the respiratory and gastrointestinal systems, the biliary epithelium is crucial in modulating immune responses to ensure tolerance. Beyond the molecular mimicry and environmental factors previously discussed, another unifying theory has put a secretory malfunctioning at the centre of the PBC pathogenesis. According to this pathogenic angle, cholestasis in PBC would be mainly due to compromised bicarbonate secretion and a malfunctioning "bicarbonate shield" on the BEC surface(105). The activation of AE2 on BEC's apical membrane facilitates bicarbonate secretion into the bile(204, 205).

Research has identified an upregulation of a microRNA, miR-506, in PBC BECs. This upregulation leads to hindered bicarbonate secretion due to diminished AE2 activity(206). The inflammatory environment of the liver seems to upregulate miR-506, causing bicarbonate secretion anomalies and intracellular pH shifts. Such changes might influence cellular metabolism, potentially leading to PDC-E2 overexpression(207). Another factor that might expose BECs to immune reactions is the heightened apoptosis observed in PBC patients. Apoptotic remnants could reveal an immunogenic form of PDC-E2. When macrophages from PBC patients are co-cultured with biliary apoptotic bodies and AMA, there's a notable release of inflammatory cytokines(208-210).

The immune response against the self-antigen PDC-E2 is likely central to PBC. Chronic BEC stimulation alters their phenotype, making them more active and

central to disease progression. These cells release mediators that influence BEC proliferation, myofibroblast differentiation, and immune cell attraction(211). The immune system can further stimulate BEC activation, and the interaction between immune cells and the biliary epithelium perpetuates a cycle driving the disease. Both innate and adaptive immune systems engage with BECs, leading to biliary damage. AMA interacts with the preserved PDC-E2 antigen in BEC apoptotic bodies, activating liver macrophages. This results in a cascade of inflammatory cytokines that sustain BEC apoptosis and inflammation(210). Gut-derived bacterial products, like LPS, also play a role in PBC pathogenesis(212-214). PBC patient BECs show increased TLR4 surface expression, and upon activation, produce elevated levels of IL-1, TNF-α, and IL-8 compared to controls(215). BECs also express the IFN-γ receptor, and its activation upregulates TLR expression and susceptibility to pathogen-associated molecular patterns (PAMPs)(216). The peroxisome proliferator-activated receptor γ (PPARγ) is consistently expressed in BECs and helps maintain biliary immune balance by dampening PAMP-induced inflammation(217, 218). Th1 cytokines can downregulate PPARγ, potentially promoting tolerance loss against the biliary epithelium. Moreover, BECs can attract immune cells through CX3CL1/fractalkine, a potent chemoattractant for cells expressing the specific receptor CX3CR1. Elevated CX3CL1 expression in PBC BECs results in significant infiltration of CX3CR1-positive CD8, CD4 T, and NK cells in these patients' portal tracts(199, 219-221). The interaction between the biliary epithelium and the immune system, especially the IL-17 axis, becomes particularly relevant in the disease's later stages. Elevated Th17 cell numbers

and cytokine secretion are observed in advanced PBC stages(193, 222). BECs express the IL-17 receptor(223) and, upon activation, promote Th17 differentiation of CD4 T cells. BECs release CCL20, attracting CCR6+ CD4 cells. The activation of these cells, along with IL-1β, IL-6, and TGF-β, is essential for CD4 T cell differentiation into Th17. The exposure to LPS augments CCL20 secretion(224). A further hit to the bile epithelium is caused by the bile acid stasis in damaged bile ducts and the therapeutic benefits of UDCA and obethicolic acid highlight bile acids' significance in PBC pathogenesis(165). The expression of AE2 is diminished in PBC, and AE2-deficient mice develop PBC-associated biliary damage(225). Proinflammatory cytokines contribute to this reduced AE2 expression in BECs(207). In a T cell-induced cholangitis mouse model, bile salt export pump expression increased, while bile acid synthesis and uptake decreased. This change is mediated by proinflammatory cytokines TNF and IFN-γ in an FXR-dependent manner(226). Conversely, bile acids can modulate both T cells and MAIT cells, emphasizing their dual role in the immune system(203, 227).

1.4.2.2. Regulatory T cells

PBC murine models strongly support the hypothesis that Tregs deficiency is a central defect in the PBC pathogenesis. The dominant-negative Transforming Growth Factor beta (dnTGF-βRII) selectively affect the TGFβ R-signaling pathway

in T cells. This affects directly the Treg suppressive capacity which heavily relies on TGF-β for their functioning. This results in the accumulation of tissue-specific autoreactive T cells, mimicking the PBC histology damage (228). Similarly, IL-

2Rα knockout model, which affects the IL-2 signalling and in turn the Treg production, develops severe autoimmune cholangitis and AMA in 100% of individuals(229). To support further the role of Treg in the loss of tolerance in PBC Zhang and colleagues reported the AMA development and autoimmune cholangitis in Scurfy mice, which have a complete Treg deletion due to a FoxP3 transcription factor mutation(230). Furthermore, Liaskou et al. demonstrated an impaired lineage stability in Treg cells from PBC patients. When exposed to relatively low levels of IL-12 leads, these cells started to increase significantly the IFN-γ expression(231). The use of Tregs as cell-therapy was also attempt in murine models. After inducing autoimmune cholangitis in recombination-activating gene (Rag)1–/– by transferring cytotoxic CD8 T cells from dnTGF-βRII, Tanaka and colleagues, successfully reduced portal inflammation transferring Tregs from C57BL/6 mice but not from dnTGF-βRII(232). This study not only suggest the potential of autologous Treg cell-therapy in the treatment of PBC but confirm the reduced functioning of Treg from PBC murine models.

1.4.2.3. Cytotoxic T CD8 cells

Murine models suggested the critical role of differentiated T CD8+ cells to inflict the ultimate bile damage. The transfer of cytotoxic T CD8+ cells from non-obese diabetic c3c4 but not T CD4+ cells can induce the autoimmune cholangitis directly mediating the bile duct injury(233, 234). Yang et al in 2008 in conducted similar experiment and demonstrated that transferring T CD4+ cells from dnTGF-βRII to Rag1 knockout mice could induce only IBD-like inflammation. Instead, transferring CD8+ T cells from triggered autoimmune cholangitis with histological features similar to PBC, with intense infiltrate of terminally differentiated T CD8+

cells(235). In humans it has been shown that chronic antigenic stimulation leads to the accumulation of terminally differentiated CD45RO^{high}CD57+CD8^{high} cytotoxic T cells around the portal area of patients with PBC (236). They can infact secrete fractalkine (CX3CL1), which attracts more T cells feeding a vicious pathogenetic loop(237).

This striking evidence shift the interest as damage mediator upon CD8+ T cells. Confirmatory data came from Yikang et al. who confirmed an enrichment of terminally differentiated T CD8+ killer cell lectin-like receptor G1+ (KRLG1+) Granzyme B+ Perforin+ cells in the portal tract of PBC patients compared with autoimmune hepatitis and viral hepatitis. Furthermore, they have shown how such accumulation correlated with a more aggressive PBC phenotype according with ALP and risk of liver transplantation (234).

The same group identified T_{RM} CD8+CD103+ as the dominant autoreactive cytotoxic population within the human PBC livers (238). In fact, this cell population was shown to be directly cytotoxic against BECs and, intriguingly, to correlate with UDCA response, which represent the most powerful prognostic factor in PBC patients.

1.4.2.4. Double hit disease hypothesis

The current data offers a pathogenic angle for the immunopathogenesis of PBC. In fact, the large amount of evidence provided by the Gershwin and Xiong groups over the last 20 years, opens to the idea that PBC could be defined a double hit disease.

The defect on both regulatory compartment and the aberrant activation toward the self-antigen is required to precipitate the bile damage. Such hypothesis has

also been tested and confirmed, by Huang et al. in 2014. They took advantage of mixed dnTGFβRII and B6 bone marrow chimeric mice to demonstrate that the T CD8 cells in dnTGF-βRII are not sufficient to generate the biliary injury. It is interesting to note that the number of Tregs in dnTGFβRII and B6 but they were defective in the PBC model. that in a of model of creating a chimeric the transferring of is insufficient to induce the cholangitis in presence of functioning Tregs(239).

The figure 1.6 summarises this pathogenic hypothesis and opens to two different potential therapeutic scenarios: target the cytotoxic T cells or increase the number of functional and stable Tregs within the liver parenchyma.

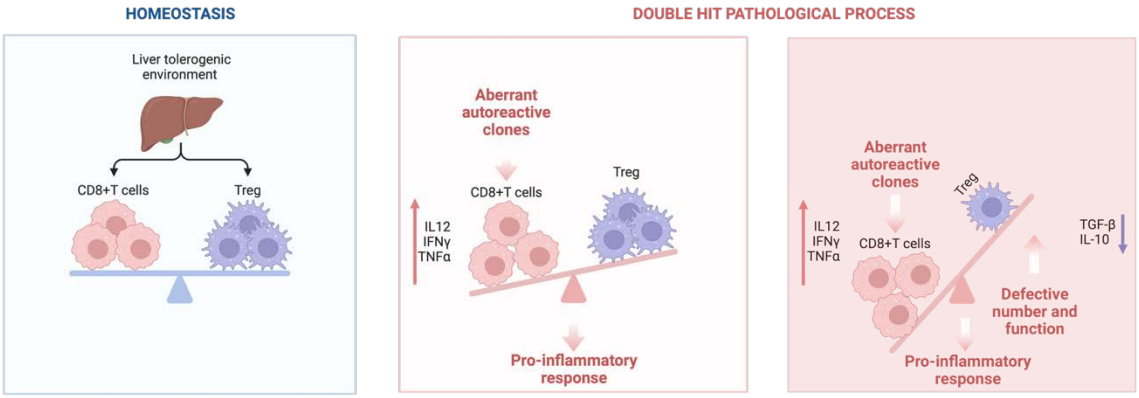

Figure 1.6 **PBC as double hit disease.** The perturbation of the immune homeostasis in the liver due to a reduction in number and function of Treg. Allows the proliferation of autoreactive T CD8+ cells clones. They aberrantly proliferate due to the continuous release of the PDC-E2 from the damaged BECs.

1.5. Cell-in-cell structure

The intricate and dynamics cell-cell interaction includes several mechanisms in which cells not only communicate with each other, but they also engage in process of invasion, engulfment, and sometimes, mutual destruction. On this background we find the captivating phenomena of the formation of cell-in-cell (CIC) structures. These phenomena have recently come under the spotlight due to their potential implications in various physiological and pathological contexts.

1.5.1. Definition and Historical Background

The first observation of cell-in-cell structure can be traced back to the early 20th century when, when researchers noticed evidence of cell residing within another. This evidence was initially considered an artifact of tissue preparation, however, as microscopy techniques advanced and our understanding of cellular biology improved, it became clear that this phenomenon was indeed a genuine biological process with potential implications in human disease processes(240, 241).

After the first evidence, the cell-in-cell process has been observed across several tissue types and in various disease states, especially in the context of cancer. The process involves the internalization of one cell (the internalized cell) by another (the host cell). The mechanism of the internalisation is heterogenous and some of them are yet to be elucidated. As much as the mechanism, the fate of both the host and the internalised cell is heterogenous and can range from the release of the internalized cell to its destruction within the host cell.

The interest in this research area was boosted around 1970 with several studies attempting to dissect the molecular and cellular mechanisms behind this cellular structure(242, 243). In this time period the term "emperipolesis" was coined, to define a specific type of cell-in-cell structure where a living cell was internalized by another, often leading to its death. This was distinct from phagocytosis, where cells engulf particles or dead cells(244, 245).

The cell-in-cell process, in its various forms, has been linked to numerous physiological processes, including tissue homeostasis, immune response modulation, and nutrient acquisition. In pathological contexts, its roles in tumour progression, metastasis, and immune evasion have been of particular interest (246-250).

1.5.2. Classification

The complexity of this biological phenomenon can be hardly captured by simple classification. There were attempt in such sense, trying to define the CIC structures based on the cells involved (hetero or homotypic) or based on the process they were involved (neoplastic or not). I found quite effective what proposed by Borensztejn et al(241) (figure 1.7). They suggest classifying the event based on the cells initiating the cascade: endocytic CIC if it has started from the outer cell or invasive CIC if it is an invasion.

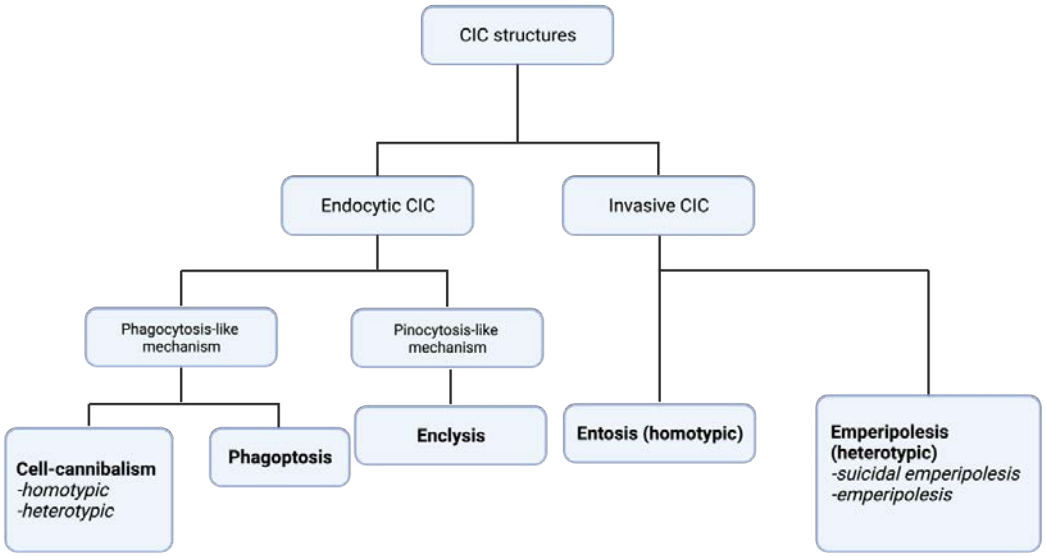

Figure 1.7 **Cell-in-cell structure classification**. Adapted from (240)

Endocytic CICs can be further classified based on their molecular mechanisms. Those resembling phagocytosis include cell cannibalism and phagoptosis, while enclysis, mirrors pinocytosis.

Phagoptosis, a variant of phagocytosis, involves a living cell's engulfment by a phagocyte. While phagoptosis typically leads to the engulfed cell's death(241, 251), cell cannibalism mirrors phagocytosis(252, 253). The distinguishing factor between the two phenomena lies in the engulfing cell's phenotype. While most cell types can exhibit cell cannibalism by adopting a cannibalistic phenotype(254), macrophages in phagoptosis retain their phagocytic phenotype, enabling them to phagocytose pathogens, dead, or living cells. Phagoptosis can be involved in physiological or pathological process, while cell cannibalism is always involved in pathological processes. Both structures typically culminate in the lysosomal death of the internalized cells(255, 256).

Enclysis refers to a structure involving hepatocytes as host cells which extends lamellipodia to engulf T lymphocytes (257, 258). Unlike phagocytosis-like CICs, the inner cell's type determines its fate. Tregs typically undergo lysosomal digestion, while other immune cells often manage to evade degradation(258).

Invasive CICs, on the other hand, are further classified into heterotypic (various emperipolesis forms) and homotypic (entosis). These CICs always are typically initiate by the inner cell, which actively penetrates the host cell's cytoplasm. Both

entosis and emperipolesis share the key proteins involved in the molecular mechanisms, like ezrin and E-cadherin(250, 259, 260), but they are differentiated by the cells involved and their roles. Emperipolesis, involving heterotypic CICs with the inner cell typically being a leukocyte, can be observed in both non-tumorigenic and cancer cell lines(261). This process can result in the death of either cell through various mechanisms(250, 262) or the inner cell's escape, leaving both cells intact(260). Emperipolesis has several variations, including suicidal emperipolesis, emperitosis, thymic cell emperipolesis, macrophage-neutrophil emperipolesis, and megakaryocyte-neutrophil emperipolesis(250, 260, 262-264).

Entosis, a homotypic CIC process, consistently involves multiple epithelial cells, often cancerous. This process can lead to the inner cell's survival or its lysosomal death(246, 265).

1.5.3. Emperipolesis

Emperipolesis, first identified in 1956, is a cellular event where one cell actively penetrates another, with both cells typically remaining intact (243). This process is predominantly heterotypic, with leukocytes often acting as the internalizing cells. Examples include neutrophils entering megakaryocytes(264), thymocytes within thymic nurse cells(263), and NK cells infiltrating cancer cells(250).

The outcomes of emperipolesis can vary. Sometimes, both cells survive, with the internalized cell eventually exiting the host. In other scenarios, the internalized cell might undergo processes like mitosis(266) or various death pathways(250,

262). The host cell can either remain unaffected or be killed, potentially through mechanisms like granzyme B activity(267).

In the context of the liver, emperipolesis involving CD8+ T lymphocytes has been observed. For instance, in certain conditions, these T cells can be engulfed and subsequently degraded by lysosomal enzymes(262), a phenomenon termed "suicidal emperipolesis". In autoimmune hepatitis (AIH), CD8+ T lymphocytes can penetrate hepatocyte lines, leading to their own apoptosis. This internalization involves proteins like ezrin, F-actin, and CD44(261). The relationship between emperipolesis and inflammation in AIH remains unclear(268).

NK cells, when interacting with cancer cells, can either exhibit cytotoxicity (267) or undergo apoptosis post-invasion(250). The molecular mechanisms involve proteins like ezrin, ICAM-2, and E-cadherin. Once inside the cancer cell, the NK cell might release granzyme B, inducing apoptosis. However, the host cell can encapsulate the NK cell, preventing granzyme B release, leading to a process termed "emperitosis"(269).

Another instance of emperipolesis involves a megakaryocyte and a neutrophil. Here, the neutrophil donates its cell membrane to emerging platelets, potentially accelerating platelet production(260).

Emperipolesis is also a hallmark of Rosai–Dorfman disease (RDD)(270), a benign disorder. The presence of emperipolesis can help differentiate RDD from

other similar conditions (270). Additionally, emperipolesis might play a role in viral transmission, as seen with the Epstein–Barr Virus (EBV)(271).

Despite advancements, emperipolesis remains a complex phenomenon, with many aspects still under investigation.

1.5.4. Entosis

Entosis is a cellular process where one epithelial cell actively invades another, marking it as a homotypic event(246, 265). Initiated by the inner cell's detachment from the matrix, it can also occur when both cells are matrix-attached or substrate-detached, such as during mitosis(272). This results in a unique cell-in-cell (CIC) structure, where the outer cell envelopes the inner cell, which remains membrane-intact within a large vacuole. The inner cell can either be digested by the host through autophagy or escape (246, 265). Both cells might undergo mitosis post-CIC formation, but the outer cell's division can be disrupted, potentially leading to aneuploidy(273).

Several molecular players and pathways facilitate entosis. Cell adhesion requires calcium ions, E-cadherin, and β-actinin. The Rho/ROCK pathway then gets activated, aiding the inner cell's engulfment (265). During this, a molecular ring forms around the inner cell, comprising proteins like vinculin, E-cadherin, catenin, and F-actin(274). Microtubules are essential for this process, and ezrin-dependent membrane blebbing in the inner cell precedes entotic invasion (259). The inner cell's digestion involves autophagy proteins like LC3(275), and a rapid pH drop in the entotic vacuole(276). Factors like glucose starvation can induce

entosis(272), and the inner cell's fate might be influenced by its autophagic activity under starvation (275). Entosis can also be triggered by ultraviolet radiation(277) and certain drugs (264).

Entosis has dual implications in cancer. It can act as a tumor suppressor, eliminating aneuploid cells from prolonged mitosis(278). However, it can also promote cancer progression by inducing aneuploidy and DNA damage. Interestingly, TP53-mutated inner entotic cells show higher survival compared to TP53-null and TP53 wild-type cells(279). Entosis also aids cancer cell survival under stress, like glucose starvation (267).

Clinically, entotic figures are observed in various cancers, including nasopharyngeal, pancreatic, breast, and lung adenocarcinoma(279-282). Their presence often correlates with increased malignancy (279) and poorer prognosis (265). Additionally, entosis is linked with specific mutations like TP53 inactivation or KRAS amplification(279, 283, 284). The relationship between cell cannibalism and entosis is evident in malignant melanoma cells, which can engulf both apoptotic and viable cells(256, 285). This engulfment is facilitated by proteins like ezrin and actin(265), and the death of entotic cells is regulated by LC3, linking entosis to autophagy(286). The occurrence of CICs in tumors can vary, even within metastases.

1.5.5. Cell-cannibalism

Cell cannibalism refers to the act where one cell engulfs another, a phenomenon observed in neoplastic tumors (287). While it can involve identical cells

(homotypic)(288), there are instances of heterotypic cannibalism, like melanoma cells engulfing lymphocytes(256). This process is seen as a nutrient source for metastatic tumors (252, 255).

The engulfment is initiated by the outer cell, without preference for viable or necrotic cells (289). This action, taking over 30 minutes, leads to the formation of an active lysosome that releases enzymes near the engulfed cell, leading to its digestion. The inner cell is surrounded by a membrane from the outer cell (290). Key proteins in this process include ezrin, caveolin-1(256, 291), and TM9SF4(292), the latter being highly expressed in cannibalistic cells. TM9SF4's exact function remains unclear, but it's believed to play a role in pH regulation of intracellular vesicles(256).

Cell cannibalism might be an evolutionary echo from our unicellular origins (256), with cancer cells exhibiting traits reminiscent of unicellular organisms like amoebas. This process was once termed "cellular phagocytosis" (287).

Cannibalism serves as a nutrient source, especially during starvation, and can also provide an advantage by eliminating immune cells. For example, melanoma cells can engulf CD8+ T lymphocytes (256), a process triggered by harsh conditions like starvation or acidic environments. This action has been linked to enhanced survival in metastatic melanoma cells.

Cell cannibalism also plays a role in cellular senescence and cancer dormancy, aiding cancer cell survival under adverse conditions. For instance, breast cancer cells (MDA-MB-231) have been observed to enter dormancy post cannibalizing mesenchymal stem cells (MSC)(293). Moreover, cell cannibalism has shown potential cancer-suppressive effects, as seen in pancreatic adenocarcinoma where its presence curbed metastases(294).

Despite its century-long recognition, the intricacies of cell cannibalism remain largely uncharted, with its molecular triggers and regulation still under exploration.

1.5.6. Phagocytosis and Phagoptosis

Since Ilya Mechnikov's observations of white blood cells engulfing bacteria, phagocytosis has been recognized as a defense mechanism against pathogens(255). However, some microorganisms, like Mycobacterium tuberculosis, can evade this process. For a long time, phagocytosis was seen merely as a cleanup mechanism for dead cells. The term "phagoptosis" was introduced to describe cell death via phagocytosis, closely resembling efferocytosis, which clears dead cell debris. Both processes are influenced by "eat me" and "do not eat me" signals on the cell surface.

Phosphatidylserine (PS) is a well-known "eat me" signal. Typically found on the inner cell membrane, certain conditions can expose PS on the outer layer(295). While PS exposure often indicates apoptosis, it can also be seen in living cells. Some external molecules can induce PS exposure without causing apoptosis (295-299), and this exposure can be reversible (296, 298, 300, 301).

CD47 acts as a "do not eat me" signal. It's a membrane protein that interacts with the macrophage's SIRPα receptor. A lack of CD47 promotes phagoptosis, while its activation inhibits the process(302). CD47 expression decreases in aging red blood cells (303), helping Kupffer cells in the liver identify and remove them (304). In cancer, CD47 overexpression helps cells evade the immune system(305). Other protective signals include PD-L1 (306) and β2-microglobulin (307).

Antibodies can stimulate phagocytosis through their Fc domain (Figure 1.3). Macrophages have Fc receptors that can either promote or inhibit phagocytosis (284). Phagoptosis can be enhanced by certain antibodies, like Hu5F9-G4 (anti-CD47) (307) and cetuximab (anti-EGFR) (284). In lab settings, phagocytosis rates can be significantly increased using specific stimulants (308). Another pathway involves Toll-like receptors, with TLR7 stimulating phagoptosis through calreticulin phosphorylation (309).

Microglia, the brain's macrophages, can engulf live neural components, affecting neural architecture(310). Factors like LPS, LTA, and β-amyloid can induce PS exposure in neurons(300). Inhibiting phagocytosis can prevent neuron loss, suggesting potential treatments for conditions like ischemic stroke(297, 298). Low β-amyloid concentrations can cause neuron death via phagoptosis, but inhibitors can prevent this (298). Blocking certain stimulants can also protect neurons (311, 312), hinting at potential treatments for neurodegenerative diseases like Alzheimer's.

1.5.7. Enclysis

In 2019 Davies et al described a novel form of cell-to-cell interaction called "enclysis" (313). Enclysis occurs when a hepatocyte actively engulfs a CD4+ T cell. Interestingly while CD8+ T cells and B cells pass through the spaces between hepatocytes it is mainly the CD4+ T cells that are targeted for engulfment. Notably among the CD4+ subset FoxP3+ regulatory T cells are commonly subjected to enclysis. These regulatory T cells are directed towards degradation unlike other T cells that remain undegraded for longer periods(258, 313).

The specific molecular mechanisms governing enclysis are still not fully understood. The precise reasons why hepatocytes selectively target CD4+ T lymphocytes and the decision-making process behind determining their fate remain elusive. Certain proteins such as ICAM 1 and β catenin have been identified in relation to enclysis. Distinguish it from other types of cell-to-cell interactions (Figure 1.4). During enclysis structures like blebs and lamellipodia form and the process is hindered by blebbistatin—a known inhibitor of myosin II. However, pinocytosis non-specific nature does not align with the nature of enclysis towards CD4+ cells, in this context(313).

It is crucial to conduct research in order to better understand the complexities of both enclysis and macropinocytosis.

1.5.8. Cell-in-cell structures in the liver

The liver, a vital organ responsible for detoxification and metabolism, is a complex environment teeming with various cell types. Among the myriads of interactions

that occur within the liver, the CIC structures stand out as particularly intriguing. These structures have been observed in various tissues, their role within the liver becomes interesting as potentially involved in the organ's unique immunological and regenerative properties.

For instance, efferocytosis plays a pivotal role in the tuning the liver immune response. The presence of dying cells within the parenchyma from either from its routine detoxification processes or from infiltrating immune cells is constant and the ability to efficiently clear these “corpse” is crucial to prevent unwanted inflammatory responses and potential autoimmune reactions(314).
According with the classification presented earlier, this is an endocytic CIC the in fact, the hepatocytes, are not just bystanders in this process. They actively engulfing dying cells, a phenomenon first observed in the 1950s. Aside having likely a role in the immunosurveillance, the process might also provide hepatocytes with nutrients from the digested cells and potentially increase their genetic diversity(258). It is intriguing how, efferocytosis could be seen as a matter to increase the liver's adaptability, it could also increase the mutation rate and eventually play a role in the carcinogenesis in hepatocellular carcinoma (HCC)(254, 314).

Unlike efferocytosis, which targets dead cells, entosis involves the internalization of live cells. It is equally ambiguous within the cancer scenarios as it is instrumental to clear cells showing early cancerous signs, however, it serves as

mechanisms to sustain cells under metabolic distress, hence it can be used by cancer cells to find nutrients, giving them selective advantage.

The liver's unique environment, with its constant exposure to toxins and its role in metabolism, might influence the occurrence and outcomes of entosis.

Furthermore, the engulfment and subsequent degradation of immune cells via entosis could serve as a source of antigens for liver-resident antigen-presenting cells. This could facilitate the presentation of these antigens to other immune cells, promoting immune regulation and tolerance. Such a mechanism would be especially vital in preventing autoimmune reactions in the liver.

Emperipolesis, has been historically observed in the biopsy of patients with viral hepatitis and autoimmune hepatitis, being for long-time a diagnostic feature for the AIH patients(262). Bertolino et al. define for the first time the mechanistical role of one of this CIC, calling it suicidal emperipolesis, involving an autoreactive CD8+ T cells and the hepatocytes(315).

In the attempt to apply the classification to this CIC structure, we should classify emperipolesis as invasive CIC, as it is an invasion of the immune cell within the hepatocytes. However, the fate of the internalised lymphocyte is lysosomal degradation.

The youngest of the CIC structure described is the enclysis which was indeed observed in the liver. It is quite plausible that the enclysis might be one of the mechanisms to disrupt the immunotolerance, however the implications of enclysis for liver function and immunity are yet to be clarified.

The CICs within the liver described so far, have as either target or host cells the hepatocyte.

As mentioned before, Zhao et al. described the emperipolesis of T CD8 cells in the BECs. Intriguingly, this phenomenon correlated with the grade of biliary damage, and it seemed to end up with the apoptosis of the biliary cells(316).

This CIC structure is so far poorly defined and both the exact mechanism and its role in the pathogenesis of the PBC remains unknown.

2. Material and Methods

N.B. *the content presented in this chapter are part of a paper recently published(317).*

2.1. Ethical approval

All human sections were cut from liver tissue, obtained from surgical procedures carried out at the Queen Elizabeth Hospital, Birmingham, UK, with written consent from patients. Ethical approval for the study was granted by the Local Research Ethics Committee (LREC) (reference number 06/Q702/61). Diseased liver tissue was obtained from explanted livers from patients undergoing transplantation for chronic liver disease or liver malignancies. Non-cirrhotic liver tissue was taken from donor livers which were rejected for transplantation or surplus to clinical requirements. Blood from patients with PBC, healthy volunteers or haemochromatosis (HFE) was collected under the same LREC when given full consent.

2.2. Human samples

I have consented and collect peripheral blood from PBC patients with established inflammation ethic approval in Liver Clinics at Queen Elizabeth Hospital, Birmingham. All the PBC cases have been diagnosed according with EASL criteria (“EASL Clinical Practice Guidelines: The Diagnosis and Management of

Patients with Primary Biliary Cholangitis," 2017). I have used as healthy controls patients undergone venesection due to hemochromatosis. All the patients with abnormal liver function tests, or with other liver or autoimmune conditions have been carefully excluded. For the experiment performed in Japan, peripheral blood mononuclear cells were isolated by centrifugation over a ficoll gradient in the Liver Lab at the University of Birmingham. PBMCs were then frozen and transferred to Sgakuchi's Lab at Osaka University, using a material transfer agreement set up with this specific purpose, under a signed agreement between the two Universities. All patients provided a written informed consent before sampling according to the Declaration of Helsinki.

2.3. Antibodies

The following antibodies were used for flow cytometry analysis:

APC-E-cadherin, BV786-CD103 and BV605-CD8 were also used to sort live E-cadherin+/- CD8+ T cells, using APC-mIGgG1 as an isotype-matched control to assist gating.

The following primary antibodies were used for immunocytochemistry: α-hCD3 mouse IgG1, α-hCD4 mouse, α-hCD8 mouse IgG2b, α-hCD69, α-hCD103 Rabbit IgG, α-hKLRG-1 rabbit IgG, α-hE-cadherin mouse IgG2a, α-hβ-catenin mouse IgG1, α-hCytokeratin-19 rabbit IgG, α-hCytokeratin-19 mouse IgG1

The following primary antibodies were used for immunocytochemistry: α-hCD8 mouse IgG2b, α-hE-cadherin mouse IgG2a, α-hβ-catenin mouse IgG1, α-hCytokeratin-19 rabbit IgG.

The full list of antibodies used for flow cytometry experiment, immunohistochemistry and immunocytochemistry is summarised in table 1 and table 2.

Target protein	Fluorochrome	Clone	Supplier	Cat No	Working dilution
Surface					
CD3	BV510	OKT3	BioLegend	317332	1:100
CD4	BUV395	RPA-T4	BD	564724	1:400
CD8	BV605	SK1	BioLegend	344742	1:400
CD45RA	BV711	HI100	Biolegend	304130	1:400
CD45RA	BV786	HI100	BioLegend	563870	1:400
CCR7	PE-594	150503	BD	562381	1:50
CD25	BV421	BC96	BioLegend	302630	1:200
CD127	BV711	A019D5	BioLegend	351328	1:100
CD107a	PE-Cy7	H4A3	BioLegend	328617	1:400
CD161	APC	HP-3G10	BioLegend	339912	1:100
CCR6	PE	11A9	BD	559562	1:50
CXCR3	AF700	G025H7	BioLegend	353742	1:33
KLRG1	FITC	SA231A2	BioLegend	367714	1:100
CD103	BV786	Ber-ACT8	BioLegend	350230	1:50
CXCR6	BV421	SA051D1	BioLegend	151109	1:100
CD69	PE	FN50	BioLegend	310906	1:100
CD27	BUV395	L128	BD	563815	1:100
CD57	PerCP	HNK-1	BioLegend	359622	1:400
CD28	BV650	CD28.2	BioLegend	302946	1:100
CD38	PE-Cy7	HIT-2	BioLegend	25038942	1:400
E-cadherin	APC	67A4	Biolegend	324107	1:25
Beta-catenin	PE	815B8	BioLegend	862604	1:100
LFA1	AF700	m24	BioLegend	363422	1:200
VLA1	APC	TS2/7	BioLegend	328314	1:100
Intracellular					
Perforin	PerCPCy5.5	DG9	Biolegend	308114	1:50
Granzyme B	PE	GB11	BD	561142	1:100
Granzyme B	PerCPCy5.5	QA16A02	Biolegend	372212	1:100

IL-17	FITC	64DEC17	eBio	11717942	1:50
IFN-γ	APC	B27	Biolegend	506510	1:100
Ki-67	BV510	Ki-67	Biolegend	350517	1:100
TNF-α	BV650	MAB11	Biolegend	502938	1:50

Table 1 List of the antibodies used for the flow cytometry experiments.

Target	**Host**	**Reactivity**	**Conjugate**	**Clonality**	**Clone number**	**Brand**	**Dilution**
Cytokeratin-19	Rabbit	Human	Unconjugated	IgG Monoclonal R	EP1580Y	Abcam	1/2000
Cytokeratin-19	Rabbit	Human	Unconjugated	IgG Monoclonal R	EP1580Y	Abcam	1/1000
Cytokeratin-19	Rabbit	Human	Unconjugated	IgG Monoclonal R	EP1580Y	Abcam	1/500
Cytokeratin-19	Mouse	Human	Unconjugated	IgG1	4E8	Invitrogen	1/1000
Cytokeratin-19	Mouse	Human	Unconjugated	IgG1	4E8	Invitrogen	1/500
Cytokeratin-19	Mouse	Human	Unconjugated	IgG1	4E8	Invitrogen	1/500
KLRG1	Rabbit	Human	Unconjugated	IgG Monoclonal R	2388C	R&D	1/200
KLRG1	Rabbit	Human	Unconjugated	IgG Monoclonal R	2388C	R&D	1/100
CD103	Rabbit	Human	Unconjugated	IgG Monoclonal R	EPR22590-27	Abcam	1/1000
CD103	Rabbit	Human	Unconjugated	IgG Monoclonal R	EPR22590-27	Abcam	1/500
CD8	Mouse	Human	Unconjugated	IgG2b	4B11	Invitrogen	1/100
CD8	Mouse	Human	Unconjugated	IgG2b	4B11	Invitrogen	1/50-100
E-cadherin	Mouse	Human	Unconjugated	IgG2a	34/E-Cadherin	BD Bioscience	1/100
E-cadherin	Mouse	Human	Unconjugated	IgG2a	34/E-Cadherin	BD Bioscience	1/100
PDCE-2	Mouse	Human	Unconjugated	IgG1	15D3G9C11	Abcam	1/200
PDCE-2	Mouse	Human	Unconjugated	IgG1	15D3G9C11	Abcam	1/100
PDCE-2	Mouse	Human	Unconjugated	IgG1	15D3G9C11	Abcam	1/100
CD4	Mouse	Human	Unconjugated	IgG2a	OTI5D9	Novus Bio	1/100
CD4	Mouse	Human	Unconjugated	IgG2a	OTI5D9	Novus Bio	1/50

Table 2 List of the antibodies used for tissue staining

2.4. Biliary epithelial cell isolation and culture

Human biliary epithelial cells (BECs) were isolated from a minimum of 200 g of explanted human liver tissue from patients with non-cholestatic disease (to avoid PBC-bias for *in vitro* experiments; a mixture of non-alcoholic steatohepatitis [NASH], cryptogenic, and alcoholic liver disease [ALD]) or non-cirrhotic tissue from donor livers rejected for transplantation. Tissue was digested enzymatically with collagenase type 1A (Sigma) and filtered through fine mesh. Density gradient centrifugation using 33%/77% Percoll (Amersham Biosciences UK Ltd) was used to separate non-parenchymal cells from BECs were extracted from the mixed nonparenchymal population via magnetic selection using antibodies against the cholangiocyte-specific receptor HEA-125 (50 µg/mL; Progen Biotechnik). HEA-125–positive BECs were plated in flasks coat with 2.5% rat-tail collagen- and kept in culture maintained in media comprising 45% Dulbeccos modified eagles medium (DMEM; Invitrogen), 45% HAMS F-12 nutrient mix, 10% heat-inactivated Fetal bovine serum (FBS,; Sigma), 10 ng/ml epidermal growth factor (EGF; Peprotech 100-15), 10 ng/ml hepatocyte growth factor (HGF; Peprotech, AF-100-39), 2 µg/ml hydrocortisone, 10 ng/ml cholera toxin (Sigma C8052), tri-iodo-thyronine (Sigma, T5516), 1% PenStep (Invitrogen), 1% L-glutamine (Invitrogen) and 0.125 IU Insulin. BECs were not used for co-culture experiments beyond their fourth passage.

2.5. T cell isolation and culture

PBMCs were isolated from blood samples by layering on Lympholyte-H separation media (Cedarlane) and centrifugation according to manufacturers while using the minimal break setting. CD8+ T cells and CD4+ T cells were then extracted using a human CD8+ T Cell Isolation Kit (Miltenyi, 130-094-156) or human CD8+ T Cell Isolation Kit (Miltenyi,130-096-533), respectively. Cells were then washed with PBS three times and and seeded in pre-warmed complete RPMI supplemented 10% heat-inactivated FBS (Sigma), 1% PenStrep, 1% L-glutamine and 500 IU IL-2 (Peprotech, 200-2) at a density of $1x10^6$/ml. All cells were cultured in incubators at 37°C, 5% CO2. After 1 h, T cells were activated with αCD3/CD28 stimulation. For CD4+ T cell vs CD8+ T cell comparisons of internalisation, Human T-Activator CD3/CD28 Dynabeads™ (ThermoFisher Scientific; 11161D) were used at a 1:4 beads to cell ratio. For all other experiments, cells were activated with 10 µl/ml TransAct (Miltenyi, 130-111-160).

2.6. Flow Cytometry

For all immune cell flow cytometry phenotyping (PBMCs or T cells alone), cells were washed in ice-cold FACS-buffer (2% FBS, 2 mM EDTA in PBS) and resuspending in round-bottom 96-well plates at concentration of $2x10^7$ cells/ml. Cells were incubated with Fc block for 10 min at 4°C. Cells were washed and resuspended in 100 ul of appropriate antibody cocktail diluted in cold FACS Buffer. Cells were incubated for 25 minutes at 4°C. Cells were washed twice in ice-cold

FACS Buffer and resuspended in 100 µL Cytofix (BD Biosciences), then incubated at room temperature in the dark for at least 20 min. Cells were washed twice in cold FACS Buffer then resuspended in 100uL of appropriate intracellular antibody cocktail made up 1X Perm buffer (Invitrogen). Cells were incubated overnight (at least 16 h) at room temperature in the dark. Cells were washed once in Perm buffer then twice in cold FACS buffer before being resuspended in cold FACS Buffer and transferred to 5 mL round-bottom polystyrene tubes. Cells were analysed on LSR Fortessa X20 (BD Biosciences).

2.7. Quantitative Co-culture Assays

BECs were seeded at $2x10^4$ cells/well in micro-clear black 96-well plates (Greiner CELLSTAR) coated with 2.5% rat-tail collagen (Sigma) and allowed 24 h to adhere. BECs were then labelled with 5 µM CellTracker Green (5-chloromethylfluorescein diacetate, CMFDA, Thermo Fisher Scientific) diluted in serum-free DMEM. CD8+ and CD4+ T cells were labelled with 5 µM CellTracker Red (CMTPX, ThermoFisher Scientific) dilution in serum-free RPMI. Cells were then washed in PBS and rested for 1 h our in their normal serum-containing media. Both cell types had their media replaced prior to their co-culture to remove leached dye. If needed, CD8+ T cells were then washed and then resuspended in normal media containing molecular inhibitors. T cells were then co-cultured with BEC at a ratio of 1:4 (BEC: T lymphocyte), unless stated otherwise, for 4 h. For CD4+ T cell vs CD8+ T cell comparisons of internalisation, cells were then fixed with 3.7% formaldehyde for 10 mins. Cells were then washed with PBS and

imaged using a ThermoFisher Scientific CellInsight CX5 high-content imager. Internalised cells were quantified manual with the assistance of cell counting tools in ImageJ software. Nine fields of view were analysed for each technical repeat. For all other experiments, cells were labelled with 5.0 µg/mL Wheat Germ Agglutinin conjugated to AlexaFlour 680 (Invitrogen, W32465) diluted in DMEM, for 10 min. Cells were then fixed with 3.7% formaldehyde for 10 mins. Cells were then washed with PBS and imaged using a Zeiss Cell Discover 7 microscope. Nine fields of view were acquired for each technical repeat. Images from these experiments were analysed by high content analysis using CellProfiler software.

2.8. CellProfiler high content analysis

Co-culture experiments imaged using the Zeiss Cell Discoverer 7 were analysed using a custom analytical pipeline developed in CellProfiler v4.2.1. Raw .czi Cell Discoverer 7 acquisition files were split into individual fields of view (“splite scene, write files”) and then single channel images were exported from each using batch processing in Zen software (Carl Zeiss), ensuring the channel or fluorophore name was present in the file name. Images were then imported into CellProfiler and then designated into channels based on their file names. BEC were detected using “IdentifyPrimaryObject” command. The generated objects were used to mask the matching T cell channel to remove T cells not found in the same areas as BEC. T cells were then detected and used to mask the membrane label image. T cells which possessed membrane labels were detected and deleted from total T cell objects detected using the “MaskObjects” feature. The newly masked

objects were then used to mask the BEC channel. Objects detected following this were T cells who possessed low membrane labelling, but were not localised at areas of displayed BEC cytoplasm. These objects were masked against objects pertaining to total CD8s without membranes. The resulting BEC cytoplasm-negative, membrane-negative cells were classed as internalised. Overlays of these cells were made over the raw BEC channel image to validate the analysis. Partially deleted cells at each masking step were removed using the "FilterObjects" feature by removing objects with an eccentricity value of more than 0.92. Numbers generated by manual counting were compared to those generated with this pipeline were analysed by linear regression to ensure the accuracy of the pipeline before conducting further experiments.

2.9. T cell siRNA knockdown

Knockdowns for CDH1 (E-cadherin) were performed using blood derived primary human CD8+ T cells from PBC patients by a reverse transfection method, 24 h post-activation with TransAct™. 750 ng of CDH1 siRNA (Flexitube Gene Solutions, QIAGEN Cat. 1027416, ID GS999 for CDH1, Human NM_004360) or Silencer Select negative control (Invitrogen, Cat. 4390843) were diluted in 100 µL Gibco OptiMEM™ (Thermo Fisher Scientific, Cat. 31985062) in 48-well plates. 6 µL Lipofectamine™ RNAiMAX (Invitrogen/Thermo Fisher Scientific, Cat. 13778100) was then added to each well, mixed gently, and incubated at room temperature for 20 min. 2 Å~ 105 activated CD8+ T cells in 100 µL OptiMEM were then added on top of siRNA complexes and incubated for 4 h at 37 °C. 400

µL RPMI, containing 1% L-Glutamine, 10% FBS, 10 µL/mL TransAct™ and 500 IU/mL IL-2, was then added to each well, (final siRNA concentration; 100 nM). After 48 hr, cells were then used in co-culture assays as described previously, with the exception that cells were co-cultured at a 1:3 ratio and performed in duplicate due to lower availability of cells. Expression of E-cadherin was also assessed by flow cytometry in parallel for each co-culture experiment and initially when validating each siRNA. The following individual siRNAs were used: siRNA1 – Hs_CDH1_13, GeneGlobe ID SI02654029, target sequence TCGGCCTGAAGTGACTCGTAA; siRNA2 – Hs_CDH1_12; GeneGlobe ID SI02653546, target sequence CTAGGTATTGTCTACTCTGAA; siRNA3 – Hs_CDH1_15, GeneGlobe ID SI04434598, target sequence TTGAATGATGATGGTGGACAA; siRNA4 – Hs_CDH1_14, GeneGlobe ID SI04434591, target sequence CAACTGGACCATTCAGTACAA.

2.10. Fluorescence Activated Cell Sorting of E-cadherin+ cells

CD8+ T cells cultured for 48 h post-activation were harvested and washed in PBS. Cells were then resuspended in ice-cold FACS buffer. Cells were stained using fluorophore-conjugated antibodies (see antibody section) and labelled using eBioscience Fixable viability Dye efluor 780 (ThermoFisher Scientific, 65-0865-14). $1x10^7$ in 200 µl were stained as the population to be sorted. $5x10^5$ cells received the staining panel containing an isotype-matched control for the E-cadherin detecting antibody. Cells were incubated with antibodies for 30 min at

4°C. Cells were then sorted using a BD FACSAria Fusion Cell sorter. Cells were gated on CD8+ positivity and viability dye negativity. Populations were then sorted into E-cadherin+ and E-cadherin- populations based on isotype-matched control staining. Cells were collected in warm RPMI, washed, and reseeded in 48-well plates in their normal culture medium at $2x10^5$ cells/well. Cells were then used within BEC co-culture assays as previously described.

2.11. Paraffin-embedding of tissue

Primary liver samples from both mice and consented human patients used paraffin-embedded for staining. All tissues were fixed in formalin (4% formaldehyde) for at least 24 h. Tissues underwent secondary processing and placed in the tissue cassettes. Tissues were then embedded in paraffin wax. 3 µm-thick sections were then cut using a rotary microtome and then floated on water to remove undesired tissue folding. Tissue sections were then mounted onto charged glass slides. Sections were then later stained using haematoxylin and eosin (H&E) or by immunohistochemistry. For 3D IHC imaging, 50 µm-thick sections were produced on a rotary microtome and after heating onto glass slides. Sections then underwent overnight low temperature epitope retrieval (ALTER), as previously described(318). Sections were then immunostained and imaged as previously described(313).

2.12. Immunohistochemistry

All immunohistochemistry was performed using paraffin-embedded tissue. Tissue sections were deparaffinized with xylene and rehydrated using 97% industrial denatured alcohol (IDA) and then underwent antigen-retrieval procedures by microwaving in Tris-based antigen unmasking solution (Vector Laboratories, UK). Endogenous peroxidase activity and non-specific antibody binding within tissue sections was blocked using Dako REAL peroxidase blocking solution (Dako) and 2X casein solution (Vectorlabs), respectively. Sections were incubated with primary antibodies at room temperature for 1 h or overnight at 4°C. Appropriate isotype-matched controls were used for all procedures. For detection using fluorophore-tagged secondary antibodies, tissue sections were stained with master mixes of appropriate secondary antibodies following their post-primary antibody washes. Slides were incubated for 1 h at room temperature and then washed with TBS. Slides were then incubated with Vector TrueView Autofluorescence quenching kit (Vectorlabs, SP-8400-15) four five min. Slides were then washed twice with TBS and mounted with VectaShield Vibrance Antifade Mounting Medium with DAPI (Vectorlabs, H-1800-10). Slides were then imaged using a Zeiss 880 confocal microscope. Where required, images were 3D-volumed rendered using Bitplane IMARIS for cell biologists, v8.3.

2.13. Semi-quantitative analysis of tissues

For the assessment of the presence of CD103+ and KLRG1+ CD8+ T cells in non-cirrhotic donors and livers with patients with different liver diseases, FFPE tissue sections were stained for CD8, E-cadherin and either CD103 or KLRG1. Slides were then imaged using a Zeiss 880 confocal microscope. Images were centred at areas of portal triads, parenchyma, fibrotic scars ,and large bile ducts for each case. 5x5 tile scans were then acquired at x40 magnification using minimal zoom. Manual ocular assessment was also conducted and supplemented with example single images. A minimum of 3 examples of CD8+ T cells expressing CD103 or KLRG1 were observed classifying each case as positive for a specific area 6 cases were analysed per disease condition.

2.14. Immunocytochemistry

BEC cells were seeded on glass coverslips in 24-well plates coated with 2.5% rat-tail collagen and allowed 24 h to adhere. Cells were then labelled with CellTracker Green (5-chloromethylfluorescein diacetate, CMFDA, Thermo Fisher Scientific and T lymphocytes were labelled with a CellTracker Red (CMTPX) at this point, if needed, and rested for 1 h our in their normal serum-containing media. BEC and CD8+ T cells were then co-cultured with BEC at a ratio of 1:4 (BEC: T lymphocyte), unless stated otherwise, for 4 h. Cells were fixed in 4% MeoH-free formaldehyde for 10 min. Cells were washed in PBS and blocked for 30 min with 1% (w/v) FBS and 1% (w/v) BSA, in PBS for a minimum of 30 min. Cells were

then stained with primary antibodies detecting membrane-bound antigens, which were were prepared in the same staining buffer at previously optimised concentration determined by titration. Cells were incubated with primary antibody for 1 h at RT, or 24 h at 4°C. Cells were washed again in staining buffer and then incubated with secondary, fluorophore-conjugated antibodies at the appropriate dilution in staining buffer containing 200 µg/ml Hoechst 33342 (Invitrogen, H3570). For intracellular stains, cells were then washed in PBS and incubated with buffer containing 1% (w/v) FBS and 1% (w/v) BSA with 0.1% Saponin (Sigma) for 10 min. Previous antibody staining rituals were then repeated, only with antibodies diluted in Saponin-containing buffer. In some cases, at this point secondary antibody cocktails also contained Alexa Fluor 594 phalloidin. Cover slips were then mounted on glass microscope slides using Vectashield Vibrance® Antifade Mounting Medium (Vectorlabs, H-1700). Cells were then imaged using a Zeiss 900 confocal microscope equipped with Airyscan 2. Where required, images were 3D-volumed rendered using Bitplane IMARIS for cell biologists, v8.3. Production of new channels depicted colocalised channels were generating using the same software and were comprised of pixels of 80% minimum colocalization.

2.15. Inhibitors

For some experiments, prior to co-culture with BEC, CD8+ T cells were treated molecular inhibitors for 30 min (1 µM Wortmannin, 5 nM H-1152 (Sigma, Cat No. 555550) or 5 µM cytochalasin D). Inhibitors were solubilised to stock

concentrations which permitted a final DMSO concentration of 0.001% during experimentation following 1/1000 dilutions. Concentrations of all treatments and relevant vehicle controls were maintained throughout the experiment duration.

2.16. Live imaging

For live cell imaging, labelled CD8+ T cells were added to BEC seeded in black 96-well plates and were then transferred to a Zeiss Cell Discoverer 7 automated microscope. Cells were then imaged overnight for 3 h at 37°C, 5% $C0_2$. Images were acquired every 4 min.

2.17. Electron microscopy

BEC were seed at a density of $5x10^4$ in 24-well plates on 12 mm glass coverslips and allowed 24 hours to adhere. 4 h co-cultures between biliary epithelial cells and CD8+ T cells were performed as they were for previous experiments, which the exception that cells were not labelled with fluorescent dyes. Following this, cells were fixed in 2.5% glutaraldehyde diluted in cacodylate buffer for at least 1 h. For scanning electron microscopy, cells underwent two 15 min washes each in increasing concentrations of Ethanol (50%, 70%, 90% then 100%). Alcohol was then replaced with liquid $C0_2$ and then samples were heated to a critical dry point to fully dehydrate the sample. Cells were then mounted on a sample stub and coated with gold. Stubs were then imaged with a ThermoFisher Scientific Apreo SEM.

For transmission electron microscopy, cells were prepared using the same methodology as SEM samples, but with the following additions: cell were treated with 1% osmium tetroxide for 1 h post-fixation, and samples received two additional sets of washed following the 100% alcohol wash; 100% dried alcohol and propylene oxide. Samples were then placed in a mixture of 1:1 propylene oxide/resin on a rotator in a fume cupboard for 1 h. Samples were then transferred to 100% resin, pulled through a vacuum for 30 min and allowed to return to atmospheric pressure. Resin was then polymerised at 60°C for at least 16 h. 100 nm-thick sections were cut with an ultramicrotome and imaged using a JEOL JEM 1400 TEM microscope with Monada Soft imaging system. All sample processing following fixation and imagined was performed at the Centre for Materials and Metallurgy at the University of Birmingham.

2.18. Characterization of the epigenetic profile of PBC T cells.

PBMCs will be stained with anti-CD4, anti-CD25, and anti-CD45RA, anti-CD127, anti-CCR6 and, anti-FOXP3 antibodies and I used fluorescence activated cell sorting (FACS) to separate them in naïve conventional T cells (naïve Tconv) and regulatory T cells (Treg). Foxp3 gene locus for STAT5 binding, H3K27ac, and chromatin status will be characterized by Chromatin immunoprecipitation followed by sequencing (ChIP-seq) and assay for

transposase-accessible Chromatin using sequencing (ATAC-seq) as previously described by Sakaguchi Lab.

2.19. Chromatin Immunoprecipitation Followed by Sequencing (ChIP-seq)

To investigate the binding of STAT5 and the histone modification H3K27ac at the Foxp3 gene locus, I performed ChIP-seq on sorted naïve conventional T cells (naïve Tconv) and regulatory T cells (Treg). Following fluorescence-activated cell sorting (FACS), cells were promptly crosslinked to preserve protein-DNA interactions. For histone modifications, cells were crosslinked in 1% formaldehyde solution for 5 minutes at room temperature. For transcription factors like STAT5, an extended crosslinking time of 30 minutes was used to ensure efficient fixation.

The crosslinking reaction was quenched by adding 125 mM glycine for 5 minutes. Cells were then lysed using a lysis buffer containing 1% SDS, 10 mM EDTA, and 50 mM Tris-HCl (pH 8.0). The chromatin was sheared to an average size of 200–500 base pairs using sonication (e.g., 30 cycles of 30 seconds on/30 seconds off at high power with a Bioruptor sonicator).

The sheared chromatin was pre-cleared with Dynabeads Protein G magnetic beads (Thermo Fisher Scientific) for 1 hour at 4°C to reduce nonspecific binding. For immunoprecipitation, the pre-cleared chromatin was incubated overnight at 4°C with antibodies specific to STAT5 (e.g., anti-STAT5 antibody, clone XYZ,

supplier) or H3K27ac (e.g., anti-H3K27ac antibody, clone ABC, supplier) that had been pre-bound to Dynabeads IgG magnetic beads. The antibody-bead complexes were preincubated for 6 hours at 4°C with gentle rotation to enhance binding efficiency.

After immunoprecipitation, the bead-bound complexes were washed sequentially with the following buffers to remove nonspecific interactions:

1. Low-salt wash buffer: 0.1% SDS, 1% Triton X-100, 20 mM Tris-HCl (pH 8.0), 150 mM NaCl, 2 mM EDTA.

2. High-salt wash buffer: same as low-salt but with 500 mM NaCl.

3. LiCl wash buffer: 0.25 M LiCl, 1% NP-40, 1% deoxycholate, 10 mM Tris-HCl (pH 8.0), 1 mM EDTA.

4. TE buffer:10 mM Tris-HCl (pH 8.0), 1 mM EDTA.

The chromatin was then eluted from the beads using an elution buffer (1% SDS, 0.1 M $NaHCO_3$) and reverse-crosslinked by incubating at 65°C overnight in the presence of proteinase K (20 µg/mL) and RNase A (10 µg/mL) to degrade proteins and RNA contaminants.

Purified DNA was extracted using a phenol-chloroform-isoamyl alcohol method followed by ethanol precipitation or purified using a commercial kit like the QIAquick PCR Purification Kit (Qiagen). DNA libraries were prepared using the KAPA HyperPrep Library Preparation Kit (Roche) according to the manufacturer's

instructions, which included end-repair, A-tailing, adapter ligation, and library amplification steps.

The quality and concentration of the DNA libraries were assessed using an Agilent 2100 Bioanalyzer or TapeStation system. Libraries were sequenced on an Illumina platform (e.g., NovaSeq 6000) to generate high-throughput sequencing data. Sequencing reads were aligned to the human reference genome (GRCh38/hg38) using Bowtie2 or BWA-MEM aligners. Peak calling to identify enriched regions of STAT5 binding or H3K27ac modification was performed using Model-Based Analysis of ChIP-Seq (MACS2) software. Data visualization and analysis were conducted using the Integrative Genomics Viewer (IGV) and additional bioinformatics tools as needed.

2.20. Assay for Transposase-Accessible Chromatin Using Sequencing (ATAC-seq)

To assess genome-wide chromatin accessibility, including at the *Foxp3* locus, ATAC-seq was performed on the sorted cell populations, following the protocol established by Buenrostro et al. (2013).

2.20.1. Cell Lysis and Nuclei Preparation:

Immediately after sorting, approximately 50,000 cells per sample were collected and washed twice with cold phosphate-buffered saline (PBS). Cells were lysed in 50 µL of cold lysis buffer composed of:

- 10 mM Tris-HCl (pH 7.4)

- 10 mM NaCl

- 3 mM $MgCl_2$

- 0.1% IGEPAL CA-630 (Nonionic surfactant)

The lysis was carried out on ice for 10 minutes to ensure efficient lysis without damaging nuclei.

2.20.2. Transposition Reaction:

Nuclei were pelleted by centrifugation at 500 × g for 10 minutes at 4°C using a refrigerated centrifuge. The supernatant was carefully removed, and the nuclear pellet was resuspended in the transposase reaction mix, which included:

- 25 µL 2× TD buffer (Illumina Nextera DNA Library Prep Kit)

- 2.5 µL Tn5 Transposase enzyme

- 22.5 µL nuclease-free water

The reaction mix (total volume of 50 µL) was incubated at 37°C for 30 minutes with gentle mixing to facilitate the integration of sequencing adapters into open chromatin regions.

2.20.3. Library Amplification:

Following transposition, DNA was purified using a Qiagen MinElute PCR Purification Kit according to the manufacturer's protocol. The purified DNA was amplified using NEBNext High-Fidelity 2X PCR Master Mix (New England Biolabs) and custom Nextera PCR primers containing sample-specific barcodes.

2.20.4. Library Purification and Quality Control:

Post-amplification, libraries were purified using AMPure XP beads (Beckman Coulter) at a ratio of 1.8× to remove fragments smaller than 100 bp, which are typically primer dimers. Library quality and fragment size distribution were assessed using an Agilent Bioanalyzer or TapeStation. The concentration of the libraries was quantified using a Qubit fluorometer (Thermo Fisher Scientific).

2.20.5. Sequencing and Data Analysis:

Sequencing was performed on an Illumina NextSeq 500 or equivalent platform to generate paired-end reads (2 × 75 bp or 2 × 150 bp). Sequencing reads were trimmed to remove adapter sequences using Trimmomatic or Cutadapt and then aligned to the human reference genome (GRCh38/hg38) using Bowtie2 with parameters optimized for ATAC-seq data.

Aligned reads were filtered to remove duplicates and mitochondrial DNA. Peaks representing regions of open chromatin were identified using MACS2 with the following parameters: `--nomodel --shift -100 --extsize 200 --keep-dup all`. Peaks were annotated relative to gene features using tools like HOMER or ChIPseeker.

Visualization of ATAC-seq peaks was performed using the Integrative Genomics Viewer (IGV) genome browser, allowing for qualitative assessment of chromatin accessibility at the *Foxp3* locus and other regions of interest. Quantitative analyses, such as differential accessibility between naïve Tconv and Treg cells, were conducted using DESeq2 or edgeR.

2.21. Bisulfite sequencing

The methylation CpG status was defined by bisulfite sequencing. After the sorting, cells were left overnight in lysis buffer (1ml 5M NaCl, 5ml 0.5M EDTA, 2.5ml 10% SDS and 500 ul 1M Tris-HCl pH 8.0) and proteinase K. After lysing, DNA was extracted by phenol reaction and by ethanol precipitation. Approximately DNA was then treated with sodium bisulfite solution and the modified DNA was amplified by PCR (CNS2, intron3a, and exon 2). The primer used are listed in the table 3. Bisulfite PCR products were extracted from gel pieces, purified and ligated to a vector. E.coli DH5α colonies were then transformed. The colonies (10-16 colonies/region) were directly amplified with the Illustra TempliPhi Amplification Kit (GE Healthcare) and sequenced using 3500xL Genetic Analyzer for Sanger sequencing.

Alternatively, after bisulfite conversion, the DNA was amplified and analysed using digital PCR for absolute quantification of nucleic acids. VIC fluorescent-tagged and FAM fluorescent-tagged TaqMan assay was used to quantify, respectively, the methylated and unmethylated FoxP3 TSDRs. The reaction

was dispensed in QuantStudio™ 3D Digital PCR 20K Chip v2 and amplified the QuantStudioTM 3D Digital PCR system.

Primer name	Sequence
mFoxp3_CNS2 - Fwd	ATT TGA ATT GGA TAT GGT TTG T
mFoxp3_CNS2 - Rev	AAC CTT AAA CCC CTC TAA CAT C
mIkzf2_intron3a_Fwd	AGG ATG GTT TTT ATT GAA GGT GAT
mIkzf2_intron3a_Rev	ATA CAC ACC AAA CAA ACA CTA CAC C
mCtla4_exon2_Fwd	TGG TGT TGG TTA GTA GTT ATG GTG T
mCtla4_exon2_Rev	AAA TTC CAC CTT ACA AAA ATA CAA TC

Table 3 Primer list

2.22. Generation and testing of Stable and functioning induced regulatory T cells.

CD4+ T cells were magnetically enriched from peripheral blood mononuclear cells (PBMCs) of PBC patients. CD4+T cells were activated by CD3+ activator beads without CD28 co-stimulatory signal, and cultured in presence of IL-2 and AS2863619 (CDK8/19 inhibitor) for 2 weeks.

The functionality of SFiTreg was investigated by vitro suppression assays using CellTrace Violet dye-labelled effector T-cells, CD3 activator beads and IL-2.

The stability of SFiTreg was evaluated after culturing the cells in presence of Th1 polarising cytokines (IL-12 and IFN-gamma) by bisulfite sequencing of Helios, FoxP3 and CTLA4 genes and flow cytometry.

2.23. Generation of antigen specific stable and functioning induced regulatory T cells

PBMCs from PBC patients or controls were resuspended at concentration of 1x106/mL and cultured in X-VIVO-15 (Lonza, BE02-054Q) enriched with 100U/ml penicillin and 0.2μg/ml streptomycin (Sigma-Merck; P4333) at concentration of 2 x 106/ml in presence of IL-4, GMC-SF and Ftl3-L in a 96-well plate for 24 hours. After taking off the supernatant, the cells were resuspended in X-VIVO-15 media in presence of LPS, IL-1Beta, R848 and with either PDC-E2 (at either 7, 10 or 14 μg/ml), PepMix Human (MOG) (JPT) or CEFT pool (JPT) for another 24 hours. The cells were then fed with a media enriched with IL-2, IL-17 and IL-15 for another 7 days and a total of 9 days of culture. The cells were then separated in two aliquots, the first part was re-stimulated with peptide and αCD49a and αCD28 antibodies for 4 hours and the second part prepared for staining and flow cytometry acquisition. After the re-stimulation, the cells were assessed for cytokine production. Cytokine secretion was blocked by addition of Brefeldin A (5μg/ml, Sigma Aldrich) and Monesin (5μg/ml, Sigma Aldrich). The re-stimulation experiment included three positive controls: Phorbal Myristate Acetate (PMA) (25ng/ml, Sigma Aldrich) and ionomycin (1μM, Sigma Aldrich), CEFT pool, or

TransActTM (MyItenibiotech) and two negative controls, the vehicle alone or MOG.

2.24. Statistics

For all experiments where the frequency of internalised T cells were measured, results were expressed as a fold-change from control parameters by dividing individual measures by control means for each individual experiment. Graphs were made and statistical tests were performed using Graphpad Prism 9.0 software. Data underwent tests for normal distribution prior to the use of parametric comparisons. The comparison of two groups of normally distributed data was performed by Student's t tests, unpaired non-parametric data by Mann-Whitney test or for paired, non-parametric data by Wilcoxon test. Correlation was determined using linear regression analysis. Statistical significance was defined as p value < 0.05. Error bars were plotted on graphs representing standard error of the mean (SEM).

3. Results

3.1. Biliary epithelial cells invaded by T CD8 cells: a cell-in-cell structure.

N.B. *the content presented in this chapter are part of a paper recently published(317) .*

3.1.1. Introduction

The onset of an aberrant and unresolved immune response is the pathophysiological ground of autoimmunity. The liver, despite not being a traditional barrier organ (like the skin or the gut) is exposed to continuous antigenic exposure, and despite possessing an immune response skewed towards tolerance at homeostasis, remains vulnerable to vulnerable to the development of autoimmune processes (55, 319, 320).

Studies in murine models have shown how the ultimate drivers of damage to the biliary epithelium in PBC are CD8+ T lymphocytes(143, 223, 239, 321). However, to date, the exact mechanism of the CD8+ T cell crosstalk with the biliary epithelium remains elusive. This particular interaction is at the basis of PBC pathogenesis, and a deeper understanding of it, it might shade the light on the tolerance breakdown (i.e. the disease onset) and the mechanism of damage (i.e. the disease progression). Recent observations suggest that CD8+ T cells are also present within the cytoplasm of BEC in liver tissues from patients with

PBC(316). The presence of internalised CD8+ T cells correlated with bile duct damage, although the mechanism of internalisation was not investigated.

The aim of this first chapter is to confirm Zhao and colleagues data(316), and better characterise what I believe is an intriguing and overlooked cell-to-cell interaction, potentially relevant in the pathogenesis of PBC. The CICs presence and feature will be assessed on PBC liver explant tissue and then modelled and replicated *in-vitro* using a platform developed with this exact purpose.

The experiments presented in the chapter 3 and chapter 4 were done in collaboration with Dr Scott Davies who shared with me the ownership of the data and was co-leading author with me on our recent published paper(317).

3.1.2. Live $CD8^+$ T cells are internalised into biliary epithelial cells in vivo and in vitro whereas $CD4^+$ T cells are not.

To confirm the observations of CD8+ T cell internalisation into BEC made by Zhao and colleagues(316), multiplex immunohistochemistry (IHC) staining of formalin-fixed paraffin-embedded (FFPE) tissue sections of liver tissue derived from PBC patients was performed (Fig. 3.1). The presence of CD3+ CD8+ T cells frequently contained within the cytoplasmic spaces of cytokeratin-19 (CK19)-expressing BEC was confirmed using fluorescence microscopy.

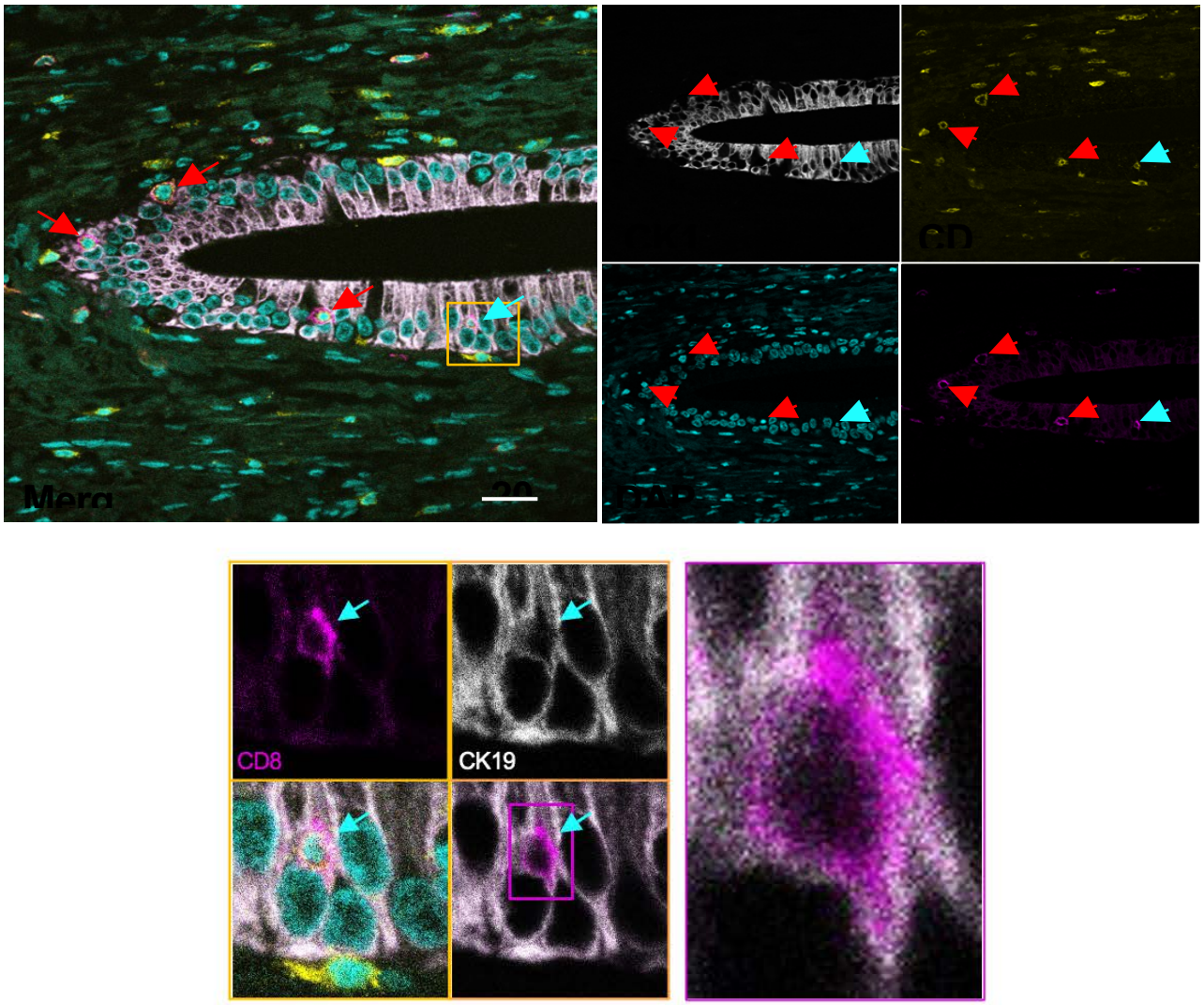

Figure 3. 1 CD8+ T cells are internalised into biliary epithelial cells in PBC liver in late disease stages. Immunohistochemistry (IHC) staining of liver tissue from a PBC patient. Red arrows indicate CD3+ (yellow) CD8+ (magenta) T cells invading cytokeratin-19+ (CK19; grey) biliary epithelial cells (BEC). Right panel shows magnified view of area outlined by yellow box in left panel and further magnified image of CD8+ T cell (blue arrow) surrounded by CK19 staining (magenta box).

The invasion of BECs by CD8+ T cell was assessed also in liver biopsies, to confirm the phenomena was also relevant for early disease. IHC staining for liver biopsies from patients with active PBC was performed (n=9; Fig. 3.2). Internalised CD8+ T cells were found within CK19+ EpCAM+ BEC in all biopsies analysed.

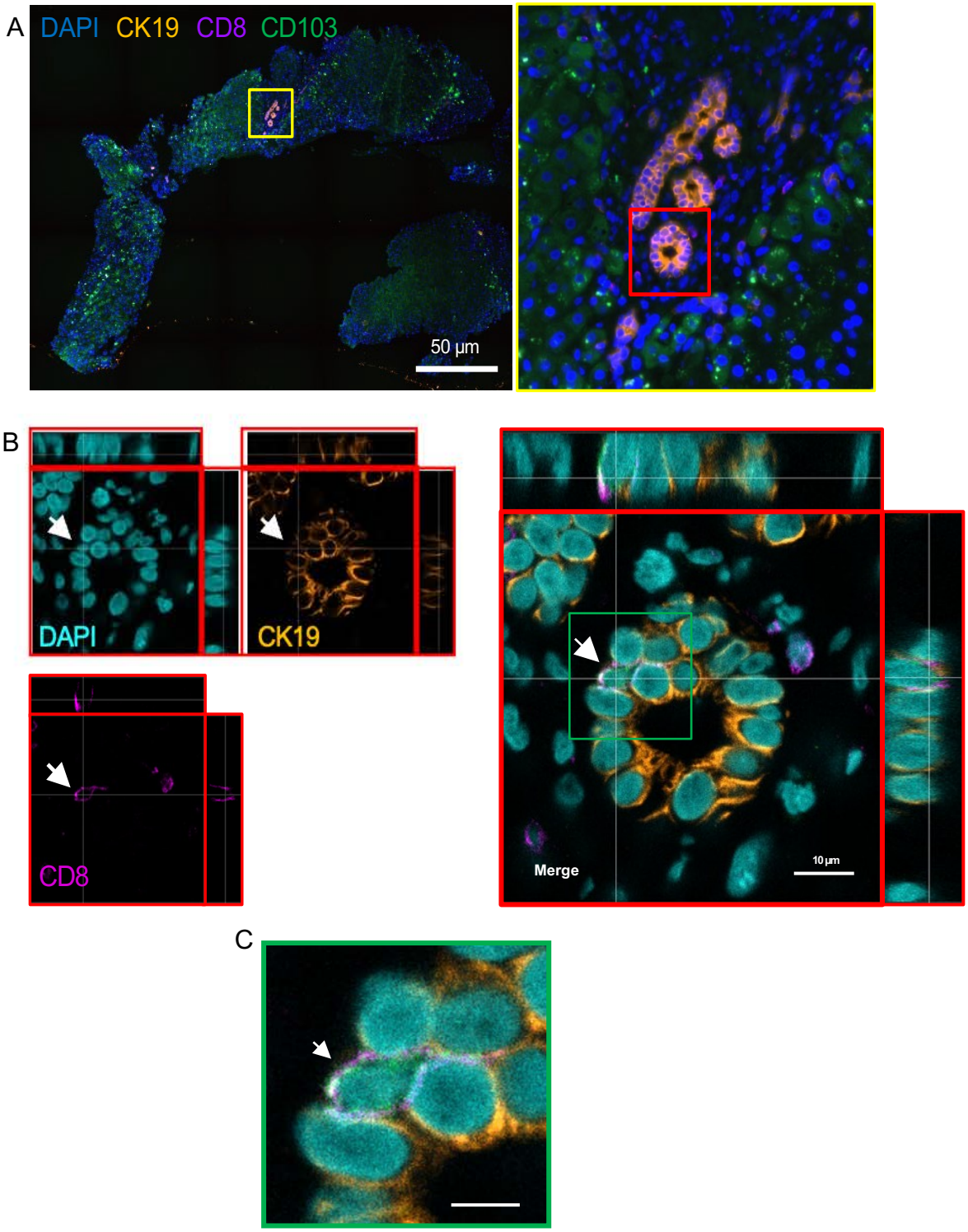

Figure 3. 2 CD8+ T cells are internalised into biliary epithelial cells in PBC livers in early disease stages. Representative fluorescence image of liver core biopsy, taken from a PBC patient with active disease, stained for CD8 (magenta), CD103 (green) and CK19 (orange) by immunohistochemistry (IHC). Yellow box identifies cluster of bile ducts. B. Multichannel representation of orthographical views showing bile duct outlined in part A (red box) showing internalised CD8+ T cell (white arrow). C. Magnified single Z-plane image of inset shown in B (green box)

To assess if this interaction could be replicated *in vitro* in absence of disease-specific stimuli, we performed co-cultures using primary human cells from non-PBC patients. Peripheral blood derived CD8+ T cells, obtained from patients who have chronic iron overload (Haemochromatosis or HFE) undergoing venesection, were co-cultured for 4 h with primary human BEC, isolated from non-cirrhotic donor livers or explanted livers from patients with chronic liver disease. Both cell types were labelled with fluorescent CellTracker™ dyes prior to co-culture and CK19 using immunocytochemistry (ICC) confirmed the identity of the BEC. Fluorescence confocal microscopy confirmed the presence of T cells within cytoplasmic spaces of the BEC (Fig. 3.3); displacement of BEC cytoplasm was concurrent with the presence of labelled T cells and Z-stack acquisition proved the complete enclosure of T cells within the BEC.

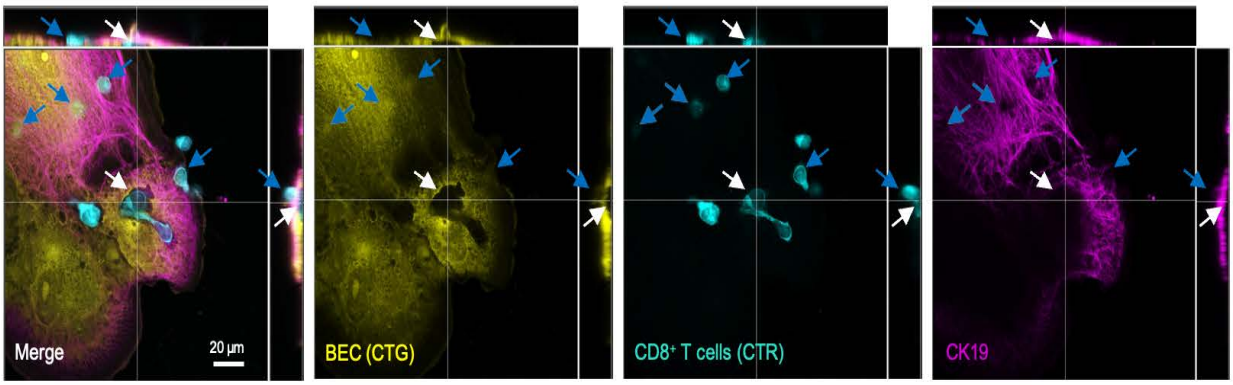

Figure 3. 3 The internalisation of activated CD8+ T cells can be replicated in vitro. Orthographical confocal micrograph showing peripheral blood-derived CD8+ T cells (CellTracker™ Red; CTR, cyan) co-cultured with BEC (CellTracker™ Green; CTG, yellow) stained for CK19 (magenta) using immunocytochemistry (ICC). Blue arrows show CD8+ T cells attached to the surface of the BEC. White arrows show flatter internalised CD8+ T cells.

Transmission electron microscopy (TEM) imaging of co-cultured BEC and CD8+ T cells further confirmed the complete internalisation of CD8+ T cells within BEC (Fig. 3.4).

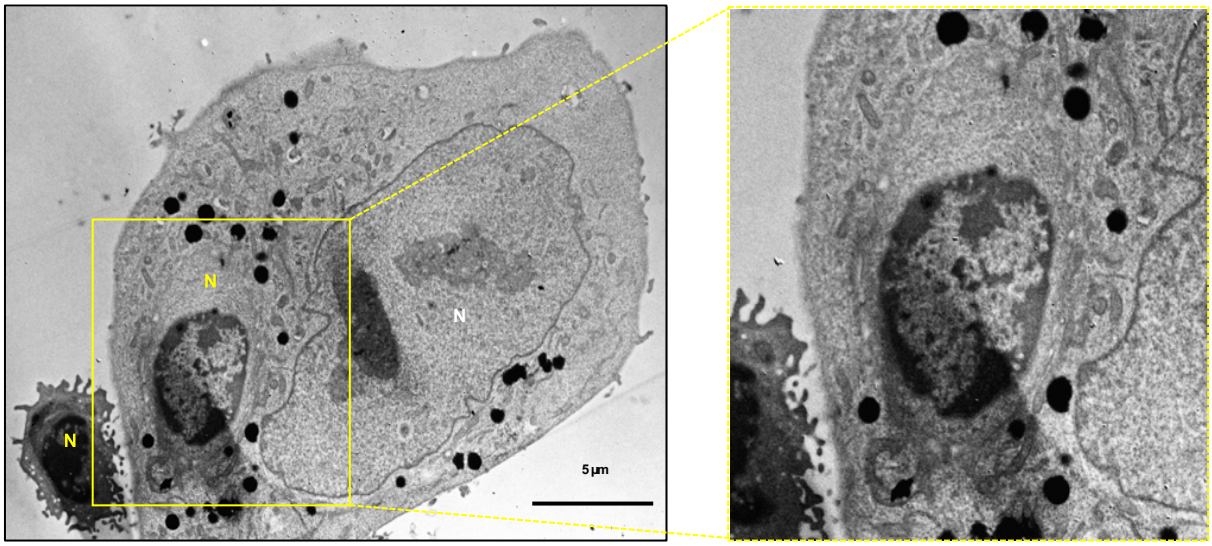

Figure 3. 4 Live and activated CD8+ T cells are internalised into biliary epithelial cells (BEC) in human livers. Transmission electron microscopy (TEM) image showing a CD8+ T cell fully internalised within a BEC.

The CICS, historically, described in the liver are defined according to the cells involved, the duration of the internalisation and the fate of the internalised cell. Transendothelial migration, involves transient occupation of T cells within the cytoplasm of the endothelial cells, with the purpose to migrate through them(322). Suicidal emperipolesis, instead, refers to autoreactive $CD8^+$ lymphocytes internalised by the hepatocytes, resulting in their deletion(262, 313).

To define the duration, and the fate of the internalised, lymphocytes, time-lapse fluorescence microscopy was performed during the CD8+ T cell-BEC co-culture (Fig. 3.5).

A

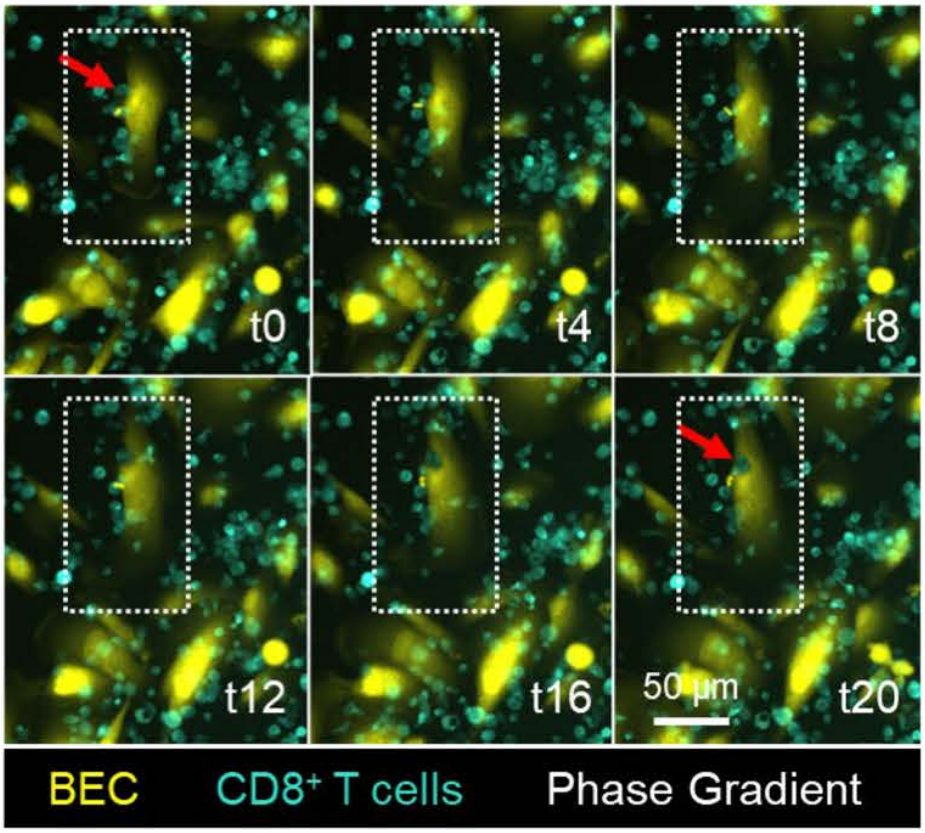
t0
t4
t8
t12
t16
50 µm
t20
BEC
CD8+ T cells
Phase Gradient

B

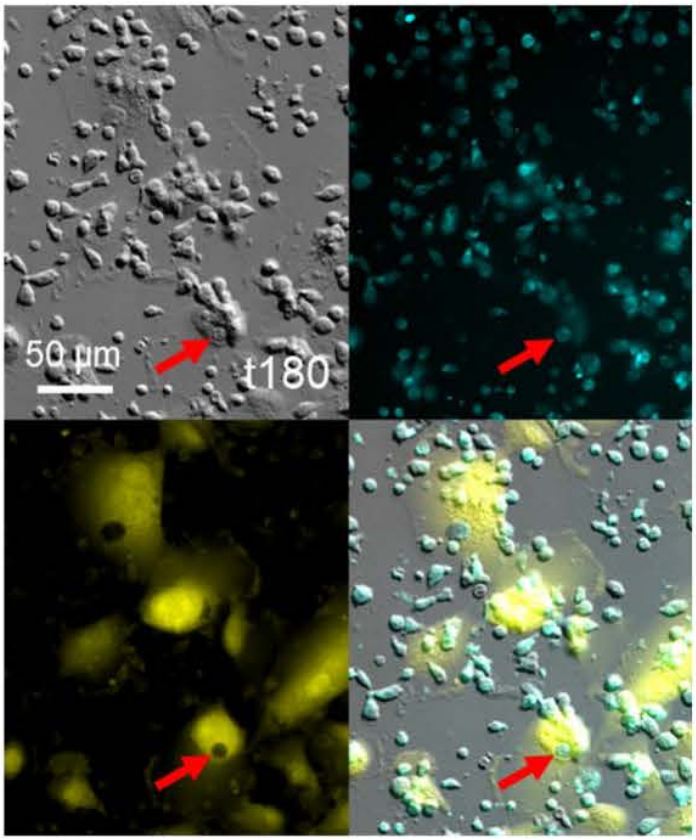
50 µm
t180

Figure 3. 5 CD8+ T cells can be internalised into BEC within 20 min of attachment and remain internalised over a longer time. A Representative time-lapse images captured at 4 min intervals showing co-cultured biliary epithelial cells (CellTracker™ Green; yellow) and peripheral blood-derived CD8+ T cells (CellTracker™ Red; cyan) 1 h after initial co-culture. T cells were activated with α-CD3/CD28 stimulation and cultured for 48 h prior to their co-culture with BEC. Red arrow shows a CD8+ T cell being internalised throughout the time course. **B** Same internalised CD8+ T cell (red arrow) after 180 min of co-culture. Phase Gradient (grey) microscopy images were acquired simultaneously.

To investigate whether CD4+ T cells were also capable of entering BEC, IHC staining of PBC liver tissue sections for CD4, CD8 and CK19 was performed (Fig. 3.6). While CD8+ T cells were found enclosed within the CK19+ BEC, CD4+ T cells were instead mostly observed to be adhering to the outer surfaces of the epithelium, but not internalised.

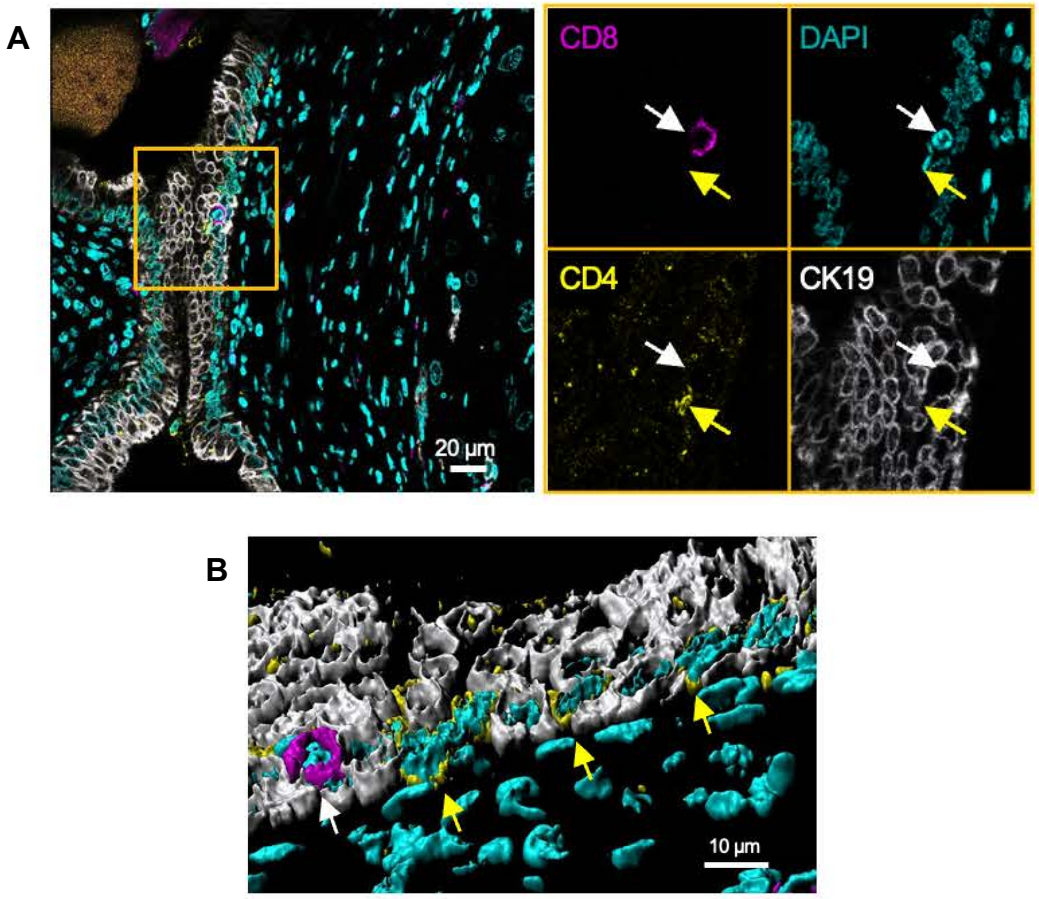

Figure 3. 6 CD8+ T cells are enclosed within BECs but not CD4+ T cells in PBC livers. IHC staining of PBC liver showing CD4+ T cells (yellow; yellow arrow), and a CD8+ T cell (magenta, white arrow) associated with the CK19+ BEC (grey). Right panel shows magnified view of area outlined by orange box in left panel. **B.** 3D-volume rendered version of Z-stack acquired from same region as **A**. White arrow identifies internalised CD8+ T cell. Yellow arrows indicate adhered and infiltrating CD4+ T cells.

Additionally, co-cultures between donor- matched CD4+ and CD8+ T cells with BEC were performed quantifying the frequency of internalisation (Fig. 3.7). Internalisations of either cell type did not occur in the absence of αCD3/CD28 stimulation. Activated CD4+ T cells demonstrated some capacity to internalise into BEC. However, the frequency of activated CD8+ T cell internalisation was significantly more than that of CD4+ T cells. Taken together, T cell internalisation within BEC is most frequent with those expressing CD8 in PBC liver tissue; this was an observation that could be reproduced *in vitro*.

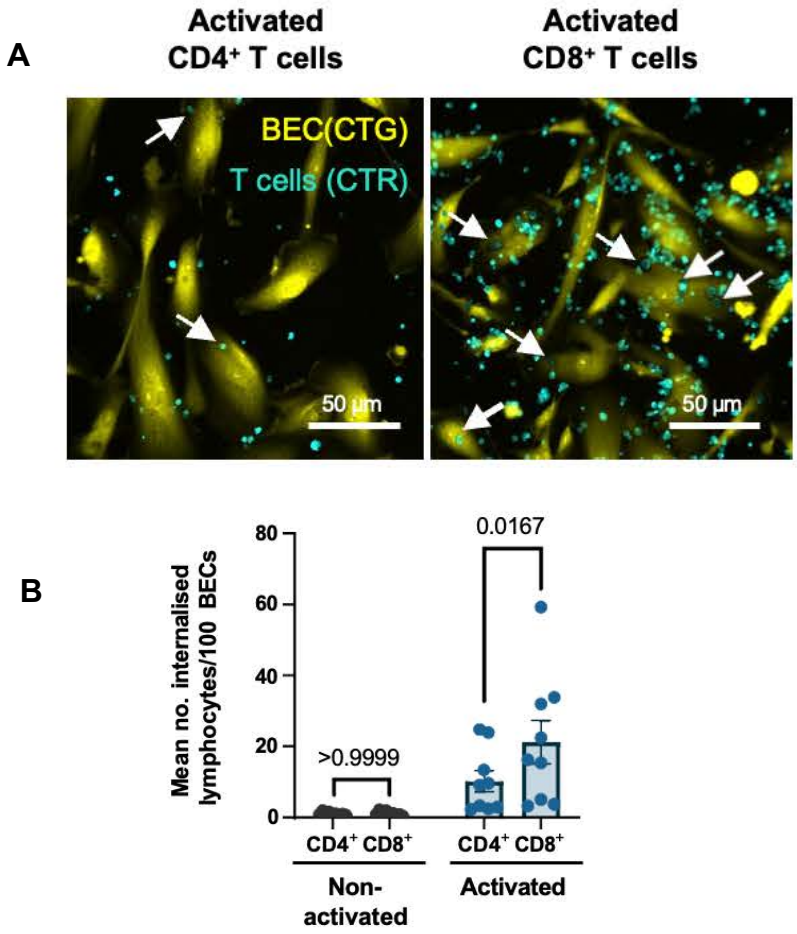

Figure 3. 7 Quantification of internalisation of CD4⁺vs CD8⁺T cells within the BECs. A. Representative images of BEC (yellow) co-cultured with α-CD3/CD28-activated CD4+ or CD8+ T cells (cyan). **B.** Quantification of internalised non-activated (black bars) or activated (blue bars) T cells per 100 BEC. Mean values from triplicate technical repeats are plotted. n=3 biologically independent experiments. Statistics were derived from paired two-tailed Student's t-tests. Error bars represent standard error of the mean (SEM).

3.1.3. CD8+ T cells are larger, more eccentric, and more frequently internalised within BEC after activation in vitro.

A morphological peculiarity of CD8+ T cells found within BEC of PBC liver tissues in the first ICH experiment was that they possessed a dendritic-like appearance and were significantly larger than those in the surrounding structures (Fig. 3.1, fig 3.6 and fig 3.8).

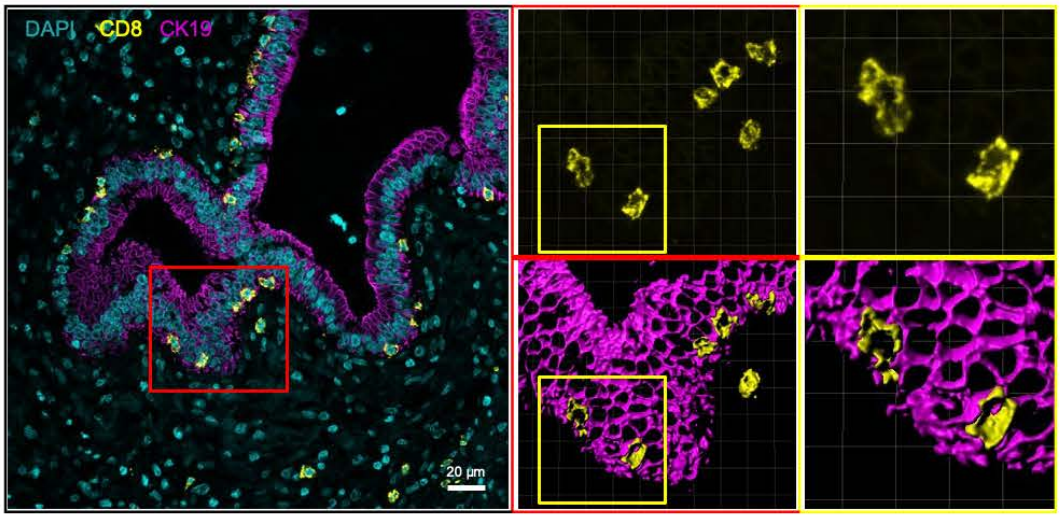

Figure 3. 8 CD8^{+} T cells are bigger and with irregular shape in PBC livers. Immunohistochemistry staining of a liver tissue section from a patient with primary biliary cholangitis (PBC), showing larger, irregularly shaped CD8^{+} T cells (yellow) invading the biliary epithelial cells (BEC). Right panels show 3D-reconstructed versions (top) and 3D-volume renders (bottom) of Z-stack images acquired for inset in left panel (red box) showing eccentric CD8^{+} T cells surrounded by cytokeratin-19 (CK19; magenta). Further magnified images of CD8^{+} T cells are also shown (far right; yellow boxes).

T cells can become enlarged because of mTOR signalling following T cell receptor (TCR)-mediated activation(323, 324), and it is possible that the chronic stimulation in the chronically inflamed PBC livers could have triggered a chronic activation state. However, similar results could not have been replicated in the *in-vitro* model, after 24-hour of activation (Fig. 3.2, 3.7). I hypothesised the reason a similar T cell morphology was not observed *in vitro* was that 24-hour activation was not sufficient to induce similar morphological changes in CD8+ T cells. To address this, I compared the sizes of non-activated human CD8+ T cells to those of donor-matched cells 24 h and 48 h post-activation using flow cytometry. Forward scatter analysis of singlet-gated CD8+ T cells revealed a substantial increase in cell size between 24 and 48 h following α-CD3/CD28 activation (Fig. 3.9).

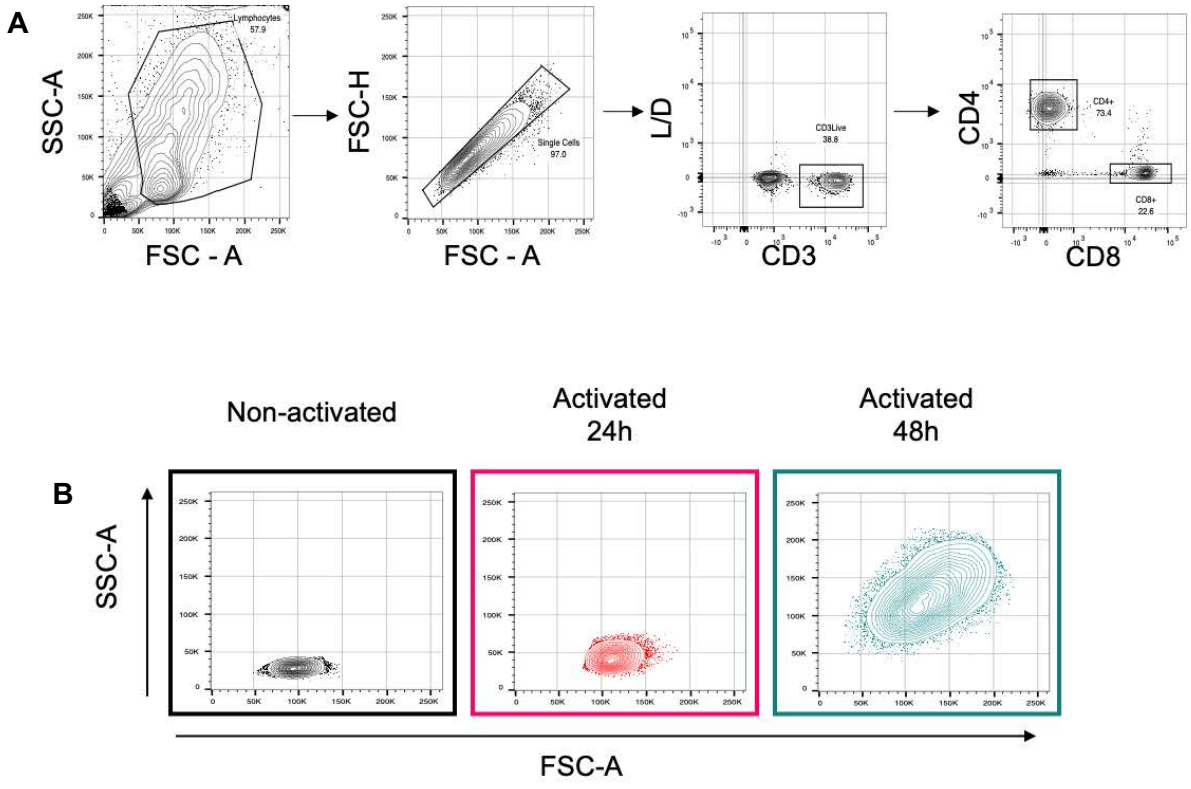

Figure 3. 9 48-hours of activation triggered the change in T-cells shape and size. A. Representative flow cytometry gating strategy for phenotyping peripheral blood-derived 1317 live, CD3+ CD4+ and CD8+ T cells. **B.** Representative flow cytometry contour plots of side and 1318 forward scatter areas (SSC-A/FSC-A), showing the difference in granularity and size, 1319 respectively, of CD8+ T cells. Cells were phenotyped in the absence of activation stimuli 1320 (black) or following 24 h (red) or 48 h (cyan) after α-CD3/CD28-mediated activation.

To determine if CD8+ T cell internalisation into BEC was increased by using T cells previously activated for 48 h, 4 h co-culture experiments were repeated, comparing 48 h activated cells to 24 h activated cells. As previously observed, activation with α-CD3/CD28 stimulation was required to promote CD8+ T cell internalisation into BEC. However, CD8+ T cells which had undergone 48 h activation displayed a significantly higher propensity to internalise into BEC. (Fig. 3.10).

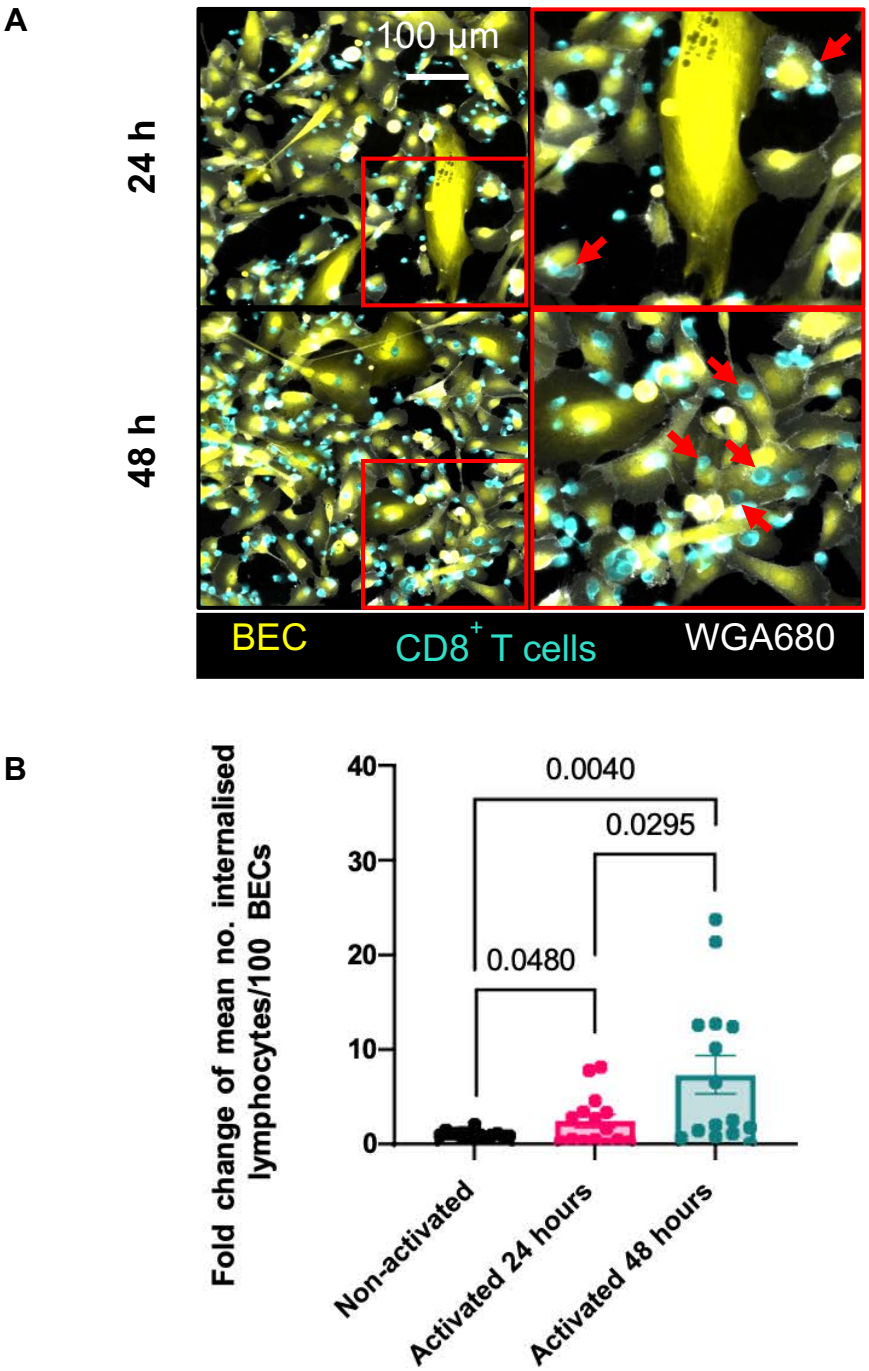

Figure 3. 10 48-hour activation increase the number of internalised CD8⁺ T cells compared with 24-hour activation. A Representative images of BEC (CellTracker™ Green; yellow) co-cultured with 24 h or 48 h-1322 activated CD8+ T cells (CellTracker™ Red; cyan). Cells were labelled with wheat germ 1323 agglutinin conjugated to Alexa Fluor 680 (WGA680, grey) after co-culture. **B** Quantification of number per 100 BEC of internalised CD8+ T cells in either non-activated, 24 h activated, or 48 h activated prior to co-culture. Nine fields of view were analysed from triplicate wells. Mean values/technical repeat are plotted. Values are normalised and displayed as a fold change from non-activated cells. n=5 biologically independent experiments. Statistics are derived from unpaired two-tailed Student's t-tests. p values are displayed for each statistical comparison made.

Additionally, the size and eccentricity (lack of roundness) of internalised cells was quantified using CellProfiler (Fig. 3.11). The size of internalised cells was consistent regardless of activation status (Fig. 3.11A). Internalised cells were, however, more eccentric 48 h post-activation compared to 24 h activation, and non-activated cells (Fig. 3.11B).

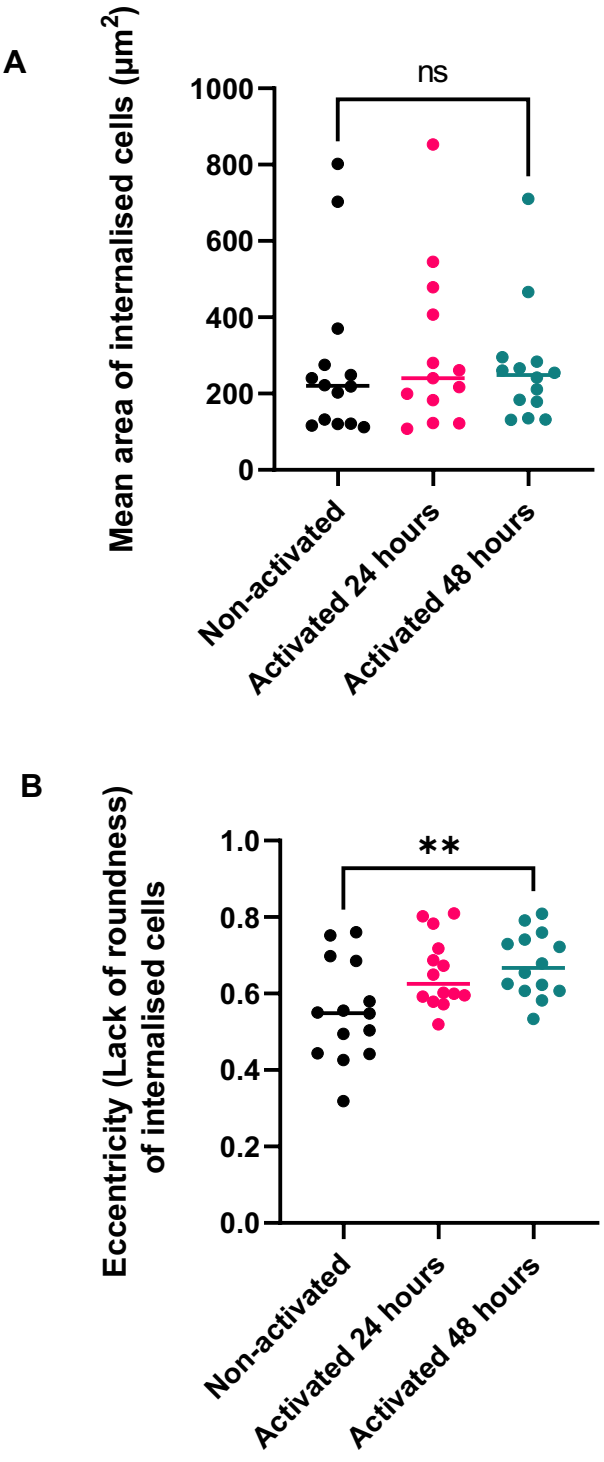

Figure 3. 11 48-hour activation increase the size and eccentricity of internalised CD8⁺ T cells compared with 24-hour activation. Quantification of size (A) and eccentricity (B) per 100 BEC of internalised CD8+ T cells in either non-activated, 24 h activated, or 48 h activated prior to co-culture. Nine fields of view were analysed from triplicate wells. Mean values/technical repeat are plotted. Values are normalised and displayed as a fold change from non-activated cells. n=5 biologically independent experiments. Statistics are derived from unpaired two-tailed Student's t-tests. p values are displayed for each statistical comparison made.

3.1.4. CD8+ T cells internalisation required actin cytoskeleton rearrangements to form discreet junctions with biliary epithelial cells and invade them.

The molecular mechanisms and cell-cell dynamics of the internalization process was assessed by electron microscopy imaging of 48 h activated CD8+ T cell interactions with BEC. I have then investigated the organisation of their actin cytoskeletons in the same model using phalloidin labelling. TEM revealed that these CD8+ T cells formed multiple discrete pseudopod-like connections with BEC at initial stages of contact (Fig. 3.12A). Airyscan confocal microscopy imaging of fluorescent dye and phalloidin-labelled CD8+ T cells demonstrated that these contacts were enriched with filopodia and that the actin cytoskeleton polarity of these CD8+ T cells was directed towards the BEC (Fig. 3.12A).

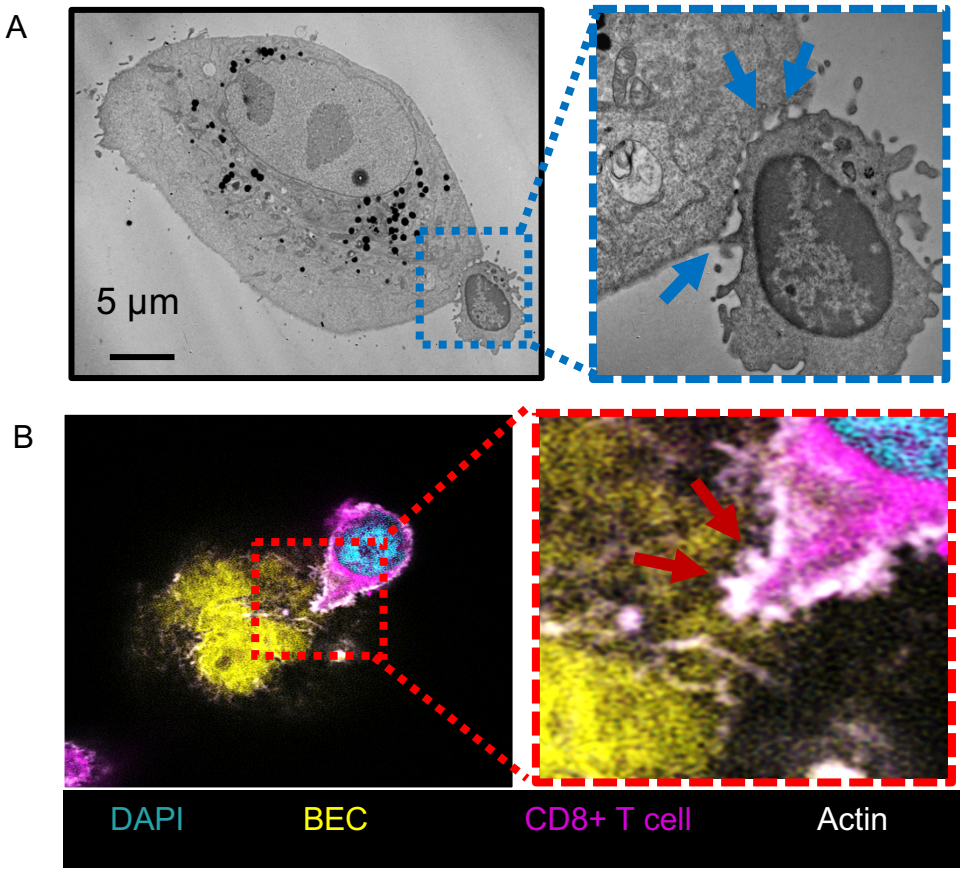

Figure 3. 12 Activated CD8 Activated CD8+ T cells undergo morphological changes and actin cytoskeleton rearrangements. A. Transmission election microscopy (TEM) micrograph showing a CD8+ T cell 1339 contacting the surface of a BEC. Right panel shows magnified image corresponding to the 1340 inset (blue box) showing pseudopodia-like elongated contacts made between the CD8+ T cell 1341 surface and BEC membrane (blue arrows). **B.** Airyscan confocal image of phalloidin-labelled 1342 (grey) co-cultured cells showing CD8+ T cell (CellTracker™ Red; magenta) polarising towards 1343 a BEC (CellTracker™ Green; yellow) and forming actin-rich filopodia at the BEC surface

Scanning electron microscopy (SEM) was used to further identify cellular interactions between BEC and T cells (Fig. 3.13). The same pseudopodia formation and discrete cell-cell contacts between BEC and CD8+ T cells were observed at locations where CD8+ T cells had adhered. Furthermore CD8+ T cells formed a higher number of discrete connections, and these T cells appeared to spread out across of the surface of the BEC.

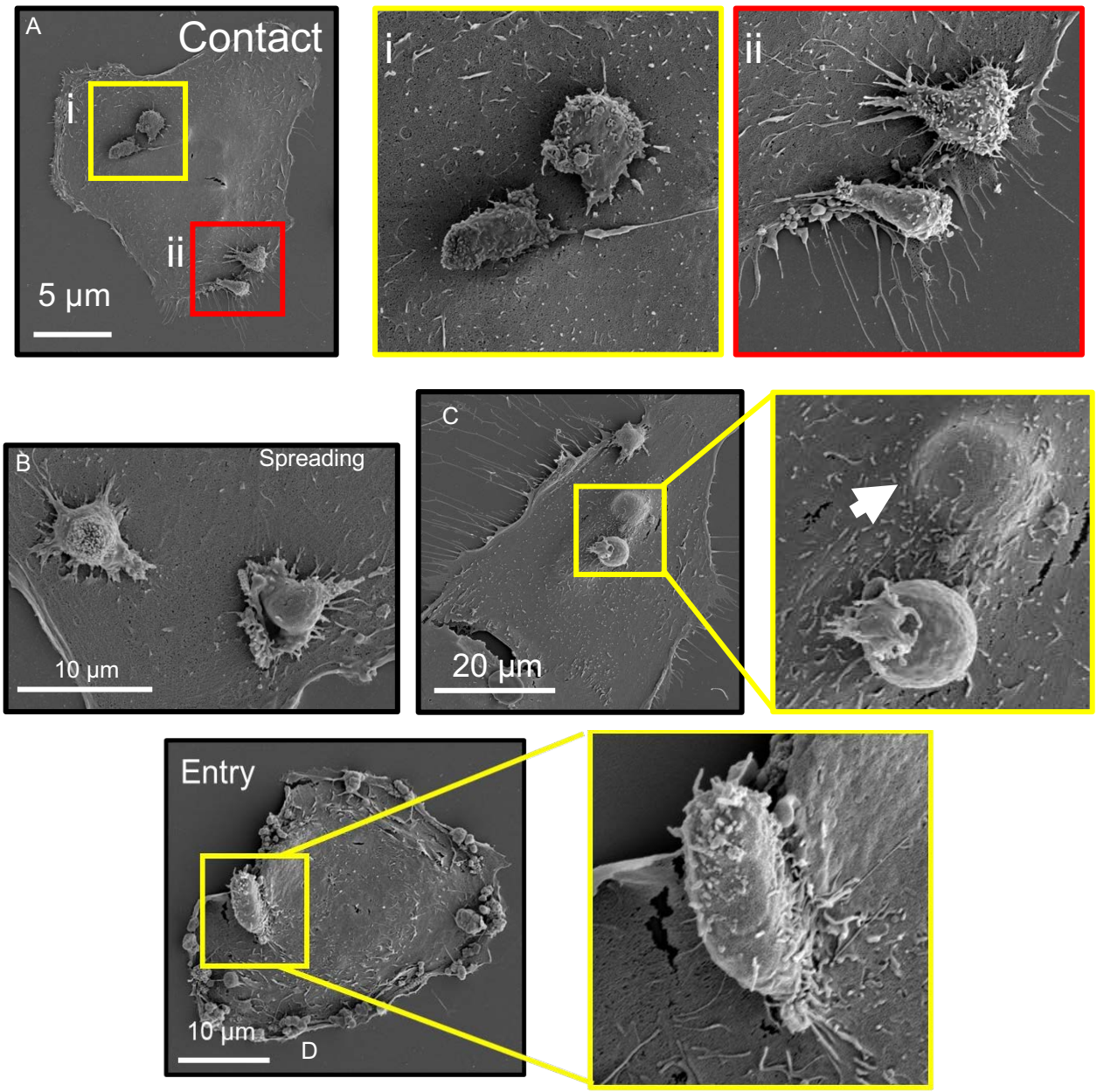

Figure 3. 13 Dynamics of CD8+ T cells interaction with BECs. A. Scanning electron microscopy (SEM) image showing CD8+ T cells on the BEC surface. Insets demonstrate T cell polarisation (i) and initial pseudopodia-like contacts (ii) between the cells. B. SEM image showing CD8+ T cells beginning to flatten out whilst formed multiple discrete contacts with BEC. C. SEM image showing two CD8+ T cells; one internalised into the BEC (white arrow) and the second one in contact with the surface. D. *Scanning electron microscopy (SEM) image showing polarised CD8+ T cell partially internalised into BEC. Inset (yellow box) shows the CD8+ T cell breaching the surface of the BEC.*

In some cases, CD8+ T cells appeared to polarise and breach the BEC membrane prior to their entry (3.13D). Additionally, some of the BECs had large bumps under their surface which resembled fully internalised T cells (3.13C).

To assess the necessity of T cell actin remodelling for the invasion of BEC, I used the co-culture HCA platform to test the effect of small molecular inhibitors which limit actin remodelling and other CICS formation processes (Fig. 3.14). Prior to co-culture with BEC, CD8+ T cells were pre-treated with wortmannin, H-1152 or cytochalasin D for 30 min. Wortmannin is a broad phosphatidylinositol 3-kinases (PI3K) inhibitor which was reported to disrupt suicidal emperipolesis(262). H-1152 is a highly-specific inhibitor of Rho Kinase (ROCK1; Ki = 1.6 nM) and has been reported to inhibit entosis(246). Cytochalasin D is a potent inhibitor of total actin remodelling which we reported to effectively inhibit enclysis(313). Pre-treatment concentrations were maintained throughout the 4 h co-culture period. Both wortmannin and cytochalasin D treatment of CD8+ T cells significantly reduced the frequency of their internalisation into BEC, whereas H-1152 did not produce the same result consistently (Fig. 3.14).

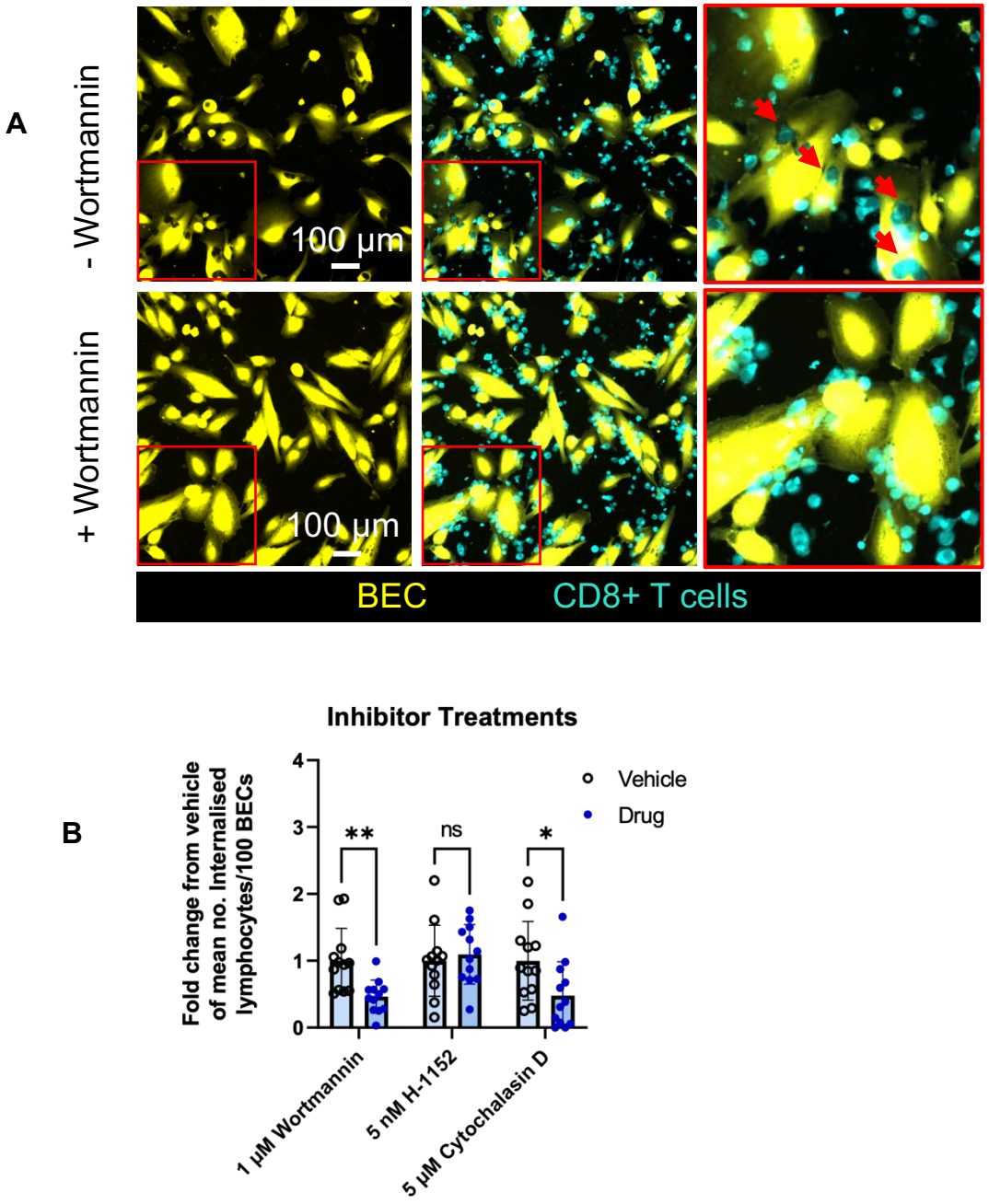

Figure 3. 14 Wortmannin and cytochalasin D treatment of CD8+ T cells significantly reduced the frequency of their internalisation into BEC. Representative images of co-cultured biliary epithelial cells (CellTracker Green™; cyan) and 48 h-activated CD8+ T cells (CellTracker Red™; cyan), comparing the frequency of internalisation of T cells into BEC following 30 min pre-treatment with 5 µM Wortmannin (broad Phosphoinositide 3-kinase inhibitor). Cells were co-cultured for 4 h and then labelled with wheat germ agglutinin conjugated with AlexaFluor 680 (WGA680, grey). G. Quantification of internalised 48 h-activated CD8+ T cells per 100 BEC in which T cells were pre-treated with 1 µM Wortmannin, 5 nM H-1152 (ROCK1 inhibitor), or 5 µM cytochalasin D (actin remodelling inhibitor) prior to co-culture. Nine fields of view were analysed from triplicate wells. Mean values of no. of internalised T cells/100 BEC/technical repeat are plotted. Values are normalised and displayed as a fold change from vehicle-treated cells.

3.1.5. Discussion

The data presented in this chapter build on the hypothesis that CD8+ T cells are indeed central in PBC pathogenesis. These experiments demonstrated that more eccentric CD8+ T cells could be found within BEC in PBC liver tissue *in vivo* and that this could be replicated *in vitro* from non-PBC blood 48 h after α-CD3/CD28 activation. The lymphocyte activation was concurrent with an overall enlargement of these cells prior to co-culture and a higher propensity for internalisation into BEC. In fact, these data demonstrate that CD8+ T cells are actively involved in their internalisation into BEC through dynamic cytoskeletal rearrangements, and inhibition of actin-remodelling reduces their entry.

The CIC events were observed in both early and late PBC stages; therefore, it is likely that CD8+ T internalisation is directly linked to its pathogenesis.

The entry mechanism of CD8+ T cells into BEC observed, was different to other described CICS of the liver, based on differences in phenotype and protein-protein interactions. Our lab recently reported the process of enclysis; the specific capture of CD4+ T cells by hepatocytes which frequently resulted in the deletion of regulatory T cells(313). In contrast to enclysis, where hepatocytes undergo membrane alterations and form ruffles to assist the engulfment of CD4+ T cells, minimal rearrangements were seen on BEC which possessed adhered or internalised CD8+ T cells. Additionally, CD4+ T cells were rarely observed to invade BEC after TCR-mediated activation. CD8+ T cell invasion into BEC did share mechanistic similarities with “suicidal emperipolesis”; both processes were sensitive to PI3K inhibition and detailed events of active invasion by CD8+ T cells into other cells(262). To corroborate the similarity Wortmannin, reported to disrupt suicidal emperipolesis(262), significantly reduced the frequency of the internalisation. However, unlike suicidal emperipolesis, in our model the T cell

internalisation were rarely associated with autoreactivity and the T cells were not deleted as consequence of the internalisation.

In the CICs herein described, the internalised cells were larger and more eccentric compared with the non-internalised cells. Therefore, these cells possess a wider surface area for forming cell-to-cell contacts and better capacity for cytoskeletal rearrangements. As such, they would be able to form more points of contact with BEC, as identified by SEM and phalloidin staining.

It should be noted that ROCK1 inhibition did not consistently reduce internalisation. Therefore, it is likely that other mechanisms may exist which permit CD8+ T cell entry into BEC which are dependent on PI3K signalling and actin remodelling but do not require ROCK1 activity.

The purpose and “immunological motivations" of CD8+ T cells internalisation into BEC remain unclear. It is unlikely that this CD8+ T cell subset has evolved specifically for intentionally killing invaded cells from the inside; BEC that were possessing T cells did not display any morphological changes associated with cell death when analysing high-content assays and viewing the cells ultrastructure with SEM. However, Zhao and colleagues reported that the frequency of CD8+ T cells found within BEC was correlated with increased apoptosis of BEC in patients with PBC(316). How BEC become apoptotic following this internalisation is still uncertain and further investigations into how internalised CD8+ T cells disrupt BEC intracellular processes would provide insight into whether this process contributes directly to BEC cytotoxicity associated with PBC.

3.2. The expression of E-cadherin is instrumental for biliary epithelial cells invasion and is expressed by T CD8 cells

N.B. *the content presented in this chapter are part of a paper recently published(317).*

3.2.1. Introduction

The presence of tissue resident cells is enriched in the liver. Among them, the tissue-resident memory CD8+ T cells are a special subset, which populate non-lymphoid organ and represent one of the first line of defence in these organs, being highly activated by antigen rechallenge(325). Huang and colleagues recently reported human data showing that cytotoxic CD8+ T cells population in PBC liver tissue was autoreactive and possessed a CD103+ tissue resident phenotype(238). Zhu and colleagues used single-cell RNA sequencing to further characterise Il12b-/-Il2ra-/- mice as model of autoimmune cholangitis. They identified a population of T CD8+ Trms highly cytotoxic and capable to induce apoptosis of BECs. They proved also that this cell subset express high level of PD-1. They took advantage of this to create a chimeric antigen receptor to target PD-1 expressing CD8+ Trm cells. This approach selectively depleted liver Trms and alleviated liver inflammation in the model. This line of evidence further demonstrates the crucial role of Trms subset in the genesis of the biliary damage in PBC. However, to date, the exact mechanism of the CD8+ T cell crosstalk with the biliary epithelium remains elusive and so it does the mechanism of damage.

In this chapter I will describe a subset of liver resident memory T cells expressing e-cadherin. The expression of such adhesion marker, more typical of epithelial cells, will be shown as key factor for the internalisation of lymphocyte within the cytoplasm of BECs. The frequency of this internalisation event was found to be notably enriched in PBC liver tissue compared to that of non-cirrhotic donor livers and those from patients with other chronic liver diseases.

3.2.2. Internalised CD8+ T cells observed within biliary epithelial cells *in vivo* are CD69+CD103+, and are enriched in patients with Primary Biliary Cholangitis.

Having identified that CD8+ T cells undergo cytoskeletal and morphological rearrangements when internalising into BEC, I hypothesised that they would express specific surface proteins that would facilitate this process. I further postulated that the frequency of CD8+ T cells expressing such proteins would be highest after 48 h activation due to the higher frequency of internalisation observed with these cells. I phenotyped and compared matched HFE-derived peripheral blood CD8+ T cells and CD4+ T cells using flow cytometry at 24 h and 48 h post-activation (Fig. 4.1). I specifically interrogated the expression of lymphocyte adhesion molecules, residency markers, and chemokine receptors associated with migration to the liver and localisation around biliary epithelium (223, 326, 327) (figure 4.1 panel A and B). The percentage of 24 h activated CD8+ cells expressing chemokine receptors, CXCR3 and CXCR6 were higher compared to patient-matched activated CD4+ T cell. Both CD8+ and CD4+ T cells displayed similar expression levels of adhesion molecules CD49a and chemokine receptor, CCR6.

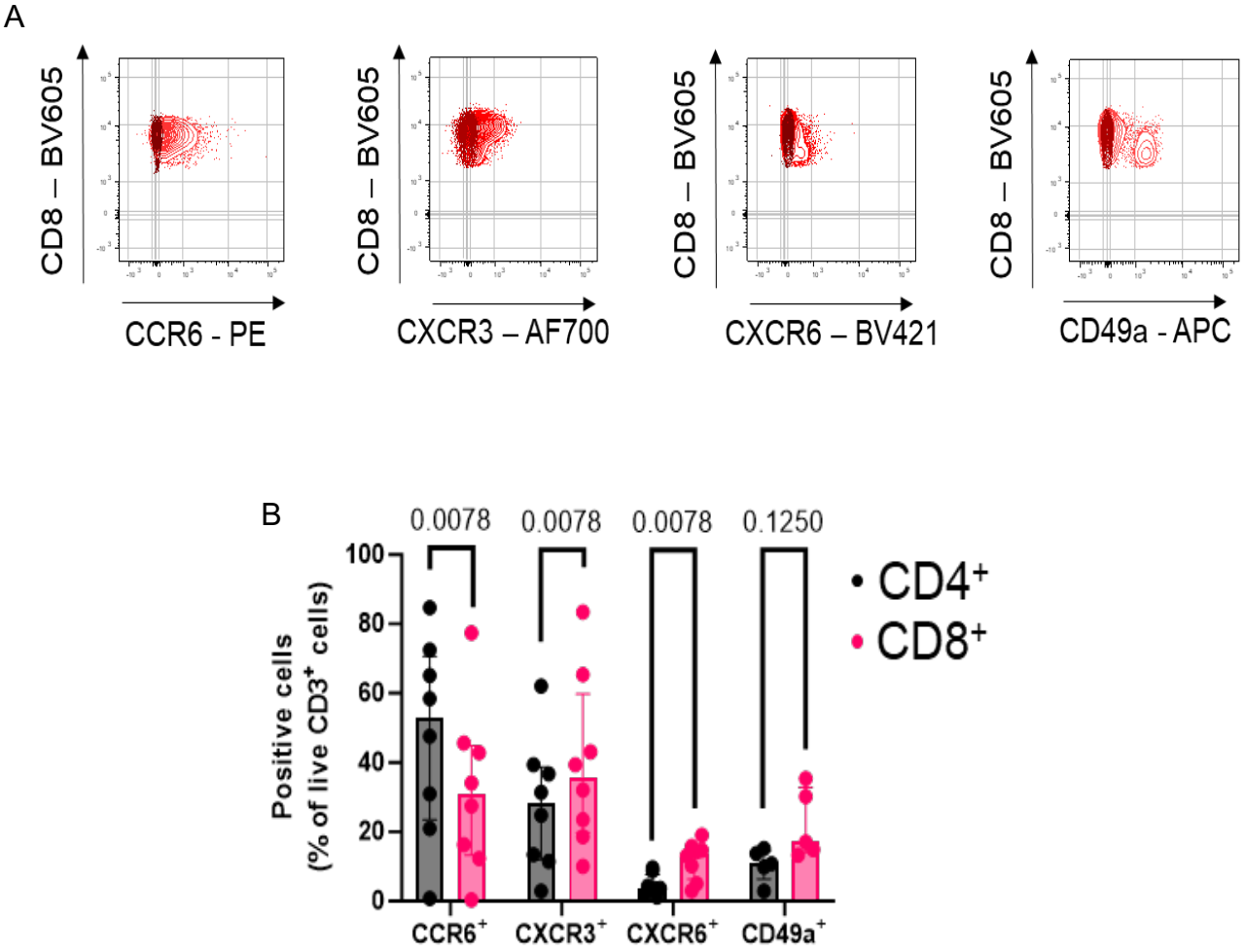

Figure 4.1 Peripheral blood derived CD8+ and CD4+ T cells express biliary epithelium homing chemokine receptors. Peripheral blood derived CD8+ and CD4+ T cells were phenotyped using flow cytometry specifically for the expression of receptors associated with recruitment, residency markers, and cytolytic enzymes. A. Representative contour plots (dark red) for CCR6 (n=8), CXCR3 (n=8), CXCR6 (n=8), and CD49a (n=5) expression by 24 h activated CD8+ T cells. Black contours show isotype match control plots for each individual marker of interest. B. Percentage of CD4+ and CD8+ T cells expressing each cell surface marker shown in A 24 h post activation with α-CD3/CD28 stimulation. Values for individual patient samples are plotted. p values were generated using two-tailed Wilcoxon Signed-Rank tests.

CD69 expression was also observed on both 24 and 48 h activated CD8+ T cells and CD4+ T cells, as expected. However, upregulation of the tissue resident memory (Trm) and intraepithelial lymphocytes (IEL) marker, CD103, was significantly higher in CD8+ T cells 48 hr post-activation compared to matched CD4+ T cells (Fig. 4.2 panel A-C).

Both CD69 and CD103 are markers of intraepithelial lymphocytes(328-330). CD8+ T cells also displayed more frequent expression of Granzyme B, compared to non-activated CD8+ T cells (Fig 4.2 panel D).

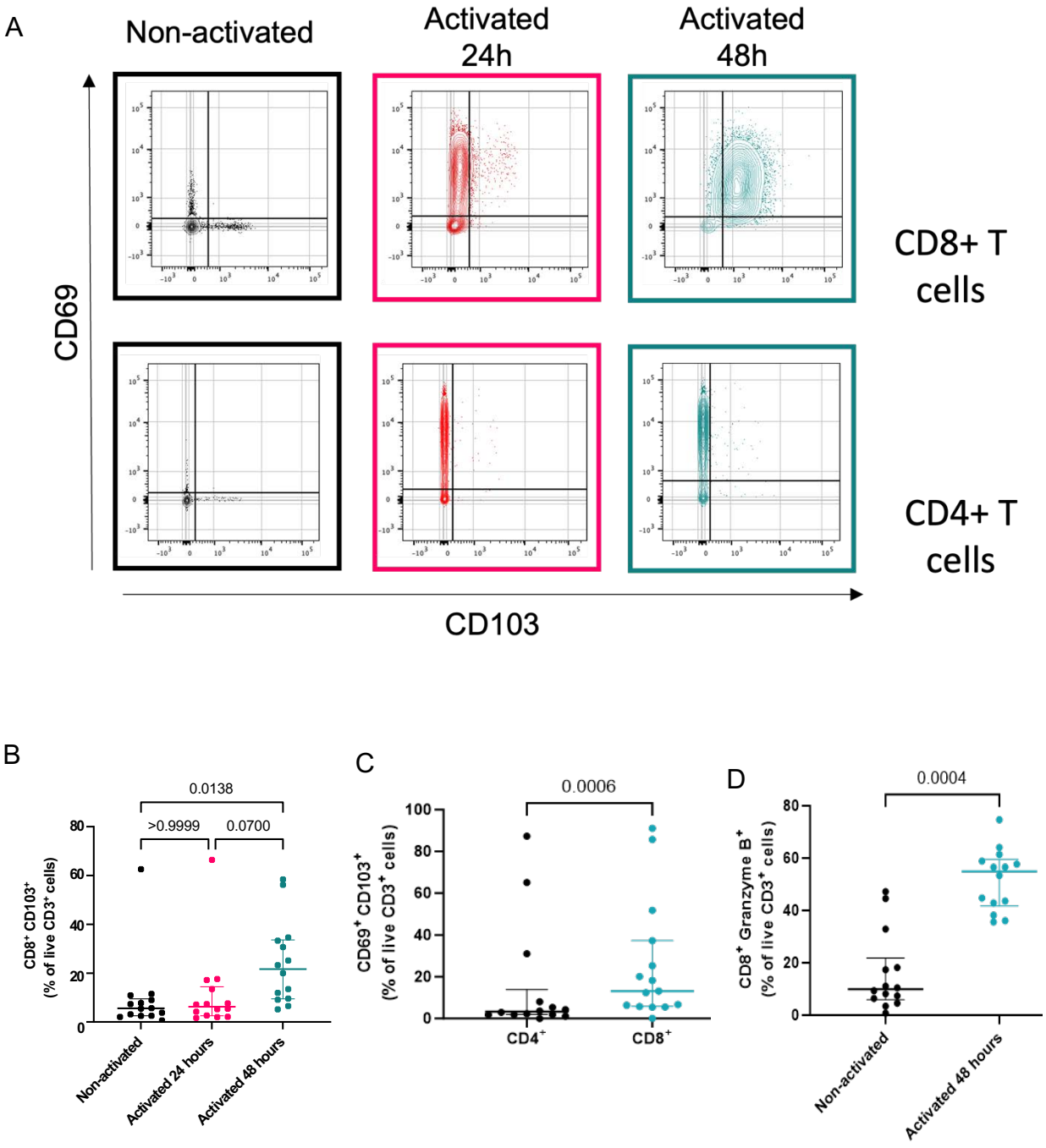

Figure 4.2 Assessment of CD69 and CD103 expression by peripheral blood-derived CD8⁺ T cells via flow cytometry. Cells were phenotyped in the absence of activation stimuli (black) or following 24 h (red) or 48 h (cyan) after α-CD3/CD28 activation. Panel A: representative contour plots showing CD69 and CD103 expression by non-activated, 24 h-activated, 48 h-activated CD8⁺ and CD4⁺T cells. Panel B: Percentage of CD8+ T cells expressing CD103. n = 14 independent patient samples. Panel C: Comparison of the percentage of CD69+ CD103+ cells between CD4+ and CD8+ T cells 48 h post α-CD3/CD28 stimulation (n=15). Panel D: comparison of percentage Granzyme B expression by CD8+ T cells between non-activated cells and 48 hr post α-CD3/CD28 stimulation (n=14).

Multiplex IHC staining of PBC liver tissues confirmed that CD8+ T cells found within BEC also expressed both CD69 and CD103 (Fig. 4.3).

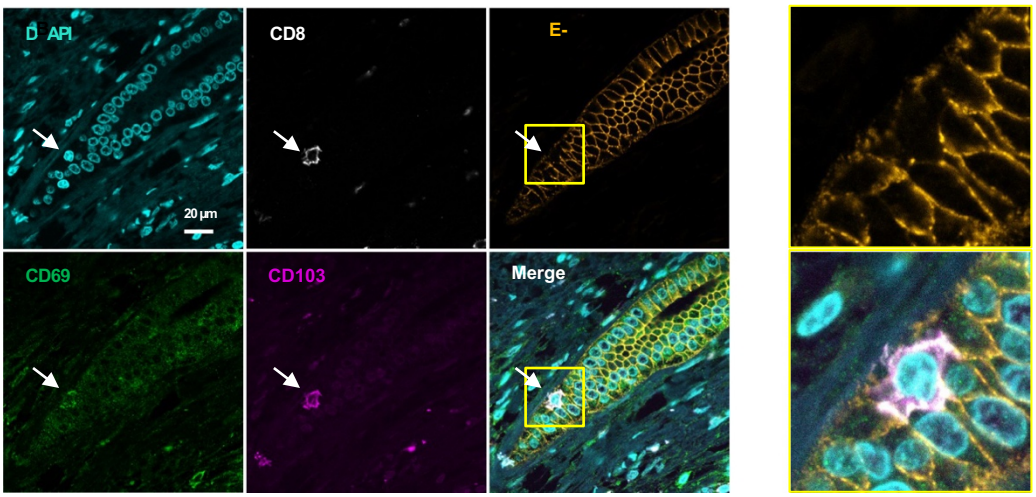

Figure 4.3 Immunohistochemistry (IHC) staining of a liver tissue section from a patient with primary biliary cholangitis (PBC) showing CD69^{+} (green), CD103^{+} (magenta) CD8^{+} (grey) T cell (white arrow) internalised within E-cadherin^{+} (orange) biliary epithelial cells (BEC) which forma bile duct. Right panel shows magnified images of left panel inset (yellow box)

To confirm complete internalisation of these cells, 50 µm-thick tissue sections (compared to the typical 3-4 µm thickness) of PBC liver were stained by IHC (Fig. 4.4) as previously described (313).

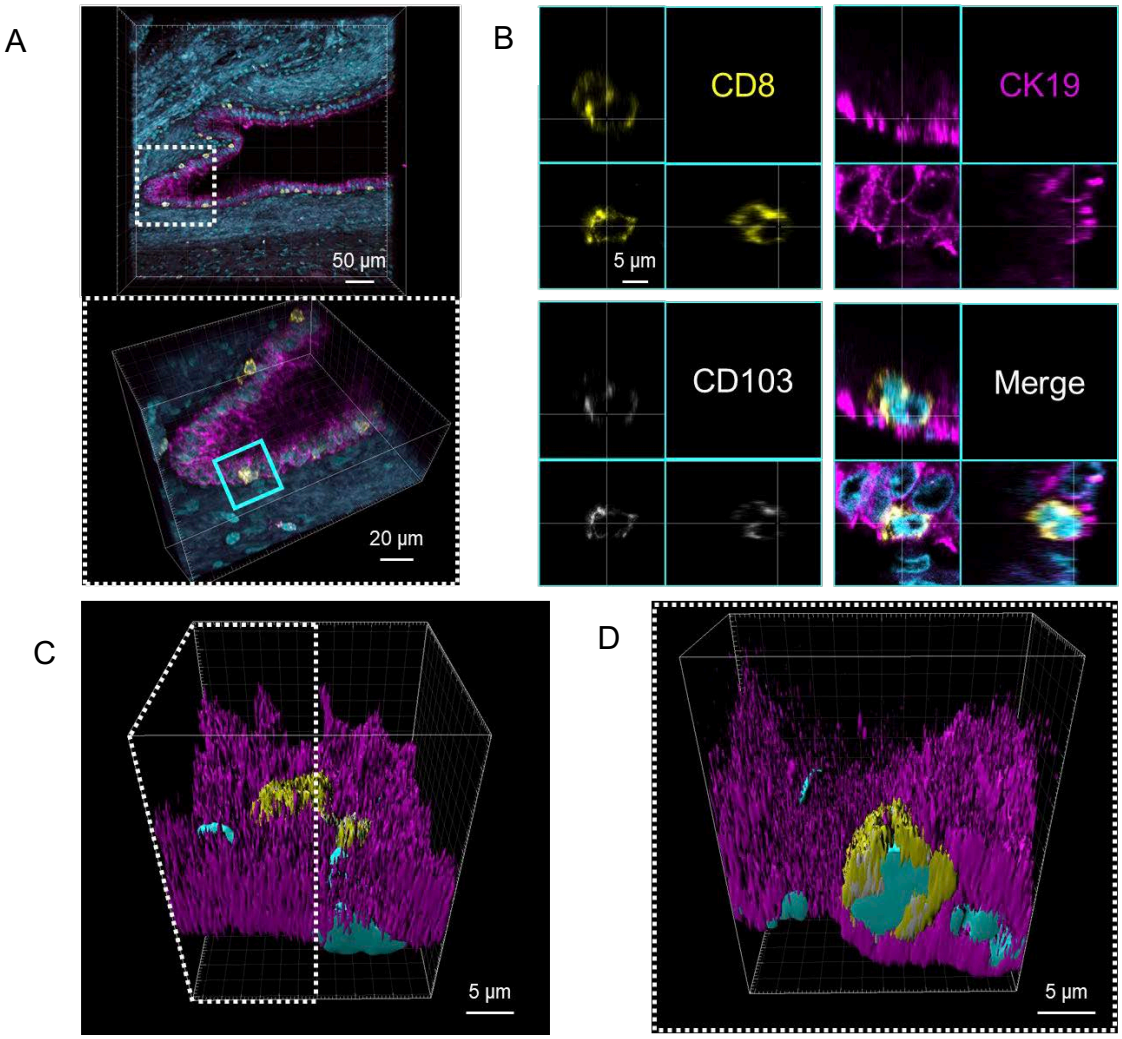

Figure 4.4 CD103+ CD8+ T cells are internalised within CK19+ BEC in human PBC livers. A. Immunohistochemistry (IHC) staining of a 50 µm-thick primary biliary cholangitis (PBC) liver tissue section showing cytokeratin-19+ (CK19; magenta) bile ducts associated with CD103+ (grey) CD8+ (yellow) T cells. Top panel shows reconstructed Z-stack as viewed from above. Bottom panel shows angled view of inset from top panel (white dotted box). **B.** Orthographical, multichannel representations of **A** bottom panel inset (white box) demonstrating CD103+ CD8+ T cell with CK19 staining of biliary epithelial cells (BEC) localised around it. **C.** 3D-volume rendered representation of merged images shown in **B**. **D.** Cross-sectional view of panel **C** representing the area highlight by the dotted line. Nuclear staining using DAPI is shown in cyan.

Z-stack confocal microscopy of this thick-cut section confirmed the presence of a CD103+ CD8+ T cell enclosed within BEC expressing CK19 and the ligand of CD103, E-cadherin(331) (Fig 4.5).

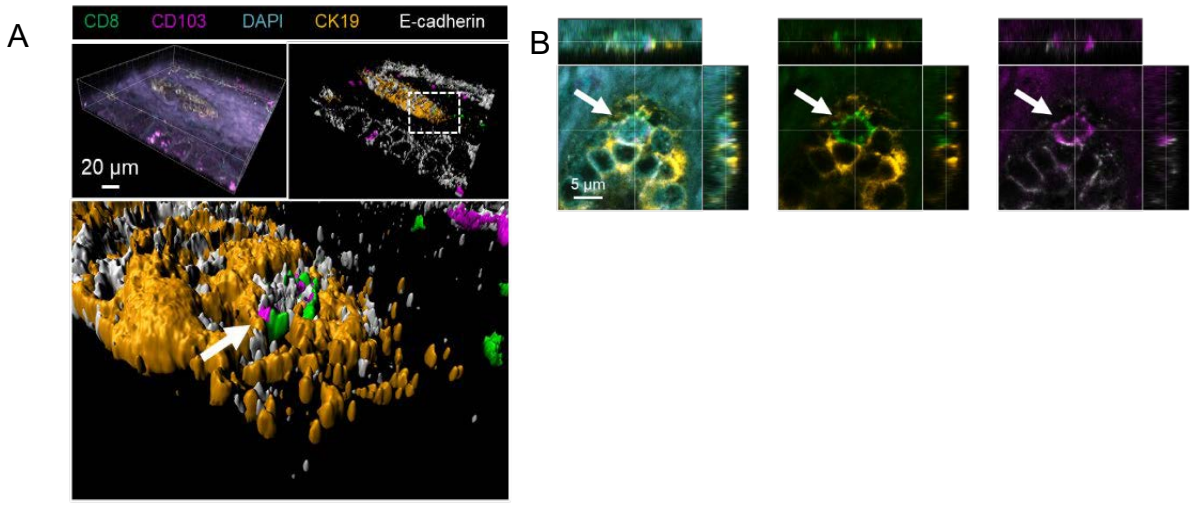

Figure 4.5 CD8+ T cells internalised by BEC express CD103. A. Immunohistochemistry (IHC) staining of a 50 µm-thick primary biliary cholangitis (PBC) liver tissue section showing a CD103+ (magenta) CD8+ (green) T cells adhered to E-cadherin+ (grey) cytokeratin-19+ (CK19; orange) biliary epithelial cells (BEC) which form the bile ducts. Top right panel shows 3D-volume rendered version of the left image. Bottom panel shows magnified image from of the top-right panel (white dotted box) demonstrating CD103+ CD8+ T cell, surrounded by E-cadherin and CK19 (white arrow). DAPI (cyan) was not rendered to enhance the visualisation of the internalised T cell. **B.** Orthographical, multichannel representations of magnified image of the part **A** bottom panel, showing the localisation of the CD103+ CD8+ T cell.

The next step has been to perform IHC-based semi-quantitative analysis of FFPE liver tissue sections from explanted diseased livers from patients with PBC, autoimmune hepatitis (AIH), and alcoholic liver disease (ArLD), as well as non-cirrhotic donor livers (N=6 each; Fig. 4.6 C; Supplementary Data 5B-C).

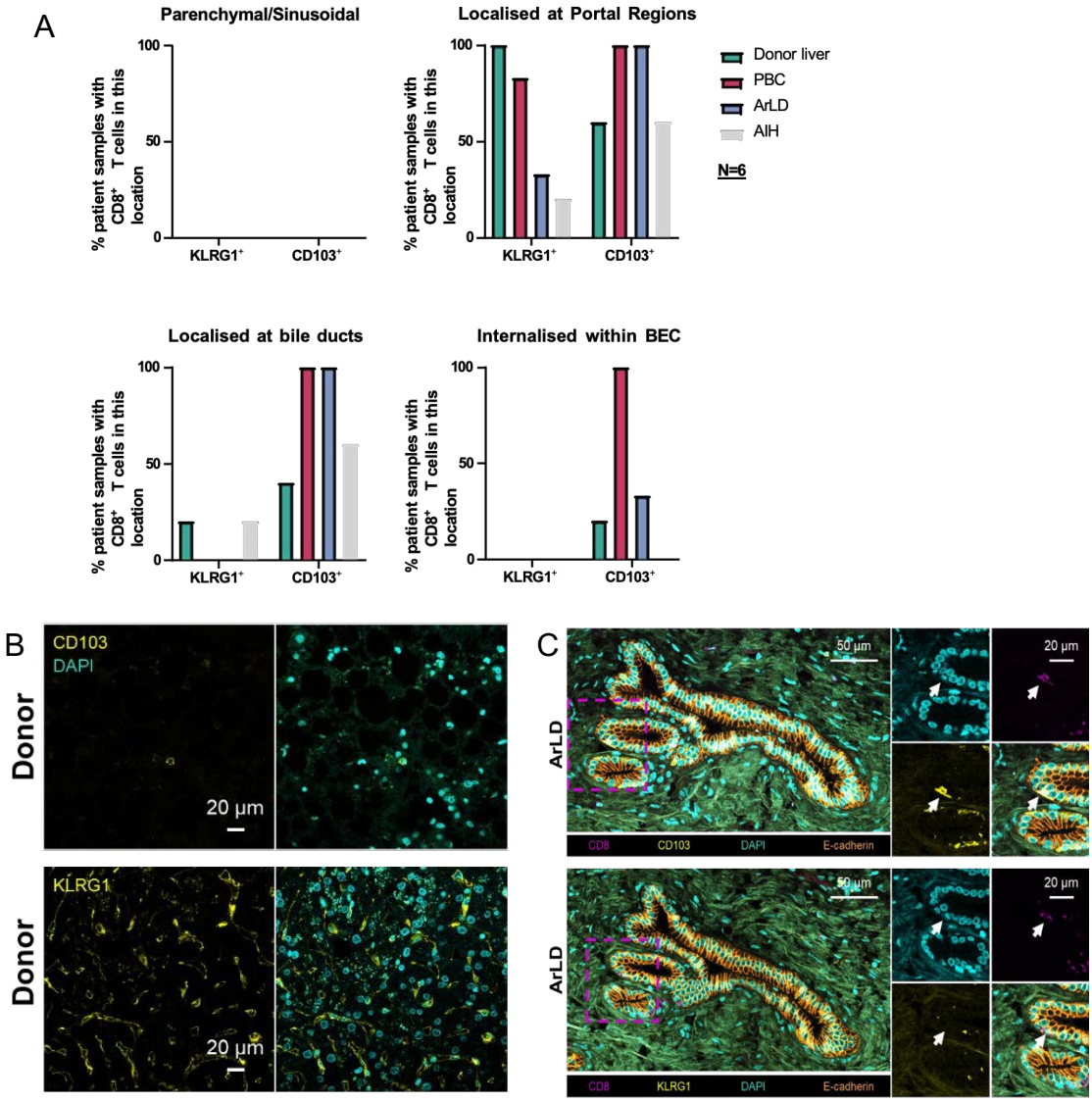

Figure 4.6 Internalised CD8$^+$ T cells are enriched for CD103 but not for KRLG1. Panel A: semi-quantification of IHC-stained liver tissues for the presence of CD103$^+$ CD8$^+$ and KLRG1$^+$ CD8$^+$ T cells in specific locations within liver tissues from non-cirrhotic donors and patients with PBC, ArLD or AIH. n = 6 independent patient samples per disease condition. Bars represent the percentage of tissues analysed displaying a minimum of three CD103+ CD8+ or KLRG1+ CD8+ T cells in the location stated in the graph titles. **Panel B**: example confocal micrographs of liver parenchyma from non-cirrhotic donor liver livers stained by IHC for CD8 and either CD103 (top panel; yellow) or KLRG1 (bottom panel; yellow). **Panel C**: location-matched representative images of serial liver tissue sections from a patient with ArLD stained for E-cadherin (orange), CD8 (magenta) and either CD103 or KLRG1 (yellow). Right panels show multichannel representations of left panel insets (purple dotted boxes). Arrows in upper panel show a CD103+ CD8+ T cell adhered to the surface of E-cadherin+ BEC. Bottom panel shows that the same cells do not express KLRG1 (bottom right panel).

The presence of CD8+ T cells in the parenchyma or sinusoids, at portal regions (within of 50 μm of portal triads), at bile ducts (within 10 μm) or within BEC (internalised) was quantified. Simultaneously, CD8+ T cells expressing CD103 were compared to Killer cell lectin-like receptor subfamily G member 1 (KLRG1), as both molecules are binding partners of E-cadherin but elicit opposite effects on T cell activity following their engagement, and are associated with different T subtypes with contrasting origins (resident vs blood derived); engagement of CD103 stimulates T cell activity and is associated with tissue resident cells, whereas KLRG1 is a co-inhibitory molecule and is typically expressed by circulating T cells (332-334). KLRG1+ CD8+ T cells were recently reported to be enriched within portal regions in patients with PBC(334). I too found that KLRG1+ CD8+ T cells were more frequently observed in portal regions compared to other diseased livers. These cells were also found in the parenchyma and portal regions of 100% of donor livers, but rarely observed within proximity of bile ducts across all conditions and were not found within the BEC. In contrast, CD103+ CD8+ T cells were observed in portal regions across all conditions and in the parenchyma or sinusoids in donor, AIH and ArLD livers, but not in PBC. These cells were also found in proximity to bile ducts in all PBC and ArLD cases (Fig 4.6 Panel B), as well as a smaller proportion of donor and AIH patients. However, despite being localised at bile ducts. internalised CD103+ CD8+ T cells were rarely internalised within BEC in donor and ArLD patients. By contrast, every PBC patient analysed possessed CD103+ CD8+ T cells contained with BEC. These observations demonstrated that the ability to invade BEC is restricted to CD103+

CD8+ T cells and, although not exclusive, was a constant histological feature of PBC.

As internalised CD8+ T cells within BEC consistently expressed CD103, we postulated that CD103 expression on CD8+ T cells and likely the interaction with E-cadherin expressed by BEC would be integral to the process of internalisation. Co-cultures were performed between BEC, and 48 h activated CD8+ T cells in the presence of αhCD103 antibodies (Figure 4.7).

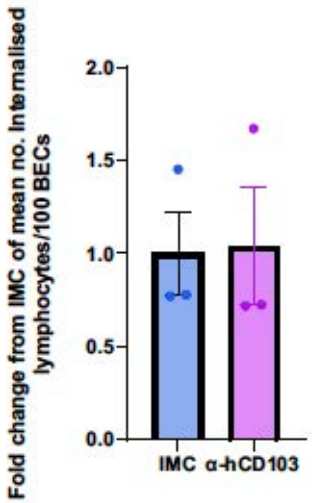

Figure 4.7 Blocking CD103 does not have any effect on the the number of internalised cells. Quantification of internalised 48 h activated CD8+ T cells per 100 BEC following 4 h co-culture. T cells were pretreated with α-CD103 antibody or an isotype-matched control (IMC). Nine fields of view were analysed from triplicate wells. Mean numbers of internalised CD8+ T cells/100 BEC/technical repeat are plotted. Values are normalised and displayed as a fold change from IMC-treated cells. n = 1 biologically independent experiment.

However, no effect was observed on CD8+ T cell internalisation following CD103 blockade. Taken together, CD8+ T cells expressing CD103 are the population capable of invading BEC regardless of disease setting, although CD103 binding is not a mechanistic requirement for CD8+ T cell internalisation.

3.2.3. The expression patterns of E-cadherin by activated T cells is consistent with the characteristics of their internalisation into biliary epithelial cells.

To understand why CD8+ T cell internalisation into BEC appeared not to require CD103 expression, we performed ICC staining of co-cultured BEC and 48h-stimulated CD8+ T cells for E-cadherin, the ligand of CD103. Surprisingly, E-cadherin appeared to be more associated with invading CD8+ T cells than the infiltrated BEC (Fig. 4.8).

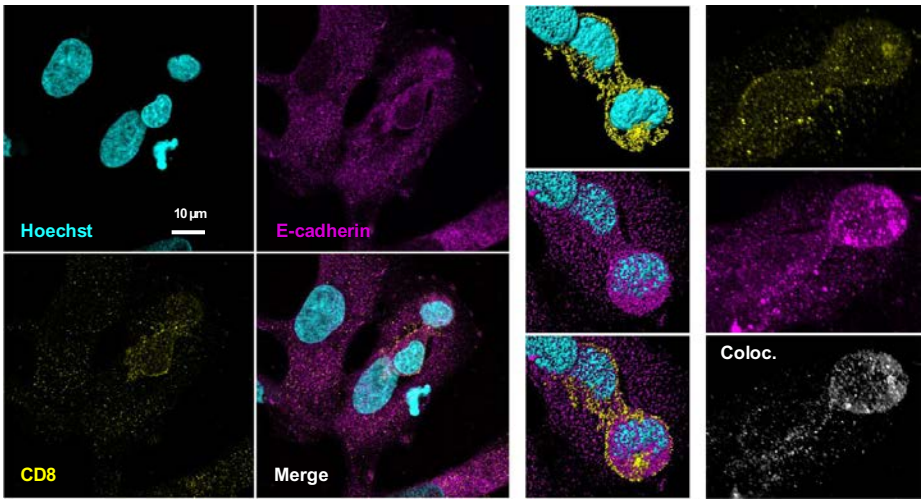

Figure 4.8 E-cadherin expression is associated with CD8$^+$T cells. Airyscan super resolution confocal micrographs of 4 h co-cultured BEC and 48 h activated CD8$^+$T cells, stained by immunocytochemistry (ICC) for CD8 (yellow) and E-cadherin (magenta). Middle panels show 3D-volume rendered versions of left panel that were acquired using Z-stack microscopy. Right panels show zoomed images of 3D reconstructed Z-stacks from left panel. Bottom section of right panels shows colocalised CD8 and E-cadherin signal (grey).

To rule out the possibility that T cells were scavenging soluble E-cadherin released from the BEC, we phenotyped peripheral blood-derived CD8+ T cells, which been activated for different lengths of time, using flow cytometry (Fig. 4.9).

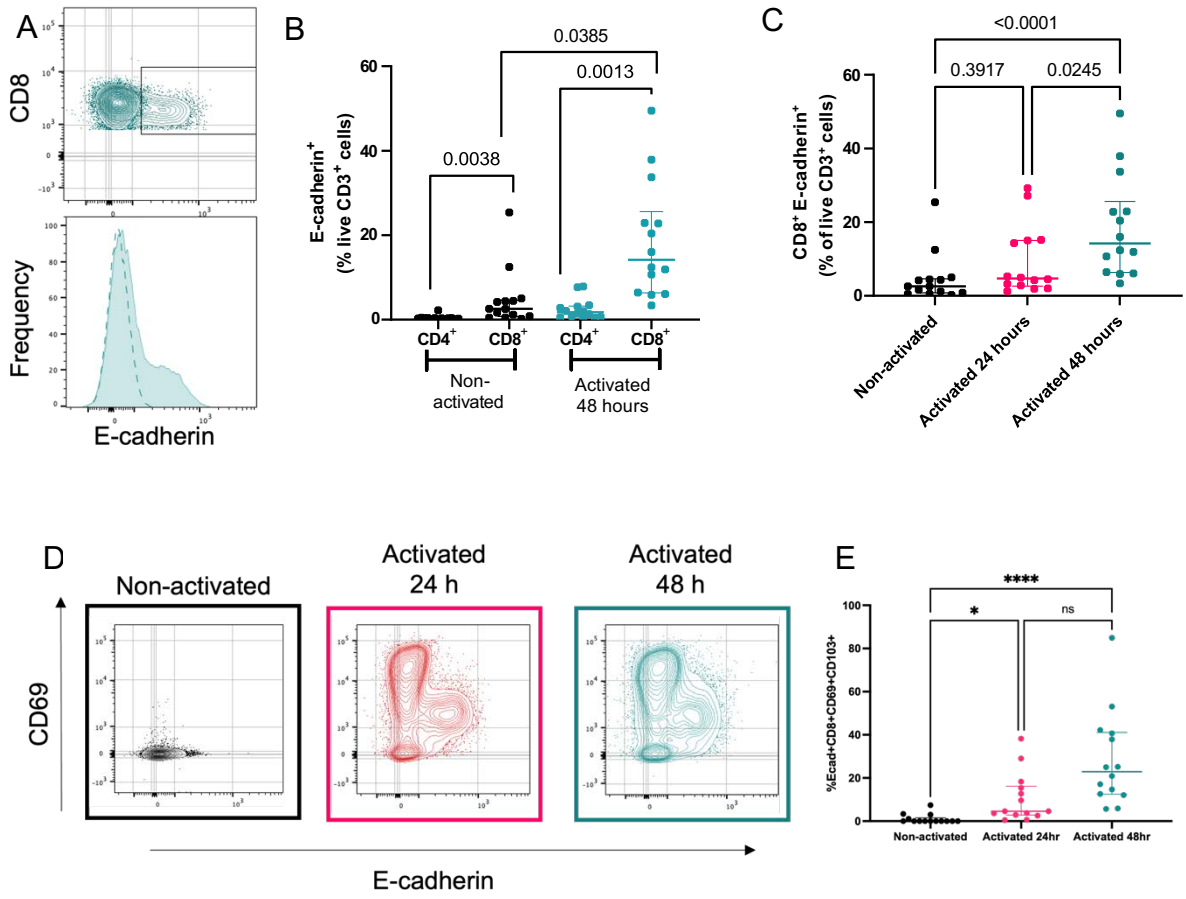

Figure 4.9 The expression patterns of E-cadherin by activated T cells are consistent with the characteristics of their internalisation into BEC. Panel A: representative graphs (contour plot and histogram) of surface E-cadherin staining of $CD8^+$ T cells 48 h following α-CD3/CD28 stimulation, as assessed by flow cytometry. Panel B-E: flow cytometry phenotyping of PBMCs isolated from patients undergoing venesection treatment for haemochromatosis (HFE). Cells were phenotyped either when non-activated or 24 h (magenta data points) or 48 h (cyan data points) after α-CD3/CD28 activation. Panel B: percentage of E-cadherin$^+$ $CD8^+$ T cells comparing non-activated and 48 h-activated $CD4^+$ and $CD8^+$ T cells. Error bars present median and interquartile range. n = 14 biologically independent patient samples. Panel C: percentage of E-cadherin$^+$ $CD8^+$ cells without activation and either 24 h or 48 h post-activation. Error bars present median and interquartile range. n = 14 biologically independent patient samples. Panel D: representative flowcytometry contour plots comparing E-cadherin and CD69 expression patterns in $CD8^+$ T cells in the absence of activation (black) or following 24 h (red) or 48 h (cyan) activation with α- CD3/CD28. Panel E: Percentage of $CD8^+$ T cells expressing E-cadherin, CD69, and CD103 assessed via flow cytometry. Error bars present median and interquartile range. n = 14 biologically independent patient samples.

CD8+ T cells were shown to express E-cadherin at 48 h post-activation (Fig. 4.9 Panel A). Matching the observed patterns of internalisation frequency, the percentage of E-cadherin+ CD8+ T cellswas significantly higher 48 h post stimulation compared to 24 h (Fig. 4.9 Panel C and E). Increases in expression of E-cadherin were primarily observed for activated CD8+ T cells and were rarely observed in CD4+ T cells (Fig. 4.9 Panel C).

Further phenotyping demonstrated that E-cadherin+ CD8+ T cells also expressed high levels of CD103 and intermediate levels of CD69 (Fig. 4.9 Panel D). The percentage of CD103+ CD69+ E-cadherin+ CD8+ T cells continued to increase 48 h post-activation (Fig. 4.9 Panel E). These data show that CD8+ T cells upregulate surface expression of E-cadherin following TCR stimulation. Furthermore, the observed expression patterns of E-cadherin were aligned with the frequency of CD8+ T cell internalisation into BEC, suggesting a mechanistic link of E-cadherin to this process.

3.2.4. CD8+ T cells from adherens junction through E-cadherin-β-catenin interaction.

E-cadherin is most widely associated with the formation of adherens junctions through homodimerization and interactions with β-catenin(335, 336). This same interaction has been linked mechanistically to entosis(246). We hypothesised that surface expressed E-cadherin on CD8+ T cells may behave similarly and be sufficient to form adherens junctions with BEC. Initially, we aimed to establish if the CD103+ CD69+ CD8+ population found within BEC in PBC tissues expressed E-cadherin. Initially, we performed multiplex fluorescence IHC staining of PBC liver tissue (Fig. 4.10).

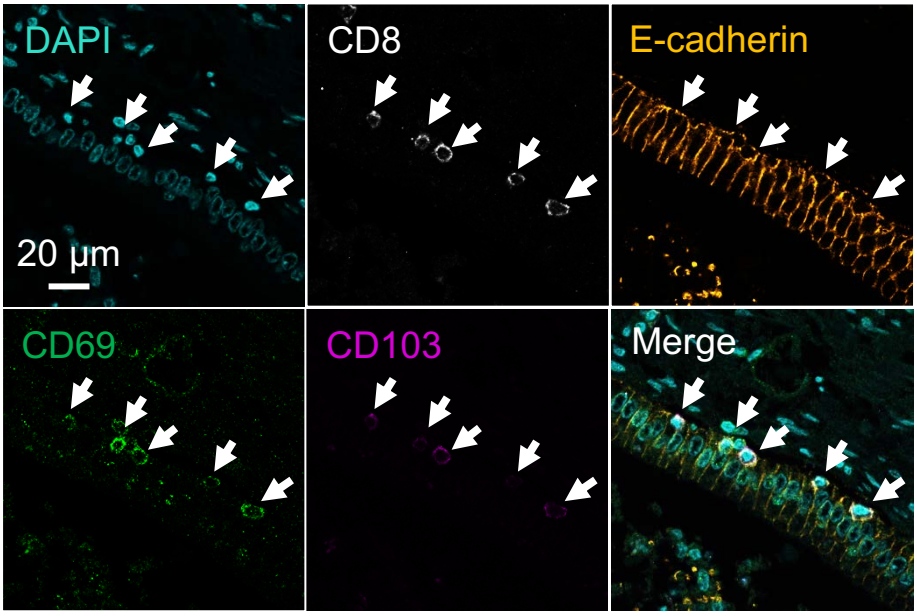

Figure 4.10 CD8+ T cells interact with biliary epithelial cell (BEC) membranes through E-cadherin – β-catenin interactions. Immunohistochemistry staining of a liver tissue section from a patient with Primary Biliary Cholangitis (PBC), showing CD69+ (green), CD103+ (magenta) CD8+ (grey) T cells adhered to bile ducts (white arrows). E-cadherin staining (orange) intensifies at contact point between T cell and epithelial cell. White arrows show attached or partially internalised CD69+ CD103+ CD8+ T cells.

To establish whether E-cadherin+ T cells could form conventional β-catenin interactions with BEC in these livers, we assessed the distribution of β-catenin expression in PBC liver in relation to E-cadherin and CD103+ CD8+ T cells using multiplex IHC (Fig. 4.11 Panel A). We observed a CD103+ CD8+ T cell adhered to the surface of a bile duct. Z-stack confocal microscopy demonstrated that CD103 expression overlapped with areas where β-catenin and E-cadherin colocalised (Fig. 4.11).

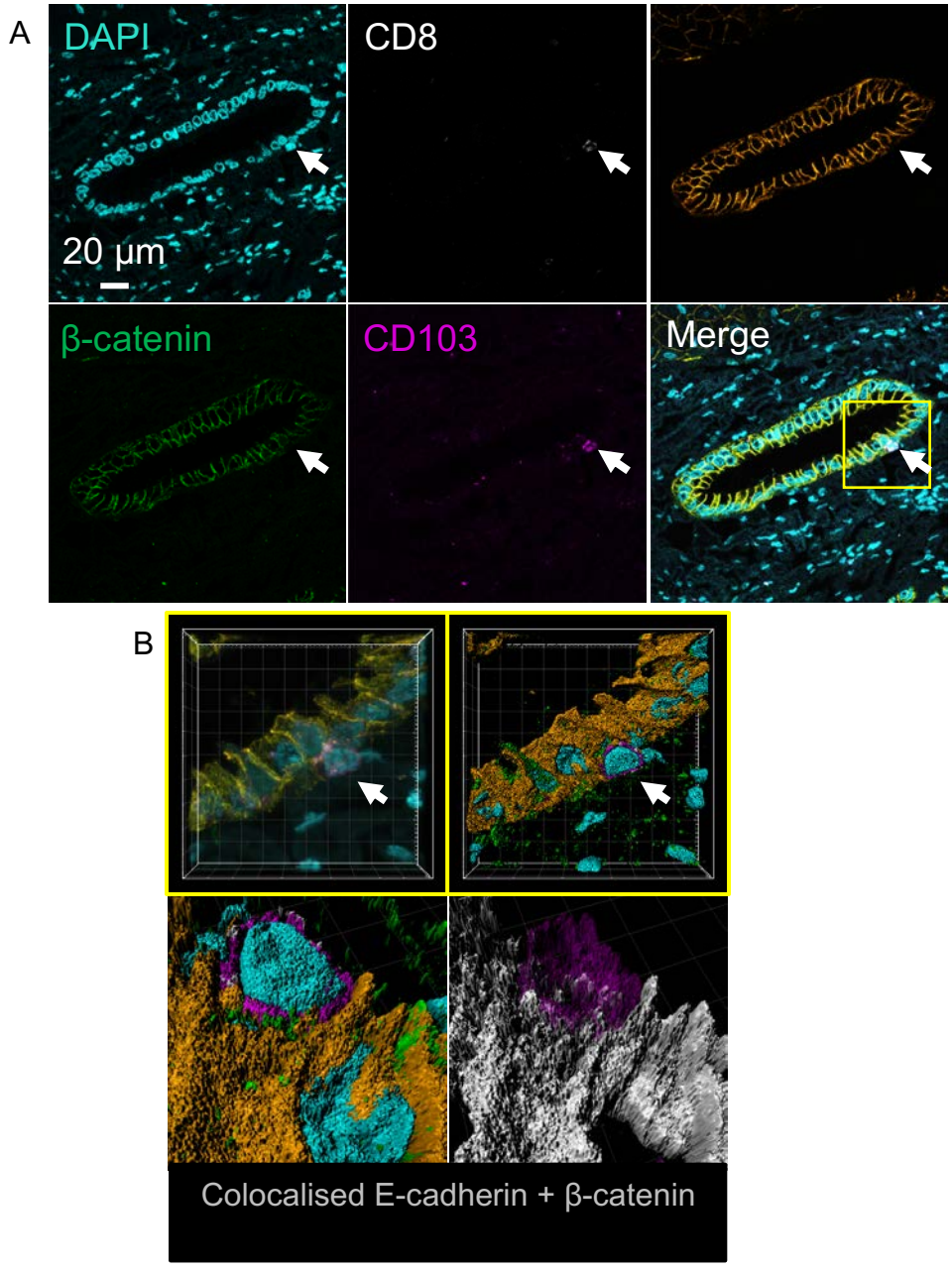

Figure 4.11E-cadherin+CD69+CD103+CD8+ T cells interaction with β-catenin. Panel A: Immunohistochemistry staining of a liver tissue section from a patient with PBC, showing CD103+ (magenta) CD8+ (grey) T cell adhered to bile ducts comprised of BEC expressing E-cadherin (orange) and β-catenin (green). **Panel B:** Higher power, Z-stack confocal micrograph showing magnified region of part B (yellow box). Top row shows 3D-reconstruction (left) and 3D-volume rendered version (right). Bottom row shows magnified image of the BEC-T cell interface. Left: rendered versions of CD103, DAPI, E-cadherin and β-catenin. Right: replication of left panel with CD103 render made semi-transparent and with only co-localising E-cadherin and β-catenin showing (grey). Orange arrow denotes area of E-cadherin expression localised to the CD8+ T cell membrane which is not co-localised with β-catenin.

Non-colocalised E-cadherin expression was also observed on the T cell membrane at areas not in contact with the BEC. To establish whether E-cadherin+ T cells could form conventional β-catenin interactions with BEC *in vitro*, ICC staining was performed for 48 h-activated CD8+ T cells co-cultured with BEC (Fig. 4.12). Intense staining of colocalised E-cadherin and β-catenin was observed at the interface between CD8+ T cells and BEC. Collectively these data suggest that E-cadherin expression by CD8+ T cells grants them the ability to form adherens junction-like interactions with BEC and potentially invade them through a mechanism resembling entosis.

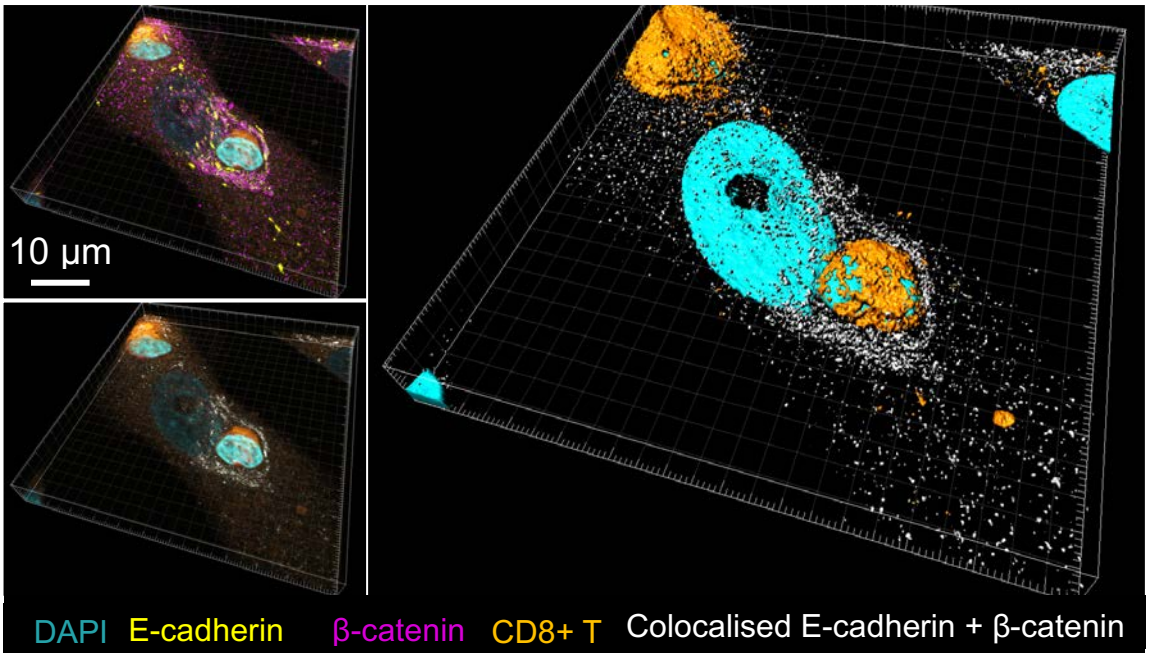

Figure 4.12 The β-catenin-E-cadherin interaction on CD8+ T cells and BECs can be replicated in-vitro. Orthographical confocal micrograph showing immunocytochemistry (ICC) for E-cadherin (yellow) and β-catenin (magenta) of BEC co-cultured with 48 h activated CD8+ T cells (CellTracker™ Red, orange). Cells were co-cultured for 4 h prior to fixation and staining. Bottom left panel shows the 3D-volume rendered version of top left image. Right image shows 3D-volume rendered image with reconstructed channel (grey) showing co-localised E-cadherin and β-catenin.

3.2.5. E-cadherin expression increases the frequency of internalisation of CD8+ T cells into biliary epithelial cells.

To directly assess the involvement of E-cadherin expression by CD8+T cells in their internalisation into BEC, we used fluorescence activated cell sorting (FACS) to isolate E-cadherin^{hi} and E-cadherin^{lo} cells from 48 h activated CD8+ T cells using isotype-matched control staining (Fig. 4.13 Panel A and Panel B). A proportion of each population expressed CD103 (Fig. 4.13 Panel C), although this subset was more frequent in the E-cadherin^{hi} population. Sorted cells were replated at equal densities and rested for 24 h following their separation. Over this period, E-cadherin^{hi} CD8+ T cells appeared to both proliferate and aggregate more than E-cadherin^{lo} cells (Fig. 4.13 Panel D).

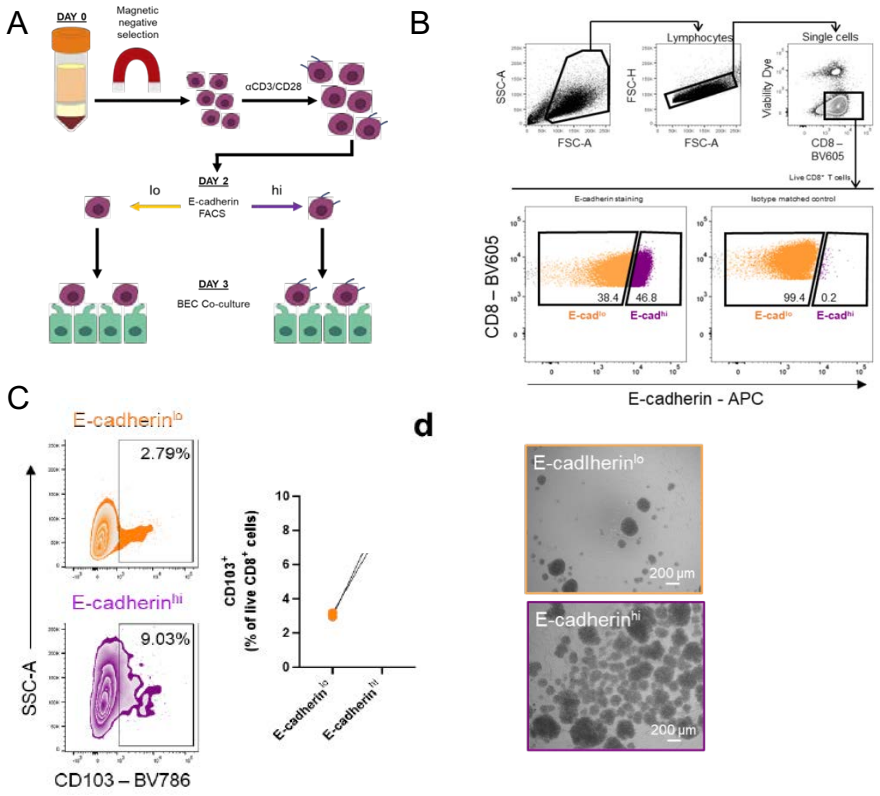

Figure 4.13 E-cadherin^{hi} CD8+ T cells show higher proliferation, aggregation and CD103 expression than E-cadherin^{lo} CD8+ T cells. **Panel A**: Graphical representation of the experiment pipeline. CD8+ T cells derived from healthy volunteer PBMCs, isolated using magnetic negative selection, were activated by α-CD3/CD28 stimulation and cultured for 48 h. E-cadherin^{hi} CD8+ T cells and E-cadherin^{lo} CD8+ T cells were then isolated using FACS. T cells were then rested for 24 h, labelled with CellTracker™ Red, and co-cultured with CellTracker™ Green-labelled biliary epithelial cells (BEC) for 4 h. Cells were fixed and then imaged by fluorescence microscopy. **Panel B:** representative gating strategy for sorting of live CD8+ T cells E-cadherin^{hi} (purple) and E-cadherinlo (orange) populations. **Panel C:** representative zebra plots of CD103+ CD8+ T cells in sorted E-cadherin^{hi} (purple) and E-cadherin^{lo} (orange) populations. n=2 biologically independent experiments. **Panel D**: phase contrast images of E-cadherin^{hi} CD8+ T cells (purple border) and E-cadherin^{lo} CD8+ T cells (orange border) 24 h after being sorted and seeded at equal concentrations.

When co-cultured with BEC for 4 h, E-cadherin^{hi} CD8+ T cells more frequently adhered to BEC compared to their E-cadherin^{lo} counterparts and remained attached to BEC after the media was removed for WGA680 labelling (Fig. 4.14a, b). E-cadherin^{hi} cells found within BEC were also larger than E-cadherin^{lo} internalised cells (Fig. 4.14c). Furthermore, the frequency of internalisation of E-cadherin^{hi} T cells by BEC was increased by 70% compared to E-cadherin^{lo} cells (Fig. 4.14d). To confirm that the internalisation of E-

cadherin^{hi} CD8+ T cells into BEC required the same actin remodelling that was observed with unsorted CD8+ T cells, we treated E-cadherin^{hi} CD8+ T cells with previously used small molecular inhibitors of actin remodelling (Fig. 4.14e). T cells received 30 min pretreatment with inhibitors, and co-cultures with BEC were performed whilst maintaining inhibitor concentrations. As with our previous co-culture experiments using total, unsorted CD8+ T cells (Fig. 3.f, g), E-cadherin^{hi} T cell internalisation into BEC was sensitive to PI3K inhibition by wortmannin (Fig. 4.14e). In contrast, H-1152 treatment also reduced the frequency of internalisation of E-cadherin^{hi} CD8+ cells by 40%. These data reveal the unique characteristics of E-cadherin^{hi} CD8+ T cells and demonstrate that invasion into BEC is actin remodelling-dependent and may require both PI3K and ROCK1- mediated signalling.

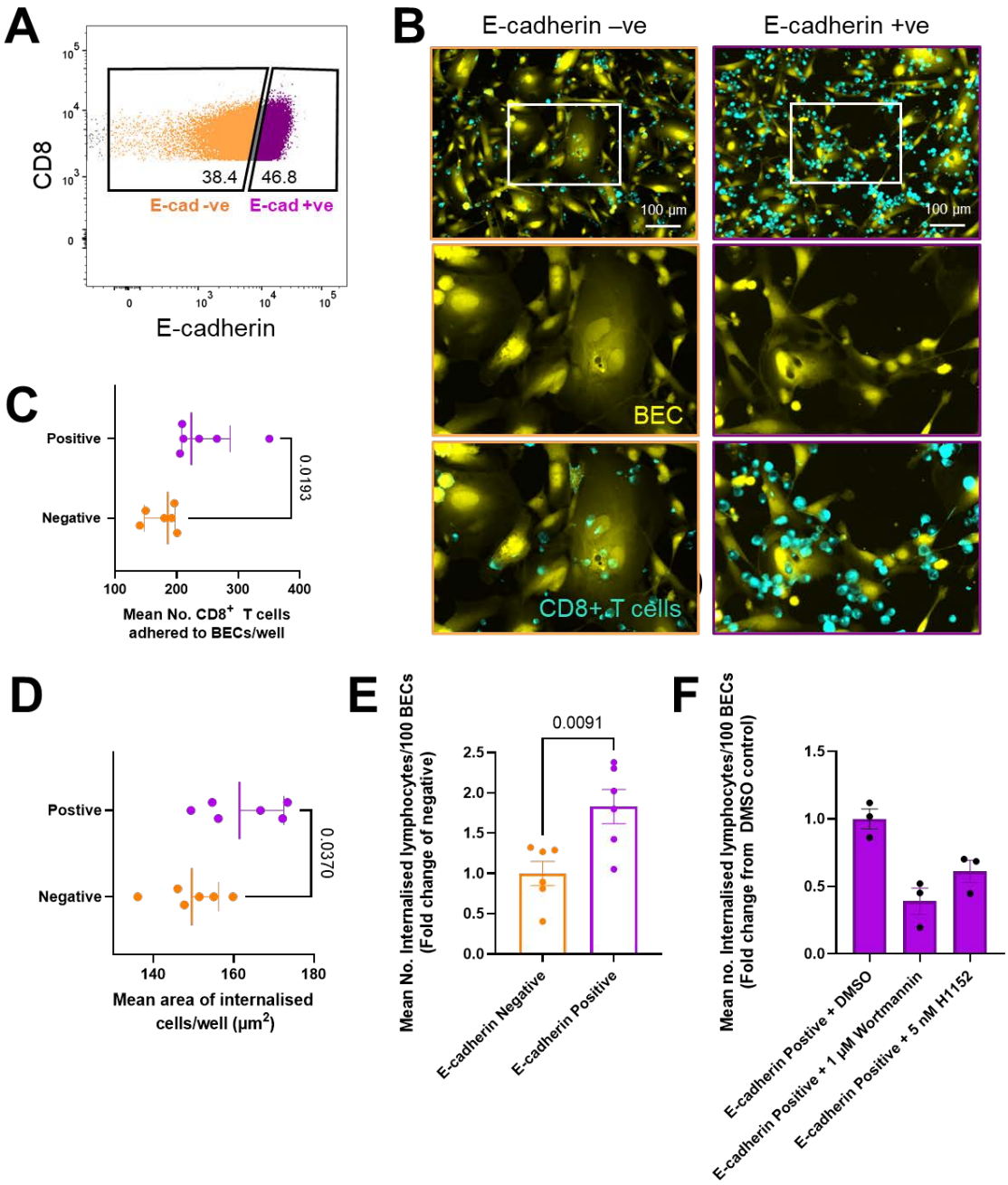

Figure 4.14 Internalisation of E-cadherin+ CD8+ T cells into BEC is more frequent than E-cadherin- CD8+ T cells and is sensitive to Rho Kinase inhibition. Peripheral blood CD8+ T cells derived from healthy volunteers were activated by α-CD3/CD28 stimulation and cultured for 48 h. E-cadherin+ CD8+ T cells and E-cadherin- CD8+ T cells were then isolated using fluorescence activated cell sorting (FACS). T cells were then rested for 24 h, labelled with Celltracker™ Red, and then co-cultured with differently labelled BEC for 4 h. Cells were fixed with 4% formaldehyde and then imaged by fluorescence microscopy. **A**. FACS-associated scatter plot showing the sorting strategy for activated CD8+ T cells either E-cadherin- (orange) or E-cadherin+ (purple) **B.** Representative images of BEC (CellTracker™ Green; yellow) co-cultured with either E-cadherin- or E-cadherin+ CD8+ T cells (CellTracker™ red, cyan). **C-E.** Quantification of CD8+

T cells attached to BEC (C) and number per 100 BEC (E), and size (D), of internalised CD8+ T cells for E-cadherin-and E-cadherin+ sorted cells. Nine fields of view were analysed from triplicate wells. Mean values/technical repeat are plotted. Experimental N=2. df=10 (C-D): Error bars represent median and interquartile range. (C) t=2.785. (D) t=2.406. (E). Error bars represent standard error of the mean. t=3.224. **F.** Quantification of internalised E-cadherin+ CD8+ T cells per 100 BEC in which T cells were pre-treated with 1 μM Wortamanin or 5 nM H-1152 (ROCK1 inhibitor), prior to co-culture. Nine fields of view were analysed from triplicate wells. Mean values of no. of internalised CD8+ T cells/technical repeat are plotted. Values are normalised and displayed as a fold change from DMSO (vehicle) treated cells. Experimental N=1. Error bars represent standard error of the mean. P values are displayed in the figure for each statistical comparison made.

3.2.6. CD8+ cell internalisation into BEC is a consistent event in PBC and driven by E-cadherin expression

Internalisation of CD8+ T cells into BEC was originally described as a histological feature in patients with PBC across a variety of stages of biliary disease progression. The experiments so far presented showed CD9+ T cells internalised at any stage of PBC. If we look at the early disease, using liver biopsies of PBC patients (Fig. 3.2), the percentage of bile ducts possessing internalised CD8+ T cells ranged from 6% to 83%, with CD103+ CD8+ T cells ranging from 2 to 50% (Fig 4.15 panel A). ALT x upper limit of normal (normalised) values were higher for patients who demonstrated a higher frequency of CD8+ and CD103+ CD8+ T cell internalisation in the biopsies we analysed (Fig 4.15 panel B).

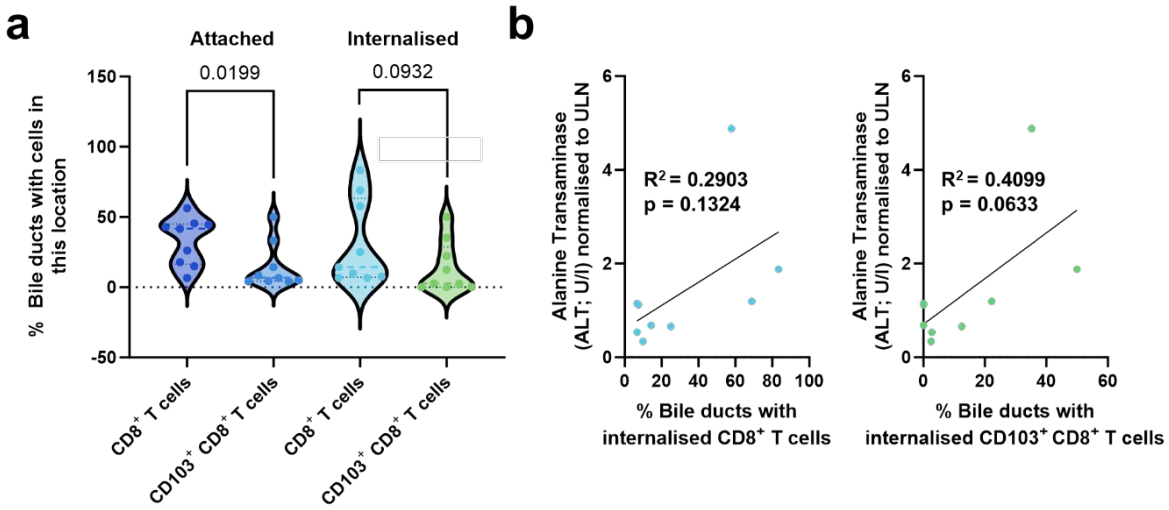

Figure 4.15 CD8+ T cells in PBC patients can be found internalised within BEC in liver biopsies and correlates with hepatocellular damage. Panel A. Violin plots showing the percentage of bile ducts with attached or internalised CD8+ or CD103+ CD8+ T cells. Liver biopsies taken from primary biliary cholangitis (PBC) patients with active disease were stained for CD8, CD103 and cytokeratin-19 (CK19) by immunohistochemistry (IHC). Bile ducts were identified using CK19 staining and the frequency of CD8+ and CD8+ CD103+ T cells either within biliary epithelial cells (BEC) or attached to bile ducts was quantified. Statistics were derived from two-tailed Mann-Whitney tests. n=9 biologically independent patient samples. **Panel B.** Linear regression of analysis comparing the percentage of bile ducts possessing internalised CD8+ or CD8+CD103+ T cells observed in patient liver biopsies against patient-matched alanine transaminase levels (ALT; U/l)

Finally, we documented the presence of CD8+ T cells within EpCAM+ BEC of bile ducts which appeared to have ruptured (Fig. 4.16). This observation was based on the incomplete continuity of the bile duct and incomplete barrier staining of both EpCAM and E-cadherin. The same bile duct also possessed EpCAM+ fragments within the duct which also colocalised with CD8+ staining.

This data suggested that the internalisation process was associated with E-cadherin expression by CD8+ T cells, so the next aim was to investigate the relationship between the presence of E-cadherin+ CD8+T cells and PBC. I then performed co-cultures using 48 h activated CD8+ T cells derived from PBC patient blood samples. These cells became larger upon activation compared to non-PBC, resembling those observed in PBC liver tissue biopsies. Flow cytometry phenotyping of peripheral blood mononuclear

cells (PBMCs) originating from PBC patients demonstrated that CD8+ T cells exhibited higher expression of E-cadherin 48 h post-activation compared to non-PBC controls (Fig. 4.17).

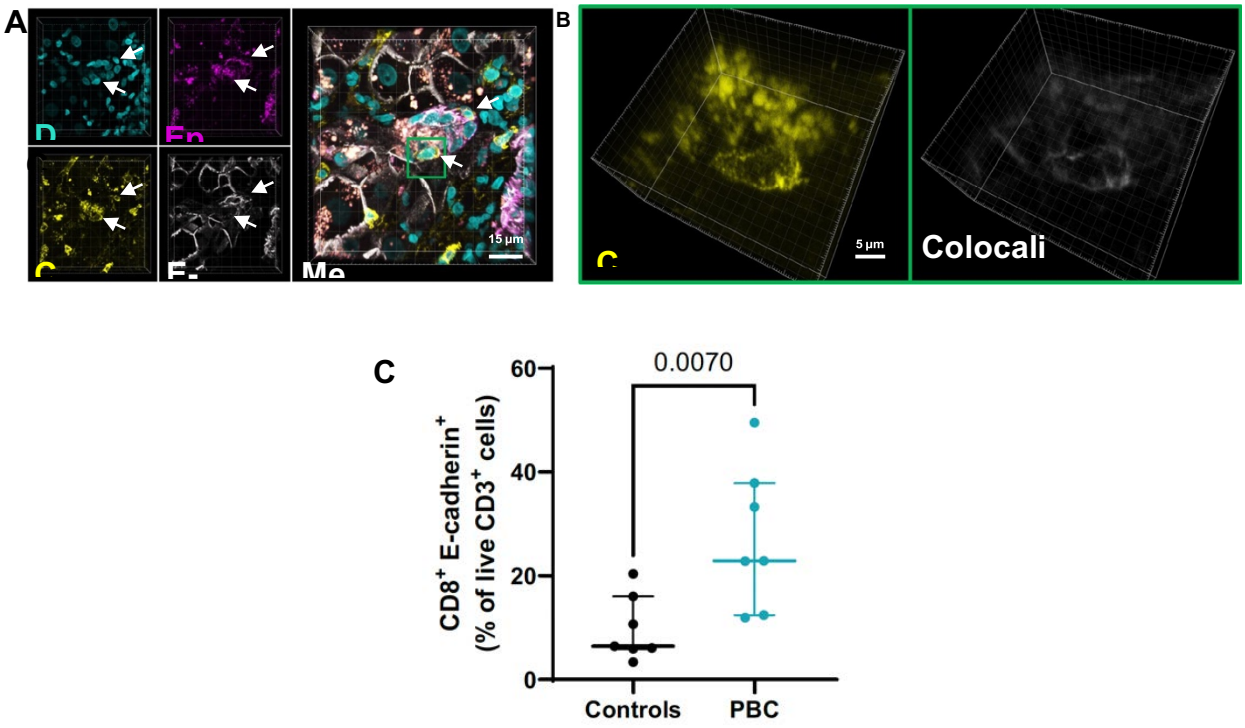

Figure 4.17 Internalisation of PBC-derived CD8+ T cells into BEC is driven by E-cadherin expression by CD8+ T cells. Panel A. Multichannel image of immunohistochemistry (IHC) staining of PBC biopsy for CD8 (yellow), E-cadherin (white) and EpCAM (magenta), showing CD8+ T cells (white arrows) within the biliary epithelial cells (BEC) of a ruptured bile duct. **Panel B.** 3D-reconstructed Z-stack of internalised CD8+ T cells highlighted in (a) (green box) which also expressed E-cadherin (colocalised signal in grey; right panel). **Panel C**. Comparison between healthy controls and PBC patients for frequency of E-cadherin expression amongst blood-derived CD8+ cells 48 h post activation, determined by flow cytometry.

E-cadherin+ CD8+ T cells from PBC patients were also more representative of terminally differentiated T effector memory cells expressing CD45RA (TEMRA) subset of T cells (CCR7- CD45RA+) compared to controls. E-cadherin+ CD8+ T cells were also enriched for the TEMRA phenotype compared to matched, total CD8+ T cell populations (Supplementary Fig. 4.18).

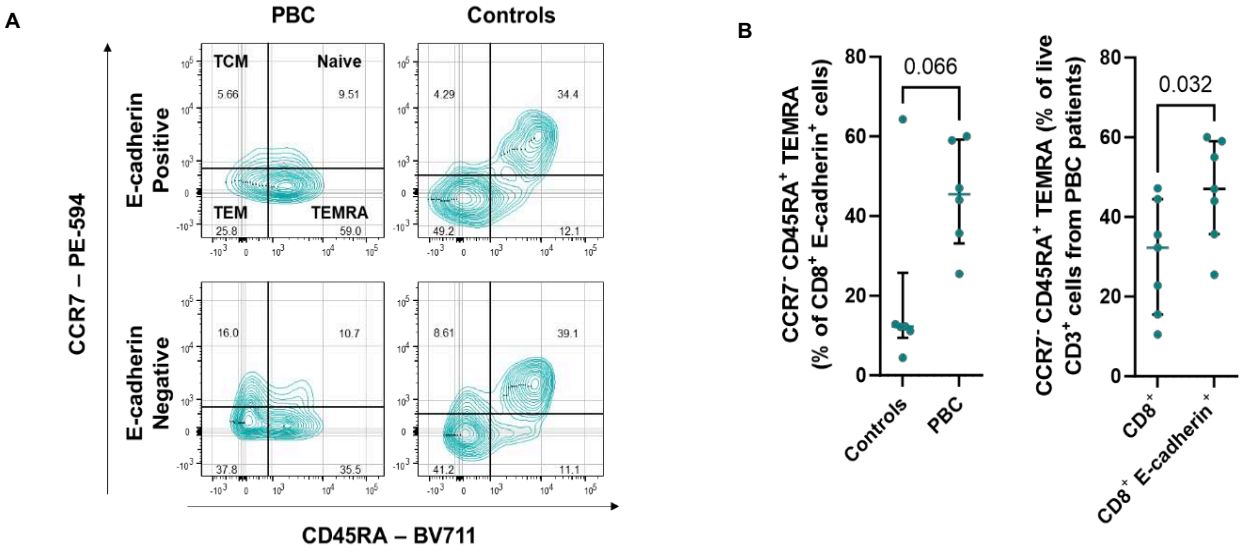

Figure 4.18 CD8+ T cells in PBC patients and represent different sub-populations compared to non-PBC controls. Peripheral blood mononuclear cells (PBMCs) from PBC patients and haemochromatosis (HFE) controls were phenotyped 48 h after activation via α-CD3/CD28 stimulation using flow cytometry. Expression of CD45RA and CCR7 was assessed to determine the subset of memory T cells that represent E-cadherin$^+$ CD8$^+$ T cells. **Panel A.** Representative contour plots for CCR7 and CD45RA expression by E-cadherin$^+$ CD8$^+$ or E-cadherin$^-$ CD8$^+$ cells from PBC and HFE patients. TCM – T central memory. TEM T effector memory. TEMRA – T effector memory expressing CD45RA. **Panel B.** *Left*: comparison of the percentage of E-cadherin$^+$ CD8$^+$ T cells expressing TEMRA markers between PBC patients and control patients. n=6 biologically independent patient samples/disease condition. p value was generated from a two-tailed Mann-Whitney test. *Right*: comparison of the percentage of total CD8$^+$ T cells and E-cadherin$^+$ CD8$^+$ T cells expressing TEMRA markers in PBC patients.

Furthermore, in our IHC-stained PBC biopsies, we observed CD8+ T cells with colocalised E-cadherin staining located within the EpCAM+ BEC of rupturing bile ducts (Fig 4.19 Panel A).

To further determine the necessity of E-cadherin expression for the internalisation of these cells, we performed siRNA-knockdowns of CDH1 for 24 h activated CD8+ T cells derived from PBC patient blood. siRNA-treated T cells were then assessed for E-cadherin expression by flow cytometry. Two out of the four individual CDH1 siRNAs tested, named siRNA 3 and siRNA 4, elicited 50% reduction of E-cadherin MFI assessed by flow cytometry, 48 h after performing knockdowns. Co-cultures were performed between BEC and CD8+ T cells treated with siRNA. Treatment with siRNA 3 or siRNA 4 resulted in a 0.5-fold change in internalisation frequency compared to CD8+ T cells treated with control siRNA, which correlated with E-cadherin MFI of CD8+ T cells determined in parallel by flow cytometry. Taken together, these data demonstrate the importance of E-cadherin expression by CD8+ T cells in driving their internalisation into BEC. Additionally, they further exemplify the consistent association between this internalisation process and PBC.

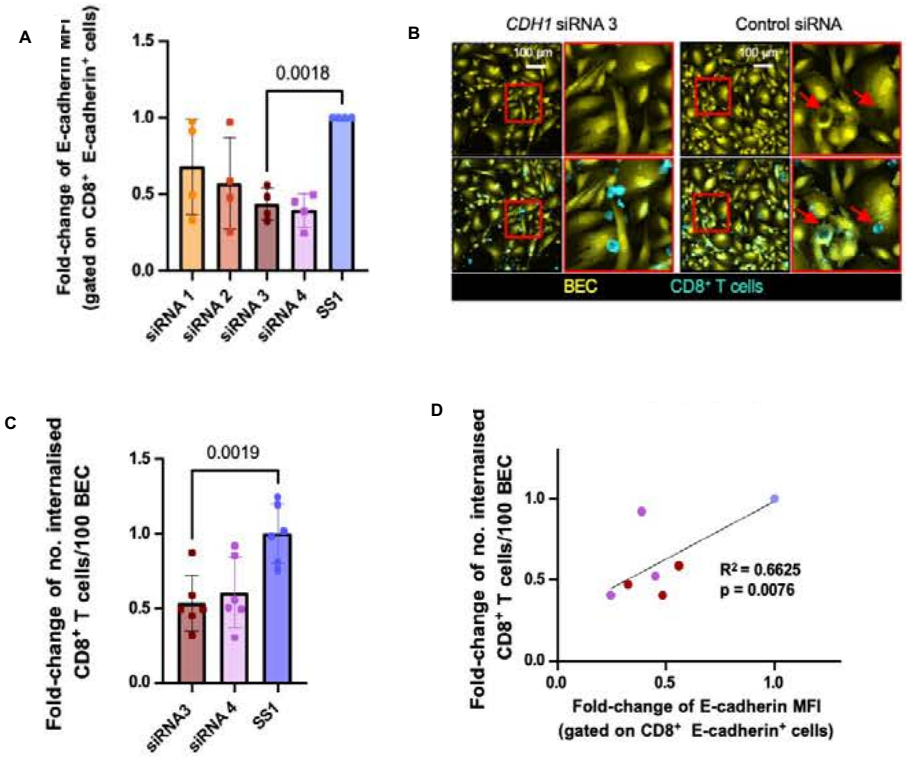

Figure 4.19. The number of internalized cells is affected by E-cadherin expression reduction. Panel A. Median fluorescence intensity (MFI) values, determined by flow cytometry, of E-cadherin staining performed for PBC patient-derived $CD8^+$ T cells treated with different *CDH1*-targeting siRNAs (siRNA1-4). **Panel B**. Representative images of BEC (CellTracker™ Green; yellow) co-cultured with siRNA- treated $CD8^+$ T cells (CellTracker™ red; cyan). Red arrows show internalized $CD8^+$ T cells. **Panel C**. Quantification of internalised $CD8^+$ T cells per 100 BEC for siRNA-treated $CD8^+$ T cells. **Panel D**. Linear regression analysis comparing matched E-cadherin MFI determined by flow cytometry (x) with mean frequency of $CD8^+$ T cell internalization (y).

3.2.7. Discussion

Overall, these experiments demonstrated that more eccentric CD8+ T cells observed within BEC in PBC liver tissue *in vivo* could be generated *in vitro* from non-PBC blood 48 h after α-CD3/CD28 activation. This change was concurrent with an overall enlargement of these cells prior to co-culture and a higher propensity for internalisation into BEC. In fact, these data demonstrate that CD8+ T cells are actively involved in their internalisation into BEC through dynamic cytoskeletal rearrangements, and inhibition of actin-remodelling reduces their entry.

CD8+ T cells within BEC in liver tissues from patients with PBC was recently observed and their presence was correlated with increased in BEC apoptosis(316). The results herein presented greatly expand on the cellular and molecular mechanisms of this interaction.

This chapter data shows the entry mechanism of CD8+ T cells into BEC was different to other described CICS of the liver, based on differences in phenotype and protein-protein interactions. Our lab recently reported the process of enclysis; the specific capture of CD4+ T cells by hepatocytes which frequently resulted in the deletion of regulatory T cells(313). In contrast to enclysis, where hepatocytes undergo membrane alterations and form ruffles to assist the engulfment of CD4+ T cells, minimal rearrangements were seen on BEC which possessed adhered or internalised CD8+ T cells. Additionally, CD4+ T cells were rarely observed to invade BEC after TCR-mediated activation. CD8+ T cell invasion into BEC did share mechanistic similarities with “suicidal emperipolesis”; both processes were sensitive to PI3K inhibition and detailed events of active invasion by CD8+ T cells into other cells(262).

The internalised cell associated with homotypic entosis possesses weaker contacts to the surrounding environment(272, 337). As CD8+ T cells would not be anchored to the stromal environment as strongly as BEC, it is likely that they “pull themselves inside”

upon E-cadherin expression. In agreement with this, the internalised cells were larger and more eccentric. These cells possess a wider surface area for forming cell-to-cell contacts and better capacity for cytoskeletal rearrangements. As such, they would be able to form more points of contact with BEC, as identified by SEM and phalloidin staining. It should be noted that ROCK1 inhibition did not consistently reduce internalisation in experiments where CD8+ T cells were not enriched for E-cadherin expression. Therefore, it is likely that other mechanisms may exist which permit CD8+ T cell entry into BEC which are dependent on PI3K signalling and actin remodelling but do not require ROCK1 activity.

The purpose and “immunological motivations" of CD8+ T cells internalisation into BEC currently remain unclear. It is unlikely that this CD8+ T cell subset has evolved specifically for intentionally killing invaded cells from the inside; BEC that were possessing T cells did not display any morphological changes associated with cell death when analysing high-content assays and viewing the cells ultrastructure with SEM. However, Zhao and colleagues reported that the frequency of CD8+ T cells found within BEC was correlated with increased apoptosis of BEC in patients with PBC(316).

3.3. The generation of PDCE-2 specific, stable and functioning induced regulatory T cells from peripheral blood of patients with PBC.

N.B. *the content presented in this chapter are part of a paper recently published (4).*

3.3.1. Introduction

Disruption of immunological homeostasis is fundamental to the onset of liver autoimmunity. Traditional autoimmune treatments rely on untargeted immunosuppression, administered as lifelong therapies. These therapies expose patients to risks of cancer, infections, and significant side effects. There is a considerable effort to develop treatment strategies to re-establish the tolerogenic mechanisms typical of the liver immune environment as a potentially curative approach for the patients suffering from these rare conditions. It is important to note that most of these strategies rely on a deep knowledge of the self-antigen which is known in PBC and in the minority of AIH cases.We tested the ex-vivo expansion of Tregs from patients with AIH and the reinfusion of the cell product. This early phase trial proved that the treatment is very well tolerated. We also showed that the Tregs after reinfusion localised mainly within the liver, most likely due to the homing to the inflamed organ(326).A similar strategy was used in combination with IL-2 in type 1 diabetes. The use of low dose of IL2 significantly boosted the number of Tregs, but with a significant effect also on NK and CD8+ T cells**(338)**.

The development of antigen specific Treg treatment in humans remains incredibly challenging. The expansion of a small component of self-reacting circulating Treg cells relies on engineering tetramers to target the epitope of interest.

Sakaguchi and colleagues suggested a novel platform to develop stable and functioning Treg cells by inhibiting cyclin dependent kinase 8 and 19. This approach allows to select CD4+ T memory cells and convert them into induced Tregs by inducing the expression of FOXP3**(339)**.

In this chapter I will present my own attempt to generate stable and functional induced regulatory T cells (SFiTreg) starting from CD4+ T cells of PBC patients. All the experiments herein presented were conducted in the Immunology Frontier Research Centre at Osaka University and funded by EMBO.

3.3.2. The generation of SFiTreg is effective and reliable.

Generating SFiTregs took two weeks. Figure 5.1 provides a schematic overview of the protocol, which is fully described in Chapter 2. The protocol's main aim was to obtain a pure population of CD4+ T cells. On day 1, in addition to isolating PBMCs from peripheral blood, magnetic negative isolation of CD14- was used to exclude monocytes, followed by magnetic positive isolation of CD4+ T cells. This last step excluded CD8+ cells which have demonstrated to affect the protocol severely, most likely as greedy binders of IL-2. The activation of the cells was obtained via beads and did not include co-stimulatory stimulation, but only through TCR stimulation. In fact, as shown by Mikami et al. (340), the activation of TCD4+ cells in presence of TGF- and IL-2, but with the deprivation of CD28 induces Treg-type DNA hypomethylation. To the first activation followed and expansion and a further activation with a step similar to the first one. The whole process included adding in the media AS2863619(339) a CDK8/19 blocker.

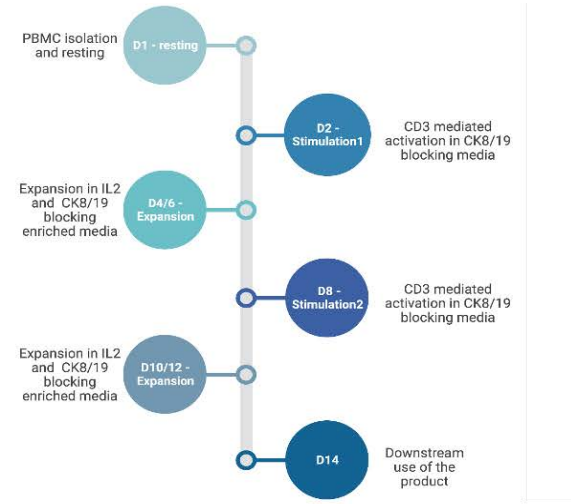

Figure 5.1 Schematic overview of the protocol to induce stable and functional regulatory T cells.

The results presented in Figure 5.2 shows a nice and clean population of CD4+ T cells expressing FoxP3 and CTLA4 already ad day 9, when according to the protocol a first purity check is indicated.

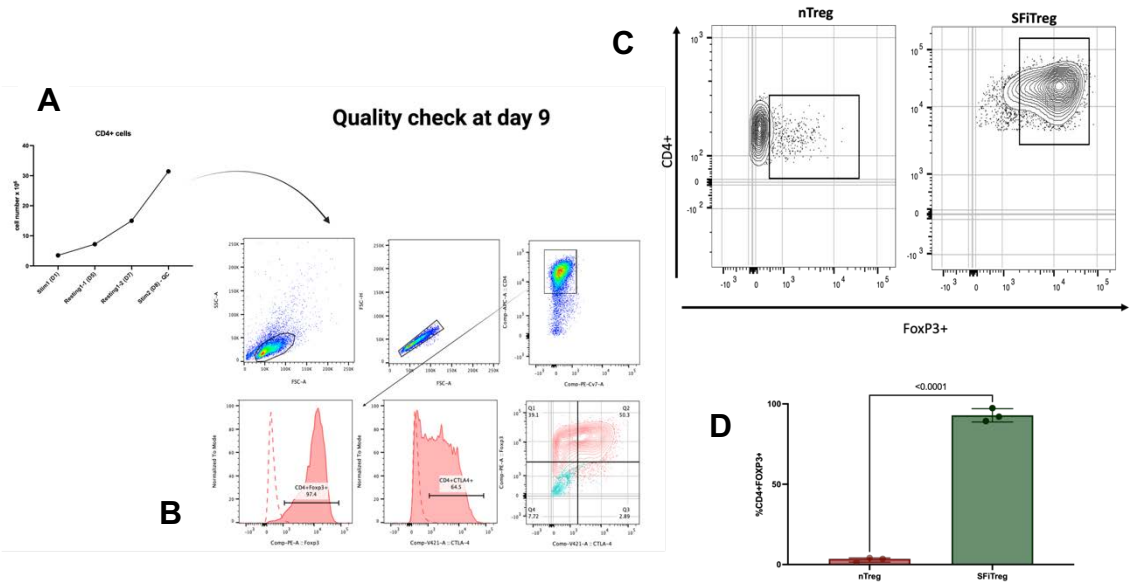

Figure 5.2 Phenotype of the CD4+ T cells at day 9 checking FOXP3 and CTLA4. Panel A. At this point of the protocol the cells have been expanded twice and after starting with less than 10 millions of TCD4+ cells, at day 9 we have already 35 millions of cells. **Panel B.** Representative flow cytometry plots showing the upregulation of both FOXP3 and CTLA4. **Panel C and D.** Frequency of induced Tregs at day 9 compared with the number of natural Tregs at the beginning of the protocol.

Figure 5.3 shows the comparison between the cell product after 9 days and 14 days in culture. While the expression of FoxP3 and CTLA4 remained similar, the markers were more stably expressed by day 14. Additionally, there was a significant increase in cell numbers, exceeding 200 million by the end of the protocol (Figure 5.3).

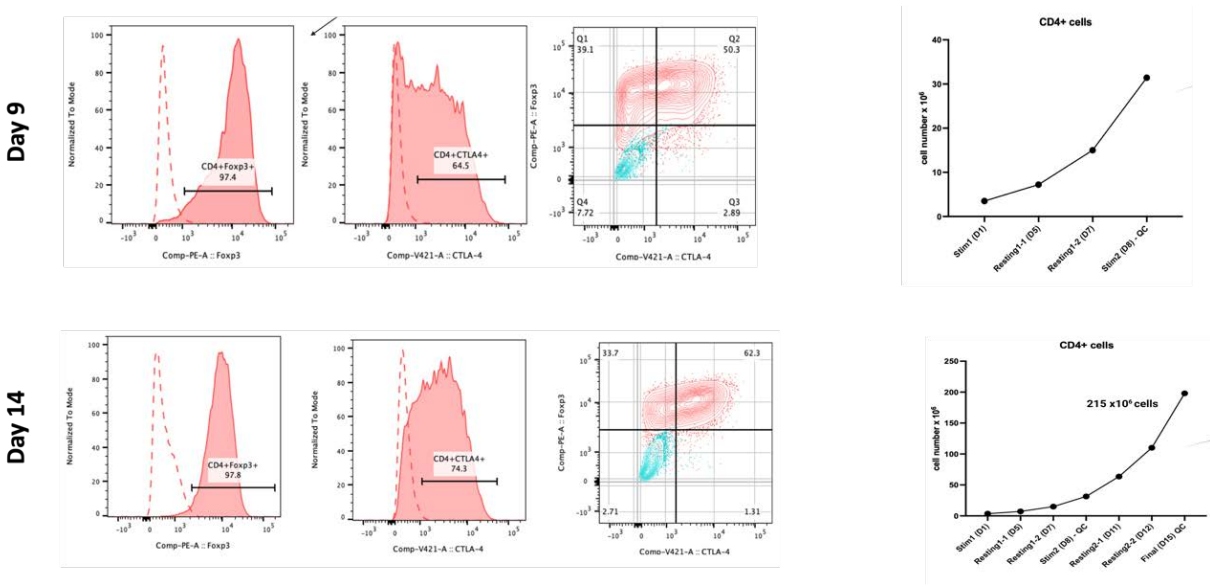

Figure 5.3 Comparing number of cells, FOXP3 and CTLA4 expression at day 9 vs day 14. Upper panels: representative plots of the cell product at day 9. Lower panels: representative plots of the cell product at day 14.

3.3.3. SFiTregs remain stable and functional in inflammatory environment.

One of the Treg feature is the plasticity. The microenvironment can affect their lineage stability and change their phenotype and function, shifting them toward a more inflammatory phenotype (i.e. Th1 or Th17).

The key action of IL-12 and IFN- has been well described in PBC. Intriguingly, Liaskou and colleagues, demonstrated, that small concentration of IL-12 can induce IFN production in Tregs from patients with PBC, confirming the lineage instability could also be a mechanism of tolerance breakdown(231).

This is potentially a significant limitation of Treg cell therapy. To test whether the cells I produced were stable in an inflammatory environment SFiTregs generated from PBC individuals were exposed *in-vitro* to a cocktail of Th1 polarising cytokines. After being cultured 6 days with IFN-gamma and IL-12, SFiTregs did not lose the expression of FOXP3 and did not upregulate significantly the expression of Tbet, specific for Th1 population (Figure 5.4).

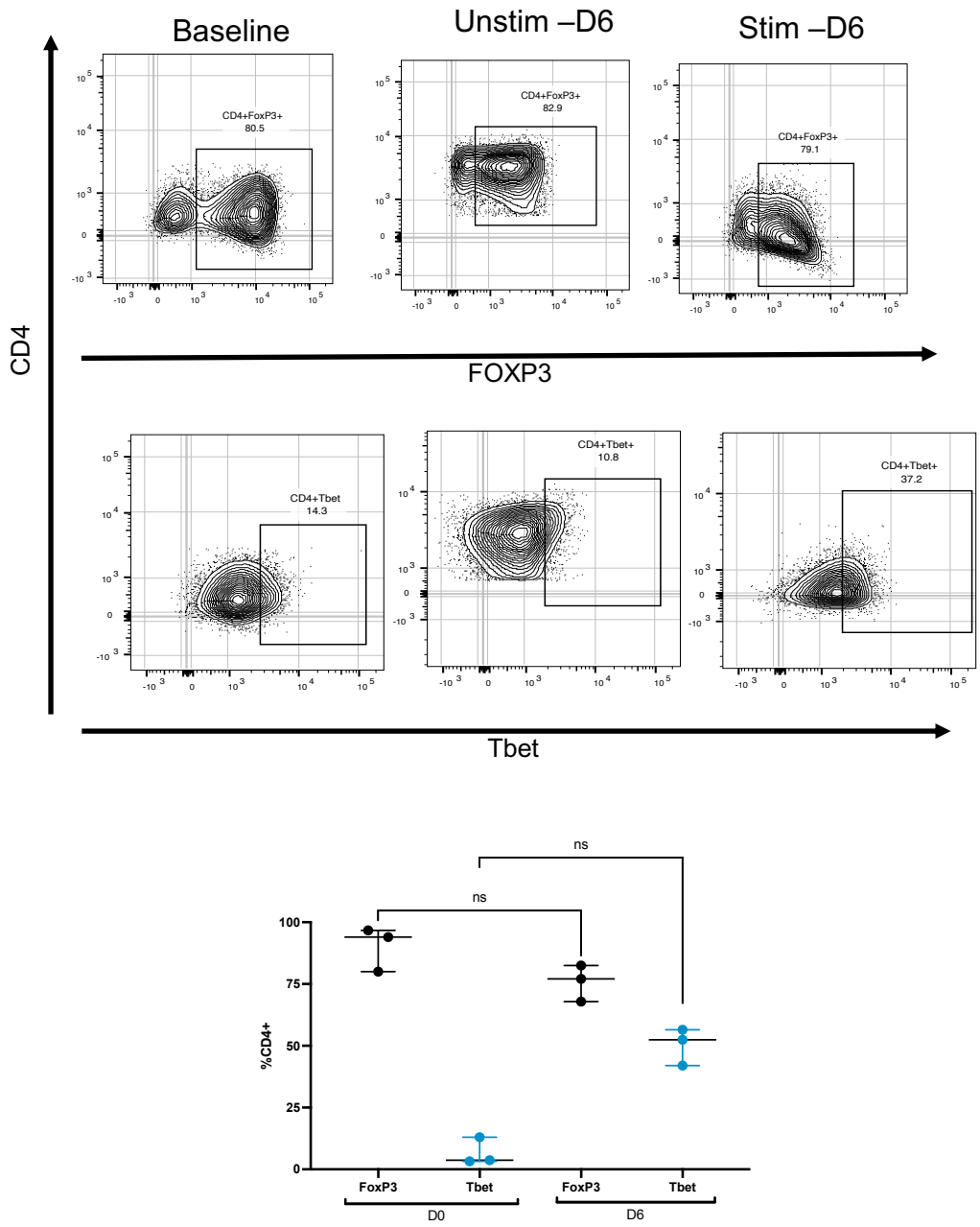

Figure 5.4 SFiTregs are stable in Th1 proinflammatory environment. Panel A Representative zebra plot showing similar expression of FOXP3 and Tbet comparing baseline vs stimulated vs unstimulated at day 6. **Panel B**. Graphical representation of the percentage of Tbet+ and FOXP3+ cells, at day 0 vs day6.

The gold standard, however, to assess the stability of FOXP3 is to look to the methylation status of CNS2 in our SFiTreg products. We assessed the methylation – demethylation ratio of the region using digital PCR and it was found significantly lower after 6 days of high dose Th1 cytokine exposure, suggesting that SFiTregs could eventually lose the FOXP3 expression, if exposed to high dose of pro-inflammatory cytokines (Figure 5.5).

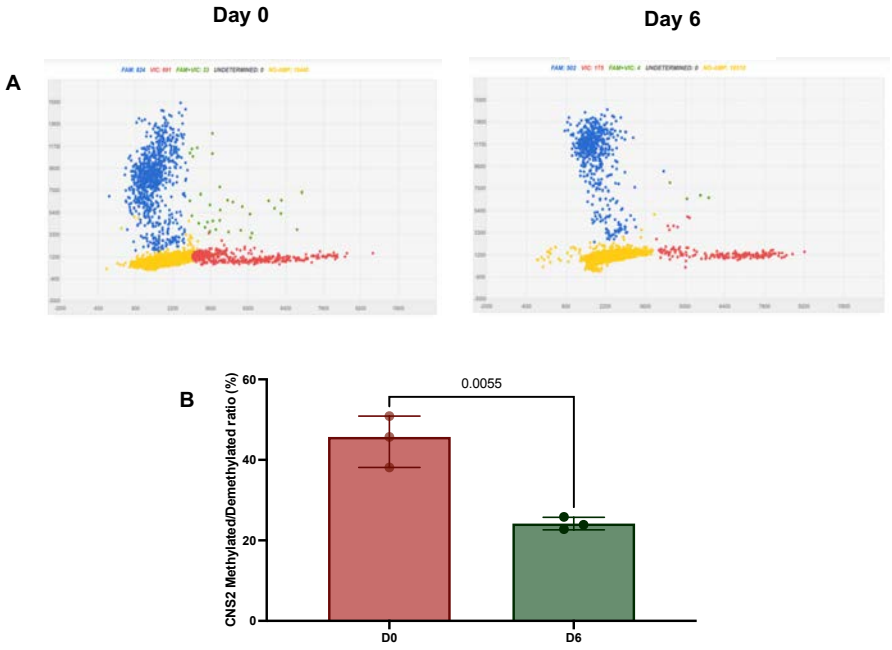

Figure 5.5 CNS2 methylation decrease overtime in SFiTregs when exposed to Th1 polarising cytokines. Panel A. Representative graph of bisulfite assessment of methylation status of CNS2 using digital PCR of SFiTregs showing a reduction in cells exhibiting methylated CNS2. **Panel B.** Graphical summary of the experiments confirming a significant reduction of the CNS2 methylation/demethylation ratio.

However, the functionality when I tested the suppressiveness of these cells using regular suppressive assay it was confirmed that the product maintains the suppressive potential (Figure 5.6).

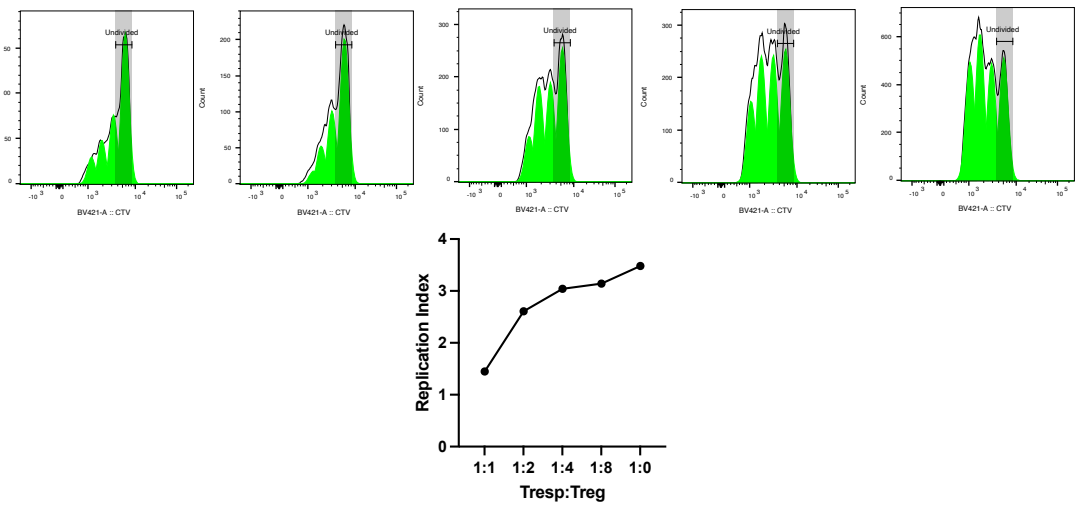

Figure 1.4.2.45.6 SFiTregs do not only express FOXP3 and Treg associated markers but remain suppressive. Representative experiment of regular suppression assay, showing suppressive effect of the produced SFiTregs.

3.3.4. SFiTregs cell epigenetic profile is different from natural Tregs.

I clearly defined the epigenome of the SFiTreg cells I generated and compared with natural Tregs, to assess the change of the initial CD4+ T cells toward Treg phenotype.

I tested CNS2, and CTLA4 methylation profile through bisulfite PCR. We could not observe any significant difference in CNS2 and CTLA4 methylation pattern using digital PCR. The assay for transposase-accessible chromatin with sequencing (ATACseq) confirmed a clear peak in CNS2 region, to confirm the epigenetic change allowing the FOXP3 expression in the SF-iTregs, not present in CD4+ T naïve cells (Figure 5.7).

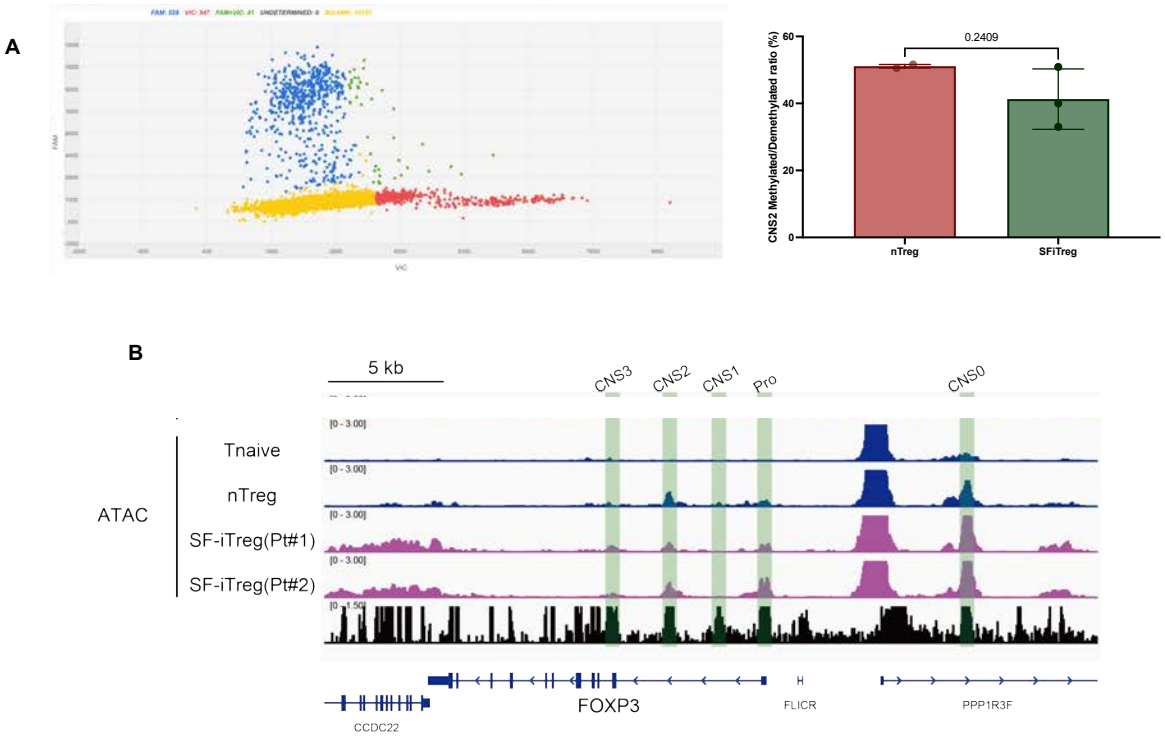

Figure 5.7. Epigenetic comparison between induced nTreg vs SF-iTregs. Panel A. CNS2, and CTLA4 methylation profile assessed through bisulfite PCR. **Panel B**. ATACs confirmed a clear peak in CNS2 region, to confirm the epigenetic change allowing the FOXP3 expression in the SF-iTregs, not present in CD4+ T naïve cells.

I then assessed the difference in the differentially accessible regions (DAR) in natural Treg vs SFiTreg (Tconv included as reference control). We found significant difference in the two subsets of cells, and in a pathway enrichment analysis, we found them associated, among others, with lymphocyte differentiation, cell adhesion and response to lipopolysaccharide (Figure 5.8).

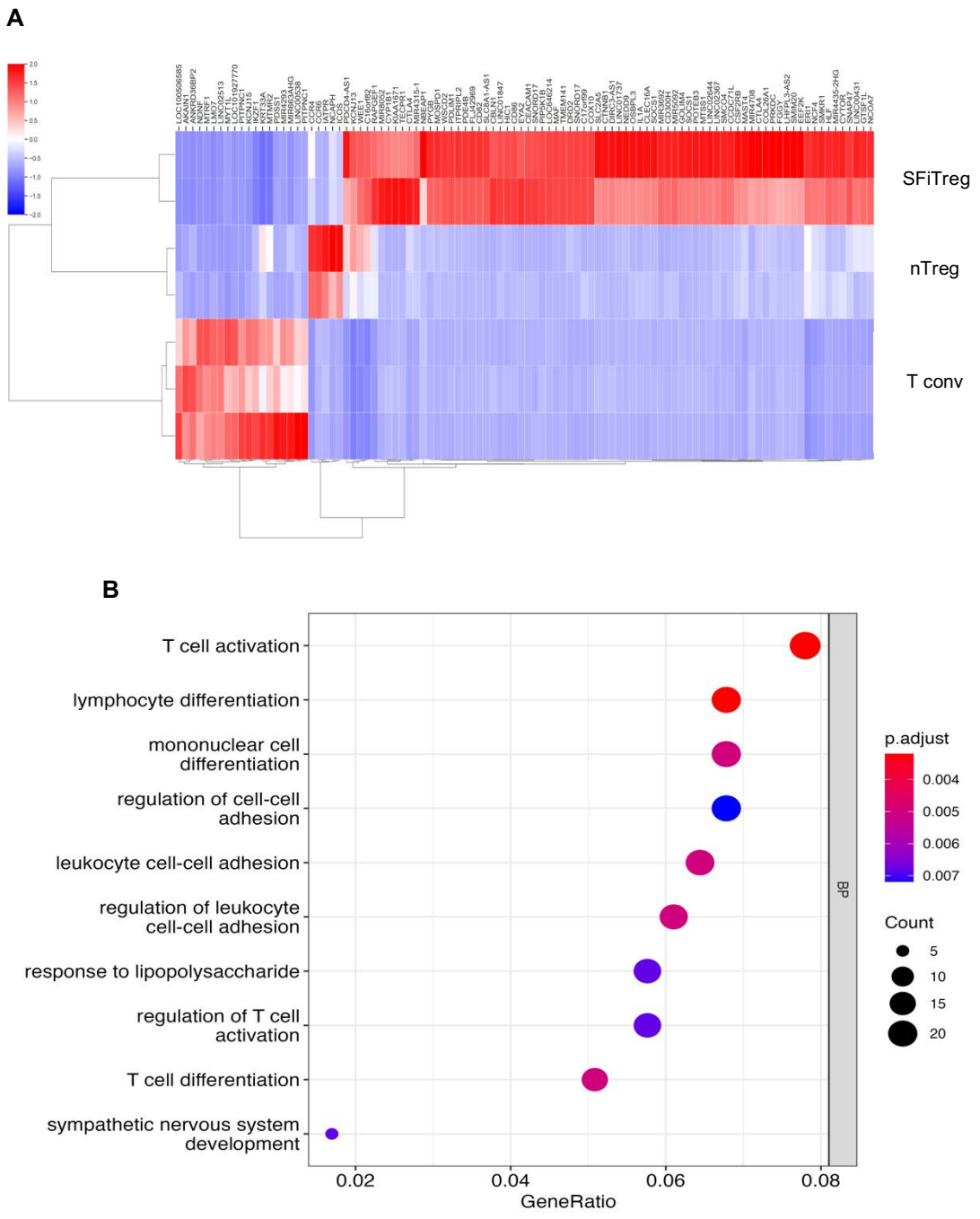

Figure 5.8 ATACs analysis of nTregs, SFiTregs and Tconv. Difference in the differentially accessible regions (DAR) in nTreg vs SFiTreg (Tconv included as reference control). **Panel A.** Heatmap of the 100 most differentially accessible regions. **Panel B.** Pathway enrichment analysis.

To test these results, we took advantage of a model of wedge perfusion optimised by Dr Angus Hann in our lab. The model is synthetised in the cartoon in Figure 5.9. Briefly, a peristaltic pump was used to infuse SFiTregs, previously generate at a concentration of 0.03 x 10^6 /mL, labelled with CellTracker Red (CMTPX) for 12 hours. A separate wedge was perfused using media as control.

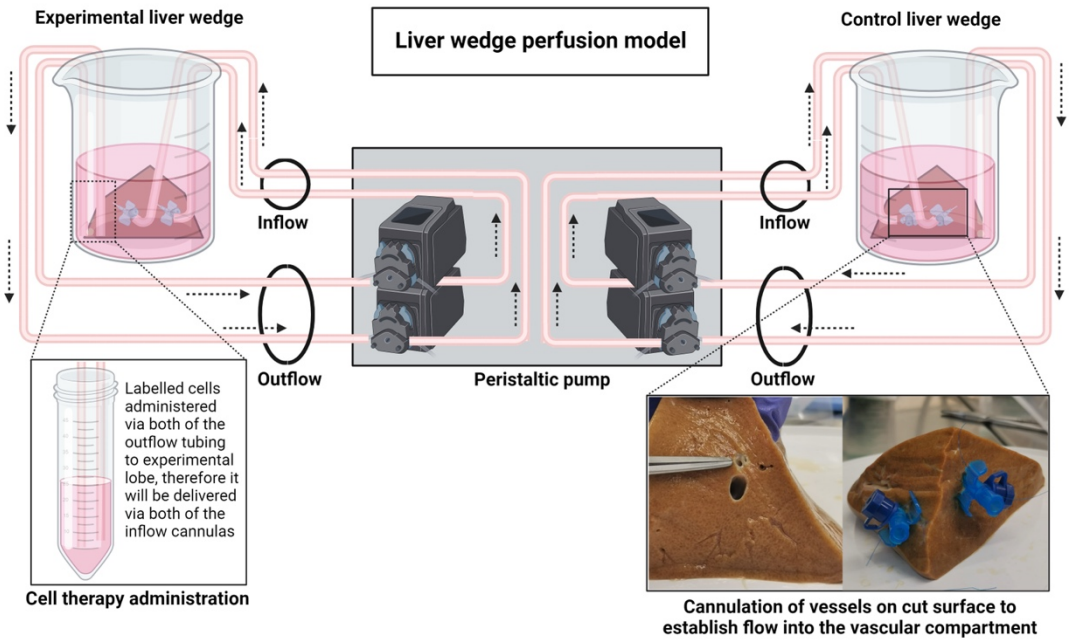

5.9 Wedge perfusion model. Two different peristaltic pumps perfuse two wedges from the same donor liver. The experimental lobe is perfused using CMPTx labelled SFiTregs, and the control lobe with cell-free media.

I phenotype the SFiTregs after thawing them to assess the stability of the FOXP3 and CTLA4 expression. The FOXP3 was expressed in more than 90% of the cells, with a slight reduction in CTLA4 (Figure 5.10).

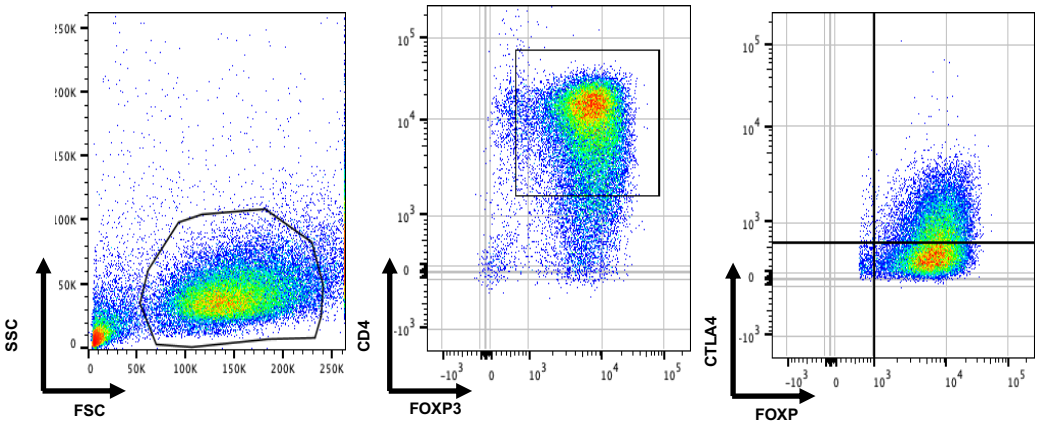

Figure 5.10 FOXP3 expression reduction in thawed SFiTreg cells. Representative flow cytometry staining of SFiTregs after thawing.

After the labelling the SFiTregs were further assessed to define the baseline expression of Treg function markers such as TIGIT, CD39 and CTLA4 (Fig 5.11).

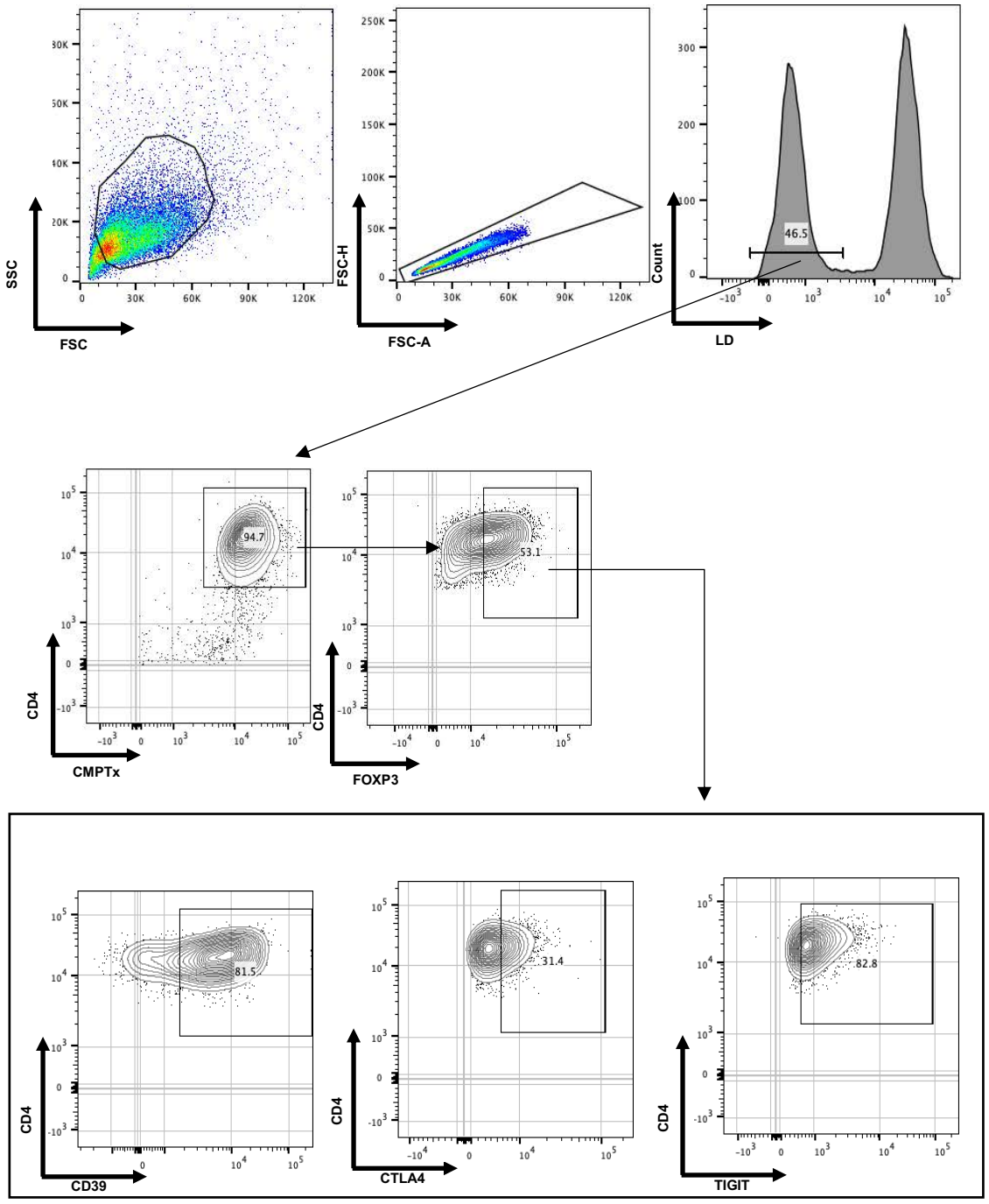

Figure 5.11 Phenotype of the SFiTreg cells after labelling them with CMTx.

After the perfusion, the wedges were processed as well as the supernatant to isolate mononuclear cells. After isolation the cells phenotype was defined using flow cytometry, using the same markers I stained before the infusion.

I could identify the cells in the perfusate, however their level of expression of FOXP3 was significantly lower compared with what it was before the infusion (94% vs 25%) (Figure 5.12).

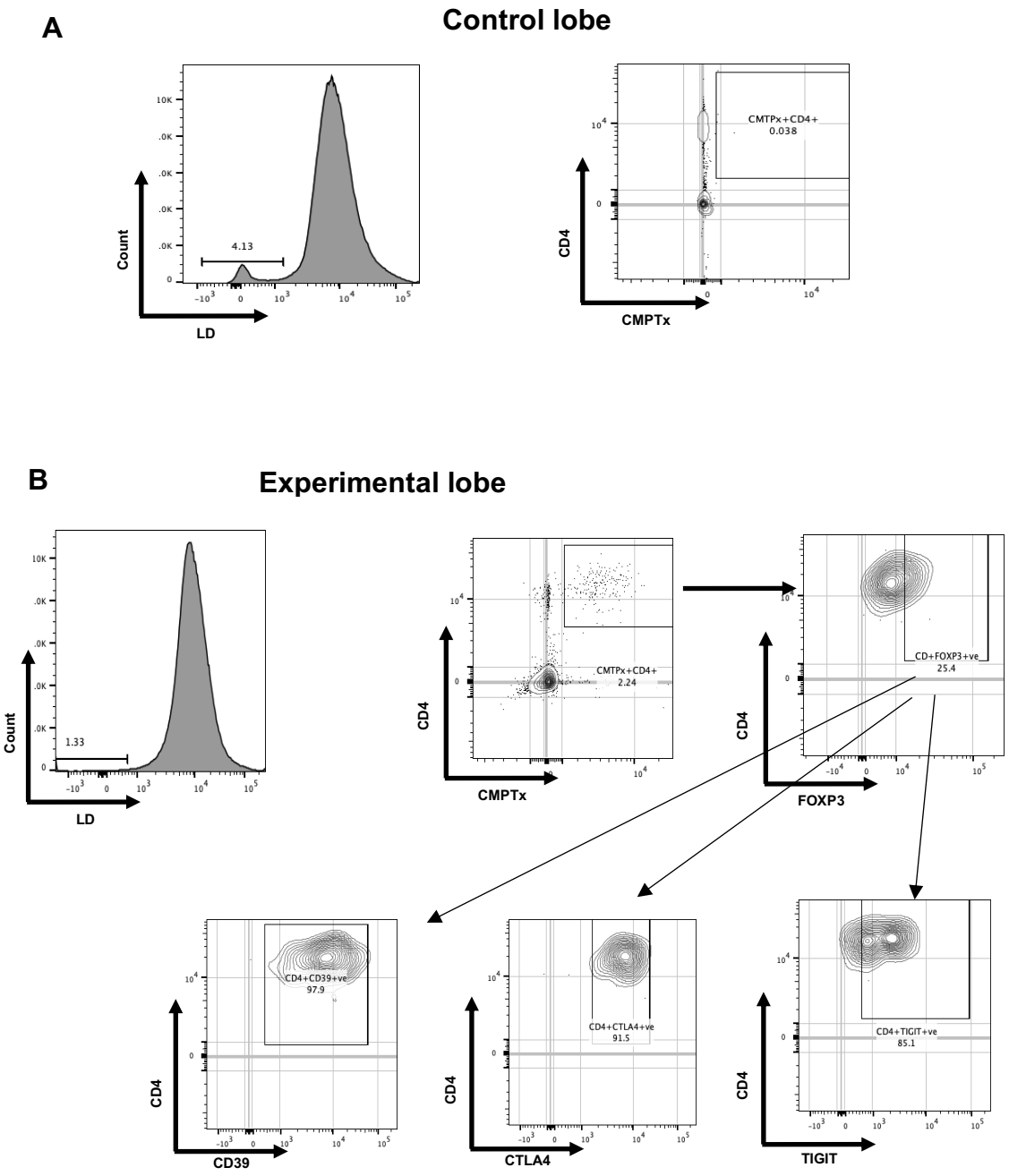

Figure 5.12 Flow cytometry analysis of the perfusate of experimental and control lobe after the perfusion. Panel A. Singlet, gated on live cells, showing CMPTx CD4+ cells. **Panel B.** Singlet lymphocytes, gated on live cells, and then on CD4+CMPTx+ cells. These cells were then stained for Treg-specific marker, such as FOXP3, CD39, CTLA4, TIGIT.

Intriguingly, when I investigated the cells within the wedges, the levels of FOXP3 were comparable with the pre-infusion levels, and the cells expressed high levels of CD39, TIGIT and CTLA4 with the latter being significantly higher compared with the pre-infusion levels. I could identify a nice population of hepatic Tregs not labelled, which showed a significantly less expression of activation markers (Figure 5.13). Overall we could infer that the infused SFiTregs upregulate FOXP3 and activation markers upon being exposed to the liver environment and, in turn, were retained within the liver.

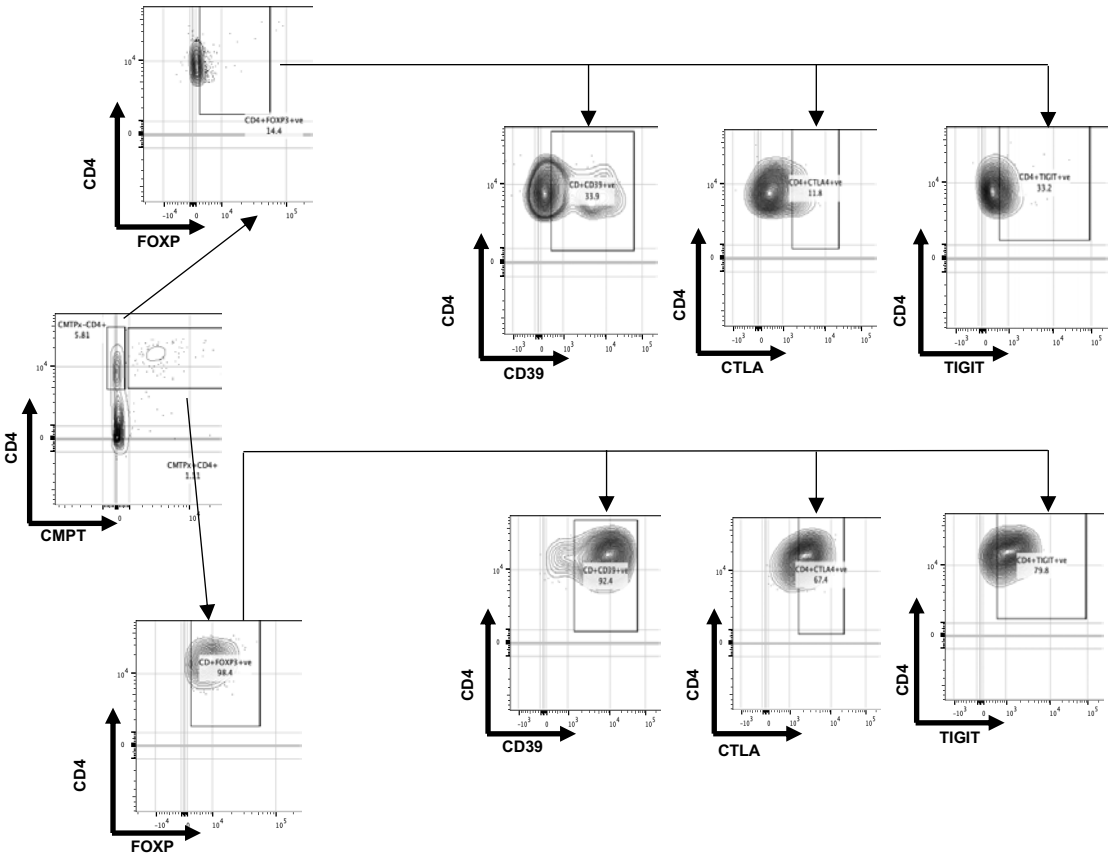

Figure 5.13 Flow cytometry phenotype of the lymphocyte isolated from the experimental lobe. The upper panels show the singlet, alive, CD4+CMPTx- FOXP3+ cells, namely the not infused Tregs (resident and circulating Tregs). The lower panels show the singlet, alive, CD4+CMPTx+FOXP3+ cells, namely the infused SFiTregs.

3.3.5. Discussion

In this chapter I presented an alternative method to produce induced Tregs as cell therapy product in PBC. The protocol I optimised in the last part of my PhD, requires two weeks to obtain more than 200 millions of cells, starting from 2 million of CD4+ T cells extracted from peripheral blood of PBC patients. This could be a way to overcome the long process needed to generate autologous cells expanded from the peripheral Treg pool.

SFiTregs demonstrated significantly higher stability in inflammatory environments, as they did not shift to the Th1 phenotype when exposed to a Th1-polarizing cytokine cocktail that simulates the liver environment in PBC patients. However, there was an observed tendency for CNS2 methylation. Liaskou and colleagues clearly showed how very small dose of IL-12 is already enough in patients with PBC to have their Treg cells starting to produce IFN-gamma and become instrumental to the inflammation rather than countering it(341).

SFiTregs, instead, not only remain fairly stable in high quantity of IL-12 and IFN-gamma, but they maintained their suppressive function too.

Another finding that could indicate a further advantage of SFiTregs compared with polyclonal autologous Tregs could be the higher expression of genes associated with the tissue adhesion and cell differentiation. In fact, this could suggest a more mature and antigen experienced phenotype and could indicate cells more prone to be retained in the inflamed tissue.

This was what we observed using wedge perfusion: SFiTregs after the infusion were more, and more activated compared with liver Tregs. Furthermore, the

number of SFiTregs recirculating in the supernatant was low and intriguingly the cells that was not retained in the liver where the ones less activated and which lost the FOXP3 expression.

The presented set of experiments, despite producing interesting results, have not negligible limitations, mostly due to the limited amount of time my funds allowed me to spend in Japan and even more to the relatively exiguous number of PBC and control samples I could ship to Japan.

For instance, I could not compare stability of SFiTregs vs natural Tregs extracted from the same individuals. These could have allowed me to replicate the results of Liaskou et al. however comparing head-to-head SFiTregs and natural Tregs.

Similarly, it would have been crucial to test the stability in Th17 polarising environment, another circumstance in which the low number of samples played a role.

Even with these limitations, I believe this data set the ground to explore SFiTregs as cell therapy platform.

4. Final Discussion and conclusions

This review explored the basis of immunological architecture of PBC. We have presented the autoimmune hypothesis well sustained by data, and described the aberrant cell states and immune pathways, found in patients and recapitulate in models, which eventually converge to drive the disease's pathogenesis. The effort in dissecting the disease pathogenesis has got an ultimate purpose which is to find a targeted treatment. However, despite extensive research and numerous attempts over the past four decades to identify effective immune-modulating treatments, significant challenges remain. The prototype immune modulators, such as corticosteroids, have proven ineffective in PBC, even when used as adjunctive therapies(342-344). Further attempts with different class of drugs, like colchicine and penicillamine(345, 346), antivirals such as lamivudine(347), as well as immunosuppressants like azathioprine and methotrexate, have been tested(348-350). However, these treatments have generally demonstrated only marginal efficacy, or have been associated with potential harm, leading to their exclusion from current treatment recommendations.

More recent attempt with targeted immunological treatment still failed in proving meaningful clinical effect. For instance, rituximab, an anti-CD20 monoclonal antibody, showed some promise by reducing alkaline phosphatase levels in a small cohort of patients, but overall clinical efficacy remained limited(351). High expectations were put on Ustekinumab, which targets the IL-12 and IL-23 pathways, having based on experimental and genetic data, a strong biological

rationale. However, it did not achieve significant improvements in alkaline phosphatase levels in larger patient groups, despite some biochemical indications of pathway modulation(352, 353). These outcomes highlight the paradoxical nature of PBC, where conventional and even specific immunosuppressive strategies fail to translate into effective disease control.

In the advanced stages of PBC, liver transplantation emerges as the only definitive treatment option, offering substantial improvements in graft and patient survival rates. Nonetheless, recurrence of PBC post-transplantation remains a frequent concern (172).

The current used treatments for PBC are active on bile acids metabolism and on the secretory machinery of BECs. These molecules, UDCA, or agonist of FXR, like obethicolic acid, and PPAR agonist, have an effect also on immune pathways. It would likely be helpful, for the general understanding of PBC pathogenesis detail the immune effects of this molecules. For instance, UDCA possesses multiple immune-modulating properties. It decreases the expression of MHC class I and II proteins on BECs, thereby reducing antigen presentation and the activation of autoreactive T cells(354). This might help restoring immune tolerance and break the inflammatory cascade driven by cytotoxic $CD8^+$ T cells, T_H1 cells, and macrophages. UDCA exerts anti-apoptotic effect, mediated through the modulation of survival signalling pathways such as nuclear factor kappa B (NF-κB), AKT, MAPK, and PI3K(355). Such effect not only prevent the biliary damage, but it also interrupts the antigen spreading, reducing inflammatory triggers. Additionally, UDCA restores NKT cell activity by reducing prostaglandin

E_2 production, fostering a balanced immune environment and preventing the shift toward a T_H17-dominated response that promotes fibrosis(356).

In cases where UDCA treatment is inadequate, second-line therapies targeting bile acid metabolism, such as obeticholic acid (OCA), an farnesoid X receptor (FXR) agonist, are used. These therapies aim to further modulate bile acid synthesis and transport, enhance intestinal barrier function, and reduce hepatic inflammation. However, even for FXR agonist, there are several and well described effects on immune system. McMahan and colleagues showed that the FXR and TGR5 agonism increase monocyte with anti-inflammatory phenotype and increase in obese mice. In vitro, upon FXR stimulation monocytes production of IL-10(357). Experimental models have demonstrated that FXR agonists can decrease the recruitment of natural killer (NK) cells and the production of IFN-γ, thereby mitigating immune-mediated liver damage and bacterial translocation from the gut(358). Also, OCA shows an effect in apoptosis reduction upon nuclear factor-κB activation.

Furthermore, peroxisome proliferator-activated receptor (PPAR)-α and PPAR-δ agonists have shown promise in inhibiting pro-fibrotic pathways and reducing inflammation. PPARs are nuclear receptors that regulate gene expression involved in lipid metabolism, inflammation, and immune responses. Activation of PPAR-α and PPAR-δ leads to the suppression of pro-inflammatory cytokine production, inhibition of NF-κB signaling, and modulation of immune cell differentiation and function. Specifically, PPAR agonists regulate T cell responses by promoting the differentiation of Treg cells while inhibiting the proliferation and function of pro-inflammatory T_H1 and T_H17 cells. This shift enhances immune

tolerance and reduces autoimmune-mediated damage to cholangiocytes. Additionally, PPAR agonists induce an anti-inflammatory phenotype in macrophages, reducing the secretion of inflammatory cytokines such as TNF-α and IL-6, and inhibiting the activation of hepatic stellate cells, which are central to fibrosis development. By regulating the expression of genes involved in bile acid transport and synthesis, PPAR agonists help maintain bile acid balance, reducing hepatobiliary stress and subsequent immune activation(359, 360).

The experimental work detailed in this thesis built on the hypothesis that CD8+ T cells play a central role in PBC pathogenesis. In particular, these cells were found to infiltrate and internalize into BECs, a novel and unexpected cellular interaction in PBC. The observed internalization of these eccentric CD8+ T cells involved dynamic cytoskeletal rearrangements and was dependent on PI3K signaling but did not involve ROCK1 activity, setting it apart from other known internalization processes in the liver such as CD4+ T cell enclysis. These findings mark an important step in understanding how CD8+ T cells interact with BECs, with further implications for how immune cells contribute to epithelial damage in autoimmune liver disease.

Despite the absence of immediate cytotoxicity following CD8+ T cell internalization into BECs, the frequent correlation between these events and BEC apoptosis in PBC patients indicates a potential long-term cytotoxic mechanism. The details of how CD8+ T cells disrupt BEC intracellular processes to cause apoptosis remain unclear, but this chapter's findings strongly suggest that the presence of these cells within BECs plays a role in disease progression. These insights into CD8+ T cell internalization help to clarify some of the previously

ambiguous aspects of PBC pathology and provide a basis for further investigation into how this process can be therapeutically targeted.

The paradigm of treatment is shifting in autoimmunity from treating to curing. The recent evidence of CAR-T cells approach targeting B cells in complex autoimmune conditions is certainly gaining attention and pushing the field forward(361). In case of the liver, remodelling the liver microenvironment, changing the cell composition and re-establishing the immune homeostasis should be set as the treatment goal. Furthermore, a more targeted approach in this instance, relies on a deep knowledge of the self-antigen which is the unique opportunity offered by PBC. The excitement surrounding new technologies in cellular engineering and therapy may drive this shift from chronic treatment to a possible cure. The recent data on CAR technology targeting PD-1$^+$ T_{RM} cells may open new treatment venues, however, it remains to be seen how these results translate to humans.

Increasing the number or reprogramming Treg cells is another therapy venue currently persued in several autoimmune conditions. The treatment approaches are several and none of them without challenges.

The *in*-situ expansion of Tregs can be obtained using low dose of IL-2, targeting selectively Tregs and avoiding the proliferation of the cytotoxic population. Such approach has been tested in several autoimmune disease, such as lupus and diabetes. The use of low dose of IL-2 significantly boosted the number of Tregs, but with a significant effect also on NK and CD8$^+$ T cells(338).

We tested the *ex vivo* expansion of Tregs from patients with AIH and the reinfusion of the cell product. This early phase trial proved that the treatment is

very well tolerated. We also showed that the Tregs after reinfusion localised mainly within the liver, most likely due to the homing to the inflamed organ(326). A similar approach is currently under investigations in our lab also for PBC.

The collateral effect of inducing a broad tolerance toward dangerous antigens, can be overcome by inducing or transferring antigen-specific Treg cells. However, moving from a polyclonal Treg therapy to an antigen specific approach in humans remains incredibly challenging. The expansion of autoreactive clones from periphery, poses two issues, first the identification of the autoreactive clones. This relies on engineered tetramers which should target the epitope of interest. The second is the isolation and the consequent expansion of the cell population that could require long time to reach a therapeutic concentration. Alternatively, engineering the TCR to generate antigen specific clones is certainly an emerging approach(362). Sakaguchi's group proposed an epigenetic reprogramming of $CD4^+$ T cells to induce stable and functioning Treg cells by inhibiting cyclin dependent kinase 8 and 19. This approach allows to select $CD4^+$ T memory cells and convert them into induced Tregs by inducing the expression of FOXP3(339).

In this thesis I presented the first attempt to introduce this novel approach for the production of stable and functional induced regulatory T cells (SFiTregs) as a potential cell therapy platform for PBC. The process for generating SFiTregs, optimized over the course of this research, demonstrated the capacity to produce over 200 million cells from a small starting population of CD4+ T cells extracted from peripheral blood. The ability of SFiTregs to remain stable and functional in inflammatory environments, even in the presence of high levels of IL-12 and IFN-

gamma, marks a significant improvement over polyclonal Tregs, which tend to lose their regulatory function and shift toward a Th1 phenotype under similar conditions.

This stability, along with the enhanced expression of tissue adhesion and cell differentiation genes, suggests that SFiTregs may have superior retention in inflamed liver tissues compared to natural Tregs. Experimental data further support this hypothesis, as the infusion of SFiTregs into wedge-perfused livers resulted in their greater retention and activation in the liver compared to circulating Tregs, providing a promising avenue for future cell-based therapies in PBC.

Over the past few decades, and especially in the last ten years, the clinical management of PBC has advanced significantly. We have now several options as second-line treatments and we have the ability to identify complex cases early using stratification tools.

However, the underlying causes of PBC remain elusive. The variety of experimental findings to date hasn't yet led to a comprehensive understanding of the disease's pathogenesis. Immunologically, PBC stands out as a unique model for studying autoimmunity. This is due to its well-defined disease epitopes, slow disease progression, and a relatively consistent phenotype among patients. Moving forward, ongoing research is crucial to decipher the complexities of PBC and to develop more targeted therapies and even reestablish the tolerance toward the antigen in these patients.

5. Reference

1. **V Ronca, Mancuso C, Milani C, Carbone M, Oo Y, and Invernizzi P**. Immune system and cholangiocytes: A puzzling affair in primary biliary cholangitis. *Journal of Leukocyte Biology* 108: 659-671 , pmid = 32349179, 2020.
2. **V Ronca, Carbone M, Bernuzzi F, Malinverno F, Mousa HS, Gershwin ME, and Invernizzi P**. From pathogenesis to novel therapies in the treatment of primary biliary cholangitis. *Expert Review of Clinical Immunology* 13: 2017.
3. **A Bozward, Cè M, Dell'oro L, Oo H Y, and Ronca V**. Breakdown in hepatic tolerance and its relation to autoimmune liver diseases. *Minerva Gastroenterology* 2021.
4. **V Ronca, Gerussi A, Collins P, Parente A, Oo YH, and Invernizzi P**. The liver as a central "hub" of the immune system: pathophysiological implications. *Physiol Rev* 2024.
5. **GD Lascaux**. Carnac. Butterworth, London, 1965.
6. **t-c Alter R**. *The Hebrew Bible*. New York: WW Norton and Company, 2019.
7. **M Jastrow**. *The liver in antiquity and the beginnings of anatomy*. 1908.
8. **Galen, and Singer C**. *Galen on Anatomical Procedures:...: Translation of the Surviving Books; with Introduction and Notes*. Wellcome Historical MedicalMuseum, 1956.
9. **F Tonelli, and Batignani G**. The modern vision of the vascular anatomy of the liver by Leonardo da Vinci. *Surgery* 167: 912-916, 2020.
10. **CD O'Malley, and de CM Saunders J**. *The Illustrations from the Works of Andreas Vesalius of Brussels: With Annotations and Translations, a Discussion of the Plates and their Background, Authorship and Influence, and a Biographical Sketch of Vesalius*. 1950.
11. **M Foster**. *Lectures on the history of physiology during the sixteenth, seventeenth, and eighteenth centuries*. University press, 1901.
12. **RY Calne, Sells RA, Pena JR, Davis DR, Millard PR, Herbertson BM, Binns RM, and Davies DAL**. Induction of immunological tolerance by porcine liver allografts. *Nature* 223: 472-476 , pmid = 4894426, 1969.
13. **S Sarnacki, Nakai H, Calise D, Azuma T, Brousse N, Révillon Y, and Cerf-Bensussan N**. Decreased expression of the interleukin 2 receptor on CD8 recipient lymphocytes in intestinal grafts rendered tolerant by liver transplantation in rats. *Gut* 43: 849-855, 1998.
14. **HM Cantor, and Dumont AE**. Hepatic suppression of sensitization to antigen absorbed into the portal system. *Nature* 215: 744-745, 1967.
15. **B Gao, Jeong WI, and Tian Z**. Liver: An organ with predominant innate immunity. *Hepatology* 47: 729-736, 2008.
16. **V Racanelli, and Rehermann B**. The liver as an immunological organ. *Hepatology* 43: S54-62, 2006.
17. **KK Sørensen, Simon-Santamaria J, McCuskey RS, and Smedsrød B**. Liver Sinusoidal Endothelial Cells. *Compr Physiol* 5: 1751-1774, 2015.

18. **F Braet, and Wisse E**. Structural and functional aspects of liver sinusoidal endothelial cell fenestrae: a review. *Comp Hepatol* 1: 1, 2002.
19. **R Saxena, Theise ND, and Crawford JM**. Microanatomy of the human liver-exploring the hidden interfaces. *Hepatology* 30: 1339-1346, 1999.
20. **A Uhrig, Banafsche R, Kremer M, Hegenbarth S, Hamann A, Neurath M, Gerken G, Limmer A, and Knolle PA**. Development and functional consequences of LPS tolerance in sinusoidal endothelial cells of the liver. *J Leukoc Biol* 77: 626-633, 2005.
21. **LP Ganesan, Mohanty S, Kim J, Clark KR, Robinson JM, and Anderson CL**. Rapid and efficient clearance of blood-borne virus by liver sinusoidal endothelium. *PLoS Pathog* 7: e1002281, 2011.
22. **HW Zimmermann, Bruns T, Weston CJ, Curbishley SM, Liaskou E, Li KK, Resheq YJ, Badenhorst PW, and Adams DH**. Bidirectional transendothelial migration of monocytes across hepatic sinusoidal endothelium shapes monocyte differentiation and regulates the balance between immunity and tolerance in liver. *Hepatology* 63: 233-246, 2016.
23. **AK Horst, Neumann K, Diehl L, and Tiegs G**. Modulation of liver tolerance by conventional and nonconventional antigen-presenting cells and regulatory immune cells. *Cell Mol Immunol* 13: 277-292, 2016.
24. **E Gomez Perdiguero, Klapproth K, Schulz C, Busch K, Azzoni E, Crozet L, Garner H, Trouillet C, de Bruijn MF, Geissmann F, and Rodewald HR**. Tissue-resident macrophages originate from yolk-sac-derived erythro-myeloid progenitors. *Nature* 518: 547-551, 2015.
25. **S Yona, Kim KW, Wolf Y, Mildner A, Varol D, Breker M, Strauss-Ayali D, Viukov S, Guilliams M, Misharin A, Hume DA, Perlman H, Malissen B, Zelzer E, and Jung S**. Fate mapping reveals origins and dynamics of monocytes and tissue macrophages under homeostasis. *Immunity* 38: 79-91, 2013.
26. **P Knolle, Schlaak J, Uhrig A, Kempf P, Meyer zum Büschenfelde KH, and Gerken G**. Human Kupffer cells secrete IL-10 in response to lipopolysaccharide (LPS) challenge. *J Hepatol* 22: 226-229, 1995.
27. **GJ Bowers, MacVittie TJ, Hirsch EF, Conklin JC, Nelson RD, Roethel RJ, and Fink MP**. Prostanoid production by lipopolysaccharide-stimulated Kupffer cells. *J Surg Res* 38: 501-508, 1985.
28. **CR Roland, Walp L, Stack RM, and Flye MW**. Outcome of Kupffer cell antigen presentation to a cloned murine Th1 lymphocyte depends on the inducibility of nitric oxide synthase by IFN-gamma. *J Immunol* 153: 5453-5464, 1994.
29. **A Schurich, Berg M, Stabenow D, Böttcher J, Kern M, Schild HJ, Kurts C, Schuette V, Burgdorf S, Diehl L, Limmer A, and Knolle PA**. Dynamic regulation of CD8 T cell tolerance induction by liver sinusoidal endothelial cells. *J Immunol* 184: 4107-4114, 2010.
30. **X Xu, Jin R, Li M, Wang K, Zhang S, Hao J, Sun X, Zhang Y, Wu H, Zhang J, and Ge Q**. Liver sinusoidal endothelial cells induce tolerance of autoreactive CD4+ recent thymic emigrants. *Sci Rep* 6: 19861, 2016.
31. **A Dangi, Sumpter TL, Kimura S, Stolz DB, Murase N, Raimondi G, Vodovotz Y, Huang C, Thomson AW, and Gandhi CR**. Selective expansion

of allogeneic regulatory T cells by hepatic stellate cells: role of endotoxin and implications for allograft tolerance. *J Immunol* 188: 3667-3677, 2012.
32. **MC Yu, Chen CH, Liang X, Wang L, Gandhi CR, Fung JJ, Lu L, and Qian S**. Inhibition of T-cell responses by hepatic stellate cells via B7-H1-mediated T-cell apoptosis in mice. *Hepatology* 40: 1312-1321, 2004.
33. **IN Crispe**. The liver as a lymphoid organ. *Annu Rev Immunol* 27: 147-163, 2009.
34. **HR Yang, Chou HS, Gu X, Wang L, Brown KE, Fung JJ, Lu L, and Qian S**. Mechanistic insights into immunomodulation by hepatic stellate cells in mice: a critical role of interferon-gamma signaling. *Hepatology* 50: 1981-1991, 2009.
35. **C Wiegard, Frenzel C, Herkel J, Kallen KJ, Schmitt E, and Lohse AW**. Murine liver antigen presenting cells control suppressor activity of CD4+CD25+ regulatory T cells. *Hepatology* 42: 193-199, 2005.
36. **M Mühlbauer, Fleck M, Schütz C, Weiss T, Froh M, Blank C, Schölmerich J, and Hellerbrand C**. PD-L1 is induced in hepatocytes by viral infection and by interferon-alpha and -gamma and mediates T cell apoptosis. *J Hepatol* 45: 520-528, 2006.
37. **J Herkel, Jagemann B, Wiegard C, Lazaro JF, Lueth S, Kanzler S, Blessing M, Schmitt E, and Lohse AW**. MHC class II-expressing hepatocytes function as antigen-presenting cells and activate specific CD4 T lymphocyutes. *Hepatology* 37: 1079-1085, 2003.
38. **A Warren, Le Couteur DG, Fraser R, Bowen DG, McCaughan GW, and Bertolino P**. T lymphocytes interact with hepatocytes through fenestrations in murine liver sinusoidal endothelial cells. *Hepatology* 44: 1182-1190, 2006.
39. **I Jomantaite, Dikopoulos N, Kröger A, Leithäuser F, Hauser H, Schirmbeck R, and Reimann J**. Hepatic dendritic cell subsets in the mouse. *Eur J Immunol* 34: 355-365, 2004.
40. **AH Rahman, and Aloman C**. Dendritic cells and liver fibrosis. *Biochim Biophys Acta* 1832: 998-1004, 2013.
41. **WK Lai, Curbishley SM, Goddard S, Alabraba E, Shaw J, Youster J, McKeating J, and Adams DH**. Hepatitis C is associated with perturbation of intrahepatic myeloid and plasmacytoid dendritic cell function. *J Hepatol* 47: 338-347, 2007.
42. **G Frumento, Rotondo R, Tonetti M, Damonte G, Benatti U, and Ferrara GB**. Tryptophan-derived catabolites are responsible for inhibition of T and natural killer cell proliferation induced by indoleamine 2,3-dioxygenase. *J Exp Med* 196: 459-468, 2002.
43. **B Jürgens, Hainz U, Fuchs D, Felzmann T, and Heitger A**. Interferon-gamma-triggered indoleamine 2,3-dioxygenase competence in human monocyte-derived dendritic cells induces regulatory activity in allogeneic T cells. *Blood* 114: 3235-3243, 2009.
44. **S Sutti, Bruzzì S, Heymann F, Liepelt A, Krenkel O, Toscani A, Ramavath NN, Cotella D, Albano E, and Tacke F**. CX. *Cells* 8: 2019.
45. **S Norris, Collins C, Doherty DG, Smith F, McEntee G, Traynor O, Nolan N, Hegarty J, and O'Farrelly C**. Resident human hepatic lymphocytes are phenotypically different from circulating lymphocytes. *J Hepatol* 28: 84-90, 1998.

46. **DG Doherty, Norris S, Madrigal-Estebas L, McEntee G, Traynor O, Hegarty JE, and O'Farrelly C**. The human liver contains multiple populations of NK cells, T cells, and CD3+CD56+ natural T cells with distinct cytotoxic activities and Th1, Th2, and Th0 cytokine secretion patterns. *J Immunol* 163: 2314-2321, 1999.
47. **HW Zimmermann, Mueller JR, Seidler S, Luedde T, Trautwein C, and Tacke F**. Frequency and phenotype of human circulating and intrahepatic natural killer cell subsets is differentially regulated according to stage of chronic liver disease. *Digestion* 88: 1-16, 2013.
48. **H Peng, Wisse E, and Tian Z**. Liver natural killer cells: subsets and roles in liver immunity. *Cell Mol Immunol* 13: 328-336, 2016.
49. **KA Stegmann, Robertson F, Hansi N, Gill U, Pallant C, Christophides T, Pallett LJ, Peppa D, Dunn C, Fusai G, Male V, Davidson BR, Kennedy P, and Maini MK**. CXCR6 marks a novel subset of T-bet(lo)Eomes(hi) natural killer cells residing in human liver. *Sci Rep* 6: 26157, 2016.
50. **J Zhao, Zhang S, Liu Y, He X, Qu M, Xu G, Wang H, Huang M, Pan J, Liu Z, Li Z, Liu L, and Zhang Z**. Single-cell RNA sequencing reveals the heterogeneity of liver-resident immune cells in human. *Cell Discov* 6: 22, 2020.
51. **P Ramachandran, Dobie R, Wilson-Kanamori JR, Dora EF, Henderson BEP, Luu NT, Portman JR, Matchett KP, Brice M, Marwick JA, Taylor RS, Efremova M, Vento-Tormo R, Carragher NO, Kendall TJ, Fallowfield JA, Harrison EM, Mole DJ, Wigmore SJ, Newsome PN, Weston CJ, Iredale JP, Tacke F, Pollard JW, Ponting CP, Marioni JC, Teichmann SA, and Henderson NC**. Resolving the fibrotic niche of human liver cirrhosis at single-cell level. *Nature* 575: 512-518, 2019.
52. **V Kumar**. NKT-cell subsets: promoters and protectors in inflammatory liver disease. *J Hepatol* 59: 618-620, 2013.
53. **PX Liew, Lee WY, and Kubes P**. iNKT Cells Orchestrate a Switch from Inflammation to Resolution of Sterile Liver Injury. *Immunity* 47: 752-765.e755, 2017.
54. **E Treiner, Duban L, Bahram S, Radosavljevic M, Wanner V, Tilloy F, Affaticati P, Gilfillan S, and Lantz O**. Selection of evolutionarily conserved mucosal-associated invariant T cells by MR1. *Nature* 422: 164-169, 2003.
55. **HC Jeffery, van Wilgenburg B, Kurioka A, Parekh K, Stirling K, Roberts S, Dutton EE, Hunter S, Geh D, Braitch MK, Rajanayagam J, Iqbal T, Pinkney T, Brown R, Withers DR, Adams DH, Klenerman P, and Oo YH**. Biliary epithelium and liver B cells exposed to bacteria activate intrahepatic MAIT cells through MR1. *J Hepatol* 64: 1118-1127, 2016.
56. **A Riva, Patel V, Kurioka A, Jeffery HC, Wright G, Tarff S, Shawcross D, Ryan JM, Evans A, Azarian S, Bajaj JS, Fagan A, Mehta K, Lopez C, Simonova M, Katzarov K, Hadzhiolova T, Pavlova S, Wendon JA, Oo YH, Klenerman P, Williams R, and Chokshi S**. Mucosa-associated invariant T cells link intestinal immunity with antibacterial immune defects in alcoholic liver disease. *Gut* 67: 918-930, 2018.
57. **K Böttcher, Rombouts K, Saffioti F, Roccarina D, Rosselli M, Hall A, Luong TV, Tsochatzis E, Thorburn D, and Pinzani M**. MAIT cells are chronically activated in patients with autoimmune liver disease and promote

profibrogenic hepatic stellate cell activation. *Hepatology* 68: 172-186 , pmid = 29023935, 2018.
58. **LJ Pallett, and Maini MK**. Liver-resident memory T cells: life in lockdown. *Semin Immunopathol* 44: 813-825, 2022.
59. **LJ Pallett, Davies J, Colbeck EJ, Robertson F, Hansi N, Easom NJW, Burton AR, Stegmann KA, Schurich A, Swadling L, Gill US, Male V, Luong T, Gander A, Davidson BR, Kennedy PTF, and Maini MK**. IL-2(high) tissue-resident T cells in the human liver: Sentinels for hepatotropic infection. *J Exp Med* 214: 1567-1580, 2017.
60. **LJ Pallett, Burton AR, Amin OE, Rodriguez-Tajes S, Patel AA, Zakeri N, Jeffery-Smith A, Swadling L, Schmidt NM, Baiges A, Gander A, Yu D, Nasralla D, Froghi F, Iype S, Davidson BR, Thorburn D, Yona S, Forns X, and Maini MK**. Longevity and replenishment of human liver-resident memory T cells and mononuclear phagocytes. *J Exp Med* 217: 2020.
61. **US Gill, Pallett LJ, Thomas N, Burton AR, Patel AA, Yona S, Kennedy PTF, and Maini MK**. Fine needle aspirates comprehensively sample intrahepatic immunity. *Gut* 68: 1493-1503, 2019.
62. **PA Szabo, Miron M, and Farber DL**. Location, location, location: Tissue resident memory T cells in mice and humans. *Sci Immunol* 4: 2019.
63. **L Kok, Masopust D, and Schumacher TN**. The precursors of CD8(+) tissue resident memory T cells: from lymphoid organs to infected tissues. *Nat Rev Immunol* 22: 283-293, 2022.
64. **D Fernandez-Ruiz, Ng WY, Holz LE, Ma JZ, Zaid A, Wong YC, Lau LS, Mollard V, Cozijnsen A, Collins N, Li J, Davey GM, Kato Y, Devi S, Skandari R, Pauley M, Manton JH, Godfrey DI, Braun A, Tay SS, Tan PS, Bowen DG, Koch-Nolte F, Rissiek B, Carbone FR, Crabb BS, Lahoud M, Cockburn IA, Mueller SN, Bertolino P, McFadden GI, Caminschi I, and Heath WR**. Liver-Resident Memory CD8(+) T Cells Form a Front-Line Defense against Malaria Liver-Stage Infection. *Immunity* 45: 889-902, 2016.
65. **EM Steinert, Schenkel JM, Fraser KA, Beura LK, Manlove LS, Igyarto BZ, Southern PJ, and Masopust D**. Quantifying Memory CD8 T Cells Reveals Regionalization of Immunosurveillance. *Cell* 161: 737-749, 2015.
66. **D Amsen, van Gisbergen K, Hombrink P, and van Lier RAW**. Tissue-resident memory T cells at the center of immunity to solid tumors. *Nat Immunol* 19: 538-546, 2018.
67. **SN Mueller, and Mackay LK**. Tissue-resident memory T cells: local specialists in immune defence. *Nat Rev Immunol* 16: 79-89, 2016.
68. **Y Koda, Teratani T, Chu PS, Hagihara Y, Mikami Y, Harada Y, Tsujikawa H, Miyamoto K, Suzuki T, Taniki N, Sujino T, Sakamoto M, Kanai T, and Nakamoto N**. CD8(+) tissue-resident memory T cells promote liver fibrosis resolution by inducing apoptosis of hepatic stellate cells. *Nat Commun* 12: 4474, 2021.
69. **T Gebhardt, Palendira U, Tscharke DC, and Bedoui S**. Tissue-resident memory T cells in tissue homeostasis, persistent infection, and cancer surveillance. *Immunol Rev* 283: 54-76, 2018.
70. **K Okla, Farber DL, and Zou W**. Tissue-resident memory T cells in tumor immunity and immunotherapy. *J Exp Med* 218: 2021.

71. **SL Park, Buzzai A, Rautela J, Hor JL, Hochheiser K, Effern M, McBain N, Wagner T, Edwards J, McConville R, Wilmott JS, Scolyer RA, Tuting T, Palendira U, Gyorki D, Mueller SN, Huntington ND, Bedoui S, Holzel M, Mackay LK, Waithman J, and Gebhardt T**. Tissue-resident memory CD8(+) T cells promote melanoma-immune equilibrium in skin. *Nature* 565: 366-371, 2019.
72. **A Gola, Silman D, Walters AA, Sridhar S, Uderhardt S, Salman AM, Halbroth BR, Bellamy D, Bowyer G, Powlson J, Baker M, Venkatraman N, Poulton I, Berrie E, Roberts R, Lawrie AM, Angus B, Khan SM, Janse CJ, Ewer KJ, Germain RN, Spencer AJ, and Hill AVS**. Prime and target immunization protects against liver-stage malaria in mice. *Sci Transl Med* 10: 2018.
73. **TM Olsen, Stone BC, Chuenchob V, and Murphy SC**. Prime-and-Trap Malaria Vaccination To Generate Protective CD8(+) Liver-Resident Memory T Cells. *J Immunol* 201: 1984-1993, 2018.
74. **SW Tse, Radtke AJ, Espinosa DA, Cockburn IA, and Zavala F**. The chemokine receptor CXCR6 is required for the maintenance of liver memory CD8(+) T cells specific for infectious pathogens. *J Infect Dis* 210: 1508-1516, 2014.
75. **LE Holz, Chua YC, de Menezes MN, Anderson RJ, Draper SL, Compton BJ, Chan STS, Mathew J, Li J, Kedzierski L, Wang Z, Beattie L, Enders MH, Ghilas S, May R, Steiner TM, Lange J, Fernandez-Ruiz D, Valencia-Hernandez AM, Osmond TL, Farrand KJ, Seneviratna R, Almeida CF, Tullett KM, Bertolino P, Bowen DG, Cozijnsen A, Mollard V, McFadden GI, Caminschi I, Lahoud MH, Kedzierska K, Turner SJ, Godfrey DI, Hermans IF, Painter GF, and Heath WR**. Glycolipid-peptide vaccination induces liver-resident memory CD8(+) T cells that protect against rodent malaria. *Sci Immunol* 5: 2020.
76. **AS Ishizuka, Lyke KE, DeZure A, Berry AA, Richie TL, Mendoza FH, Enama ME, Gordon IJ, Chang LJ, Sarwar UN, Zephir KL, Holman LA, James ER, Billingsley PF, Gunasekera A, Chakravarty S, Manoj A, Li M, Ruben AJ, Li T, Eappen AG, Stafford RE, K CN, Murshedkar T, DeCederfelt H, Plummer SH, Hendel CS, Novik L, Costner PJ, Saunders JG, Laurens MB, Plowe CV, Flynn B, Whalen WR, Todd JP, Noor J, Rao S, Sierra-Davidson K, Lynn GM, Epstein JE, Kemp MA, Fahle GA, Mikolajczak SA, Fishbaugher M, Sack BK, Kappe SH, Davidson SA, Garver LS, Bjorkstrom NK, Nason MC, Graham BS, Roederer M, Sim BK, Hoffman SL, Ledgerwood JE, and Seder RA**. Protection against malaria at 1 year and immune correlates following PfSPZ vaccination. *Nat Med* 22: 614-623, 2016.
77. **S Inoue, Niikura M, Mineo S, and Kobayashi F**. Roles of IFN-gamma and gammadelta T Cells in Protective Immunity Against Blood-Stage Malaria. *Front Immunol* 4: 258, 2013.
78. **SP Kurup, Butler NS, and Harty JT**. T cell-mediated immunity to malaria. *Nat Rev Immunol* 19: 457-471, 2019.
79. **LS Lau, Fernandez-Ruiz D, Mollard V, Sturm A, Neller MA, Cozijnsen A, Gregory JL, Davey GM, Jones CM, Lin YH, Haque A, Engwerda CR, Nie CQ, Hansen DS, Murphy KM, Papenfuss AT, Miles JJ, Burrows SR, de Koning-Ward T, McFadden GI, Carbone FR, Crabb BS, and Heath WR**.

CD8+ T cells from a novel T cell receptor transgenic mouse induce liver-stage immunity that can be boosted by blood-stage infection in rodent malaria. *PLoS Pathog* 10: e1004135, 2014.
80. **P Hombrink, Helbig C, Backer RA, Piet B, Oja AE, Stark R, Brasser G, Jongejan A, Jonkers RE, Nota B, Basak O, Clevers HC, Moerland PD, Amsen D, and van Lier RA**. Programs for the persistence, vigilance and control of human CD8(+) lung-resident memory T cells. *Nat Immunol* 17: 1467-1478, 2016.
81. **LG Guidotti, Ando K, Hobbs MV, Ishikawa T, Runkel L, Schreiber RD, and Chisari FV**. Cytotoxic T lymphocytes inhibit hepatitis B virus gene expression by a noncytolytic mechanism in transgenic mice. *Proc Natl Acad Sci U S A* 91: 3764-3768, 1994.
82. **R Thimme, Wieland S, Steiger C, Ghrayeb J, Reimann KA, Purcell RH, and Chisari FV**. CD8(+) T cells mediate viral clearance and disease pathogenesis during acute hepatitis B virus infection. *J Virol* 77: 68-76, 2003.
83. **K Kakimi, Lane TE, Wieland S, Asensio VC, Campbell IL, Chisari FV, and Guidotti LG**. Blocking chemokine responsive to gamma-2/interferon (IFN)-gamma inducible protein and monokine induced by IFN-gamma activity in vivo reduces the pathogenetic but not the antiviral potential of hepatitis B virus-specific cytotoxic T lymphocytes. *J Exp Med* 194: 1755-1766, 2001.
84. **M Dudek, Pfister D, Donakonda S, Filpe P, Schneider A, Laschinger M, Hartmann D, Huser N, Meiser P, Bayerl F, Inverso D, Wigger J, Sebode M, Ollinger R, Rad R, Hegenbarth S, Anton M, Guillot A, Bowman A, Heide D, Muller F, Ramadori P, Leone V, Garcia-Caceres C, Gruber T, Seifert G, Kabat AM, Mallm JP, Reider S, Effenberger M, Roth S, Billeter AT, Muller-Stich B, Pearce EJ, Koch-Nolte F, Kaser R, Tilg H, Thimme R, Boettler T, Tacke F, Dufour JF, Haller D, Murray PJ, Heeren R, Zehn D, Bottcher JP, Heikenwalder M, and Knolle PA**. Auto-aggressive CXCR6(+) CD8 T cells cause liver immune pathology in NASH. *Nature* 592: 444-449, 2021.
85. **D Pfister, Nunez NG, Pinyol R, Govaere O, Pinter M, Szydlowska M, Gupta R, Qiu M, Deczkowska A, Weiner A, Muller F, Sinha A, Friebel E, Engleitner T, Lenggenhager D, Moncsek A, Heide D, Stirm K, Kosla J, Kotsiliti E, Leone V, Dudek M, Yousuf S, Inverso D, Singh I, Teijeiro A, Castet F, Montironi C, Haber PK, Tiniakos D, Bedossa P, Cockell S, Younes R, Vacca M, Marra F, Schattenberg JM, Allison M, Bugianesi E, Ratziu V, Pressiani T, D'Alessio A, Personeni N, Rimassa L, Daly AK, Scheiner B, Pomej K, Kirstein MM, Vogel A, Peck-Radosavljevic M, Hucke F, Finkelmeier F, Waidmann O, Trojan J, Schulze K, Wege H, Koch S, Weinmann A, Bueter M, Rossler F, Siebenhuner A, De Dosso S, Mallm JP, Umansky V, Jugold M, Luedde T, Schietinger A, Schirmacher P, Emu B, Augustin HG, Billeter A, Muller-Stich B, Kikuchi H, Duda DG, Kutting F, Waldschmidt DT, Ebert MP, Rahbari N, Mei HE, Schulz AR, Ringelhan M, Malek N, Spahn S, Bitzer M, Ruiz de Galarreta M, Lujambio A, Dufour JF, Marron TU, Kaseb A, Kudo M, Huang YH, Djouder N, Wolter K, Zender L, Marche PN, Decaens T, Pinato DJ, Rad R, Mertens JC, Weber A, Unger K, Meissner F, Roth S, Jilkova ZM, Claassen M, Anstee QM, Amit I, Knolle P, Becher B, Llovet JM, and Heikenwalder M**. NASH limits anti-tumour surveillance in immunotherapy-treated HCC. *Nature* 592: 450-456, 2021.

86. **JH Kim, Han JW, Choi YJ, Rha MS, Koh JY, Kim KH, Kim CG, Lee YJ, Kim AR, Park J, Kim HK, Min BS, Seo SI, Kang M, Park HJ, Han DH, Kim SI, Kim MS, Lee JG, Lee DH, Kim W, Park JY, Park SH, Joo DJ, and Shin EC**. Functions of human liver CD69(+)CD103(-)CD8(+) T cells depend on HIF-2alpha activity in healthy and pathologic livers. *J Hepatol* 72: 1170-1181, 2020.
87. **CA Chapin, Burn T, Meijome T, Loomes KM, Melin-Aldana H, Kreiger PA, Whitington PF, Behrens EM, and Alonso EM**. Indeterminate pediatric acute liver failure is uniquely characterized by a CD103(+) CD8(+) T-cell infiltrate. *Hepatology* 68: 1087-1100, 2018.
88. **Z You, Li Y, Wang Q, Zhao Z, Li Y, Qian Q, Li B, Zhang J, Huang B, Liang J, Chen R, Lyu Z, Chen Y, Lian M, Xiao X, Miao Q, Fang J, Lian Z, Eric Gershwin M, Tang R, and Ma X**. The Clinical Significance of Hepatic CD69(+) CD103(+) CD8(+) Resident-Memory T Cells in Autoimmune Hepatitis. *Hepatology* 74: 847-863, 2021.
89. **F Schaffner, and Popper H**. Electron microscopic studies of normal and proliferated bile ductules. *Am J Pathol* 38: 393-410, 1961.
90. **J Ludwig**. New concepts in biliary cirrhosis. *Semin Liver Dis* 7: 293-301, 1987.
91. **H Sasaki, Schaffner F, and Popper H**. Bile ductules in cholestasis: morphologic evidence for secretion and absorption in man. *Lab Invest* 16: 84-95, 1967.
92. **A Benedetti, Bassotti C, Rapino K, Marucci L, and Jezequel AM**. A morphometric study of the epithelium lining the rat intrahepatic biliary tree. *J Hepatol* 24: 335-342, 1996.
93. **Al Masyuk, Masyuk TV, and LaRusso NF**. Cholangiocyte primary cilia in liver health and disease. *Dev Dyn* 237: 2007-2012, 2008.
94. **M Trauner, and Boyer JL**. Bile salt transporters: molecular characterization, function, and regulation. *Physiol Rev* 83: 633-671, 2003.
95. **S Afroze, Meng F, Jensen K, McDaniel K, Rahal K, Onori P, Gaudio E, Alpini G, and Glaser SS**. The physiological roles of secretin and its receptor. *Ann Transl Med* 1: 29, 2013.
96. **G Alpini, Roberts S, Kuntz SM, Ueno Y, Gubba S, Podila PV, LeSage G, and LaRusso NF**. Morphological, molecular, and functional heterogeneity of cholangiocytes from normal rat liver. *Gastroenterology* 110: 1636-1643, 1996.
97. **SS Glaser, Gaudio E, Rao A, Pierce LM, Onori P, Franchitto A, Francis HL, Dostal DE, Venter JK, DeMorrow S, Mancinelli R, Carpino G, Alvaro D, Kopriva SE, Savage JM, and Alpini GD**. Morphological and functional heterogeneity of the mouse intrahepatic biliary epithelium. *Lab Invest* 89: 456-469, 2009.
98. **R Mancinelli, Franchitto A, Gaudio E, Onori P, Glaser S, Francis H, Venter J, Demorrow S, Carpino G, Kopriva S, White M, Fava G, Alvaro D, and Alpini G**. After damage of large bile ducts by gamma-aminobutyric acid, small ducts replenish the biliary tree by amplification of calcium-dependent signaling and de novo acquisition of large cholangiocyte phenotypes. *Am J Pathol* 176: 1790-1800, 2010.
99. **AK Dutta, Khimji AK, Kresge C, Bugde A, Dougherty M, Esser V, Ueno Y, Glaser SS, Alpini G, Rockey DC, and Feranchak AP**. Identification

and functional characterization of TMEM16A, a Ca2+-activated Cl- channel activated by extracellular nucleotides, in biliary epithelium. *J Biol Chem* 286: 766-776, 2011.
100. **R Mancinelli, Franchitto A, Glaser S, Meng F, Onori P, Demorrow S, Francis H, Venter J, Carpino G, Baker K, Han Y, Ueno Y, Gaudio E, and Alpini G**. GABA induces the differentiation of small into large cholangiocytes by activation of Ca(2+) /CaMK I-dependent adenylyl cyclase 8. *Hepatology* 58: 251-263, 2013.
101. **H Francis, Glaser S, Demorrow S, Gaudio E, Ueno Y, Venter J, Dostal D, Onori P, Franchitto A, Marzioni M, Vaculin S, Vaculin B, Katki K, Stutes M, Savage J, and Alpini G**. Small mouse cholangiocytes proliferate in response to H1 histamine receptor stimulation by activation of the IP3/CaMK I/CREB pathway. *Am J Physiol Cell Physiol* 295: C499-513, 2008.
102. **G Alpini, Lenzi R, Sarkozi L, and Tavoloni N**. Biliary physiology in rats with bile ductular cell hyperplasia. Evidence for a secretory function of proliferated bile ductules. *J Clin Invest* 81: 569-578, 1988.
103. **D Alvaro, Mancino MG, Glaser S, Gaudio E, Marzioni M, Francis H, and Alpini G**. Proliferating cholangiocytes: a neuroendocrine compartment in the diseased liver. *Gastroenterology* 132: 415-431, 2007.
104. **A Renzi, Glaser S, Demorrow S, Mancinelli R, Meng F, Franchitto A, Venter J, White M, Francis H, Han Y, Alvaro D, Gaudio E, Carpino G, Ueno Y, Onori P, and Alpini G**. Melatonin inhibits cholangiocyte hyperplasia in cholestatic rats by interaction with MT1 but not MT2 melatonin receptors. *Am J Physiol Gastrointest Liver Physiol* 301: G634-643, 2011.
105. **U Beuers, Hohenester S, de Buy Wenniger LJ, Kremer AE, Jansen PL, and Elferink RP**. The biliary HCO(3)(-) umbrella: a unifying hypothesis on pathogenetic and therapeutic aspects of fibrosing cholangiopathies. *Hepatology* 52: 1489-1496, 2010.
106. **T Kumagi, Guindi M, Fischer SE, Arenovich T, Abdalian R, Coltescu C, Heathcote EJ, and Hirschfield GM**. Baseline ductopenia and treatment response predict long-term histological progression in primary biliary cirrhosis. *Am J Gastroenterol* 105: 2186-2194, 2010.
107. **DC Yamaguti, and Patricio FR**. Morphometrical and immunohistochemical study of intrahepatic bile ducts in biliary atresia. *Eur J Gastroenterol Hepatol* 23: 759-765, 2011.
108. **A Farina, Dumonceau JM, Delhaye M, Frossard JL, Hadengue A, Hochstrasser DF, and Lescuyer P**. A step further in the analysis of human bile proteome. *J Proteome Res* 10: 2047-2063, 2011.
109. **WR Brown, and Kloppel TM**. The liver and IgA: immunological, cell biological and clinical implications. *Hepatology* 9: 763-784, 1989.
110. **P Brandtzaeg, Bjerke K, Kett K, Kvale D, Rognum TO, Scott H, Sollid LM, and Valnes K**. Production and secretion of immunoglobulins in the gastrointestinal tract. *Ann Allergy* 59: 21-39, 1987.
111. **BD Aagaard, Heyworth MF, Oesterle AL, Jones AL, and Way LW**. Intestinal immunisation with Escherichia coli protects rats against Escherichia coli induced cholangitis. *Gut* 39: 136-140, 1996.

112. **PR Harmatz, Kleinman RE, Bunnell BW, Bloch KJ, and Walker WA**. Hepatobiliary clearance of IgA immune complexes formed in the circulation. *Hepatology* 2: 328-333, 1982.
113. **K Harada, Ohba K, Ozaki S, Isse K, Hirayama T, Wada A, and Nakanuma Y**. Peptide antibiotic human beta-defensin-1 and -2 contribute to antimicrobial defense of the intrahepatic biliary tree. *Hepatology* 40: 925-932, 2004.
114. **K Saito, and Nakanuma Y**. Lactoferrin and lysozyme in the intrahepatic bile duct of normal livers and hepatolithiasis. An immunohistochemical study. *J Hepatol* 15: 147-153, 1992.
115. **XM Chen, O'Hara SP, Nelson JB, Splinter PL, Small AJ, Tietz PS, Limper AH, and LaRusso NF**. Multiple TLRs are expressed in human cholangiocytes and mediate host epithelial defense responses to Cryptosporidium parvum via activation of NF-kappaB. *J Immunol* 175: 7447-7456, 2005.
116. **H Ikeda, Sasaki M, Ishikawa A, Sato Y, Harada K, Zen Y, Kazumori H, and Nakanuma Y**. Interaction of Toll-like receptors with bacterial components induces expression of CDX2 and MUC2 in rat biliary epithelium in vivo and in culture. *Lab Invest* 87: 559-571, 2007.
117. **S Oya, Yokoyama Y, Kokuryo T, Uno M, Yamauchi K, and Nagino M**. Inhibition of Toll-like receptor 4 suppresses liver injury induced by biliary obstruction and subsequent intraportal lipopolysaccharide injection. *Am J Physiol Gastrointest Liver Physiol* 306: G244-252, 2014.
118. **H Yokomori, Oda M, Ogi M, Wakabayashi G, Kawachi S, Yoshimura K, Nagai T, Kitajima M, Nomura M, and Hibi T**. Expression of adhesion molecules on mature cholangiocytes in canal of Hering and bile ductules in wedge biopsy samples of primary biliary cirrhosis. *World J Gastroenterol* 11: 4382-4389, 2005.
119. **RC Ayres, Neuberger JM, Shaw J, Joplin R, and Adams DH**. Intercellular adhesion molecule-1 and MHC antigens on human intrahepatic bile duct cells: effect of pro-inflammatory cytokines. *Gut* 34: 1245-1249, 1993.
120. **K Takeda, Kojima Y, Ikejima K, Harada K, Yamashina S, Okumura K, Aoyama T, Frese S, Ikeda H, Haynes NM, Cretney E, Yagita H, Sueyoshi N, Sato N, Nakanuma Y, Smyth MJ, and Okumura K**. Death receptor 5 mediated-apoptosis contributes to cholestatic liver disease. *Proc Natl Acad Sci U S A* 105: 10895-10900, 2008.
121. **DI Godfrey, Uldrich AP, McCluskey J, Rossjohn J, and Moody DB**. The burgeoning family of unconventional T cells. *Nat Immunol* 16: 1114-1123, 2015.
122. **SP O'Hara, Karlsen TH, and LaRusso NF**. Cholangiocytes and the environment in primary sclerosing cholangitis: where is the link? *Gut* 66: 1873-1877, 2017.
123. **SP O'Hara, Tabibian JH, Splinter PL, and LaRusso NF**. The dynamic biliary epithelia: molecules, pathways, and disease. *J Hepatol* 58: 575-582, 2013.
124. **M Strazzabosco, Fiorotto R, Cadamuro M, Spirli C, Mariotti V, Kaffe E, Scirpo R, and Fabris L**. Pathophysiologic implications of innate immunity

and autoinflammation in the biliary epithelium. *Biochim Biophys Acta Mol Basis Dis* 1864: 1374-1379, 2018.
125. **C Pinto, Giordano DM, Maroni L, and Marzioni M**. Role of inflammation and proinflammatory cytokines in cholangiocyte pathophysiology. *Biochim Biophys Acta Mol Basis Dis* 1864: 1270-1278, 2018.
126. **PL Maria, Margaret FB, Julia LW, Simi A, Michael T, and John AK**. Immunogenicity of biliary epithelium: Investigation of antigen presentation to CD4+ T cells. *Hepatology* 24: 561-567, 1996.
127. **BH Barnes, Tucker RM, Wehrmann F, Mack DG, Ueno Y, and Mack CL**. Cholangiocytes as immune modulators in rotavirus-induced murine biliary atresia. *Liver International* 29: 1253-1261, 2009.
128. **M Heydtmann, Lalor PF, Eksteen JA, Hubscher SG, Briskin M, and Adams DH**. CXC chemokine ligand 16 promotes integrin-mediated adhesion of liver-infiltrating lymphocytes to cholangiocytes and hepatocytes within the inflamed human liver. *J Immunol* 174: 1055-1062, 2005.
129. **MP Leon, Kirby JA, Gibbs P, Burt AD, and Bassendine MF**. Immunogenicity of biliary epithelial cells: study of the expression of B7 molecules. *J Hepatol* 22: 591-595, 1995.
130. **U Broome, Scheynius A, and Hultcrantz R**. Induced expression of heat-shock protein on biliary epithelium in patients with primary sclerosing cholangitis and primary biliary cirrhosis. *Hepatology* 18: 298-303, 1993.
131. **SJ Zweers, Shiryaev A, Komuta M, Vesterhus M, Hov JR, Perugorria MJ, de Waart DR, Chang JC, Tol S, Te Velde AA, de Jonge WJ, Banales JM, Roskams T, Beuers U, Karlsen TH, Jansen PL, and Schaap FG**. Elevated interleukin-8 in bile of patients with primary sclerosing cholangitis. *Liver Int* 36: 1370-1377, 2016.
132. **R Dong, and Zheng S**. Interleukin-8: A critical chemokine in biliary atresia. *J Gastroenterol Hepatol* 30: 970-976, 2015.
133. **K Isse, Harada K, and Nakanuma Y**. IL-8 expression by biliary epithelial cells is associated with neutrophilic infiltration and reactive bile ductules. *Liver Int* 27: 672-680, 2007.
134. **CM Morland, Fear J, Joplin R, and Adams DH**. Inflammatory cytokines stimulate human biliary epithelial cells to express interleukin-8 and monocyte chemotactic protein-1. *Biochem Soc Trans* 25: 232S, 1997.
135. **KV Fumi, Joe W, and Timothy RC**. An increased risk of urinary tract infection precedes development of primary biliary cirrhosis. *BMC gastroenterology* 11: 95 , pmid = 21871059, 2011.
136. **SA Morshed, Nishioka M, Saito I, Komiyama K, and Moro I**. Increased expression of Epstein-Barr virus in primary biliary cirrhosis patients. *Gastroenterologia Japonica* 27: 751-758 , pmid = 1334891, 1992.
137. **CYC Richy, Phornnop N, Shang-An S, Jinjun W, Guo-Xiang Y, Thomas PK, Kathryn CG, Jeffrey DB, Christopher B, Mi-Hua T, Mark JK, Aftab AA, Marshall K, Ross LC, Ana L, Gershwin ME, and Patrick SCL**. Antimitochondrial antibody heterogeneity and the xenobiotic etiology of primary biliary cirrhosis. *Hepatology (Baltimore, Md)* 57: 1498-1508 , pmid = 23184636, 2013.
138. **SCL Patrick, Jinjun W, Phornnop N, Thomas PK, Kit SL, Mark JK, and Gershwin ME**. Environment and primary biliary cirrhosis: electrophilic

drugs and the induction of AMA. *Journal of autoimmunity* 41: 79-86 , pmid = 23352659, 2013.
139. **PB Dimitrios, Harold B, Diego V, and Andrew KB**. The role of E. coli infection in the pathogenesis of primary biliary cirrhosis. *Disease markers* 29: 301-311 , pmid = 21297249, 2010.
140. **C Corpechot, Chrétien Y, Chazouillères O, and Poupon R**. Demographic, lifestyle, medical and familial factors associated with primary biliary cirrhosis. *J Hepatol* 53: 162-169, 2010.
141. **R Roman, Patrick SCL, Melissa RJ, Mark JK, Michael HN, Kit SL, Daniel B, Aftab AA, Ross LC, Ian RM, and Gershwin ME**. Identification of 2-nonynoic acid, a cosmetic component, as a potential trigger of primary biliary cirrhosis. *Journal of autoimmunity* 27: 7-16 , pmid = 16876981, 2006.
142. **ME Gershwin, Selmi C, Worman HJ, Gold EB, Watnik M, Utts J, Lindor KD, Kaplan MM, Vierling JM, and Group UPE**. Risk factors and comorbidities in primary biliary cirrhosis: a controlled interview-based study of 1032 patients. *Hepatology* 42: 1194-1202, 2005.
143. **A Lleo, Wang GQ, Gershwin ME, and Hirschfield GM**. Primary biliary cholangitis. *Lancet* 396: 1915-1926, 2020.
144. **K Boonstra, Beuers U, and Ponsioen CY**. Epidemiology of primary sclerosing cholangitis and primary biliary cirrhosis: a systematic review. *J Hepatol* 56: 1181-1188, 2012.
145. **T Lv, Chen S, Li M, Zhang D, Kong Y, and Jia J**. Regional variation and temporal trend of primary biliary cholangitis epidemiology: A systematic review and meta-analysis. *J Gastroenterol Hepatol* 36: 1423-1434, 2021.
146. **PJ Trivedi, Bowlus CL, Yimam KK, Razavi H, and Estes C**. Epidemiology, Natural History, and Outcomes of Primary Sclerosing Cholangitis: A Systematic Review of Population-based Studies. *Clin Gastroenterol Hepatol* 2021.
147. **R Asselta, Paraboschi EM, Gerussi A, Cordell HJ, Mells GF, Sandford RN, Jones DE, Nakamura M, Ueno K, Hitomi Y, Kawashima M, Nishida N, Tokunaga K, Nagasaki M, Tanaka A, Tang R, Li Z, Shi Y, Liu X, Xiong M, Hirschfield G, Siminovitch KA, Canadian USPBCC, Italian PBCGSG, Consortium U-P, Japan PBCGC, Carbone M, Cardamone G, Duga S, Gershwin ME, Seldin MF, and Invernizzi P**. X Chromosome Contribution to the Genetic Architecture of Primary Biliary Cholangitis. *Gastroenterology* 160: 2483-2495 e2426, 2021.
148. **HJ Cordell, Fryett JJ, Ueno K, Darlay R, Aiba Y, Hitomi Y, Kawashima M, Nishida N, Khor SS, Gervais O, Kawai Y, Nagasaki M, Tokunaga K, Tang R, Shi Y, Li Z, Juran BD, Atkinson EJ, Gerussi A, Carbone M, Asselta R, Cheung A, de Andrade M, Baras A, Horowitz J, Ferreira MAR, Sun D, Jones DE, Flack S, Spicer A, Mulcahy VL, Byan J, Han Y, Sandford RN, Lazaridis KN, Amos CI, Hirschfield GM, Seldin MF, Invernizzi P, Siminovitch KA, Ma X, Nakamura M, Mells GF, Consortia P, Consortium CP, Consortium CP, Group IPS, Consortium J-P-G, Consortium UP, and Consortium U-P**. An international genome-wide meta-analysis of primary biliary cholangitis: Novel risk loci and candidate drugs. *J Hepatol* 75: 572-581, 2021.

149. **GF Mells, Floyd JA, Morley KI, Cordell HJ, Franklin CS, Shin SY, Heneghan MA, Neuberger JM, Donaldson PT, Day DB, Ducker SJ, Muriithi AW, Wheater EF, Hammond CJ, Dawwas MF, Consortium UP, Wellcome Trust Case Control C, Jones DE, Peltonen L, Alexander GJ, Sandford RN, and Anderson CA**. Genome-wide association study identifies 12 new susceptibility loci for primary biliary cirrhosis. *Nat Genet* 43: 329-332, 2011.
150. **L Bossini-Castillo, Martin JE, Broen J, Gorlova O, Simeon CP, Beretta L, Vonk MC, Callejas JL, Castellvi I, Carreira P, Garcia-Hernandez FJ, Fernandez Castro M, Spanish Scleroderma G, Coenen MJ, Riemekasten G, Witte T, Hunzelmann N, Kreuter A, Distler JH, Koeleman BP, Voskuyl AE, Schuerwegh AJ, Palm O, Hesselstrand R, Nordin A, Airo P, Lunardi C, Scorza R, Shiels P, van Laar JM, Herrick A, Worthington J, Denton C, Tan FK, Arnett FC, Agarwal SK, Assassi S, Fonseca C, Mayes MD, Radstake TR, and Martin J**. A GWAS follow-up study reveals the association of the IL12RB2 gene with systemic sclerosis in Caucasian populations. *Hum Mol Genet* 21: 926-933, 2012.
151. **GM Hirschfield, Liu X, Han Y, Gorlov IP, Lu Y, Xu C, Lu Y, Chen W, Juran BD, Coltescu C, Mason AL, Milkiewicz P, Myers RP, Odin JA, Luketic VA, Speiciene D, Vincent C, Levy C, Gregersen PK, Zhang J, Heathcote EJ, Lazaridis KN, Amos CI, and Siminovitch KA**. Variants at IRF5-TNPO3, 17q12-21 and MMEL1 are associated with primary biliary cirrhosis. *Nat Genet* 42: 655-657, 2010.
152. **GM Hirschfield, Liu X, Xu C, Lu Y, Xie G, Lu Y, Gu X, Walker EJ, Jing K, Juran BD, Mason AL, Myers RP, Peltekian KM, Ghent CN, Coltescu C, Atkinson EJ, Heathcote EJ, Lazaridis KN, Amos CI, and Siminovitch KA**. Primary biliary cirrhosis associated with HLA, IL12A, and IL12RB2 variants. *N Engl J Med* 360: 2544-2555, 2009.
153. **JK Dyson, Blain A, Foster Shirley MD, Hudson M, Rushton S, and Jeffreys Jones DE**. Geo-epidemiology and environmental co-variate mapping of primary biliary cholangitis and primary sclerosing cholangitis. *JHEP Rep* 3: 100202, 2021.
154. **MI Prince, Ducker SJ, and James OFW**. Case-control studies of risk factors for primary biliary cirrhosis in two United Kingdom populations. *Gut* 59: 508-512 , pmid = 20332522, 2010.
155. **C Corpechot, Abenavoli L, Rabahi N, Chretien Y, Andreani T, Johanet C, Chazouilleres O, and Poupon R**. Biochemical response to ursodeoxycholic acid and long-term prognosis in primary biliary cirrhosis. *Hepatology* 48: 871-877, 2008.
156. **C Corpechot, Carrat F, Bonnand AM, Poupon RE, and Poupon R**. The effect of ursodeoxycholic acid therapy on liver fibrosis progression in primary biliary cirrhosis. *Hepatology (Baltimore, Md)* 32: 1196-1199 , pmid = 11093724, 2000.
157. **A Pares, Caballeria L, and Rodes J**. Excellent long-term survival in patients with primary biliary cirrhosis and biochemical response to ursodeoxycholic Acid. *Gastroenterology* 130: 715-720, 2006.
158. **EM Kuiper, Zondervan PE, and van Buuren HR**. Paris criteria are effective in diagnosis of primary biliary cirrhosis and autoimmune hepatitis overlap syndrome. *Clin Gastroenterol Hepatol* 8: 530-534, 2010.

159. **M Carbone, Sharp SJ, Flack S, Paximadas D, Spiess K, Adgey C, Griffiths L, Lim R, Trembling P, Williamson KD, Wareham NJ, Aldersley M, Bathgate A, Burroughs AK, Heneghan MA, Neuberger JM, Thorburn D, Hirschfield GM, Cordell HJ, Alexander GJ, Jones DEJ, Sandford RN, and Mells GF**. The UK-PBC Risk Scores: Derivation and validation of a scoring system for long-term prediction of end-stage liver disease in primary biliary cirrhosis. *Hepatology (Baltimore, Md)* 2015.
160. **WJ Lammers, van Buuren HR, Hirschfield GM, Janssen HL, Invernizzi P, Mason AL, Ponsioen CY, Floreani A, Corpechot C, Mayo MJ, Battezzati PM, Pares A, Nevens F, Burroughs AK, Kowdley KV, Trivedi PJ, Kumagi T, Cheung A, Lleo A, Imam MH, Boonstra K, Cazzagon N, Franceschet I, Poupon R, Caballeria L, Pieri G, Kanwar PS, Lindor KD, Hansen BE, and Global PBCSG**. Levels of alkaline phosphatase and bilirubin are surrogate end points of outcomes of patients with primary biliary cirrhosis: an international follow-up study. *Gastroenterology* 147: 1338-1349 e1335; quiz e1315, 2014.
161. **M Carbone, Mells GF, Pells G, Dawwas MF, Newton JL, Heneghan MA, Neuberger JM, Day DB, Ducker SJ, Consortium UP, Sandford RN, Alexander GJ, and Jones DE**. Sex and age are determinants of the clinical phenotype of primary biliary cirrhosis and response to ursodeoxycholic acid. *Gastroenterology* 144: 560-569 e567; quiz e513-564, 2013.
162. **M Carbone, and Neuberger J**. Liver transplantation in PBC and PSC: indications and disease recurrence. *Clin Res Hepatol Gastroenterol* 35: 446-454, 2011.
163. **RC de Veer, van Hooff MC, da Silva G, Harms MH, Metselaar HJ, Willemse J, Utomo E, and van der Meer AJ**. Quality of life in Dutch patients with primary biliary cholangitis: Discrepancies between patients' perspectives and objective disease parameters. *Hepatol Res* 53: 401-408, 2023.
164. EASL Clinical Practice Guidelines: The diagnosis and management of patients with primary biliary cholangitis. *Journal of Hepatology* 67: 145-172 , publisher = Elsevier, 2017.
165. **F Nevens, Andreone P, Mazzella G, Strasser SI, Bowlus C, Invernizzi P, Drenth JP, Pockros PJ, Regula J, Beuers U, Trauner M, Jones DE, Floreani A, Hohenester S, Luketic V, Shiffman M, van Erpecum KJ, Vargas V, Vincent C, Hirschfield GM, Shah H, Hansen B, Lindor KD, Marschall HU, Kowdley KV, Hooshmand-Rad R, Marmon T, Sheeron S, Pencek R, MacConell L, Pruzanski M, Shapiro D, and Group PS**. A Placebo-Controlled Trial of Obeticholic Acid in Primary Biliary Cholangitis. *N Engl J Med* 375: 631-643, 2016.
166. **U Beuers, Spengler U, Kruis W, Aydemir U, Wiebecke B, Heldwein W, Weinzierl M, Pape GR, Sauerbruch T, and Paumgartner G**. Ursodeoxycholic acid for treatment of primary sclerosing cholangitis: a placebo-controlled trial. *Hepatology* 16: 707-714, 1992.
167. **U Beuers, Boyer JL, and Paumgartner G**. Ursodeoxycholic acid in cholestasis: potential mechanisms of action and therapeutic applications. *Hepatology* 28: 1449-1453, 1998.
168. **R Pellicciari, Fiorucci S, Camaioni E, Clerici C, Costantino G, Maloney PR, Morelli A, Parks DJ, and Willson TM**. 6alpha-ethyl-

chenodeoxycholic acid (6-ECDCA), a potent and selective FXR agonist endowed with anticholestatic activity. *J Med Chem* 45: 3569-3572, 2002.
169. **T Inagaki, Choi M, Moschetta A, Peng L, Cummins CL, McDonald JG, Luo G, Jones SA, Goodwin B, Richardson JA, Gerard RD, Repa JJ, Mangelsdorf DJ, and Kliewer SA**. Fibroblast growth factor 15 functions as an enterohepatic signal to regulate bile acid homeostasis. *Cell Metab* 2: 217-225, 2005.
170. **S Zhang, Wang J, Liu Q, and Harnish DC**. Farnesoid X receptor agonist WAY-362450 attenuates liver inflammation and fibrosis in murine model of non-alcoholic steatohepatitis. *J Hepatol* 51: 380-388, 2009.
171. **C Corpechot, Chazouillères O, Rousseau A, Guyader D, Habersetzer F, Mathurin P, Goria O, Potier P, Minello A, Silvain C, Abergel A, Debette-Gratien M, Larrey D, Roux O, Bronowicki JP, Boursier J, Ledhingen Vd, Heurgue-Berlot A, Nguyen-Khac E, Zoulim F, Ollivier-Hourmand I, Zarski JP, Nkontchou G, Gaouar F, Simon T, and Poupon R**. A 2-year multicenter, double-blind, randomized, placebo-controlled study of bezafibrate for the treatment of primary biliary cholangitis in patients with inadequate biochemical response to ursodeoxycholic acid therapy (Bezurso) abstract. *Journal of Hepatology* 66: Supplement, Page S89 , publisher = Elsevier, 2017.
172. **AJ Montano-Loza, Hansen BE, Corpechot C, Roccarina D, Thorburn D, Trivedi P, Hirschfield G, McDowell P, Poupon R, Dumortier J, Bosch A, Giostria E, Conti F, Pares A, Reig A, Floreani A, Russo FP, Goet JC, Harms MH, van Buuren H, Van den Ende N, Nevens F, Verhelst X, Donato MF, Malinverno F, Ebadi M, Mason AL, and Global PBCSG**. Factors Associated With Recurrence of Primary Biliary Cholangitis After Liver Transplantation and Effects on Graft and Patient Survival. *Gastroenterology* 156: 96-107 e101, 2019.
173. **C Sun, Xiao X, Yan L, Sheng L, Wang Q, Jiang P, Lian M, Li Y, Wei Y, Zhang J, Chen Y, Li B, Li Y, Huang B, Li Y, Peng Y, Chen X, Fang J, Qiu D, Hua J, Tang R, Leung P, Gershwin ME, Miao Q, and Ma X**. Histologically proven AMA positive primary biliary cholangitis but normal serum alkaline phosphatase: Is alkaline phosphatase truly a surrogate marker? *J Autoimmun* 99: 33-38, 2019.
174. **K Sultan, Petkar M, and Derbala M**. Florid biliary duct lesions in an AMA -positive patient in absence of cholestatic liver biochemistry. *J Autoimmun* 101: 153-155, 2019.
175. **GD Benson, Kikuchi K, Miyakawa H, Tanaka A, Watnik MR, and Gershwin ME**. Serial analysis of antimitochondrial antibody in patients with primary biliary cirrhosis. *Clin Dev Immunol* 11: 129-133, 2004.
176. **S Moteki, Leung PS, Coppel RL, Dickson ER, Kaplan MM, Munoz S, and Gershwin ME**. Use of a designer triple expression hybrid clone for three different lipoyl domain for the detection of antimitochondrial autoantibodies. *Hepatology* 24: 97-103, 1996.
177. **S Moteki, Leung PS, Dickson ER, Van Thiel DH, Galperin C, Buch T, Alarcon-Segovia D, Kershenobich D, Kawano K, Coppel RL, and et al.** Epitope mapping and reactivity of autoantibodies to the E2 component of 2-oxoglutarate dehydrogenase complex in primary biliary cirrhosis using

recombinant 2-oxoglutarate dehydrogenase complex. *Hepatology* 23: 436-444, 1996.
178. **PS Leung, Coppel RL, and Gershwin ME**. Etiology of primary biliary cirrhosis: the search for the culprit. *Semin Liver Dis* 25: 327-336, 2005.
179. **S Oertelt, Rieger R, Selmi C, Invernizzi P, Ansari AA, Coppel RL, Podda M, Leung PS, and Gershwin ME**. A sensitive bead assay for antimitochondrial antibodies: Chipping away at AMA-negative primary biliary cirrhosis. *Hepatology* 45: 659-665, 2007.
180. **A Tanaka, Nezu S, Uegaki S, Mikami M, Okuyama S, Kawamura N, Aiso M, Gershwin ME, Takahashi S, Selmi C, and Takikawa H**. The clinical significance of IgA antimitochondrial antibodies in sera and saliva in primary biliary cirrhosis. *Ann N Y Acad Sci* 1107: 259-270, 2007.
181. **K Amano, Leung PS, Rieger R, Quan C, Wang X, Marik J, Suen YF, Kurth MJ, Nantz MH, Ansari AA, Lam KS, Zeniya M, Matsuura E, Coppel RL, and Gershwin ME**. Chemical xenobiotics and mitochondrial autoantigens in primary biliary cirrhosis: identification of antibodies against a common environmental, cosmetic, and food additive, 2-octynoic acid. *J Immunol* 174: 5874-5883, 2005.
182. **SA Long, Quan C, Van de Water J, Nantz MH, Kurth MJ, Barsky D, Colvin ME, Lam KS, Coppel RL, Ansari A, and Gershwin ME**. Immunoreactivity of organic mimeotopes of the E2 component of pyruvate dehydrogenase: connecting xenobiotics with primary biliary cirrhosis. *J Immunol* 167: 2956-2963, 2001.
183. **R Rieger, Leung PS, Jeddeloh MR, Kurth MJ, Nantz MH, Lam KS, Barsky D, Ansari AA, Coppel RL, Mackay IR, and Gershwin ME**. Identification of 2-nonynoic acid, a cosmetic component, as a potential trigger of primary biliary cirrhosis. *J Autoimmun* 27: 7-16, 2006.
184. **Z Shuai, Wang J, Badamagunta M, Choi J, Yang G, Zhang W, Kenny TP, Guggenheim K, Kurth MJ, Ansari AA, Voss J, Coppel RL, Invernizzi P, Leung PSC, and Gershwin ME**. The fingerprint of antimitochondrial antibodies and the etiology of primary biliary cholangitis. *Hepatology* 65: 1670-1682, 2017.
185. **K Wakabayashi, Yoshida K, Leung PSC, Moritoki Y, Yang GX, Tsuneyama K, Lian ZX, Hibi T, Ansari AA, Wicker LS, Ridgway WM, Coppel RL, Mackay IR, and Gershwin ME**. Induction of autoimmune cholangitis in non-obese diabetic (NOD).1101 mice following a chemical xenobiotic immunization. *Clinical and experimental immunology* 155: 577-586 , pmid = 19094117, 2009.
186. **K Wakabayashi, Lian ZX, Leung PS, Moritoki Y, Tsuneyama K, Kurth MJ, Lam KS, Yoshida K, Yang GX, Hibi T, Ansari AA, Ridgway WM, Coppel RL, Mackay IR, and Gershwin ME**. Loss of tolerance in C57BL/6 mice to the autoantigen E2 subunit of pyruvate dehydrogenase by a xenobiotic with ensuing biliary ductular disease. *Hepatology* 48: 531-540, 2008.
187. **H Kita, Matsumura S, He XS, Ansari AA, Lian ZX, Van de Water J, Coppel RL, Kaplan MM, and Gershwin ME**. Quantitative and functional analysis of PDC-E2-specific autoreactive cytotoxic T lymphocytes in primary biliary cirrhosis. *J Clin Invest* 109: 1231-1240, 2002.
188. **H Kita, Naidenko OV, Kronenberg M, Ansari AA, Rogers P, He XS, Koning F, Mikayama T, Van De Water J, Coppel RL, Kaplan M, and**

Gershwin ME. Quantitation and phenotypic analysis of natural killer T cells in primary biliary cirrhosis using a human CD1d tetramer. *Gastroenterology* 123: 1031-1043, 2002.
189. **H Kita, Lian ZX, Van de Water J, He XS, Matsumura S, Kaplan M, Luketic V, Coppel RL, Ansari AA, and Gershwin ME**. Identification of HLA-A2-restricted CD8(+) cytotoxic T cell responses in primary biliary cirrhosis: T cell activation is augmented by immune complexes cross-presented by dendritic cells. *J Exp Med* 195: 113-123, 2002.
190. **S Shimoda, Van de Water J, Ansari A, Nakamura M, Ishibashi H, Coppel RL, Lake J, Keeffe EB, Roche TE, and Gershwin ME**. Identification and precursor frequency analysis of a common T cell epitope motif in mitochondrial autoantigens in primary biliary cirrhosis. *J Clin Invest* 102: 1831-1840, 1998.
191. **D Luger, Silver PB, Tang J, Cua D, Chen Z, Iwakura Y, Bowman EP, Sgambellone NM, Chan CC, and Caspi RR**. Either a Th17 or a Th1 effector response can drive autoimmunity: conditions of disease induction affect dominant effector category. *J Exp Med* 205: 799-810, 2008.
192. **A Lleo, Gershwin ME, Mantovani A, and Invernizzi P**. Towards common denominators in primary biliary cirrhosis: the role of IL-12. *J Hepatol* 56: 731-733, 2012.
193. **RY Lan, Salunga TL, Tsuneyama K, Lian ZX, Yang GX, Hsu W, Moritoki Y, Ansari AA, Kemper C, Price J, Atkinson JP, Coppel RL, and Gershwin ME**. Hepatic IL-17 responses in human and murine primary biliary cirrhosis. *J Autoimmun* 32: 43-51, 2009.
194. **CY Yang, Ma X, Tsuneyama K, Huang S, Takahashi T, Chalasani NP, Bowlus CL, Yang GX, Leung PS, Ansari AA, Wu L, Coppel RL, and Gershwin ME**. IL-12/Th1 and IL-23/Th17 biliary microenvironment in primary biliary cirrhosis: implications for therapy. *Hepatology* 59: 1944-1953, 2014.
195. **TK Mao, Lian ZX, Selmi C, Ichiki Y, Ashwood P, Ansari AA, Coppel RL, Shimoda S, Ishibashi H, and Gershwin ME**. Altered monocyte responses to defined TLR ligands in patients with primary biliary cirrhosis. *Hepatology* 42: 802-808, 2005.
196. **YH Chuang, Lian ZX, Tsuneyama K, Chiang BL, Ansari AA, Coppel RL, and Gershwin ME**. Increased killing activity and decreased cytokine production in NK cells in patients with primary biliary cirrhosis. *J Autoimmun* 26: 232-240, 2006.
197. **S Shimoda, Harada K, Niiro H, Yoshizumi T, Soejima Y, Taketomi A, Maehara Y, Tsuneyama K, Nakamura M, Komori A, Migita K, Nakanuma Y, Ishibashi H, Selmi C, and Gershwin ME**. Biliary epithelial cells and primary biliary cirrhosis: the role of liver-infiltrating mononuclear cells. *Hepatology* 47: 958-965, 2008.
198. **K Chen, Liu J, and Cao X**. Regulation of type I interferon signaling in immunity and inflammation: A comprehensive review. *J Autoimmun* 83: 1-11, 2017.
199. **S Shimoda, Hisamoto S, Harada K, Iwasaka S, Chong Y, Nakamura M, Bekki Y, Yoshizumi T, Shirabe K, Ikegami T, Maehara Y, He XS, Gershwin ME, and Akashi K**. Natural killer cells regulate T cell immune responses in primary biliary cirrhosis. *Hepatology* 62: 1817-1827, 2015.

200. **SC Afford, Ahmed-Choudhury J, Randhawa S, Russell C, Youster J, Crosby HA, Eliopoulos A, Hubscher SG, Young LS, and Adams DH**. CD40 activation-induced, Fas-dependent apoptosis and NF-kappaB/AP-1 signaling in human intrahepatic biliary epithelial cells. *FASEB journal : official publication of the Federation of American Societies for Experimental Biology* 15: 2345-2354 , pmid = 11689460, 2001.
201. **A Lleo, Liao J, Invernizzi P, Zhao M, Bernuzzi F, Ma L, Lanzi G, Ansari AA, Coppel RL, Zhang P, Li Y, Zhou Z, Lu Q, and Gershwin ME**. Immunoglobulin M levels inversely correlate with CD40 ligand promoter methylation in patients with primary biliary cirrhosis. *Hepatology* 55: 153-160, 2012.
202. **XZ Tang, Jo J, Tan AT, Sandalova E, Chia A, Tan KC, Lee KH, Gehring AJ, De Libero G, and Bertoletti A**. IL-7 licenses activation of human liver intrasinusoidal mucosal-associated invariant T cells. *J Immunol* 190: 3142-3152, 2013.
203. **X Jiang, Lian M, Li Y, Zhang W, Wang Q, Wei Y, Zhang J, Chen W, Xiao X, Miao Q, Bian Z, Qiu D, Fang J, Ansari AA, Leung PSC, Coppel RL, Tang R, Gershwin ME, and Ma X**. The immunobiology of mucosal-associated invariant T cell (MAIT) function in primary biliary cholangitis: Regulation by cholic acid-induced Interleukin-7. *J Autoimmun* 90: 64-75, 2018.
204. **JM Banales, Arenas F, Rodriguez-Ortigosa CM, Saez E, Uriarte I, Doctor RB, Prieto J, and Medina JF**. Bicarbonate-rich choleresis induced by secretin in normal rat is taurocholate-dependent and involves AE2 anion exchanger. *Hepatology* 43: 266-275, 2006.
205. **M Strazzabosco, Mennone A, and Boyer JL**. Intracellular pH regulation in isolated rat bile duct epithelial cells. *The Journal of clinical investigation* 87: 1503-1512 , pmid = 2022723, 1991.
206. **JM Banales, Saez E, Uriz M, Sarvide S, Urribarri AD, Splinter P, Tietz Bogert PS, Bujanda L, Prieto J, Medina JF, and LaRusso NF**. Up-regulation of microRNA 506 leads to decreased Cl-/HCO3- anion exchanger 2 expression in biliary epithelium of patients with primary biliary cirrhosis. *Hepatology* 56: 687-697, 2012.
207. **O Erice, Munoz-Garrido P, Vaquero J, Perugorria MJ, Fernandez-Barrena MG, Saez E, Santos-Laso A, Arbelaiz A, Jimenez-Aguero R, Fernandez-Irigoyen J, Santamaria E, Torrano V, Carracedo A, Ananthanarayanan M, Marzioni M, Prieto J, Beuers U, Oude Elferink RP, LaRusso NF, Bujanda L, Marin JJG, and Banales JM**. MicroRNA-506 promotes primary biliary cholangitis-like features in cholangiocytes and immune activation. *Hepatology* 67: 1420-1440, 2018.
208. **K Takeda, Kojima Y, Ikejima K, Harada K, Yamashina S, Okumura K, Aoyama T, Frese S, Ikeda H, Haynes NM, Cretney E, Yagita H, Sueyoshi N, Sato N, Nakanuma Y, Smyth MJ, and Okumura K**. Death receptor 5 mediated-apoptosis contributes to cholestatic liver disease. *Proceedings of the National Academy of Sciences* 105: 10895-10900, 2008.
209. **A Lleo, Selmi C, Invernizzi P, Podda M, Coppel RL, Mackay IR, Gores GJ, Ansari AA, Van de Water J, and Gershwin ME**. Apotopes and the biliary specificity of primary biliary cirrhosis. *Hepatology* 49: 871-879, 2009.

210. **A Lleo, Bowlus CL, Yang GX, Invernizzi P, Podda M, Van de Water J, Ansari AA, Coppel RL, Worman HJ, Gores GJ, and Gershwin ME**. Biliary apotopes and anti-mitochondrial antibodies activate innate immune responses in primary biliary cirrhosis. *Hepatology* 52: 987-998, 2010.
211. **K Harada, Shimoda S, Sato Y, Isse K, Ikeda H, and Nakanuma Y**. Periductal interleukin-17 production in association with biliary innate immunity contributes to the pathogenesis of cholangiopathy in primary biliary cirrhosis. *Clinical and Experimental Immunology* 157: 261-270, 2009.
212. **J Mattner**. Impact of Microbes on the Pathogenesis of Primary Biliary Cirrhosis (PBC) and Primary Sclerosing Cholangitis (PSC). *Int J Mol Sci* 17: 2016.
213. **DM Giordano, Pinto C, Maroni L, Benedetti A, and Marzioni M**. Inflammation and the Gut-Liver Axis in the Pathophysiology of Cholangiopathies. *Int J Mol Sci* 19: 2018.
214. **R Tang, Wei Y, Li Y, Chen W, Chen H, Wang Q, Yang F, Miao Q, Xiao X, Zhang H, Lian M, Jiang X, Zhang J, Cao Q, Fan Z, Wu M, Qiu D, Fang JY, Ansari A, Gershwin ME, and Ma X**. Gut microbial profile is altered in primary biliary cholangitis and partially restored after UDCA therapy. *Gut* 67: 534-541, 2018.
215. **J Zhao, Zhao S, Zhou G, Liang L, Guo X, Mao P, Zhou X, Wang H, Nan Y, Xu D, and Yu J**. Altered biliary epithelial cell and monocyte responses to lipopolysaccharide as a TLR ligand in patients with primary biliary cirrhosis. *Scand J Gastroenterol* 46: 485-494, 2011.
216. **K Harada, Isse K, and Nakanuma Y**. Interferon gamma accelerates NF-kappaB activation of biliary epithelial cells induced by Toll-like receptor and ligand interaction. *J Clin Pathol* 59: 184-190, 2006.
217. **K Harada, Isse K, Kamihira T, Shimoda S, and Nakanuma Y**. Th1 cytokine-induced downregulation of PPARgamma in human biliary cells relates to cholangitis in primary biliary cirrhosis. *Hepatology* 41: 1329-1338, 2005.
218. **T Nakajima, Kamijo Y, Tanaka N, Sugiyama E, Tanaka E, Kiyosawa K, Fukushima Y, Peters JM, Gonzalez FJ, and Aoyama T**. Peroxisome proliferator-activated receptor alpha protects against alcohol-induced liver damage. *Hepatology* 40: 972-980, 2004.
219. **W Zhang, Ono Y, Miyamura Y, Bowlus CL, Gershwin ME, and Maverakis E**. T cell clonal expansions detected in patients with primary biliary cirrhosis express CX3CR1. *J Autoimmun* 37: 71-78, 2011.
220. **K Isse, Harada K, Zen Y, Kamihira T, Shimoda S, Harada M, and Nakanuma Y**. Fractalkine and CX3CR1 are involved in the recruitment of intraepithelial lymphocytes of intrahepatic bile ducts. *Hepatology* 41: 506-516, 2005.
221. **M Sasaki, Miyakoshi M, Sato Y, and Nakanuma Y**. Chemokine-chemokine receptor CCL2-CCR2 and CX3CL1-CX3CR1 axis may play a role in the aggravated inflammation in primary biliary cirrhosis. *Dig Dis Sci* 59: 358-364, 2014.
222. **G Rong, Zhou Y, Xiong Y, Zhou L, Geng H, Jiang T, Zhu Y, Lu H, Zhang S, Wang P, Zhang B, and Zhong R**. Imbalance between T helper type 17 and T regulatory cells in patients with primary biliary cirrhosis: the serum

cytokine profile and peripheral cell population. *Clinical & Experimental Immunology* 156: 2009.
223. **YH Oo, Banz V, Kavanagh D, Liaskou E, Withers DR, Humphreys E, Reynolds GM, Lee-Turner L, Kalia N, Hubscher SG, Klenerman P, Eksteen B, and Adams DH**. CXCR3-dependent recruitment and CCR6-mediated positioning of Th-17 cells in the inflamed liver. *Journal of hepatology* 57: 1044-1051, 2012.
224. **HC Jeffery, Hunter S, Humphreys EH, Bhogal R, Wawman RE, Birtwistle J, Atif M, Bagnal CJ, Rodriguez Blanco G, Richardson N, Warner S, Dunn WB, Afford SC, Adams DH, and Oo YH**. Bidirectional Cross-Talk between Biliary Epithelium and Th17 Cells Promotes Local Th17 Expansion and Bile Duct Proliferation in Biliary Liver Diseases. *J Immunol* 203: 1151-1159, 2019.
225. **JT Salas, Banales JM, Sarvide S, Recalde S, Ferrer A, Uriarte I, Oude Elferink RP, Prieto J, and Medina JF**. Ae2a,b-deficient mice develop antimitochondrial antibodies and other features resembling primary biliary cirrhosis. *Gastroenterology* 134: 1482-1493, 2008.
226. **F Glaser, John C, Engel B, Hoh B, Weidemann S, Dieckhoff J, Stein S, Becker N, Casar C, Schuran FA, Wieschendorf B, Preti M, Jessen F, Franke A, Carambia A, Lohse AW, Ittrich H, Herkel J, Heeren J, Schramm C, and Schwinge D**. Liver infiltrating T cells regulate bile acid metabolism in experimental cholangitis. *J Hepatol* 71: 783-792, 2019.
227. **TWH Pols, Puchner T, Korkmaz HI, Vos M, Soeters MR, and de Vries CJM**. Lithocholic acid controls adaptive immune responses by inhibition of Th1 activation through the Vitamin D receptor. *PLoS One* 12: e0176715, 2017.
228. **S Oertelt, Lian ZX, Cheng CM, Chuang YH, Padgett KA, He XS, Ridgway WM, Ansari AA, Coppel RL, Li MO, Flavell RA, Kronenberg M, Mackay IR, and Gershwin ME**. Anti-mitochondrial antibodies and primary biliary cirrhosis in TGF-beta receptor II dominant-negative mice. *J Immunol* 177: 1655-1660, 2006.
229. **K Wakabayashi, Lian ZX, Moritoki Y, Lan RY, Tsuneyama K, Chuang YH, Yang GX, Ridgway W, Ueno Y, Ansari AA, Coppel RL, Mackay IR, and Gershwin ME**. IL-2 receptor alpha(-/-) mice and the development of primary biliary cirrhosis. *Hepatology* 44: 1240-1249, 2006.
230. **W Zhang, Sharma R, Ju ST, He XS, Tao Y, Tsuneyama K, Tian Z, Lian ZX, Fu SM, and Gershwin ME**. Deficiency in regulatory T cells results in development of antimitochondrial antibodies and autoimmune cholangitis. *Hepatology* 49: 545-552, 2009.
231. **E Liaskou, Patel SR, Webb G, Bagkou Dimakou D, Akiror S, Krishna M, Mells G, Jones DE, Bowman SJ, Barone F, Fisher BA, and Hirschfield GM**. Increased sensitivity of Treg cells from patients with PBC to low dose IL-12 drives their differentiation into IFN-gamma secreting cells. *J Autoimmun* 94: 143-155, 2018.
232. **H Tanaka, Zhang W, Yang GX, Ando Y, Tomiyama T, Tsuneyama K, Leung P, Coppel RL, Ansari AA, Lian ZX, Ridgway WM, Joh T, and Gershwin ME**. Successful immunotherapy of autoimmune cholangitis by adoptive transfer of forkhead box protein 3(+) regulatory T cells. *Clin Exp Immunol* 178: 253-261, 2014.

233. **GX Yang, Wu Y, Tsukamoto H, Leung PS, Lian ZX, Rainbow DB, Hunter KM, Morris GA, Lyons PA, Peterson LB, Wicker LS, Gershwin ME, and Ridgway WM**. CD8 T cells mediate direct biliary ductule damage in nonobese diabetic autoimmune biliary disease. *J Immunol* 186: 1259-1267, 2011.
234. **Y Li, Li B, You Z, Zhang J, Wei Y, Li Y, Chen Y, Huang B, Wang Q, Miao Q, Peng Y, Fang J, Gershwin ME, Tang R, Greenberg SA, and Ma X**. Cytotoxic KLRG1 expressing lymphocytes invade portal tracts in primary biliary cholangitis. *J Autoimmun* 103: 102293, 2019.
235. **GX Yang, Lian ZX, Chuang YH, Moritoki Y, Lan RY, Wakabayashi K, Ansari AA, Flavell RA, Ridgway WM, Coppel RL, Tsuneyama K, Mackay IR, and Gershwin ME**. Adoptive transfer of CD8(+) T cells from transforming growth factor beta receptor type II (dominant negative form) induces autoimmune cholangitis in mice. *Hepatology* 47: 1974-1982, 2008.
236. **M Tsuda, Ambrosini YM, Zhang W, Yang GX, Ando Y, Rong G, Tsuneyama K, Sumida K, Shimoda S, Bowlus CL, Leung PS, He XS, Coppel RL, Ansari AA, Lian ZX, and Gershwin ME**. Fine phenotypic and functional characterization of effector cluster of differentiation 8 positive T cells in human patients with primary biliary cirrhosis. *Hepatology* 54: 1293-1302, 2011.
237. **T Masanobu, Yoko A, Yuki M, Katsunori Y, Weici Z, Guo-Xiang Y, Yugo A, Guanghua R, Toshio N, and Christopher B**. CD45ROhighCD57+ CD8high T cells in primary biliary cirrhosis (101.4). 2011.
238. **B Huang, Lyu Z, Qian Q, Chen Y, Zhang J, Li B, Li Y, Liang J, Liu Q, Chen R, Lian M, Xiao X, Miao Q, Wang Q, Fang J, Lian Z, Tang R, Helleday T, Gershwin ME, You Z, and Ma X**. NUDT1 promotes the accumulation and longevity of CD103. *J Hepatol* 77: 1311-1324, 2022.
239. **W Huang, Kachapati K, Adams D, Wu Y, Leung PS, Yang GX, Zhang W, Ansari AA, Flavell RA, Gershwin ME, and Ridgway WM**. Murine autoimmune cholangitis requires two hits: cytotoxic KLRG1(+) CD8 effector cells and defective T regulatory cells. *J Autoimmun* 50: 123-134, 2014.
240. **M Overholtzer, and Brugge JS**. The cell biology of cell-in-cell structures. *Nat Rev Mol Cell Biol* 9: 796-809, 2008.
241. **K Borensztejn, Tyrna P, Gawel AM, Dziuba I, Wojcik C, Bialy LP, and Mlynarczuk-Bialy I**. Classification of Cell-in-Cell Structures: Different Phenomena with Similar Appearance. *Cells* 10: 2021.
242. **N Fujinami, Zucker-Franklin D, and Valentine F**. Interaction of mononuclear leukocytes with malignant melanoma. *Lab Invest* 45: 28-37, 1981.
243. **JG Humble, Jayne WH, and Pulvertaft RJ**. Biological interaction between lymphocytes and other cells. *Br J Haematol* 2: 283-294, 1956.
244. **A Aderem, and Underhill DM**. Mechanisms of phagocytosis in macrophages. *Annu Rev Immunol* 17: 593-623, 1999.
245. **AE Wright, Douglas SR, and Sanderson JB**. An experimental investigation of the role of the blood fluids in connection with phagocytosis. 1903. *Rev Infect Dis* 11: 827-834, 1989.
246. **M Overholtzer, Mailleux AA, Mouneimne G, Normand G, Schnitt SJ, King RW, Cibas ES, and Brugge JS**. A nonapoptotic cell death process, entosis, that occurs by cell-in-cell invasion. *Cell* 131: 966-979, 2007.

247. **S Fais, and Overholtzer M**. Cell-in-cell phenomena in cancer. *Nat Rev Cancer* 18: 758-766, 2018.
248. **P Xia, Zhou J, Song X, Wu B, Liu X, Li D, Zhang S, Wang Z, Yu H, Ward T, Zhang J, Li Y, Wang X, Chen Y, Guo Z, and Yao X**. Aurora A orchestrates entosis by regulating a dynamic MCAK-TIP150 interaction. *J Mol Cell Biol* 6: 240-254, 2014.
249. **M Wang, Ning X, Chen A, Huang H, Ni C, Zhou C, Yu K, Lan S, Wang Q, Li S, Liu H, Wang X, Chen Z, Ma L, and Sun Q**. Impaired formation of homotypic cell-in-cell structures in human tumor cells lacking alpha-catenin expression. *Sci Rep* 5: 12223, 2015.
250. **S Wang, He MF, Chen YH, Wang MY, Yu XM, Bai J, Zhu HY, Wang YY, Zhao H, Mei Q, Nie J, Ma J, Wang JF, Wen Q, Ma L, Wang Y, and Wang XN**. Rapid reuptake of granzyme B leads to emperitosis: an apoptotic cell-in-cell death of immune killer cells inside tumor cells. *Cell Death Dis* 4: e856, 2013.
251. **GC Brown, and Neher JJ**. Microglial phagocytosis of live neurons. *Nat Rev Neurosci* 15: 209-216, 2014.
252. **S Fais**. Cannibalism: a way to feed on metastatic tumors. *Cancer Lett* 258: 155-164, 2007.
253. **GS Sarode, Sarode SC, and Karmarkar S**. Complex cannibalism: an unusual finding in oral squamous cell carcinoma. *Oral Oncol* 48: e4-6, 2012.
254. **M Marquez-Ropero, Benito E, Plaza-Zabala A, and Sierra A**. Microglial Corpse Clearance: Lessons From Macrophages. *Front Immunol* 11: 506, 2020.
255. **F Lozupone, and Fais S**. Cancer Cell Cannibalism: A Primeval Option to Survive. *Curr Mol Med* 15: 836-841, 2015.
256. **L Lugini, Matarrese P, Tinari A, Lozupone F, Federici C, Iessi E, Gentile M, Luciani F, Parmiani G, Rivoltini L, Malorni W, and Fais S**. Cannibalism of live lymphocytes by human metastatic but not primary melanoma cells. *Cancer Res* 66: 3629-3638, 2006.
257. **PD Scott, Gary MR, Alex LW, Xiaoyan L, Rebecca R, Maanav L, Yuxin SL, Ratnam G, Emma B, Joe G, Nicholas MB, Robin CM, Stefan GH, David HA, Yuehua H, Omar Q, and Zania S**. Hepatocytes Delete Regulatory T Cells by Enclysis, a CD4+ T Cell Engulfment Process. *Cell Reports* 29: 1610-1620.e1614, 2019.
258. **SP Davies, Terry LV, Wilkinson AL, and Stamataki Z**. Cell-in-Cell Structures in the Liver: A Tale of Four E's. *Front Immunol* 11: 650, 2020.
259. **LS Hinojosa, Holst M, Baarlink C, and Grosse R**. MRTF transcription and Ezrin-dependent plasma membrane blebbing are required for entotic invasion. *J Cell Biol* 216: 3087-3095, 2017.
260. **P Cunin, Bouslama R, Machlus KR, Martinez-Bonet M, Lee PY, Wactor A, Nelson-Maney N, Morris A, Guo L, Weyrich A, Sola-Visner M, Boilard E, Italiano JE, and Nigrovic PA**. Megakaryocyte emperipolesis mediates membrane transfer from intracytoplasmic neutrophils to platelets. *Elife* 8: 2019.
261. **MF Bauer, Hader M, Hecht M, Buttner-Herold M, Fietkau R, and Distel LVR**. Cell-in-cell phenomenon: leukocyte engulfment by non-tumorigenic cells and cancer cell lines. *BMC Mol Cell Biol* 22: 39, 2021.

262. **V Benseler, Warren A, Vo M, Holz LE, Tay SS, Le Couteur DG, Breen E, Allison AC, van Rooijen N, McGuffog C, Schlitt HJ, Bowen DG, McCaughan GW, and Bertolino P**. Hepatocyte entry leads to degradation of autoreactive CD8 T cells. *Proc Natl Acad Sci U S A* 108: 16735-16740, 2011.
263. **JC Guyden, Martinez M, Chilukuri RV, Reid V, Kelly F, and Samms MO**. Thymic Nurse Cells Participate in Heterotypic Internalization and Repertoire Selection of Immature Thymocytes; Their Removal from the Thymus of Autoimmune Animals May be Important to Disease Etiology. *Curr Mol Med* 15: 828-835, 2015.
264. **Y Yener, and Dikmenli M**. The effects of acrylamide on the frequency of megakaryocytic emperipolesis and the mitotic activity of rat bone marrow cells. *J Sci Food Agric* 91: 1810-1813, 2011.
265. **I Mlynarczuk-Bialy, Dziuba I, Sarnecka A, Platos E, Kowalczyk M, Pels KK, Wilczynski GM, Wojcik C, and Bialy LP**. Entosis: From Cell Biology to Clinical Cancer Pathology. *Cancers (Basel)* 12: 2020.
266. **YH Chen, Wang S, He MF, Wang Y, Zhao H, Zhu HY, Yu XM, Ma J, Che XJ, Wang JF, and Wang XN**. Prevalence of heterotypic tumor/immune cell-in-cell structure in vitro and in vivo leading to formation of aneuploidy. *PLoS One* 8: e59418, 2013.
267. 王小宁**, and** 李文简. Mechanisms of natural killer cell-mediated tumor cell cytolysis at a single cell level. *Journal of Medical Colleges of PLA* 1987.
268. **Q Miao, Bian Z, Tang R, Zhang H, Wang Q, Huang S, Xiao X, Shen L, Qiu D, and Krawitt EL**. Emperipolesis mediated by CD8 T cells is a characteristic histopathologic feature of autoimmune hepatitis. *Clinical reviews in allergy & immunology* 48: 226-235, 2015.
269. **I Rousalova, and Krepela E**. Granzyme B-induced apoptosis in cancer cells and its regulation. *International journal of oncology* 37: 1361-1378, 2010.
270. **S Dalia, Sagatys E, Sokol L, and Kubal T**. Rosai-Dorfman disease: tumor biology, clinical features, pathology, and treatment. *Cancer Control* 21: 322-327, 2014.
271. **C Ni, Chen Y, Zeng M, Pei R, Du Y, Tang L, Wang M, Hu Y, Zhu H, and He M**. In-cell infection: a novel pathway for Epstein-Barr virus infection mediated by cell-in-cell structures. *Cell research* 25: 785-800, 2015.
272. **J Durgan, Tseng YY, Hamann JC, Domart MC, Collinson L, Hall A, Overholtzer M, and Florey O**. Mitosis can drive cell cannibalism through entosis. *eLife* 6: 2017.
273. **M Krajcovic, Johnson NB, Sun Q, Normand G, Hoover N, Yao E, Richardson AL, King RW, Cibas ES, and Schnitt SJ**. A non-genetic route to aneuploidy in human cancers. *Nature cell biology* 13: 324-330, 2011.
274. **M Wang, Niu Z, Qin H, Ruan B, Zheng Y, Ning X, Gu S, Gao L, Chen Z, and Wang X**. Mechanical ring interfaces between adherens junction and contractile actomyosin to coordinate entotic cell-in-cell formation. *Cell reports* 32: 2020.
275. **O Florey, Kim SE, Sandoval CP, Haynes CM, and Overholtzer M**. Autophagy machinery mediates macroendocytic processing and entotic cell death by targeting single membranes. *Nature cell biology* 13: 1335-1343, 2011.

276. **Y Su, Ren H, Tang M, Zheng Y, Zhang B, Wang C, Hou X, Niu Z, Wang Z, and Gao X**. Role and dynamics of vacuolar pH during cell-in-cell mediated death. *Cell death & disease* 12: 119, 2021.
277. **R Chen, Ram A, Albeck JG, and Overholtzer M**. Entosis is induced by ultraviolet radiation. *iScience* 24: 102902, 2021.
278. **J Liang, Niu Z, Zhang B, Yu X, Zheng Y, Wang C, Ren H, Wang M, Ruan B, and Qin H**. p53-dependent elimination of aneuploid mitotic offspring by entosis. *Cell Death & Differentiation* 28: 799-813, 2021.
279. **HL Mackay, Moore D, Hall C, Birkbak NJ, Jamal-Hanjani M, Karim SA, Phatak VM, Piñon L, Morton JP, and Swanton C**. Genomic instability in mutant p53 cancer cells upon entotic engulfment. *Nature communications* 9: 3070, 2018.
280. **H Schenker, Büttner-Herold M, Fietkau R, and Distel LV**. Cell-in-cell structures are more potent predictors of outcome than senescence or apoptosis in head and neck squamous cell carcinomas. *Radiation Oncology* 12: 1-9, 2017.
281. **M Schwegler, Wirsing AM, Schenker HM, Ott L, Ries JM, Büttner-Herold M, Fietkau R, Putz F, and Distel LV**. Prognostic value of homotypic cell internalization by nonprofessional phagocytic cancer cells. *BioMed research international* 2015: 359392, 2015.
282. **X Zhang, Niu Z, Qin H, Fan J, Wang M, Zhang B, Zheng Y, Gao L, Chen Z, and Tai Y**. Subtype-based prognostic analysis of cell-in-cell structures in early breast cancer. *Frontiers in oncology* 9: 895, 2019.
283. **A Hayashi, Yavas A, McIntyre CA, Ho Y-j, Erakky A, Wong W, Varghese AM, Melchor JP, Overholtzer M, and O'Reilly EM**. Genetic and clinical correlates of entosis in pancreatic ductal adenocarcinoma. *Modern Pathology* 33: 1822-1831, 2020.
284. **N Gül, and van Egmond M**. Antibody-dependent phagocytosis of tumor cells by macrophages: a potent effector mechanism of monoclonal antibody therapy of cancer. *Cancer research* 75: 5008-5013, 2015.
285. **L Lugini, Lozupone F, Matarrese P, Funaro C, Luciani F, Malorni W, Rivoltini L, Castelli C, Tinari A, and Piris A**. Potent phagocytic activity discriminates metastatic and primary human malignant melanomas: a key role of ezrin. *Laboratory Investigation* 83: 1555-1567, 2003.
286. **JC Hamann, Kim SE, and Overholtzer M**. Methods for the study of entotic cell death. *Autophagy: Methods and Protocols* 447-454, 2019.
287. **K Gupta, and Dey P**. Cell cannibalism: diagnostic marker of malignancy. *Diagn Cytopathol* 28: 86-87, 2003.
288. **CA Tonnessen-Murray, Frey WD, Rao SG, Shahbandi A, Ungerleider NA, Olayiwola JO, Murray LB, Vinson BT, Chrisey DB, and Lord CJ**. Chemotherapy-induced senescent cancer cells engulf other cells to enhance their survival. *Journal of Cell Biology* 218: 3827-3844, 2019.
289. **R Caruso, Fedele F, Finocchiaro G, Arena G, and Venuti A**. Neutrophil-tumor cell phagocytosis (cannibalism) in human turoms: an update and literature review. *Experimental oncology* 2012.
290. **X Wang, Li Y, Li J, Li L, Zhu H, Chen H, Kong R, Wang G, Wang Y, and Hu J**. Cell-in-cell phenomenon and its relationship with tumor microenvironment and tumor progression: A review. *Frontiers in cell and developmental biology* 7: 311, 2019.

291. **F Lozupone, Perdicchio M, Brambilla D, Borghi M, Meschini S, Barca S, Marino ML, Logozzi M, Federici C, and Iessi E**. The human homologue of Dictyostelium discoideum phg1A is expressed by human metastatic melanoma cells. *EMBO reports* 10: 1348-1354, 2009.
292. **F Lozupone, Borghi M, Marzoli F, Azzarito T, Matarrese P, Iessi E, Venturi G, Meschini S, Canitano A, and Bona R**. TM9SF4 is a novel V-ATPase-interacting protein that modulates tumor pH alterations associated with drug resistance and invasiveness of colon cancer cells. *Oncogene* 34: 5163-5174, 2015.
293. **TJ Bartosh, Ullah M, Zeitouni S, Beaver J, and Prockop DJ**. Cancer cells enter dormancy after cannibalizing mesenchymal stem/stromal cells (MSCs). *Proceedings of the National Academy of Sciences* 113: E6447-E6456, 2016.
294. **CE Cano, Sandí MJ, Hamidi T, Calvo EL, Turrini O, Bartholin L, Loncle C, Secq V, Garcia S, and Lomberk G**. Homotypic cell cannibalism, a cell‐death process regulated by the nuclear protein 1, opposes to metastasis in pancreatic cancer. *EMBO molecular medicine* 4: 964-979, 2012.
295. **VA Fadok, De Cathelineau A, Daleke DL, Henson PM, and Bratton DL**. Loss of phospholipid asymmetry and surface exposure of phosphatidylserine is required for phagocytosis of apoptotic cells by macrophages and fibroblasts. *Journal of Biological Chemistry* 276: 1071-1077, 2001.
296. **M Dias-Baruffi, Zhu H, Cho M, Karmakar S, McEver RP, and Cummings RD**. Dimeric galectin-1 induces surface exposure of phosphatidylserine and phagocytic recognition of leukocytes without inducing apoptosis. *Journal of Biological Chemistry* 278: 41282-41293, 2003.
297. **JJ Neher, Neniskyte U, Zhao J-W, Bal-Price A, Tolkovsky AM, and Brown GC**. Inhibition of microglial phagocytosis is sufficient to prevent inflammatory neuronal death. *The Journal of Immunology* 186: 4973-4983, 2011.
298. **U Neniskyte, Neher JJ, and Brown GC**. Neuronal death induced by nanomolar amyloid β is mediated by primary phagocytosis of neurons by microglia. *Journal of Biological Chemistry* 286: 39904-39913, 2011.
299. **YY Tyurina, Basova LV, Konduru NV, Tyurin VA, Potapovich AI, Cai P, Bayir H, Stoyanovsky D, Pitt BR, and Shvedova AA**. Nitrosative stress inhibits the aminophospholipid translocase resulting in phosphatidylserine externalization and macrophage engulfment: implications for the resolution of inflammation. *Journal of Biological Chemistry* 282: 8498-8509, 2007.
300. **Y Zhang, Li H, Li X, Wu J, Xue T, Wu J, Shen H, Li X, Shen M, and Chen G**. TMEM16F aggravates neuronal loss by mediating microglial phagocytosis of neurons in a rat experimental cerebral ischemia and reperfusion model. *Frontiers in Immunology* 11: 1144, 2020.
301. **P-A Oldenborg, Zheleznyak A, Fang Y-F, Lagenaur CF, Gresham HD, and Lindberg FP**. Role of CD47 as a marker of self on red blood cells. *Science* 288: 2051-2054, 2000.
302. **K Weiskopf, Jahchan NS, Schnorr PJ, Cristea S, Ring AM, Maute RL, Volkmer AK, Volkmer J-P, Liu J, and Lim JS**. CD47-blocking

immunotherapies stimulate macrophage-mediated destruction of small-cell lung cancer. *The Journal of clinical investigation* 126: 2610-2620, 2016.
303. **S Khandelwal, Van Rooijen N, and Saxena RK**. Reduced expression of CD47 during murine red blood cell (RBC) senescence and its role in RBC clearance from the circulation. *Transfusion* 47: 1725-1732, 2007.
304. **H Basit, Tan ML, and Webster DR**. Histology, Kupffer Cell. 2018.
305. **M Feng, Jiang W, Kim BY, Zhang CC, Fu Y-X, and Weissman IL**. Phagocytosis checkpoints as new targets for cancer immunotherapy. *Nature Reviews Cancer* 19: 568-586, 2019.
306. **SR Gordon, Maute RL, Dulken BW, Hutter G, George BM, McCracken MN, Gupta R, Tsai JM, Sinha R, and Corey D**. PD-1 expression by tumour-associated macrophages inhibits phagocytosis and tumour immunity. *Nature* 545: 495-499, 2017.
307. **AA Barkal, Weiskopf K, Kao KS, Gordon SR, Rosental B, Yiu YY, George BM, Markovic M, Ring NG, and Tsai JM**. Engagement of MHC class I by the inhibitory receptor LILRB1 suppresses macrophages and is a target of cancer immunotherapy. *Nature immunology* 19: 76-84, 2018.
308. !!! INVALID CITATION !!! {}.
309. **M Feng, Chen JY, Weissman-Tsukamoto R, Volkmer J-P, Ho PY, McKenna KM, Cheshier S, Zhang M, Guo N, and Gip P**. Macrophages eat cancer cells using their own calreticulin as a guide: roles of TLR and Btk. *Proceedings of the National Academy of Sciences* 112: 2145-2150, 2015.
310. **A Vilalta, and Brown GC**. Neurophagy, the phagocytosis of live neurons and synapses by glia, contributes to brain development and disease. *The FEBS journal* 285: 3566-3575, 2018.
311. **JJ Neher, Neniskyte U, Hornik T, and Brown GC**. Inhibition of UDP/P2Y6 purinergic signaling prevents phagocytosis of viable neurons by activated microglia in vitro and in vivo. *Glia* 62: 1463-1475, 2014.
312. **U Neniskyte, and Brown GC**. Lactadherin/MFG‐E8 is essential for microglia‐mediated neuronal loss and phagoptosis induced by amyloid β. *Journal of neurochemistry* 126: 312-317, 2013.
313. **SP Davies, Reynolds GM, Wilkinson AL, Li X, Rose R, Leekha M, Liu YS, Gandhi R, Buckroyd E, Grove J, Barnes NM, May RC, Hubscher SG, Adams DH, Huang Y, Qureshi O, and Stamataki Z**. Hepatocytes Delete Regulatory T Cells by Enclysis, a CD4(+) T Cell Engulfment Process. *Cell Rep* 29: 1610-1620.e1614, 2019.
314. **TN Bukong, Cho Y, Iracheta-Vellve A, Saha B, Lowe P, Adejumo A, Furi I, Ambade A, Gyongyosi B, Catalano D, Kodys K, and Szabo G**. Abnormal neutrophil traps and impaired efferocytosis contribute to liver injury and sepsis severity after binge alcohol use. *J Hepatol* 69: 1145-1154, 2018.
315. **P Bertolino, Heath WR, Hardy CL, Morahan G, and Miller JF**. Peripheral deletion of autoreactive CD8+ T cells in transgenic mice expressing H-2Kb in the liver. *Eur J Immunol* 25: 1932-1942, 1995.
316. **SX Zhao, Li WC, Fu N, Zhou GD, Liu SH, Jiang LN, Zhang YG, Wang RQ, Nan YM, and Zhao JM**. Emperipolesis mediated by CD8 + T cells correlates with biliary epithelia cell injury in primary biliary cholangitis. *Journal of Cellular and Molecular Medicine* 24: 1268-1275, 2020.

317. **SP Davies, Ronca V, Wootton GE, Krajewska NM, Bozward AG, Fiancette R, Patten DA, Yankouskaya K, Reynolds GM, Pat S, Osei-Bordom DC, Richardson N, Grover LM, Weston CJ, and Oo YH**. Expression of E-cadherin by CD8(+) T cells promotes their invasion into biliary epithelial cells. *Nat Commun* 15: 853, 2024.
318. **GM Reynolds, Visentin B, and Sabbadini R**. Immunohistochemical Detection of Sphingosine-1-Phosphate and Sphingosine Kinase-1 in Human Tissue Samples and Cell Lines. *Methods Mol Biol* 1697: 43-56, 2018.
319. **HC Jeffery, Hunter S, Humphreys EH, Bhogal R, Wawman RE, Birtwistle J, Atif M, Bagnal CJ, Rodriguez Blanco G, Richardson N, Warner S, Dunn WB, Afford SC, Adams DH, and Oo YH**. Bidirectional Cross-Talk between Biliary Epithelium and Th17 Cells Promotes Local Th17 Expansion and Bile Duct Proliferation in Biliary Liver Diseases. *Journal of immunology (Baltimore, Md : 1950)* 203: 1151-1159, 2019.
320. **V Ronca, Mancuso C, Milani C, Carbone M, Oo YH, and Invernizzi P**. Immune system and cholangiocytes: A puzzling affair in primary biliary cholangitis. *J Leukoc Biol* 108: 659-671, 2020.
321. **K Kawata, Yang GX, Ando Y, Tanaka H, Zhang W, Kobayashi Y, Tsuneyama K, Leung PS, Lian ZX, Ridgway WM, Ansari AA, He XS, and Gershwin ME**. Clonality, activated antigen-specific CD8(+) T cells, and development of autoimmune cholangitis in dnTGFβRII mice. *Hepatology (Baltimore, Md)* 58: 1094-1104, 2013.
322. **S Shetty, Weston CJ, Oo YH, Westerlund N, Stamataki Z, Youster J, Hubscher SG, Salmi M, Jalkanen S, Lalor PF, and Adams DH**. Common lymphatic endothelial and vascular endothelial receptor-1 mediates the transmigration of regulatory T cells across human hepatic sinusoidal endothelium. *J Immunol* 186: 4147-4155, 2011.
323. **DC Fingar, Salama S, Tsou C, Harlow E, and Blenis J**. Mammalian cell size is controlled by mTOR and its downstream targets S6K1 and 4EBP1/eIF4E. *Genes Dev* 16: 1472-1487, 2002.
324. **KN Pollizzi, Waickman AT, Patel CH, Sun IH, and Powell JD**. Cellular size as a means of tracking mTOR activity and cell fate of CD4+ T cells upon antigen recognition. *PLoS One* 10: e0121710, 2015.
325. **HX Zhu, Yang SH, Gao CY, Bian ZH, Chen XM, Huang RR, Meng QL, Li X, Jin H, Tsuneyama K, Han Y, Li L, Zhao ZB, Gershwin ME, and Lian ZX**. Targeting pathogenic CD8(+) tissue-resident T cells with chimeric antigen receptor therapy in murine autoimmune cholangitis. *Nat Commun* 15: 2936, 2024.
326. **YH Oo, Ackrill S, Cole R, Jenkins L, Anderson P, Jeffery HC, Jones N, Jeffery LE, Lutz P, Wawman RE, Athwal AK, Thompson J, Gray J, Guo K, Barton D, Hirschfield GM, Wong T, Guest P, and Adams DH**. Liver homing of clinical grade Tregs after therapeutic infusion in patients with autoimmune hepatitis. *JHEP Rep* 1: 286-296, 2019.
327. **SM Curbishley, Eksteen B, Gladue RP, Lalor P, and Adams DH**. CXCR 3 activation promotes lymphocyte transendothelial migration across human hepatic endothelium under fluid flow. *The American journal of pathology* 167: 887-899, 2005.

328. **T Mayassi, and Jabri B**. Human intraepithelial lymphocytes. *Mucosal Immunol* 11: 1281-1289, 2018.
329. **M Baumgart, Witt C, Hüge W, and Müller B**. Increase in the expression of alpha E beta 7, characteristic of intestinal intraepithelial lymphocytes, on T cells in the lung epithelium of patients with interstitial lung diseases and in synovial fluid of patients with rheumatic diseases. *Immunobiology* 196: 415-424, 1996.
330. **LF Risnes, Eggesbø LM, Zühlke S, Dahal-Koirala S, Neumann RS, Lundin KEA, Christophersen A, and Sollid LM**. Circulating CD103(+) γδ and CD8(+) T cells are clonally shared with tissue-resident intraepithelial lymphocytes in celiac disease. *Mucosal Immunol* 14: 842-851, 2021.
331. **SE Jenkinson, Whawell SA, Swales BM, Corps EM, Kilshaw PJ, and Farthing PM**. The αE(CD103)β7 integrin interacts with oral and skin keratinocytes in an E-cadherin-independent manner*. *Immunology* 132: 188-196, 2011.
332. **H Bottois, Ngollo M, Hammoudi N, Courau T, Bonnereau J, Chardiny V, Grand C, Gergaud B, Allez M, and Le Bourhis L**. KLRG1 and CD103 Expressions Define Distinct Intestinal Tissue-Resident Memory CD8 T Cell Subsets Modulated in Crohn's Disease. *Frontiers in immunology* 11: 2020.
333. **D Herndler-Brandstetter, Ishigame H, Shinnakasu R, Plajer V, Stecher C, Zhao J, Lietzenmayer M, Kroehling L, Takumi A, Kometani K, Inoue T, Kluger Y, Kaech SM, Kurosaki T, Okada T, and Flavell RA**. KLRG1(+) Effector CD8(+) T Cells Lose KLRG1, Differentiate into All Memory T Cell Lineages, and Convey Enhanced Protective Immunity.
334. **Y Li, Li B, You Z, Zhang J, Wei Y, Li Y, Chen Y, Huang B, Wang Q, Miao Q, Peng Y, Fang J, Gershwin ME, Tang R, Greenberg SA, Ma X, Ma HD, Ma WT, Liu QZ, Zhao ZB, Liu MZ, Tsuneyama K, Gao JM, Ridgway WM, Ansari AA, Gershwin ME, Fei YY, and Lian ZX**. Cytotoxic KLRG1 expressing lymphocytes invade portal tracts in primary biliary cholangitis Chemokine receptor CXCR3 deficiency exacerbates murine autoimmune cholangitis by promoting pathogenic CD8(+) T cell activation.
335. **Z Guo, Neilson LJ, Zhong H, Murray PS, Zanivan S, and Zaidel-Bar R**. E-cadherin interactome complexity and robustness resolved by quantitative proteomics. *Sci Signal* 7: rs7, 2014.
336. **O Shafraz, Xie BA-O, Yamada S, Sivasankar SA-O, Koirala RA-O, Priest AV, Yen CA-O, Cheah JS, Pannekoek WA-O, Gloerich M, Yamada S, and Sivasankar SA-O**. Mapping transmembrane binding partners for E-cadherin ectodomains
Inside-out regulation of E-cadherin conformation and adhesion. LID - 10.1073/pnas.2104090118 [doi] LID - e2104090118.
337. **Q Sun, Luo T, Ren Y, Florey O, Shirasawa S, Sasazuki T, Robinson DN, and Overholtzer M**. Competition between human cells by entosis. *Cell research* 24: 1299-1310, 2014.
338. **S Dong, Hiam-Galvez KJ, Mowery CT, Herold KC, Gitelman SE, Esensten JH, Liu W, Lares AP, Leinbach AS, Lee M, Nguyen V, Tamaki SJ, Tamaki W, Tamaki CM, Mehdizadeh M, Putnam AL, Spitzer MH, Ye CJ, Tang Q, and Bluestone JA**. The effect of low-dose IL-2 and Treg adoptive cell therapy in patients with type 1 diabetes. *JCI Insight* 6: 2021.

339. **M Akamatsu, Mikami N, Ohkura N, Kawakami R, Kitagawa Y, Sugimoto A, Hirota K, Nakamura N, Ujihara S, Kurosaki T, Hamaguchi H, Harada H, Xia G, Morita Y, Aramori I, Narumiya S, and Sakaguchi S**. Conversion of antigen-specific effector/memory T cells into Foxp3-expressing T(reg) cells by inhibition of CDK8/19. *Sci Immunol* 4: 2019.
340. **N Mikami, Kawakami R, Chen KY, Sugimoto A, Ohkura N, and Sakaguchi S**. Epigenetic conversion of conventional T cells into regulatory T cells by CD28 signal deprivation. *Proc Natl Acad Sci U S A* 117: 12258-12268, 2020.
341. **L Evaggelia, Samita RP, Gwilym W, Danai Bagkou D, Sarah A, Mahesh K, George M, Dave EJ, Simon JB, Francesca B, Benjamin AF, and Gideon MH**. Increased sensitivity of Treg cells from patients with PBC to low dose IL-12 drives their differentiation into IFN-γ secreting cells. *Journal of Autoimmunity* 94: 143-155, 2018.
342. **HC Mitchison, Bassendine MF, Malcolm AJ, Watson AJ, Record CO, and James OF**. A pilot, double-blind, controlled 1-year trial of prednisolone treatment in primary biliary cirrhosis: hepatic improvement but greater bone loss. *Hepatology (Baltimore, Md)* 10: 420-429 , pmid = 2777203, 1989.
343. **M Leuschner, Maier KP, Schlichting J, Strahl S, Herrmann G, Dahm HH, Ackermann H, Happ J, and Leuschner U**. Oral budesonide and ursodeoxycholic acid for treatment of primary biliary cirrhosis: results of a prospective double-blind trial. *Gastroenterology* 117: 918-925 , pmid = 10500075, 1999.
344. **M Leuschner, Güldütuna S, You T, Hübner K, Bhatti S, and Leuschner U**. Ursodeoxycholic acid and prednisolone versus ursodeoxycholic acid and placebo in the treatment of early stages of primary biliary cirrhosis. *Journal of hepatology* 25: 49-57 , pmid = 8836901, 1996.
345. **O Epstein, Jain S, Lee RG, Cook DG, Boss AM, Scheuer PJ, and Sherlock S**. D-penicillamine treatment improves survival in primary biliary cirrhosis. *Lancet* 1: 1275-1277, 1981.
346. **MM Kaplan, Alling DW, Zimmerman HJ, Wolfe HJ, Sepersky RA, Hirsch GS, Elta GH, Glick KA, and Eagen KA**. A prospective trial of colchicine for primary biliary cirrhosis. *N Engl J Med* 315: 1448-1454, 1986.
347. **AL Mason, Lindor KD, Bacon BR, Vincent C, Neuberger JM, and Wasilenko ST**. Clinical trial: randomized controlled study of zidovudine and lamivudine for patients with primary biliary cirrhosis stabilized on ursodiol. *Aliment Pharmacol Ther* 28: 886-894, 2008.
348. **MK Marshall, Alan B, Robin R, and Peter ALB**. Methotrexate in patients with primary biliary cirrhosis who respond incompletely to treatment with ursodeoxycholic acid. *Digestive diseases and sciences* 55: 3207-3217 , pmid = 20559727, 2010.
349. **C Burton, Scott SE, Nancy LF, Santiago JM, Velimir AL, Marlyn JM, Timothy MM, Rowen KZ, Marion GP, Adrian MDB, Kent GB, Kris VK, Robert LC, Leonard R, Guadalupe G-T, James LB, Thomas DB, Enrique JM, Nathan MB, John RL, David SB, Maurizio B, Karen LL, Mills AS, Rodney SM, Raphael R, West AB, Donald EW, Melissa JC, and Alan FH**. Methotrexate (MTX) plus ursodeoxycholic acid (UDCA) in the treatment of

primary biliary cirrhosis. *Hepatology (Baltimore, Md)* 42: 1184-1193 , pmid = 16250039, 2005.
350. **E Christensen, Neuberger J, Crowe J, Altman DG, Popper H, Portmann B, Doniach D, Ranek L, Tygstrup N, and Williams R**. Beneficial effect of azathioprine and prediction of prognosis in primary biliary cirrhosis. Final results of an international trial. *Gastroenterology* 89: 1084-1091, 1985.
351. **T Masanobu, Yuki M, Zhe-Xiong L, Weici Z, Katsunori Y, Kanji W, Guo-Xiang Y, Toshio N, John V, Keith L, Gershwin ME, and Christopher LB**. Biochemical and immunologic effects of rituximab in patients with primary biliary cirrhosis and an incomplete response to ursodeoxycholic acid. *Hepatology* 55: 512-521 , publisher = Wiley Subscription Services, Inc., A Wiley Company, 2012.
352. **MH Gideon, Gershwin ME, Richard S, Marlyn JM, Cynthia L, Bin Z, Jewel J, Ivo PN, Bidisha D, Katherine L, Carlo S, Hanns-Ulrich M, David J, and Keith L**. Ustekinumab for patients with primary biliary cholangitis who have an inadequate response to ursodeoxycholic acid: A proof-of-concept study. *Hepatology* 64: 2016.
353. **GM Hirschfield, Gershwin ME, Strauss R, Mayo MJ, Levy C, Zou B, Selmi C, Marschall HU, and Lindor K**. P367 Phase 2 Study Evaluating the Efficacy and Safety of Ustekinumab in Patients with Primary Biliary Cirrhosis Who Had an Inadequate Response to Ursodeoxycholic Acid. *Journal of Hepatology* 60: S189-S190 , publisher = Elsevier, 2014.
354. **S Terasaki, Nakanuma Y, Ogino H, Unoura M, and Kobayashi K**. Hepatocellular and biliary expression of HLA antigens in primary biliary cirrhosis before and after ursodeoxycholic acid therapy. *Am J Gastroenterol* 86: 1194-1199, 1991.
355. **P Raoul**. Ursodeoxycholic acid and bile-acid mimetics as therapeutic agents for cholestatic liver diseases: an overview of their mechanisms of action. *Clinics and research in hepatology and gastroenterology* 36 Suppl 1: S3-12 , pmid = 23141891, 2012.
356. **Y Nishigaki, Ohnishi H, Moriwaki H, and Muto Y**. Ursodeoxycholic acid corrects defective natural killer activity by inhibiting prostaglandin E2 production in primary biliary cirrhosis. *Dig Dis Sci* 41: 1487-1493, 1996.
357. **RH McMahan, Wang XX, Cheng LL, Krisko T, Smith M, El Kasmi K, Pruzanski M, Adorini L, Golden-Mason L, Levi M, and Rosen HR**. Bile acid receptor activation modulates hepatic monocyte activity and improves nonalcoholic fatty liver disease. *J Biol Chem* 288: 11761-11770, 2013.
358. **L Verbeke, Farre R, Verbinnen B, Covens K, Vanuytsel T, Verhaegen J, Komuta M, Roskams T, Chatterjee S, Annaert P, Vander Elst I, Windmolders P, Trebicka J, Nevens F, and Laleman W**. The FXR agonist obeticholic acid prevents gut barrier dysfunction and bacterial translocation in cholestatic rats. *Am J Pathol* 185: 409-419, 2015.
359. **A Christofides, Konstantinidou E, Jani C, and Boussiotis VA**. The role of peroxisome proliferator-activated receptors (PPAR) in immune responses. *Metabolism* 114: 154338, 2021.
360. **F Colapietro, Gershwin ME, and Lleo A**. PPAR agonists for the treatment of primary biliary cholangitis: Old and new tales. *J Transl Autoimmun* 6: 100188, 2023.

361. **W Merkt, Lorenz HM, and Schmitt M**. CAR T-Cell Therapy in Autoimmune Disease. *N Engl J Med* 390: 1628-1629, 2024.
362. **JL McGovern, Wright GP, and Stauss HJ**. Engineering Specificity and Function of Therapeutic Regulatory T Cells. *Front Immunol* 8: 1517, 2017.

6. Appendix

The PhD work generated several manuscripts and abstract presentation which has been used to build this thesis.

I list below the reference of publications:

Ronca V, Gerussi A, Collins P, Parente A, Oo YH, Invernizzi P. The liver as a central "hub" of the immune system: pathophysiological implications. Physiol Rev. 2024 Sep 19. doi: 10.1152/physrev.00004.2023. Epub ahead of print. PMID: 39297676.

Montano-Loza AJ, Corpechot C, Burra P, Schramm C, Selzner N, Ronca V, Oo YH. Recurrence of autoimmune liver diseases after liver transplantation: Review and expert opinion statement. Liver Transpl. 2024 Jun 11. doi: 10.1097/LVT.0000000000000419. Epub ahead of print. PMID: 38857316.

Davies SP, Ronca V, Wootton GE, Krajewska NM, Bozward AG, Fiancette R, Patten DA, Yankouskaya K, Reynolds GM, Pat S, Osei-Bordom DC, Richardson N, Grover LM, Weston CJ, Oo YH. Expression of E-cadherin by $CD8^+$ T cells promotes their invasion into biliary epithelial cells. Nat Commun. 2024 Jan 29;15(1):853. doi: 10.1038/s41467-024-44910-2. PMID: 38286990; PMCID: PMC10825166.

Montano-Loza AJ, Ronca V, Ebadi M, Hansen BE, Hirschfield G, Elwir S, Alsaed M, Milkiewicz P, Janik MK, Marschall HU, Burza MA, Efe C, Calışkan AR, Harputluoglu M, Kabaçam G, Terrabuio D, de Quadros Onofrio F, Selzner N, Bonder A, Parés A, Llovet L, Akyıldız M, Arikan C, Manns MP, Taubert R, Weber AL, Schiano TD, Haydel B, Czubkowski P, Socha P, Ołdak N, Akamatsu

N, Tanaka A, Levy C, Martin EF, Goel A, Sedki M, Jankowska I, Ikegami T, Rodriguez M, Sterneck M, Weiler-Normann C, Schramm C, Donato MF, Lohse A, Andrade RJ, Patwardhan VR, van Hoek B, Biewenga M, Kremer AE, Ueda Y, Deneau M, Pedersen M, Mayo MJ, Floreani A, Burra P, Secchi MF, Beretta-Piccoli BT, Sciveres M, Maggiore G, Jafri SM, Debray D, Girard M, Lacaille F, Lytvyak E, Mason AL, Heneghan M, Oo YH; International Autoimmune Hepatitis Group (IAIHG). Risk factors and outcomes associated with recurrent autoimmune hepatitis following liver transplantation. J Hepatol. 2022 Jul;77(1):84-97. doi: 10.1016/j.jhep.2022.01.022. Epub 2022 Feb 8. PMID: 35143897.

Bozward AG, Ronca V, Osei-Bordom D, Oo YH. Gut-Liver Immune Traffic: Deciphering Immune-Pathogenesis to Underpin Translational Therapy. Front Immunol. 2021 Aug 25;12:711217. doi: 10.3389/fimmu.2021.711217. PMID: 34512631; PMCID: PMC8425300.

Ronca V, Wootton G, Milani C, Cain O. The Immunological Basis of Liver Allograft Rejection. Front Immunol. 2020 Sep 2;11:2155. doi: 10.3389/fimmu.2020.02155. PMID: 32983177; PMCID: PMC7492390.

Carbone M, Milani C, Gerussi A, Ronca V, Cristoferi L, Invernizzi P. Primary biliary cholangitis: a multifaceted pathogenesis with potential therapeutic targets. J Hepatol. 2020 Oct;73(4):965-966. doi: 10.1016/j.jhep.2020.05.041. Epub 2020 Jul 21. PMID: 32709365.

Ronca V, Mancuso C, Milani C, Carbone M, Oo YH, Invernizzi P. Immune system and cholangiocytes: A puzzling affair in primary biliary cholangitis. J

Leukoc Biol. 2020 Aug;108(2):659-671. doi: 10.1002/JLB.5MR0320-200R. Epub 2020 Apr 29. PMID: 32349179.